En Route to Tailor-made Oligosaccharides – Chemo-enzymatic Synthesis and Physiological Functions of Novel Carbohydrate Structures

Von der Fakultät für Lebenswissenschaften

der Technischen Universität Carolo-Wilhelmina

zu Braunschweig

zur Erlangung des Grades eines

Doktors der Naturwissenschaften

(Dr. rer. nat.)

genehmigte

D i s s e r t a t i o n

von Arne Homann

aus Gifhorn

1. Referent: Prof. Dr. Jürgen Seibel

2. Referent: Prof. Dr. Dieter Jahn

eingereicht am: 19.10.2009

mündliche Prüfung (Disputation) am: 17.12.2009

Druckjahr 2009

Vorveröffentlichungen der Dissertation

Teilergebnisse aus dieser Arbeit wurden mit Genehmigung der Fakultät für Lebenswissenschaften, vertreten durch den Mentor der Arbeit, in folgenden Beiträgen vorab veröffentlicht:

Publikationen

Homann, A., Seibel, J., “Chemo-enzymatic synthesis and functional analysis of natural and modified glycostructures.” (2009) Nat Prod Rep., 26 (12),1555-1571

Homann, A., Seibel, J., “Towards tailor-made oligosaccharides – Chemo-enzymatic approaches by enzyme and substrate engineering.” (2009) Appl Microbiol Biotechnol., 83 (2), 209-16.

Homann, A., Biedendieck, R., Götze, S., Jahn, D. Seibel, J., "Insights into polymer *versus* oligosaccharide synthesis - Mutagenesis and mechanistic studies of a novel levansucrase from *Bacillus megaterium.*" (2007) Biochem J., 407 (2), 189-198.

Eingereichte Publikationen

Homann, A., Riaz-ul-Qamar, Serim, S., Dersch, P., Seibel, J., “Bioorthogonal metabolic glycoengineering of human larynx carcinoma (HEp-2) cells targeting sialic acid.” (submitted in 2009 to Beilstein Journal of Organic Chemistry)

Einzureichende Publikationen

Homann, A., Strube, C., Gamer, M., Jahn, D., Heinz, D., Seibel, J., “Synthesis of tailor-made oligosaccharides - Engineering the transfructosylation process of the levansucrase SacB from *Bacillus megaterium.*”

Homann, A., Pasche, B., Dersch, P., Schughart, K., Seibel, J., “Immuno-stimulating properties of novel fructo-oligosaccharides”.

Homann, A., Seibel, J. “Shift of the linkage type of the sucrose analogue Gal-Fru – Substrate engineering of a sucrose isomerase from *Protaminobacter rubrum*.”

Tagungsbeiträge

Homann, A., Strube, C., Pasche, B., Schughart, K., Heinz, D., Seibel, J., “Enzymatic synthesis and immuno-assay of novel carbohydrate structures.” EMBL International PhD Symposium, Heidelberg, 2009 (Poster)

Homann, A., Strube, C., Pasche, B., Schughart, K., Heinz, D., Seibel, J., “Towards tailor-made oligosaccharides – Chemo-enzymatic synthesis and physiological functions of novel carbohydrate structures.” SFB 630 International Symposium, Novel agents against Infectious diseases – An Interdisciplinary approach, Würzburg, 2009 (Poster Award, Oral Presentation)

Homann, A., Strube, C., Jahn, D., Heinz, D., Seibel, J., “Towards tailor-made oligosaccharides by enzyme and substrate engineering.” 15th European Carbohydrate Symposium, Wien, 2009 (Poster Award)

Homann, A., Hillringhaus, L., Höbbel, S. and Seibel, J., “Modified thio-sugars on carbohydrate microarrays to study interactions with glycosyltransferases and glycosidases.” EMBL Conference on Chemical Biology, Heidelberg, 2008 (Poster)

Homann, A., Zuccaro, A. Götze, S., Strube, C., Dersch, P., Heinz, D. and Seibel, J., “Novel fructo-oligosaccharides as pharma-/nutraceuticals.” European Bioperspectives, Hannover, 2008 (Poster)

Homann, A., Strube, C., Heinz, D. und Seibel, J., “Oligo- *vs*. polysaccharide formation – Production of oligofructosides and structure-function analysis of a novel fructosyltransferase from *Bacillus megaterium.”* International Congress on Biocatalysis, Hamburg, 2008 (Poster)

Strube, C., Homann, A., Biedendieck, R., Gamer, M., Jahn, D., Heinz, D., Seibel, J., „Strukturbiologie von Glykosyltransferasen zur Optimierung von biotechnologischen Prozessen.“, Begutachtung SFB 578, Braunschweig, 2008 (Poster)

Homann, A., Biedendieck, R., Götze, S., Buchholz, K. and Seibel, J., “Kinetic studies of a novel fructosyltransferase from *Bacillus megaterium* provide insights into the reaction mechanism.” European Bioperspectives, Köln, 2007 (Poster)

Strube, C., Homann, A., Biedendieck, R., Jahn, D., Heinz, D., Seibel, J., „Strukturbiologie von Glykosyltransferasen zur Optimierung von biotechnologischen Prozessen.“ Berichtskolloquium SFB 578, Braunschweig, 2007 (Vortrag)

Homann, A., Götze, S., Biedendieck, S., Jahn, D., Buchholz, K. and Seibel, J., “Characterization and mechanistic insights of a novel fructosyltransferase from *Bacillus megaterium* by site-directed mutagenesis.” 7th Carbohydrate Bioengineering Meeting, Braunschweig, 2007 (Poster)

Hillringhaus, L., Homann, A., Hellmuth, H., Moraru, R., Götze, S., Beine, R. and Seibel, J., „Neuartige chemo-enzymatische Glykosylierungsmethoden zur Synthese von Oligosacchariden, Glykopeptiden und Glykokonjugaten.“ Jahrestagung Deutscher Katalytiker, Weimar, 2007 (Poster)

Götze, S., Moraru, R., Homann, A., Hecht, H.-J., Na'amnieh, S., Pawlowski, A., Buchholz, K. and Seibel, J., „Sucrose analogues synthesis with the fructosyltransferase of *Bacillus subtilis* NCIMB 11871 provides mechanistic insights." International Congress on Biocatalysis, Hamburg, 2006 (Poster)

"Wahrlich es ist nicht das Wissen, sondern das Lernen, nicht das Besitzen, sondern das Erwerben, nicht das Da-Seyn, sondern das Hinkommen, was den größten Genuss gewährt."

(*Carl Friedrich Gauß, Schreiben Gauß an Wolfgang Bolyai, Göttingen, 2. 9. 1808)*

Contents

I Abbreviations

Amino acid	Three letter code	One letter code
alanine	Ala	A
arginine	Arg	R
asparagine	Asn	N
aspartic acid	Asp	D
cysteine	Cys	C
glutamic acid	Glu	E
glutamine	Gln	Q
glycine	Gly	G
histidine	His	H
isoleucine	Ile	I
leucine	Leu	L
lysine	Lys	K
methionine	Met	M
phenylalanine	Phe	F
proline	Pro	P
serine	Ser	S
threonine	Thr	T
tryptophan	Try	W
tyrosine	Tyr	Y
valine	Val	V

Carbohydrates	
AcGlcNAz	2-azidoacetylamino-2-deoxy-(1,3,4,6)-tetraacetyl-β-D-glucopyranoside
Fuc, F	fucose
FF, Fuc-Fru	fucosylfructoside (α-L-fucopyranosyl-β-D-fructofuranoside)
Fru, F	fructose
Gal, G	galactose

GalNAc	*N*-acetylgalactosamine
GF, Gal-Fru	galactosylfructoside (α-D-galactopyranosyl-β-D-fructofuranoside)
Glc	glucose
GlcNAc	*N*-acetylglucosamine
GlcNAz	2-azidoacetylamino-2-deoxy-β-D-glucopyranoside
Kest	1-kestose
Man	mannose
ManNAc	*N*-acetylmannosamine
MF, Man-Fru	mannosylfructoside (α-D-mannopyranosyl-β-D-fructofuranoside)
NeuNAc	neuraminic acid
NeuNAz	*N*-azido-acetylneuraminic acid
NeuNHex	*N*-(1-oxohex-5inyl) neuraminic acid
Nyst	1-nystose
Pala	palatinose
Suc	sucrose
Xyl, X	xylose
XF, Xyl-Fru	xylosylfructoside (α-D-xylopyranosyl-β-D-fructofuranoside)

1D	one dimensional
2D	two dimensional
3D	three dimensional
Å	Ångstrøm [10^{-10} m]
A	exponential factor of the Arrhenius equation
bp	base pair
BRENDA	Braunschweiger Enzymdatenbank
BSA	bovine serum albumine
c	concentration
C	Celsius
CAZy	carbohydrate-active enzymes database

CHO	Chinese Hamster Ovary
CM	carboxymethyl
COSY	homonuclear correlation spectroscopy
Da	Dalton
DIFO	difluoronated cyclooctyne
DMEM	Dulbecco`s modified Eagle`s medium
DMF	dimethylformamide
DMSO	dimethylsulfoxide
DNA	desoxyribonucleic acid
DSMZ	Deutsche Sammlung für Mikroorganismen und Zellkulturen
E	enzyme concentration
E_0	starting concentration
E_A	activation energy
EC	Enzyme Commission
EDTA	ethylendiaminetetraacetate
EP	enzyme-product complex
Epo	erythropoietin
epPCR	error-prone polymerase chain reaction
ER	endoplasmatic reticulum
ES	enzyme-substrate complex
ESI/MS	electro-spray ionisation mass spectroscopy
FACS	fluorescence-activated cell sorting
FCS	fetal calf serum

FOS	fructo-oligosaccharide
FPLC	fast protein liquid chromatography
g	gram
g	gravitation constant
Gb3	globotriaosyl
GH	glycoside hydrolase
GM-CSF	Granulocyte-macrophage colony-stimulating factor
Golgi	Golgi apparatus
GRAS	generally regarded as safe
H	hemagglutinin
h	hour
HMBC	hetero multiple bond coherence
HPAEC	high-performance anion-exchange chrromatography
HSQC	heteronuclear single quantum coherence
IFN	interferon
Ig	immunoglobulin
IL	interleukin
IPTG	isopropyl-ß-D-galactopyranoside
K_m	Michaelis-Menten constant [mM]
k_{cat}	turnover number [s^{-1}]
KLH	keyhole limpet hemocyanin
l	litre
Le^x	Lewis X

Ln	ligand
M_w	molecular weight
MALDI/MS	matrix-assisted laser desorption mass spectroscopy
MCP	monocyte chemoattractant protein
MIG	monokine induced by gamma interferon
min	minute
MIP	macrophage inflammatory protein
MIG	monokine induced by γ-interferon
MRS	medium after deMan, Rogosa and Sharp
MWCO	molecular weight cut-off
N	neuraminidase
N-N	(N-(1-naphthyl)-ethylendiamindihydrochlorid)
NCS	newborn calf serum
NMR	nuclear magnetic resonance
NOESY	nuclear Overhauser effect spectroscopy
OS	oligosaccharide
PBS	phosphate buffered saline
PCR	polymerase chain reaction
PS	polysaccharide
R	gas constant
RANTES	regulated upon activation, normal T-cell expressed and secreted
RNA	ribonucleic acid
rpm	rounds per minute

RPMI	Roswell Park Memorial Insitute
S	substrate concentration [M]
SDS-PAGE	sodiumdodecylsulfate-polyacrylamide gel electrophoresis
sec	second
sLe^x	sialyl Lewis X
ssDNA	single-stranded desoxyribonucleic acid
T	temperature
t	time
TAMRA	tetramethylrhodamine
TBTA	Tris-[(1-benzyl-1-H-1,2,3-triazol-4-yl) methyl]amine
TLC	thin layer chromatography
TNF	tumour necrosis factor
TOCSY	total correlation spectroscopy
TU	Technical University
UDP	uridine diphosphate
UV	ultraviolet
v	velocity
v_{max}	maximum velocity
v/v	volume per volume
w/o	without
w/v	weight per volume
WT	wild-type

1 Theoretical Background

1.1 What is Glycobiology?

The term “carbohydrate” was first used over a 100 years ago to label molecules of the sum formula $(CH_2O)_n$. Today this term also includes carbohydrate derivatives and refers to the whole class of molecules. Other names for carbohydrates are saccharides, sugars or glycans. The term “saccharide” was derived from the ancient Greek word *sakhar* meaning sugar or sweetness. In the 19th century, Emil Fischer elucidated the structure of the first monosaccharide, glucose, which was also called dextrose after Kekulé due to its ability to refract polarised light. This was the development of chirality (from the greek “*cheir*” meaning “hand”), *i.e.* the differentiation between the D (*dexter* meaning “right”)- and L (*laevus* meaning “left”)-forms of carbohydrates. But science was still far from realising the true biological impact of carbohydrates on living organisms.

In 1953 Watson and Crick discovered the helix structure of the DNA which was a major breakthrough for biological sciences (Watson *et al.*, 1953). Since then, more and more “molecules of life” were discovered and their impact on the biochemical properties of cells and whole organisms was investigated. The central dogma is that DNA is transcribed into RNA which is subsequently translated into proteins.

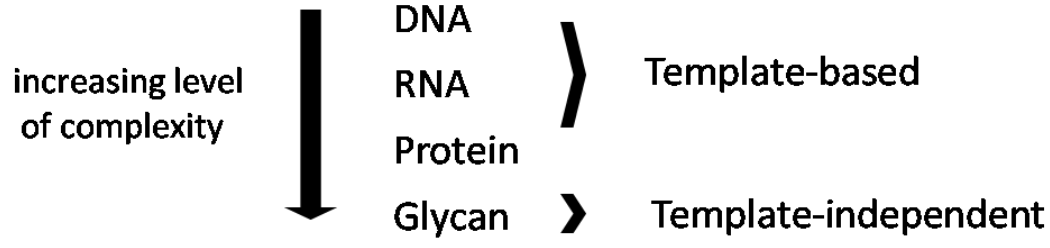

Figure 1 The increasing level of complexity of the “molecules of life” from DNA, to RNA, proteins and glycans. The biosynthesis and transfer of glycans are not template-based.

This unidirectional theory became more and more perforated as transcriptional and translational control and regulation mechanisms were discovered. Furthermore, complex co- and posttranslational modifications like glycosylation were identified which made our picture of a cell more complete but also significantly more complicated. The dynamic or microheterogeneity of the glycosylation mechanism is a great challenge for scientists these days. What makes glycobiology even more challenging is the diversity of carbohydrates. The possible structure of an oligosaccharide far exceeds the complexity of DNA and even proteins. The degree of polymerisation, the linkage type and anomeric state of carbohydrates are the factors which make them so diverse. Fortunately for glycobiologists, nature uses limited monosaccharide resources and linkage types.

1.2 Natural bioactive carbohydrate structures

Oligosaccharides are crucial for the development and differentiation of cells (Ungar, 2009). Glycoconjugates are involved in processes like inflammation, cell-cell signalling, cell differentiation and infections. These interactions of cells with their environment require accessible carbohydrate patterns on the surface of the cells. This so-called glycocalyx covers the surface of every eukaryotic cell.

Major classes of glycosylation patterns are *N*- and *O*-glycosylation of proteins, glycosaminoglycans, glycophospholipids and glycosphingolipids. *N*-glycosylation occurs at an asparagine residue of a protein which is part of an N-X-S/T sequon where X can be any amino acid except proline (Bause, 1983; Jones *et al.*, 2005). However, this is a necessary but not a sufficient condition. It is estimated that approximately 90 % of the sequons are glycosylated. Glycosylation ensures and even accelerates proper protein folding (Hanson *et al.*, 2009). Unfortunately, no motif has yet been identified for the *O*-glycosylation mechanism. *O*-glycans are mostly of lower molecular weight than the *N*-glycosylation patterns. In glycophospholipids, carbohydrates function as a bridge between phophatidylinositol and phosphoethanolamine. The latter is coupled to the C-terminus of a glycoprotein by an amide bond which anchors the glycoprotein in a cell membrane. Glycosphingolipids or simply glycolipids are glycosylated fatty acids carrying a long-chain amino alcohol,

e.g. sphingosin (figure 2). Glycoproteins as well as glycolipids form the glycocalyx on the surface of a cell.

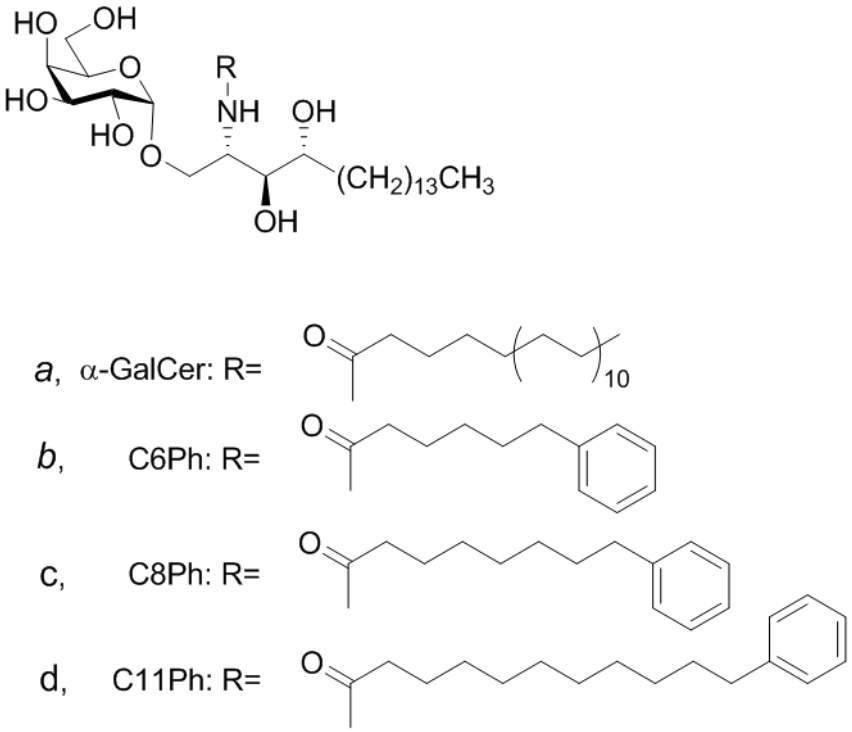

Figure 2 Structure of the glycolipid galactosylceramide and aromatic fatty acyl chain analogues.

In the following paragraphs, two examples of cell surface glycans are introduced which represent the impact of the monosaccharide structure and the linkage type between two monosaccharides. The first example is the human blood type. The structures of the blood types A and B are highly similar except of one *N*-linked acetyl group of the terminal galactose unit (figure 3). The blood type 0 misses the terminal galactose or *N*-acetylgalactosamine, respectively. As it is commonly known, this small change in the structure of the tetrasaccharide has a dramatic effect. The immune system recognises each structure as “self” or “non-self” and induces inflammation against non-self glycosylation patterns

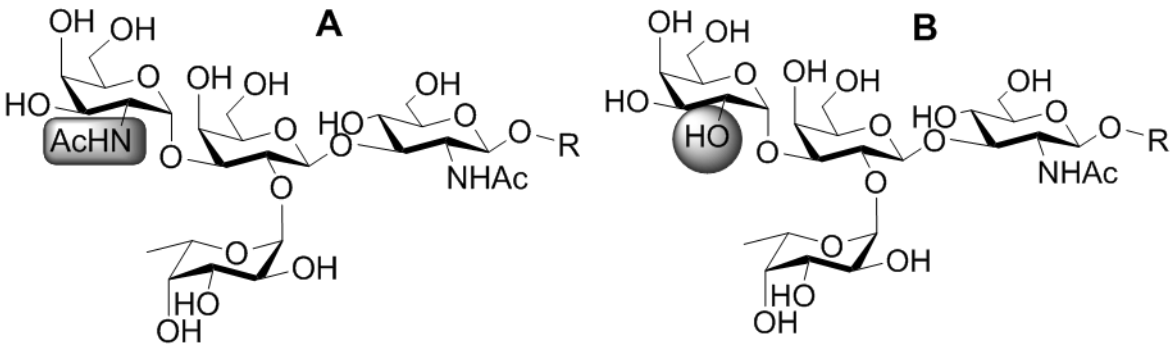

Figure 3 Carbohydrate structures of A) blood type A with terminal galactosamine, B) blood type B with terminal galactose. R is a cell surface protein or ceramide.

One recent topic concerning oligosaccharide structures with terminal sialic acids is flu. Bird flu (H5N1) and swine flu (H1N1) are termed after different variations of hemagglutinin (H) and neuraminidase (N). Hemagglutinin binds to terminal sialic acids of cells which are target for infection processes (Kunisaki *et al.*, 2009). The binding mode of the sialic acid determines the infectiousness of the flu virus type. The human respiratory tract contains α-(2,6)-linked sialic acids whereas the bird flu virus is specific for α-(2,3) linkages (figure 4). However, a mutation of just one amino acid residue is required to change the specificity from α-(2,3) to α-(2,6) (Kunisaki *et al.*, 2009). Moreover, swines can become infected by both types and therefore can act as a “mixing vessel” to eventually enhance the pathogenicity of the virus (Ding *et al.*, 2009).

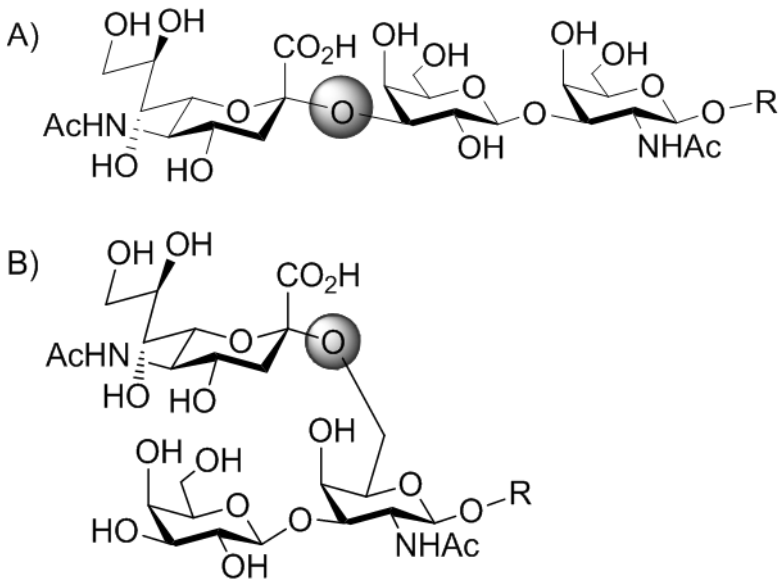

Figure 4 Glycosylation pattern of A) the α-(2,3)-linked sialic acid involved in “bird flu” infection and B) the α-(2,6)-linked sialic acid involved in “swine flu” infection.

1.3 Carbohydrate-active enzymes

In contrast to the long-standing opinion that one enzyme is specific for one substrate or catalyses one reaction it is nowadays clear that many enzymes have a certain promiscuity in donor or acceptor substrate recognition. Additionally, molecular biology techniques like directed evolution and rational design help to create enzymes with new functionalities (Hancock *et al.*, 2006; Eltis *et al.*, 2008). It was shown that glycosyltransferases can transfer carbohydrates to different kinds of acceptors, *e.g.* alcohols, amino acids, lipids, proteins or other carbohydrates (Seibel *et al.*, 2006a; Eltis *et al.*, 2008; Shaikh *et al.*, 2008). The natural promiscuity of glycosyltransferases already is surprisingly high. Enzyme and substrate engineering gives further access to tailor-made glycan products (Kim *et al.*, 2006; Lairson *et al.*, 2006; Seibel *et al.*, 2006a; Homann *et al.*, 2009).

Two major classes of these enzymes exist depending on their substrates: Leloir and non-Leloir glycosyltransferases. They are termed after the Argentinian chemist and Nobel-prize winner Luis Leloir. Leloir-type glycosyltransferases use nucleotide-activated carbohydrates as substrates while non-Leloir enzymes use the energy of the glycosidic bond for the transfer of monosaccharides to an acceptor (figure 5).

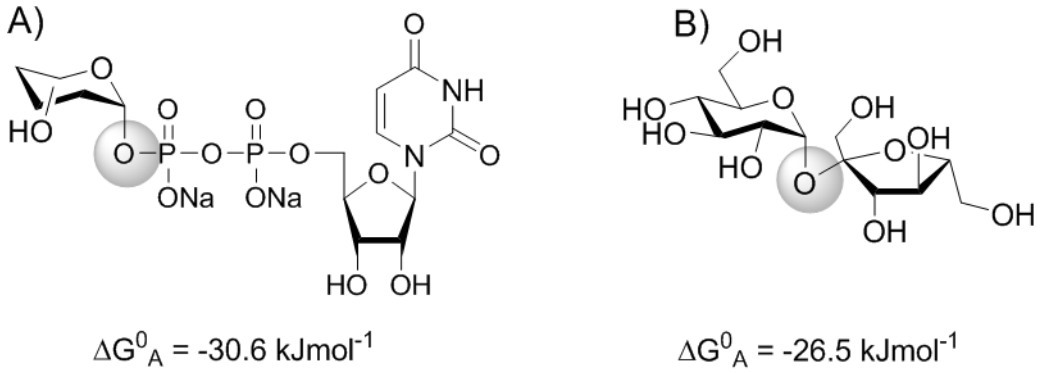

Figure 5 The A) Leloir-type, nucleotide-activated and B) non-Leloir-type substrate sucrose for glycosyltransferases. The carbohydrate moiety shown in red can be a wide variety of monosaccharides, *e.g.* mannose, galactose or fucose. The similar binding energy of the glycosidic bond is indicated.

1.4 Glycosyltransferases catalyse hydrolysis and transfer reactions

As mentioned above, carbohydrates play a very important role both as polymers and short-chain oligo- or even monosaccharides with biological functions. Polysaccharides can act as structural motifs, energy reserve or protection against environmental factors (van Hijum *et al.*, 2006; Comstock, 2009; Kline *et al.*, 2009). The polysaccharides as well as the oligosaccharide structures are synthesised by glycosyltransferases. Two different kinds of reaction mechanisms were identified: The retaining and the inverting mechanism. In the two-step retaining hydrolysis mechanism, a nucleophile (generally glutamate or aspartate) attacks the anomeric C1 hydroxyl group and forms a covalent intermediate temporarely inverting the anomeric state. This intermediate is attacked by a water molecule again in position C1 and the hydrolysed carbohydrate is released under overall anomeric retention (figure 6). The inverting mechanism takes place in one step. The nucleophile attacks a proton from a water molecule and at the same time the water hydroxyl residue attacks the C1 carbon of the carbohydrate inverting the anomeric configuration (figure 7).

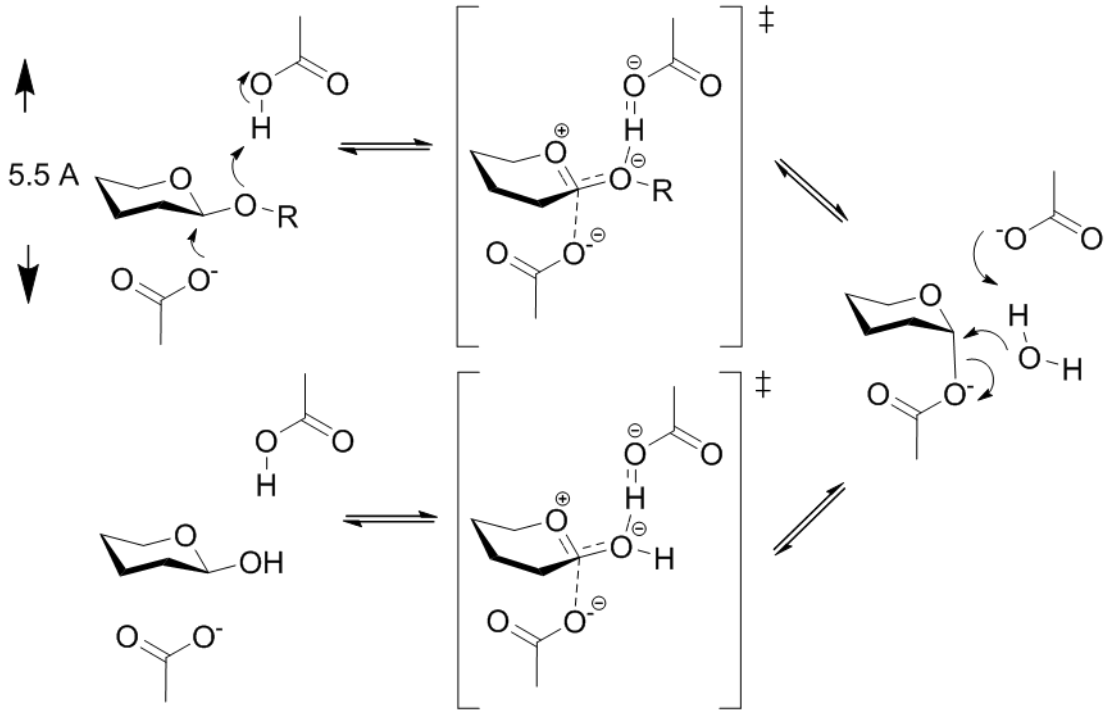

Figure 6 The double-displacement reaction mechanism of glycosyltransferases retaining the anomeric centre.

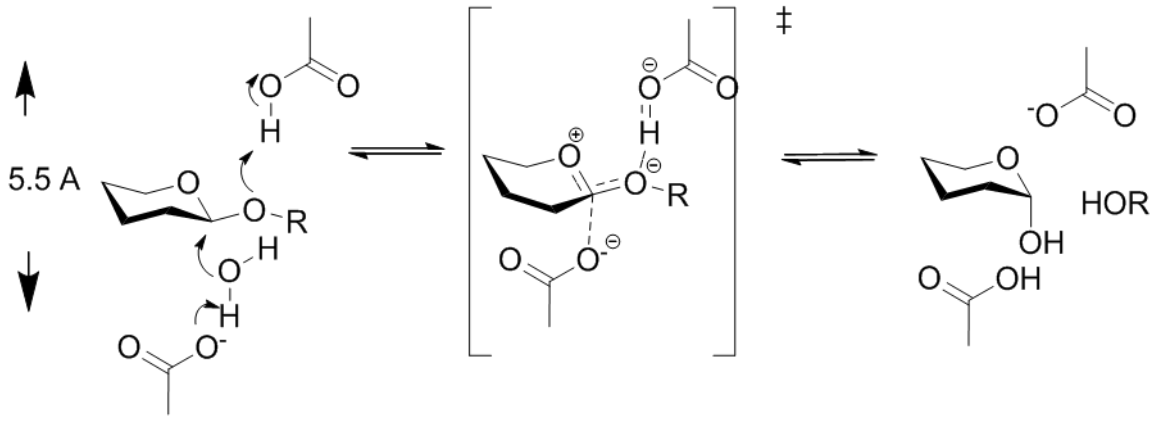

Figure 7 The reaction mechanism of glycosyltransferases inverting the anomeric centre.

Bacterial and fungal fructosyltransferases synthesise fructans by the non-Leloir pathway with the double-displacement retaining mechanism. Products are β-(2,6) linked levan or β-(2,1) linked inulin (van Hijum *et al.*, 2006). In this process, a

fructosyl unit is transferred to an acceptor molecule. This can be water in case of hydrolysation, an oligosaccharide substrate like sucrose forming a trisaccharide or a polysaccharide yielding an elongated polymer. However, it remains unclear which mechanisms influence the stereospecificity of the reaction or hydrolysis, oligo- or polysaccharide formation.

1.5 Determination of the kinetic parameters of an enzyme reaction – The kinetic model of Michaelis-Menten

The kinetic model after Michaelis-Menten is a mathematical description of an enzyme reaction under some simplified conditions. Not all enzymes are following these laws, especially when inhibitory effects occur (Lasch, 1987).

During an enzyme reaction, an enzyme-substrate-complex (ES) is formed. The substrate (S) is subsequently converted to a product (P) and dissociates from the enzyme (Lasch, 1987). This is described by equation 1.1.

$$E + S \underset{k_{-1}}{\overset{k_1}{\rightleftharpoons}} ES \underset{k_{-2}}{\overset{k_2}{\rightleftharpoons}} EP \underset{k_{-3}}{\overset{k_3}{\rightleftharpoons}} E + P \qquad [1.1]$$

The simplification assumptions of Michaelis-Menten include no back reaction at the beginning of the enzyme reaction ($k_{-2,\ -3} = 0$) and only the measurement of the product formation. The result is equation 1.2.

$$E + S \underset{k_{-1}}{\overset{k_1}{\rightleftharpoons}} ES \xrightarrow{k_2} E + P \qquad [1.2]$$

The equation for the saturation hyperbola of the Michaelis-Menten ansatz is equation 1.3.

$$v = \frac{v_{max} \cdot [S]}{K_m + [S]} \qquad [1.3]$$

The K_m-value represents the substrate concentration at the point of half-maximal reaction velocity and contains the velocity constants from equation 1.2. The situation

at the point of half-saturation of the enzyme (K_m) and the point of saturation (v_{max}) is illustrated in figure 8.

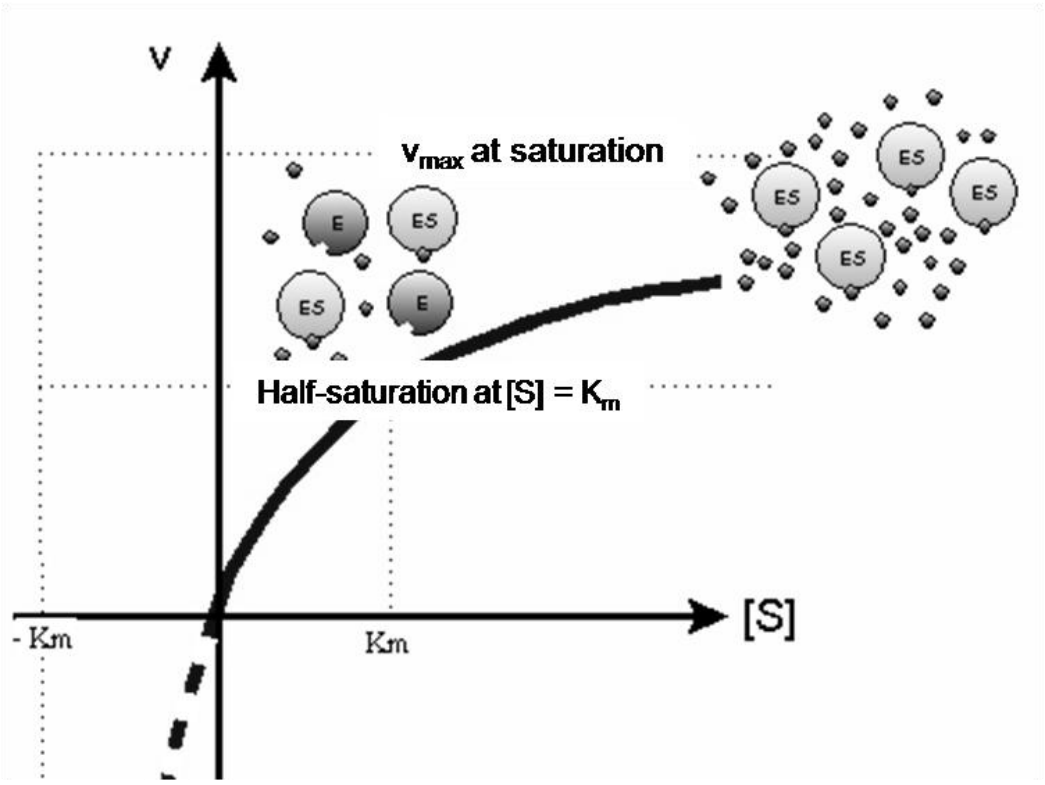

Figure 8 Kinetics of an enzyme reaction after Michaelis-Menten.

For the saturation of the enzyme the velocity of the product formation is crucial. By equation 1.4 the k_{cat} is determined which describes the turnover rate of substrate molecules per time.

$$k_2 = k_{cat} = \frac{v_{\max}}{E_0} \qquad [1.4]$$

For the determination of the catalytic efficiency it is assumed that [S] << K_m under physiological conditions (1.5).

$$v = \left(\frac{v_{\max}}{K_m} \right) \cdot [S] \qquad [1.5]$$

Equation 1.4 is solved for v_{max} and inserted in 1.5.

$$v = \left(\frac{k_{cat}}{K_m} \right) \cdot [E_0] \cdot [S] \qquad [1.6]$$

The ratio $\left(\frac{k_{cat}}{K_m} \right)$ is the catalytic efficiency.

1.6 The pH-dependency of an enzyme reaction

As enzymes consist of amino acids with different functional groups, they are polyelectrolytes. The result is a characteristic isoelectric point for each enzyme. At this point an identical number of positively and negatively charged groups are present. The charge depends on the surrounding medium. By a change of the pH a conformational change of the enzyme occurs. Because the enzyme reaction depends on the steric orientation of the amino acid residues there is a clear dependence on the pH of the environment. Statistically every five amino acid residues there is a functional group whose charge depends on the pH of the medium.

Another issue is the influence of the pH on the substrate. During enzyme-substrate interactions ionic groups and the substrate conformation plays a crucial role for the activity of the enzyme. When choosing a buffer for an enzyme reaction the ions of the buffer must not or at least very fewly interact with the enzyme. Phosphate buffer systems ensure few enzyme interactions (Stoll *et al.*, 1990).

A plot of the pH and the enzyme activity usually looks like a bell-shaped curve with a maximum (Lasch, 1987). The Gauß-function is the basis for the plot (figure 9).

$$y = y_0 + A \cdot e^{-\frac{(x - x_c)^2}{w^2}} \qquad [1.7]$$

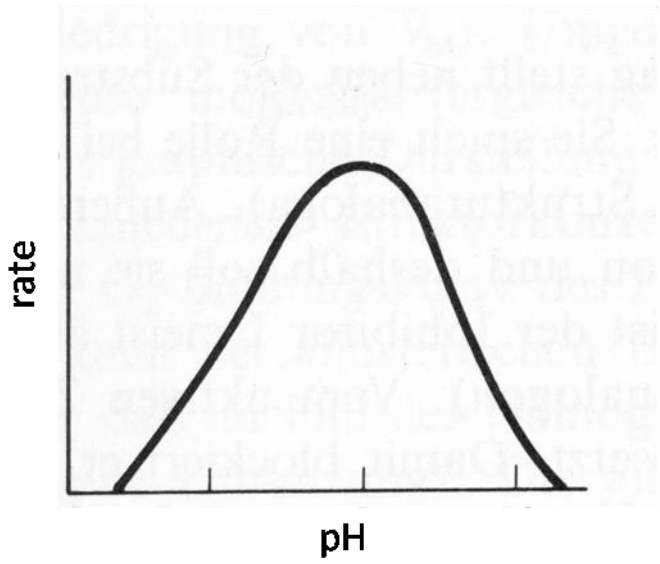

Figure 9 Scheme of the pH-dependency of an enzyme reaction.

1.7 The temperature-dependency of an enzyme reaction

Analogous to chemical reactions the velocity of enzymatic reactions is generally increased with higher temperatures (Arrhenius, 1889). But one has to consider that enzymes denature rapidly at temperatures above the normal physiological conditions. These are temperature-dependent denaturing effects influencing the structural conformation of the enzyme. As a rule, an enzyme is the more temperature-sensitive the purer it is (Lasch, 1987). Under physiological conditions, enzymes are often associated with other proteins or membranes which have stabilising effects (Alberts *et al.*, 1995). The temperature-dependency of the velocity constant is described by the Arrhenius equation (1.9).

$$k = A \cdot e^{\frac{-E_a}{RT}} \qquad [1.9]$$

A, Arrhenius factor; E_a, activation energy; R, gas constant and T, temperature.

The plot shows a slow increase with a maximum of the reaction rate. When the temperature is further increased a denaturation of the enzyme and thus a fast decrease of the reaction rate occurs (figure 10).

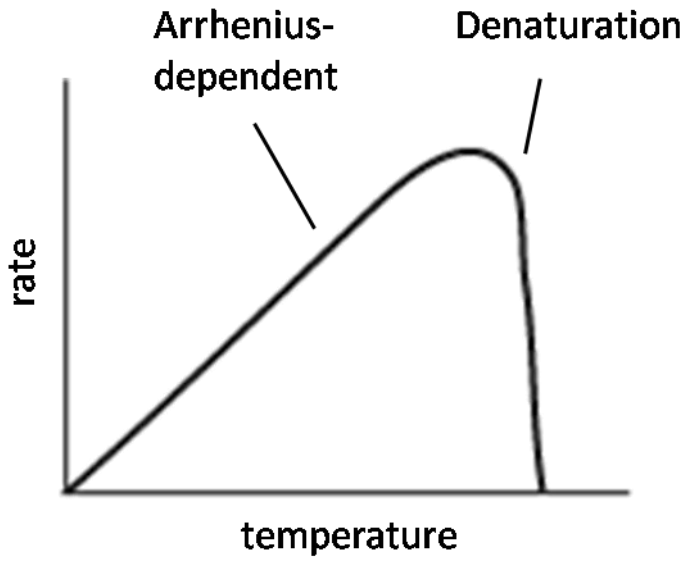

Figure 10 The temperature-dependency of an enzyme reaction.

1.8 En route to tailor-made oligosaccharides

1.8.1 Tailor-made carbohydrates by enzyme engineering

Many enzymes have been targets for directed evolution and rational design approaches to enhance their temperature- or pH-stability, to perform the catalysis of a novel reaction as well as the acceptance of a new substrate. The crucial point for the success of these strategies is the screening system. According to the so-called first law of directed evolution “You get what you screen for” (Schmidt-Dannert *et al.*, 1999) the resulting enzyme variants can have unexpected properties. Nevertheless, the strategy proved very useful in terms of novel acceptor substrates and novel activities of the engineered enzymes (Hancock *et al.*, 2006; Gantt *et al.*, 2008). Withers and co-workers turned a glycosidase into a glycosynthase or a glycothiosynthase, respectively (Hancock *et al.*, 2006). The group of Fairbanks engineered an endo-β-*N*-acetylglucosaminidase to act as an oligosaccharyltransferase (Heidecke *et al.*, 2008).

The strategy of directed evolution includes the creation of as many mutants as suitable. Techniques are error-prone polymerase chain reaction (epPCR) or the use of DNA-intercalating chemicals such as nitrous acid or hydroxylamine. The resulting enzyme variants are screened and the positive ones are isolated. The elucidation of

the protein structure as well as the biochemical data of the chosen variants may help to explain the effect of amino acid mutations. With the structure of desired variants at hand, rational design may follow the directed evolution. In this work, we combined the techniques of directed evolution and rational design to create variants of the fructosyltransferase from *B. megaterium* in order to synthesise tailor-made oligosaccharides (figure 11).

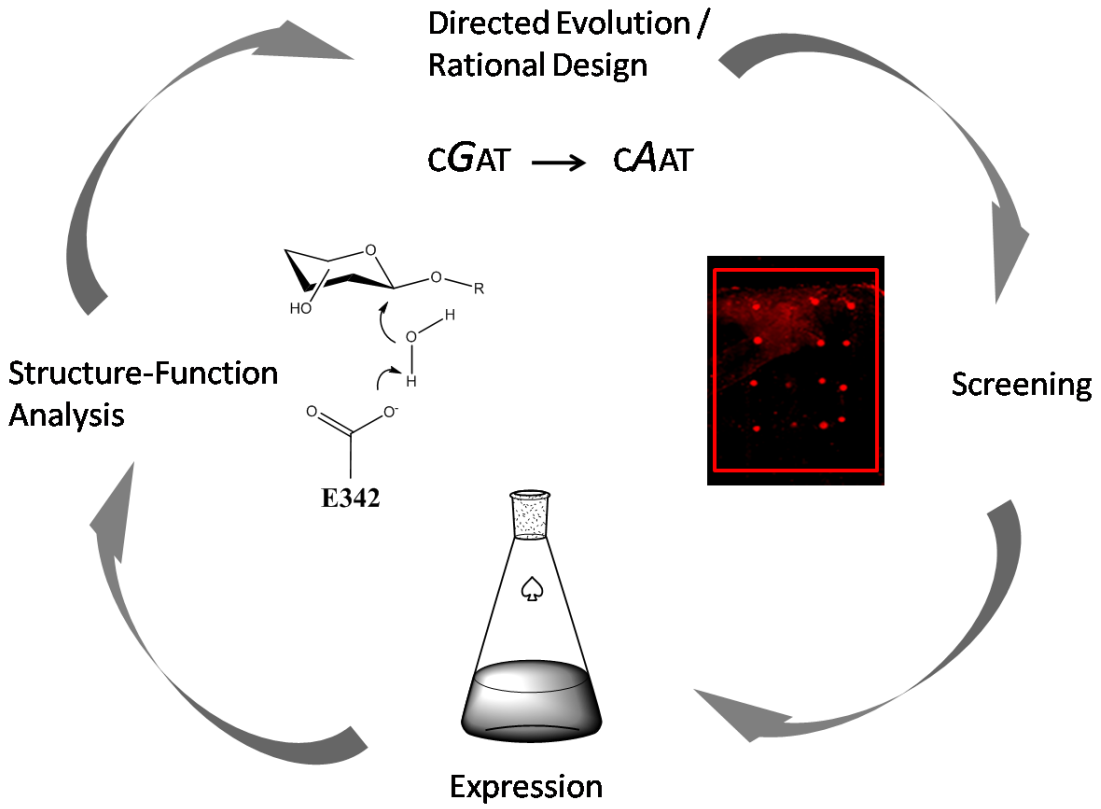

Figure 11 Combined directed evolution and screening cycle. Structural biology permits rational enzyme design.

1.8.2 Tailor-made carbohydrates by substrate engineering

The growing impact of chemical biology is not surprising considering the success of engineered substrates over the very recent years. Glycosyltransferases accept a bunch of modified natural substrate analogues sometimes even keeping their wild-type activity (Fazio *et al.*, 2002; Perez *et al.*, 2007; Lairson *et al.*, 2008). Bacterial glycosyltransferases like the fructosyltransferase from *A. niger* readily synthesises 1-

kestose and 1-nystose analogues with sucrose analogues as substrates (Zuccaro *et al.*, 2008). The engineered fructosyltransferase from *B. subtilis* synthesises 6-kestose and 6-nystose analogues with the same substrates (Beine *et al.*, 2008). Short-chain oligofructosides are known as prebiotics with beneficial effects on the human intestinal flora (Yun, 1996; Saavedra *et al.*, 2002; Boehm *et al.*, 2004; Hirayama *et al.*, 2005; Comstock, 2009). Also the L-forms of various sucrose analogues are accepted by the levanucrase SacB from *B. subtilis* (figure 12; Seibel *et al.*, 2006a). Engineered substrates with thio-functionalities offer further chemical modification steps (Pachamuthu *et al.*, 2006; Hellmuth *et al.*, 2007).

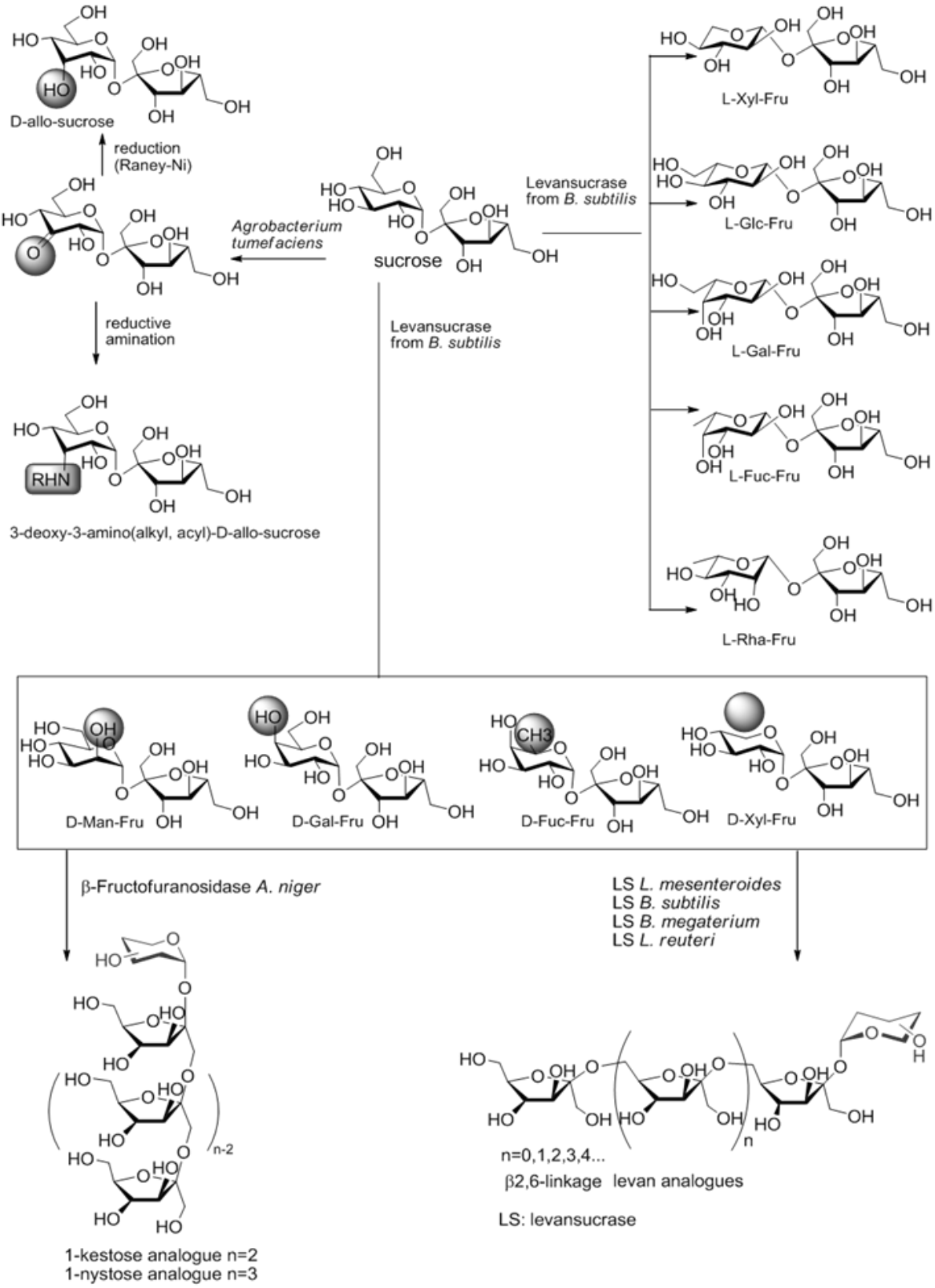

Figure 12 Possible chemo-enzymatic synthesis of various oligosaccharide structures (Stoppok *et al.*, 1995; Seibel *et al.*, 2006b; van Hijum *et al.*, 2006).

1.9 Isomerases as tools for controlling the linkage type of oligosaccharides

Sucrose isomerases convert sucrose (α-D-glucopyranosyl-β-(1,2)-D-fructofuranoside) to the sucrose analogues isomaltulose (α-D-glucopyranosyl-β-D-(1,6)-fructofuranoside, also referred to as the commercial name palatinose) (yield up to 75-85 %) or trehalulose (α-D-glucopyranosyl-β-(1,1)-D–fructofuranoside, yield up to 90 %) depending on the bacterial strain and the reaction conditions (figure 13; Cheetham, 1984; Nagai *et al.*, 1994; Veronese *et al.*, 1998; Zhang *et al.*, 2003; Wu *et al.*, 2005). Palatinose (synonym for isomaltulose) is an established commercial product. It is used as a substitute for sucrose beneficial in the treatment of diabetics and sports in food and drinks (Lina *et al.*, 2002). The structures of PalI, an isomaltulose synthase from *Klebsiella* sp. strain LX3 (Zhang *et al.*, 2003), MutB, a trehalulose synthase from *Pseudomonas mesoacidophila* MX-45 (Ravaud *et al.*, 2005; Ravaud *et al.*, 2007) and SmuA, a sucrose isomerase from *Protaminobacter rubrum* have been solved (Ravaud *et al.*, 2009). Sucrose isomerases are classified as GH 13 retaining glycoside hydrolysases according to CAZy database (Cantarel *et al.*, 2009). Other enzymes of this class are starch-acting, branching enzymes and amylase for example. They are glycosidases containing a highly conserved active site and act via a double-displacement mechanism forming a glycosyl intermediate (Davies *et al.*, 1995; Mosi *et al.*, 1997; Yoshioka *et al.*, 1997; Uitdehaag *et al.*, 1999; Jensen *et al.*, 2004). The catalytic triad of the sucrose isomerase from *P. rubrum* consists of the amino acid residues D214, E268 and E342 (Ravaud *et al.*, 2009). An aromatic clamp with impact on the hydrolysis *versus* transfructosylation activity has been described for GH 5 enzymes*, i.e*. the fungal exo-glucanase subfamily (Cutfield *et al.*, 1999) and an endocellulase (Ducros *et al.*, 1995). In the sucrose isomerase from *P. rubrum* it is formed by the amino acid residues F270 and F294 (Ravaud *et al.*, 2009).

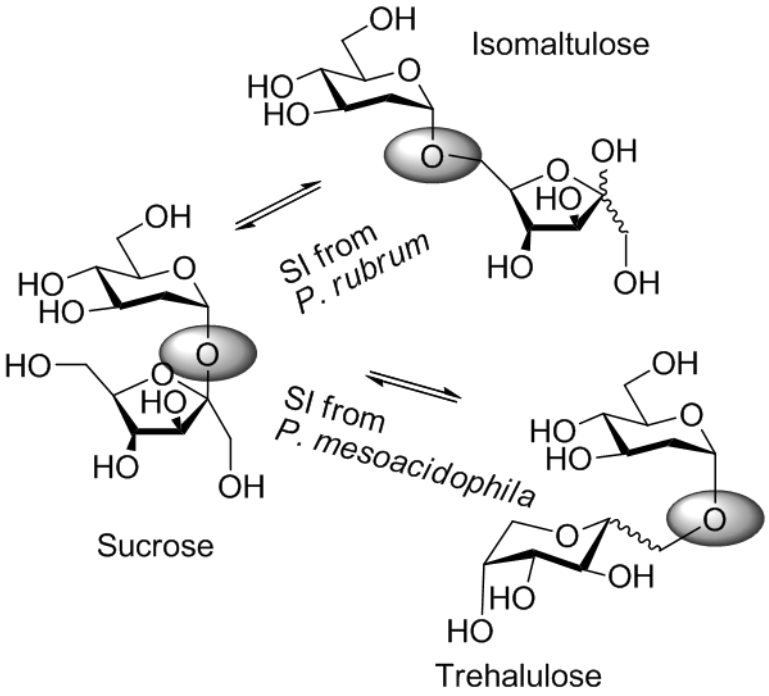

Figure 13 Sucrose isomerase (SI) activity depending on the bacterial strain. Sucrose is converted predominantly to isomaltulose (SI from *Protaminobacter rubrum*) or trehalulose (SI from *Pseudomonas mesoacidophila;* Zhang *et al.*, 2003; Ravaud *et al.*, 2006; Ravaud *et al.*, 2007).

1.10 Physiological effects of novel oligosaccharides

1.10.1 Applications of oligo- and polysaccharides

Oligo- and polysaccharides are already used frequently in many commercial products, *e.g.* cosmetics, functional food and medicine. Various polysaccharides like hyaluronan, galactan and oligofructose are used in cosmetic products. Functional food with beneficial effect for the intestinal flora includes inulin, oligofructose and isomaltose for example. The isomers of sucrose (trehalulose and isomaltulose) are sweet but non-cariogenic and metabolised without the release of glucose. The pharma industry currently investigates the bioengineering of oligosaccharides for various applications (table 1). One recent example is the synthesis of erythropoietin (Epo), a glycosylated cytokine involved in the control of the red blood cell population, with the exact human glycosylation pattern (Sinclair *et al.*, 2005; Kim *et al.*, 2008).

Table 1 Chemo-enzymatically synthesised carbohydrate structures and their possible applications.

Oligosaccharide	**Synthesis**	**(potential) Application**	**Structure**
Sucrose analogue	Donor: Sucrose Acceptor: Glycopyranosyl residue Fructosyltransferase SacB from *Bacillus subtilis* or *megaterium*	Nutrition (low caloric, non-caryogenic sweetener, prebiotic)	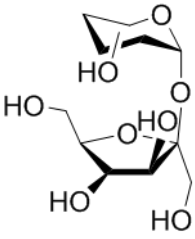
Fructo-oligosaccharides	Donor: Sucrose analogue Acceptor: Sucrose analogue β-fructofuranosidase Suc1 from *Aspergillus niger*	Nutrition (prebiotic), Pharma (immuno-stimulation)	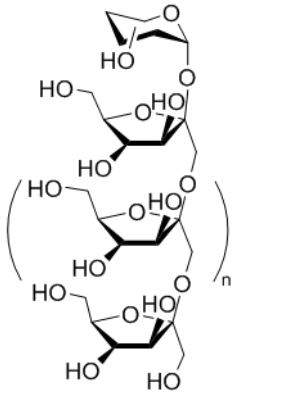 n=0 : kestose-analogue n=1 : nystose-analogue
Isomaltose	Donor: Sucrose Acceptor: Glucose *Lactobacillus reuteri* GTFR variant S628D	Nutrition (low caloric sweetener), cosmetic	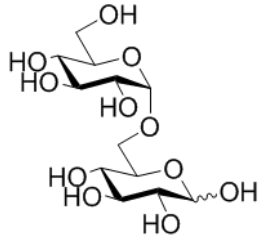
Novel α–(1,3) glucan with α–(1,6) branches	Donor: Sucrose Acceptor: Glucan *Lactobacillus reuteri* GTFR variant R624G/V630I/D717A	New material (surfactant), cosmetic	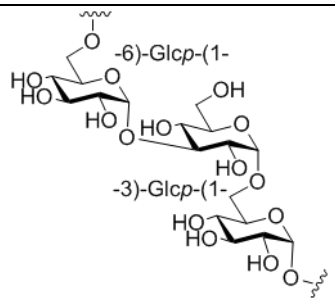

Gal-Tn analogue	Donor: UDP-Gal Acceptor: 1-allyl-2-N-acetyl-glucosamine β-(1,4) galactosyltransferase from bovine milk	Medicine (vaccine)	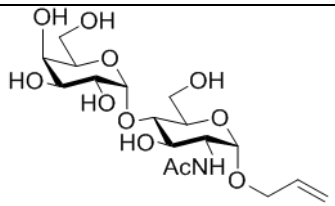
Le^X analogue	Donor: β-L-1-thio-fucose Acceptor: 1-allyl-6-*p*-toluenesulfonyl-Gal-Tn DMF, 80° C	Medicine (vaccine)	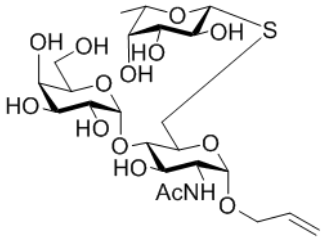

1.10.2 Carbohydrates as prebiotics

Lactobacilli and *Bifidobacteria* are known for their beneficial effects in the human intestinal tract (Yun, 1996). In functional food like cereals and yoghurt they are already applicated to humans. Their growth is stimulated by prebiotics like oligofructose and inulin which are also components of functional food. *Lactobacilli* are micro-aerophile, rod-shaped cells found in pairs or short chains (figure 14). They grow at temperatures of up to 45 °C and acidic conditions (pH 4-5). They were isolated from milk, wheat, meat and fish. In humans, they are found in the gut area. *Lactobacilli* metabolise lactose and form lactic acid in a homofermentative process. Some heterofermentative strains produce ethanol, carbon dioxide and acetic acid. *Lactobacilli* help to improve the intestinal function and prevent unwanted bacteria from growth by creating an acidic environment thus increasing their own population. In the intestinal tract, *Lactobacilli* synthesise the beneficial metabolites niacin, folic acid and pyridoxine (Schlegel, 1992).

Bifidobacteria are anaerobic intestinal rod-shaped bacteria. They metabolise carbohydrates like glucose and form acetic acid and lactic acid (Schlegel, 1992). *Bifidobacteria* like the *Lactobacilli* are considered as beneficial for the gut function and human health.

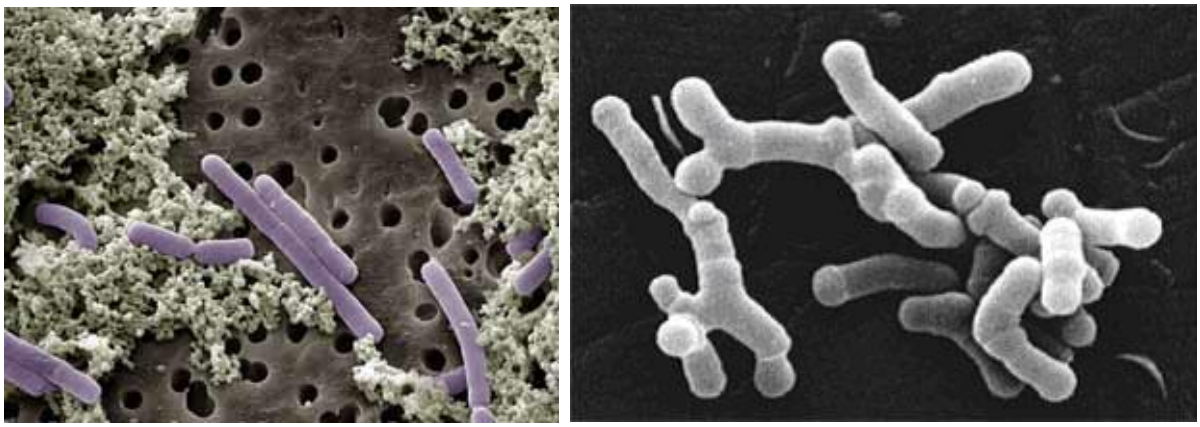

Figure 14 On the left: Rod-shaped *Lactobacilli* forming chains are shown in purple. The right picture shows *Bifidobacteria*.

1.10.3 Small proteins as immuno-stimulating agents - Characteristics of cytokines and chemokines

Inflammation processes are essential for the viability of a host organism attacked by bacteria, viruses or other pathogens. These hostile organisms carry surface agents recognised by the host as non-self. The factors which trigger cytokines and inflammation have been investigated thoroughly over the last decade but still the process is yet not fully understood. Cytokines are proteins of a small molecular weight (< 30 kDa) synthesised by T-cells, macrophages and monocytes. The molecular weight of chemokines is in the range of 8-12 kDa. Chemokines are synthesised by a broad variety of cells, not only involved in blood coagulation and hematopoeity processes as suggested previously. For a detailed characterisation of chemokines and their physiological effects see the reviews by Rollins and Springer (Springer, 1994; Rollins, 1997). Some are introduced in table 2 and figures 15 and 16. All chemokines are structurally homologue and they affect the G-protein-coupled 7-helix-type receptor (Paul, 2008). Cytokines can be triggered by lipopolysaccharides on the surface of Gram-negative bacteria (Ulevitch *et al.*, 1995; Stevens, 1997) or capsular polysaccharides and lipoteichoic acid from Gram-positive species (Standiford *et al.*, 1994; Massion *et al.*, 1995; Soell *et al.*, 1995; Miller *et al.*, 1996a; Miller *et al.*, 1996b; Yao *et al.*, 1997). Recent studies suggest a connection between auto-immune diseases and mutations in glycosyltransferase genes leading to defections in the *N*-glycosylation pattern of proteins. In mice, the knock-out of a

mannosidase (αM-II) involved in the trimming of the *N*-glycosylation patterns of glycoproteins in the Golgi yields exposed hybrid-type mannose patterns. These are recognised as non-self and act as inducers for innate immune responses under the release of cytokines and chemokines, *e.g.* MCP-1 (Green *et al.*, 2007). Another investigation of immune-stimulating effects of carbohydrate structures is the incubation of the probiotic *E. coli* strain Nissle 1917 with human epithelial colorectal adenocarcinoma (Caco-2) cells. An increase in the release of cytokines and chemokines, *e.g.* MCP-1 and IL-8, was observed. It was shown that the triggering of the cytokine and chemokine release is due to a capsular polysaccharide (K5) on the surface of *E. coli* Nissle 1917 (Hafez *et al.*, 2009).

IL-8, representing the CXC-class of chemokines, is an ubiqitious chemokine synthesised by monocytes, T lymphocytes, neutrophils, fibroblasts, endothelial cells, and epithelial cells (Rollins, 1997). Two cysteine residues form disulfide bridges at its amino-terminal end separated by one amino acid residue (CXC motif). After the induction of IL-8 expression during inflammation, IL-8 is stored for days in Weibel-Palade bodies of endothelial cells along with other proteins like the von-Willebrand factor involved in blood coagulation (Sadler, 1998; Wolff *et al.*, 1998). This is considered as a memory function of the inflammation process. Upon repeated inflammatory stimulation, IL-8 can be released from the Weibel-Palade bodies without *de novo* synthesis. Recent findings include the stimulation of IL-8 during integrin-mediated infection of HEp-2 cells by *Yersinia* (Uliczka *et al.*, 2009).
MCP-1 (monocyte chemoattractant protein 1) is a potent chemoattractor for monocytes *in vitro* (500 pmol l^{-1}). It represents the chemokine class CC because of two adjacent cysteine residues at its amino-terminal end. MCP-1 induces the expression of integrins for chemotaxis during monocyte migration processes (Jiang *et al.*, 1992; Vaddi *et al.*, 1994). T lymphocytes like CD4 are a target of MCP-1 (Carr *et al.*, 1994). MCP-1 is one factor responsible for the release of histamine by basophils (Alam *et al.*, 1992; Bischoff *et al.*, 1992; Kuna *et al.*, 1992).

Table 2 Cytokine and chemokine families and receptor types. Adapted from Callard and Gearing, Cytokine Facts Book (Callard *et al.*, 1994).

Family	**Members**	**Receptor type**
Hematopoietins (4 α-helical bundles)	IL-2, IL-3, IL-4, IL-5, Il-6, IL-7, IL-9, IL-13, G-CSF, GM-CSF, CNTF, OSM, LIF, Epo	Cytokine receptor class I
	IL-10, IFNα, IFNβ, IFNγ	Cytokine receptor class II
	M-CSF	Tyrosine kinase
EGF (β-sheet)	EGF, TGFα	Tyrosine kinase
β-trefoil	FGFα, FGFβ	Split tyrosine kinase
	IL-1α, IL-1β, IL-1Rα	IL-1 receptor
TNF (jelly roll motif, cysteine knot)	TNFα, TNFβ, LTβ	NGF receptor
	NGF	NGF receptor
	TGFβ1, TGFβ2, TGFβ3	Serine/threonine kinase
	PDGF, VEGF	Tyrosine kinase
Chemokines (triple-stranded, anti-parallel β-sheet)	IL-8, MIP-1α, MIP-1β, MIP-2, PF-4, PBP, I-309/TCA-3, MCP-1, MCP-2, MCP-3, gIP-10	Rhodopsin superfamily

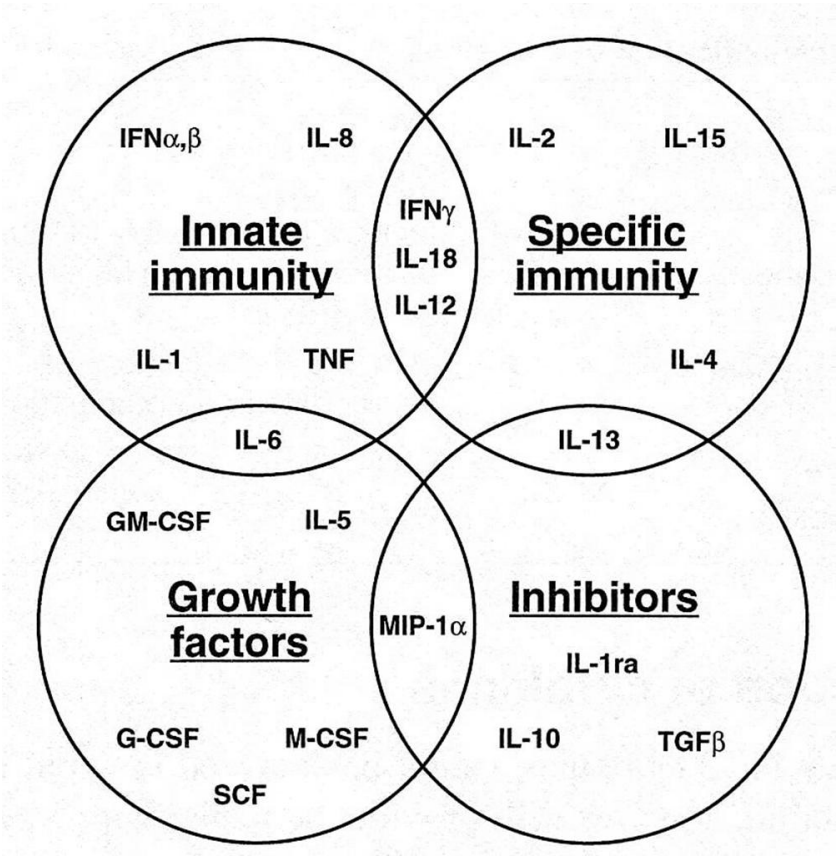

Figure 15 Functional classification of cytokines (Mantovani *et al.*, 2000).

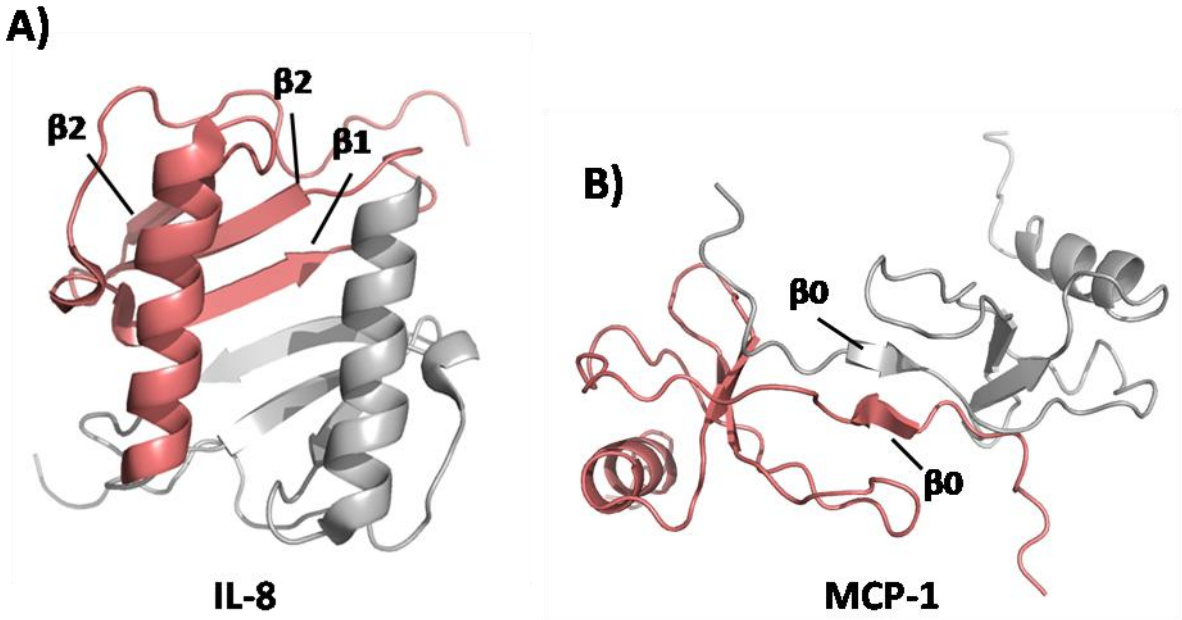

Figure 16 Dimeric structures of A) CC-class IL-8 (Clore *et al.*, 1990) and B) CXC-type MCP-1 (Handel *et al.*, 1996). The monomers are shown in grey and rosé. A) The three β-sheets of each monomer form a plane for the two parallel α-helices. B) The

two subunits interact by two β-sheets (β0) forming an elongated, cylindrical-shaped dimer.

1.11 Metabolic labelling of cell surfaces

1.11.1 Glycan target structures

The surface of eukaryotic cells is highly decorated with glycan structures of various types forming the glycocalyx (figures 17 and 18). Glycolipids and glycoproteins mediate cell-cell recognition and signal transduction processes. The highly diverse *N*-glycosylation patterns of glycoproteins are built by a surprisingly low pool of monosaccharides. The complexity of the oligosaccharides results from branches and different linkage types of the monosaccharides.

The carbohydrates derive from the periplasma or yield from various metabolic cellular processes. *N*-glycosylation occurs in the Endoplasmatic Reticulum (ER) and the Golgi. In the ER a defined glycosylation pattern is synthesised and transferred to the asparagine residue of a glycoprotein`s sequon Asn-X-Se/Thr. In the ER, the *N*-glycosylation motif acts as a protein folding sensor. Recent findings show an even enhanced fold when the glycosylation pattern is correct (Hanson *et al.*, 2009). The ER-*N*-glycosylation pattern also interacts with the calnexin/calreticulin cycle to ensure proper glycosylation and correct folding of the enzyme. In this process one glucose unit is cleft and retransferred (Totani *et al.*, 2009). After this process of enzyme quality control, the glycoproteins proceed to the Golgi where further trimming of the glycan patterns occurs. The result is a protein with a glycosylation pattern depending on the cell type, environmental conditions and development state of the cell and organism (Ungar, 2009). The terminal units of glycoproteins are often sialic acids (figure 18).

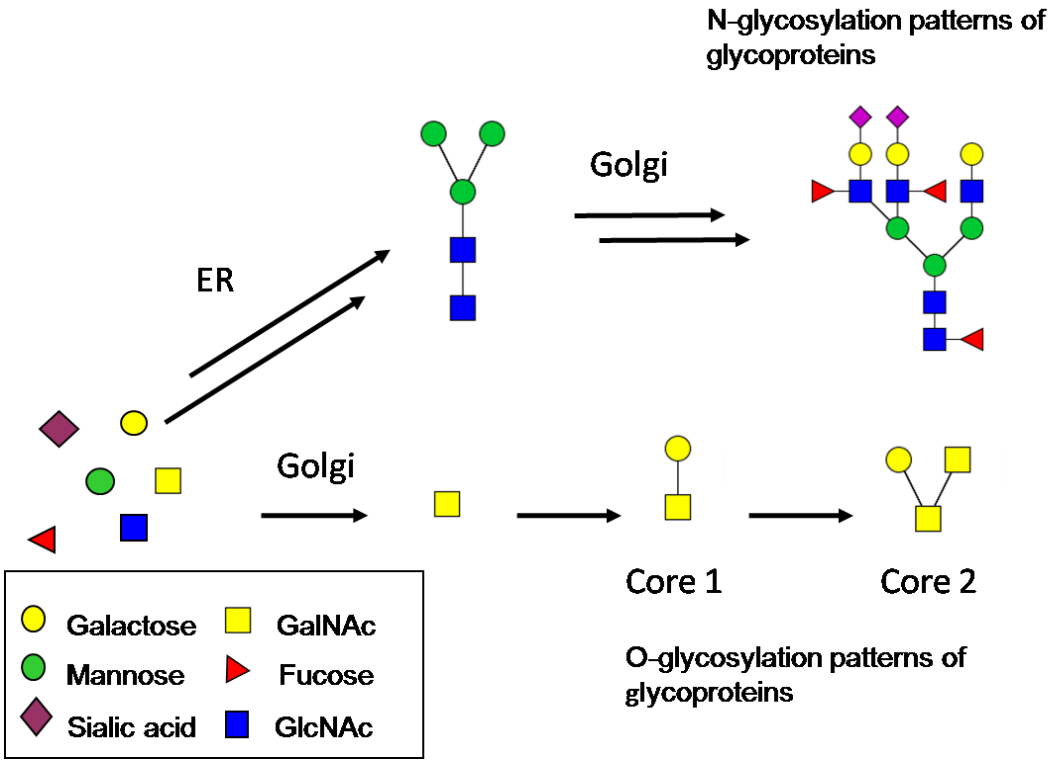

Figure 17 Examples of *N*- and *O*-glycosylation patterns of proteins.

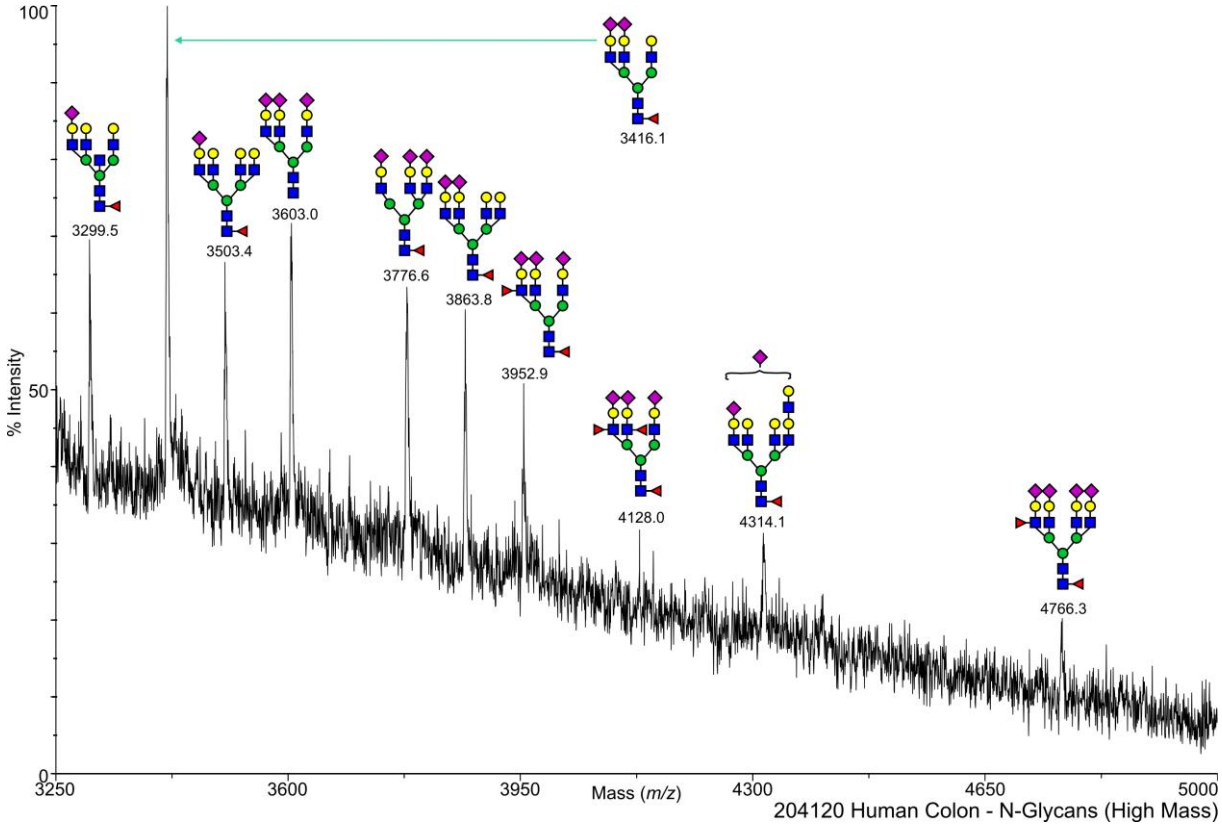

Figure 18 Glycosylation pattern of a human colon cancer cell line from the database of the consortium of functional glycomics (http://www.functionalglycomics.org). For the sign code see the figure above.

1.11.2 Metabolic labelling and engineering of the cell surfaces of eukaryotic cell lines *in vitro* and *in vivo*

Bertozzi and coworkers showed that functionalised carbohydrates can be incorporated into cells *in vitro* (Saxon *et al.*, 2002; Dube *et al.*, 2003; figure 19). This process works by active transporters and diffusion procedures depending on the modification of the carbohydrates. Acetylated sugars can easily pass the cell membrane whereas neuraminic acid derivatives carrying no acetylated hydroxyl groups enter the cell by special transporter systems (Bardor *et al.*, 2005). Acetylated monosaccharides are processed by unspecific deacetylases, activated by nucleotide transferases and metabolised by isomerases and epimerases (Prescher *et al.*, 2006; Chang *et al.*, 2007; Codelli *et al.*, 2008; Laughlin *et al.*, 2008; Chang *et al.*, 2009). These activated carbohydrate analogues are incorporated into the natural carbohydrate patterns of the cell (figure 19). Some of the modified sugars are part of

the glycosylated cell surface and therefore are accessible to chemical conversion without destruction of the cell. Depending on the modified carbohydrate added to the growth medium of the cell line or organism, *N*- or *O*-glycosylation patterns are addressed. However, the exact mechanism of incorporation remains to be investigated.

The major classes of functionalised bioorthogonal monosaccharide analogues successfully incorporated into cells are azides and alkynes (figure 19). One chemical detection method is the (1,3)-dipolar cycloaddition reaction after Sharpless and Huisgen which proofed suitable for bioorthogonal metabolic labelling (figure 20) (Kolb *et al.*, 2001; Agard *et al.*, 2004). Alternative strategies include the modification of cysteine residues of proteins and the introduction of aldehyde groups on modified substrate analogues (Prescher *et al.*, 2005; figure 21).

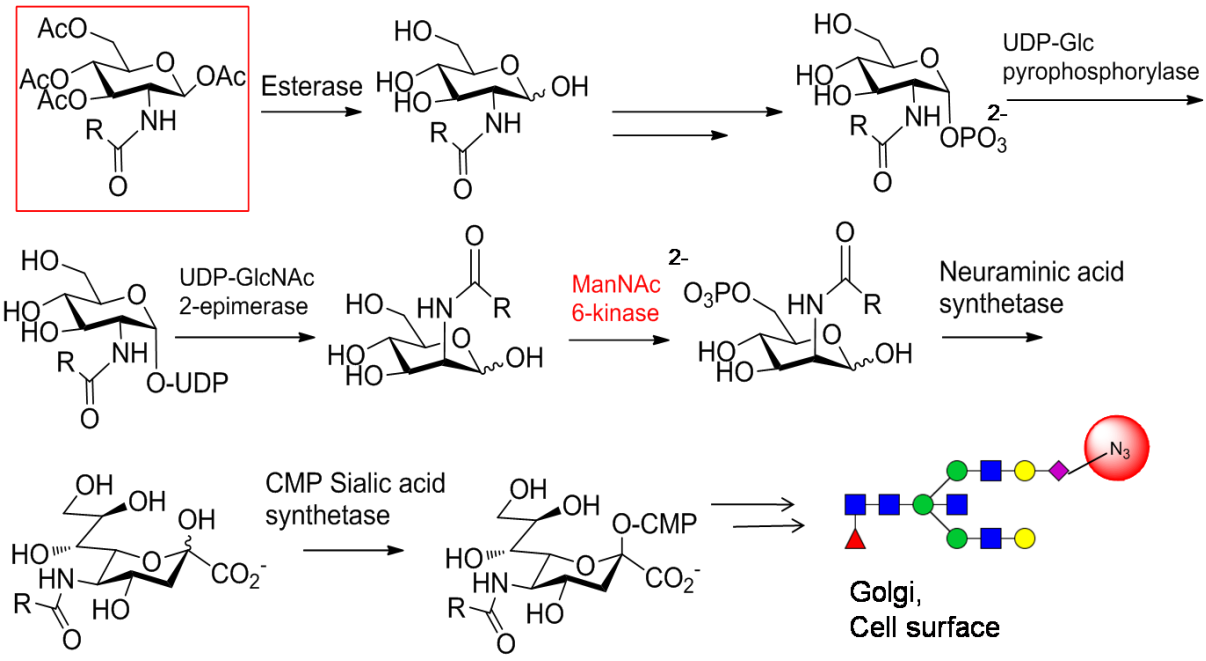

Figure 19 The biosynthesis pathway of sialic acid. Incorporation of modified AcGlcNAz and its entrance in the carbohydrate metabolic process. R is an azide or alkyne (up to hexyne) group. ManNAc-6-kinase was described as a bottleneck for sterically large functional groups in position “R” (Dube *et al.*, 2003). It was shown that it is also possible to enter the metabolic process at different stages, *e.g.* AcManNAz (Chang *et al.*, 2007) or AcGlcNAz, GlcNAz, NeuNAz and NeuNHex (this thesis) can be used for metabolic labelling.

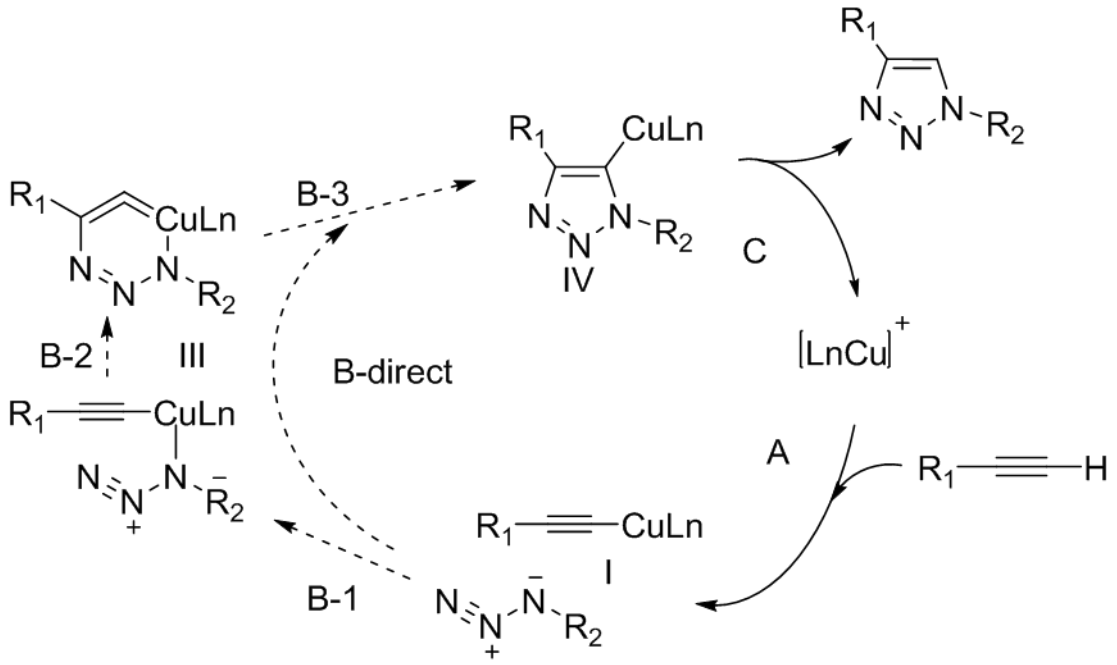

Figure 20 Reaction mechanism of the triazole formation by a (1,3)-dipolar cycloaddition (“click reaction”).

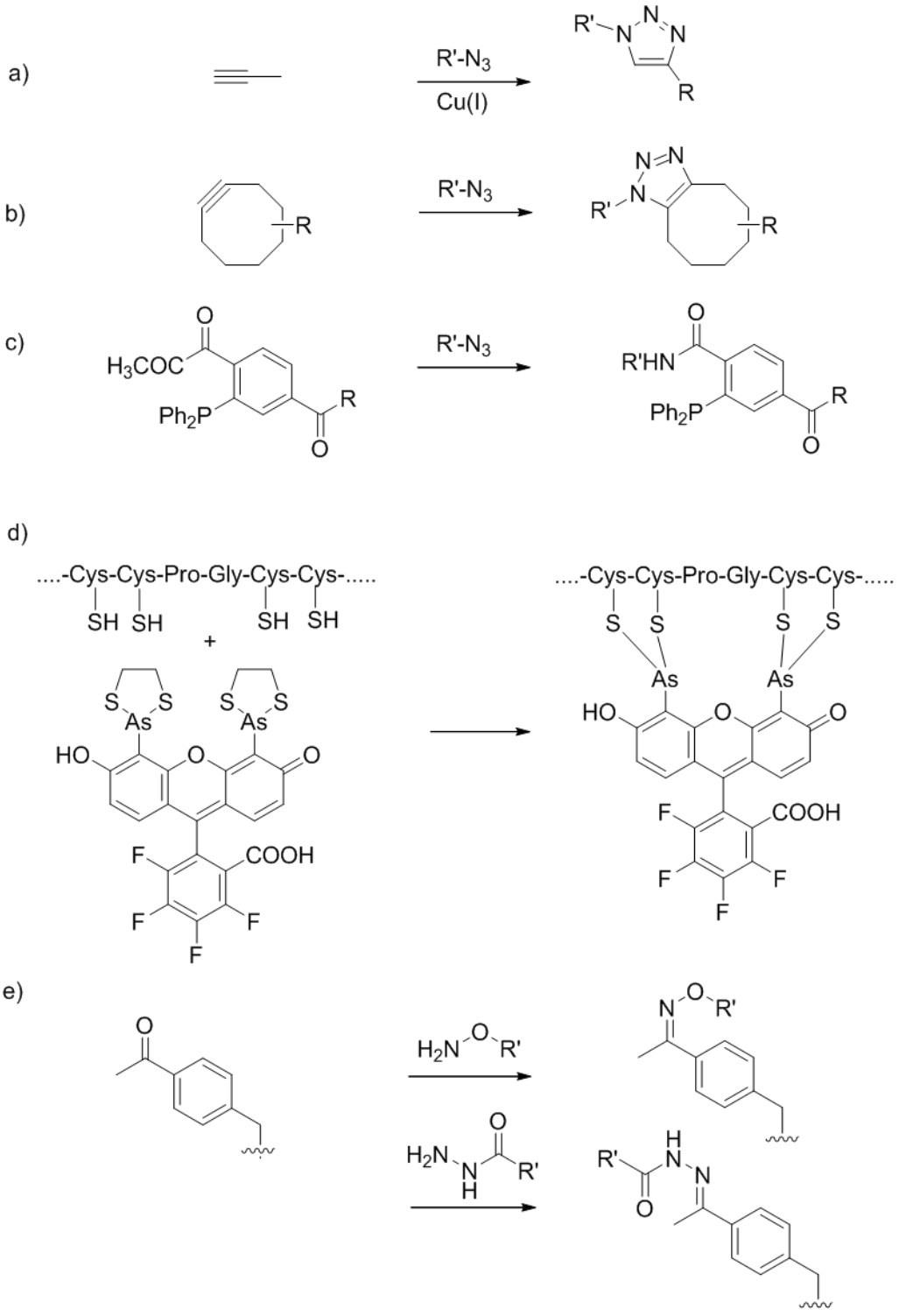

Figure 21 Possible bioorthogonal metabolic labelling reactions. a)-c) A metabolically incorporated carbohydrate analogue with an azide function (R-N_3) can be coupled to a phosphine, an alkyne activated by Cu(I) or an *in vivo* compatible strain-promoted cycloaddition (Kolb *et al.*, 2001; Baskin *et al.*, 2007). d) A genetically encoded tetracysteine motif is modified with a biarsenical labelling reagent (FlAsH-EDT2). Fluorescence is induced upon binding to recombinant proteins containing the

tetracysteine motif Cys-Cys-Pro-Gly-Cys-Cys; e) *p*-acetyl phenylalanine in response to the stop codon TAG during protein biosynthesis *in vivo*. The ketone can be derivatised with amino-derivatives, *e.g.* aminooxysaccharides (Prescher *et al.*, 2006; Sletten *et al.*, 2009).

In case of the azide-alkyne “click reaction”, Cu(I) needs a ligand for its activation which can be [Tris(benzyl-1H-1,2,3-triazol-4-yl)-methylamine] (TBTA (Ln) (step A in figure 20). The functionalised alkyne is in turn activated by the Cu(I)-Ln complex and forms an intermediate with the nitrogen bound to R2 (B-1). The now activated azide performs an attack at the C-group of the alkyne coupled to R1 forming the (1,3)-intermediate with copper as a hetero ring member (B-3). An electrophilic attac of the carbon in position 2 to R2-bound nitrogen forms the 5-membered triazole ring with ligand-activated-copper as the leaving group (C).

The eukaryotic carbohydrate metabolism can be exploited *in vivo* by functionalised monosaccharide analogues (figure 22; Baskin *et al.*, 2007). Recent approaches include the *in vivo* incorporation of azido-carbohydrates. Bertozzi and co-workers established a labelling method without the use of toxic copper by a strain-promoted cycloaddition using a fluorescence-labelled difluorinated cyclooctyne (DIFO, figure 21b (Baskin *et al.*, 2007; Laughlin *et al.*, 2008). The multi-step labelling reaction was performed in zebrafish embryos with different dyes and during different states of development in the same embryo (Laughlin *et al.*, 2008). The change in the glycosylation pattern over time shows in which glycosylation processes of the organism take place at which point of time (figure 23).

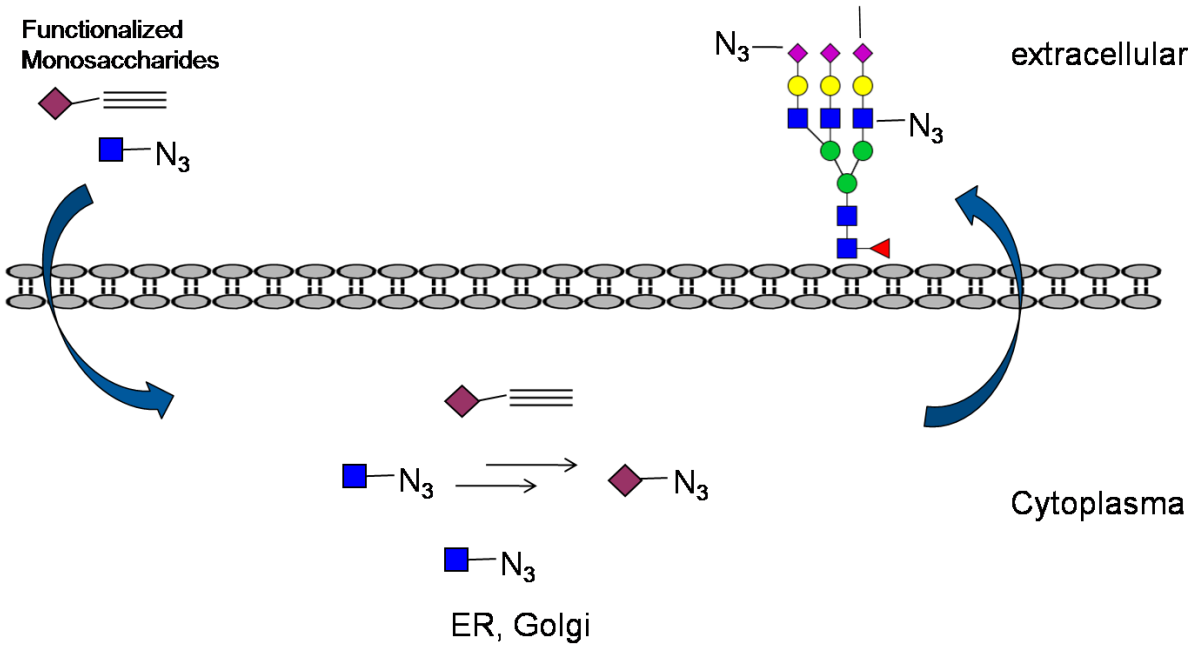

Figure 22 Metabolic labelling of cell surfaces by the incorporation of modified monosaccharides. They pass the membrane by diffusion (acetylated carbohydrates) or active transport mechanisms (Bardor *et al.*, 2005).

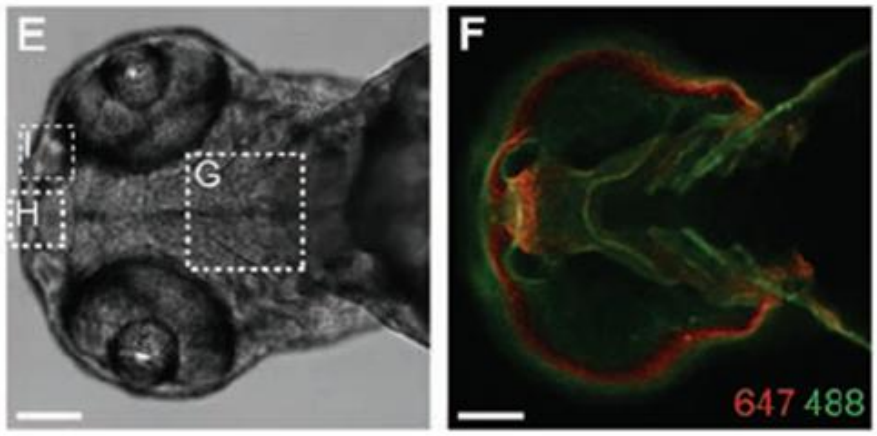

Figure 23 Adapted from Laughlin *et al.*, 2008: Identification of temporally distinct glycan populations during zebrafish development using two colour labelling. Zebrafish embryos metabolically labelled with Ac4GalNAz from 3 to 60 h were reacted with DIFO-647 between 60 and 61 hours and then reacted with DIFO-488 between 62 and 63 hours. E) Brightfield image of a ventral view of an embryo at 63 hours. F) Single z-plane fluorescence image of E) displaying intense DIFO-488 fluorescence but not DIFO-647 fluorescence. Scale bars are 100 mm.

As a further example of cell surface functionality, the cell surface functionalised with azido-carbohydrates was modified with phosphine-labelled single-stranded (ss) DNA (figure 24) (Chandra *et al.*, 2006). By the application of defined oligonucleotides the labelled surface is specifically identified by fluorescence-labelled complementary DNA or other complementary DNA-labelled cells of the same type or another (figures 25 and 26). In this way interactions can be studied that happen *in vivo* or do not occur naturally (Gartner *et al.*, 2009). In one experiment, Jurkat cells were labelled with a fluorescent agent and assembled with cells containing the complementary ssDNA on their surface (figure 25). In another approach, different cell types which were labelled with different fluorescent molecules. First, the two populations were sorted by FACS and subsequently incubated with a third population which was not fluorescent but labelled with complementary DNA. The result is an assembly of the three cell types (figure 26).

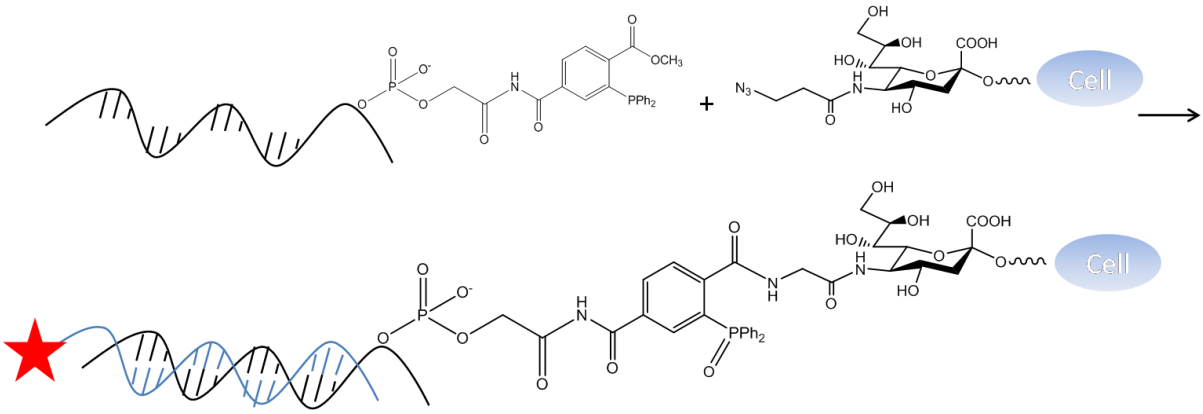

Figure 24 DNA-based cell-cell assembly. The red star label indicates a fluorescent marker or another cell.

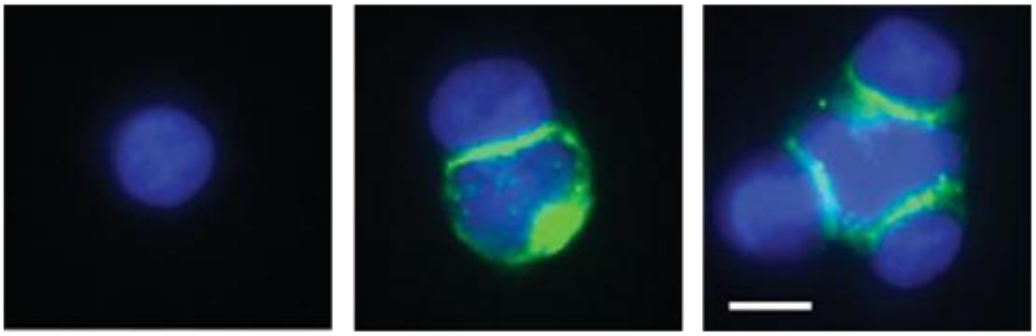

Figure 25 Adapted from Gartner *et al.*, 2009: Jurkat cells labelled with fluorescein-conjugated DNA (single cell, left panel) were assembled with cells bearing a non-fluorescent complementary strand (middle and right panel). Scale bar is 10 µm.

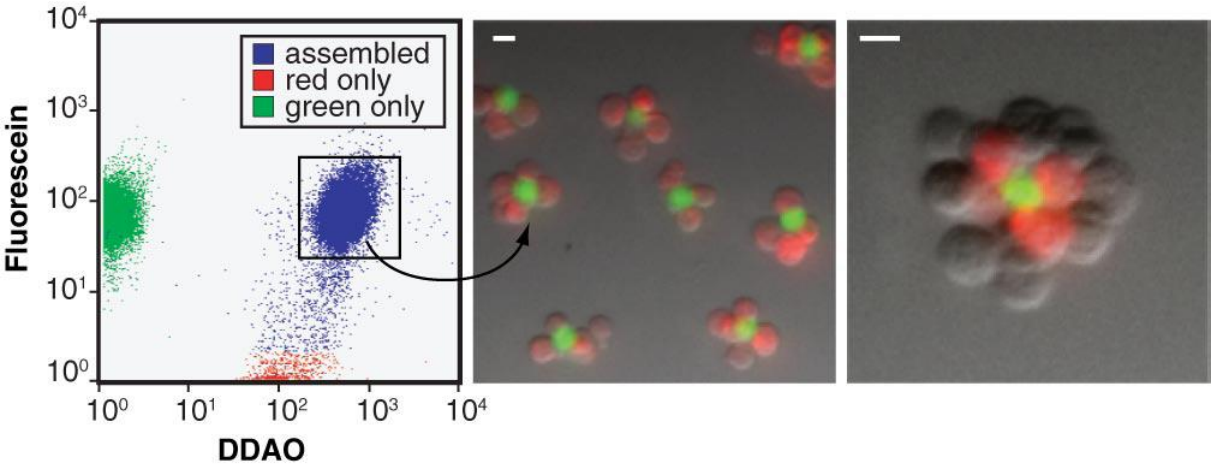

Figure 26 Adapted from Gartner *et al.*, 2009: Fluorescence-activated cell-sorting (FACS) separates cell assemblies based on their fluorescence properties. On the left picture Jurkat cell-based structures were isolated by FACS based on red and green fluorescence proportional to the number of each cell type in the cluster. Middle and right picture: Higher-order multicellular structure generated by incubation of the labelled cells with a third population of unstained Jurkat cells bearing cell surface oligonucleotides complementary to those on the red-stained cells. Red, Texas Red; green, fluorescein; scale bars, 10 µm.

1.12 Oligosaccharides as potential vaccines

During the recent years there is a growing attention towards carbohydrate-based vaccines for infection and cancer therapies. Oligosaccharides and glycoconjugates like proteoglycans and glycolipids were synthesised and tested *in vitro* and *in vivo* with promising results. However, the major breakthrough has not been achieved yet. Carbohydrates alone mostly do not evoke a full immune answer. The task is to find the right combination regarding the aglycon and the structural presentation of the glycans. In this chapter some examples will be presented which are steps to future carbohydrate-based vaccination strategies.

Bacteria forming biofilms play a role in a wide variety of human infection processes (Potera, 1999; Donlan *et al.*, 2002). Polysaccharide-promoted intercellular adhesion processes are known to evoke immunogenic responses in mice (McKenney *et al.*, 1999; Maira-Litran *et al.*, 2002). Anticancer vaccines were developed by a couple of working groups over the recent years (Dziadek *et al.*, 2004; Buskas *et al.*, 2005; Ingale *et al.*, 2007; Wittrock *et al.*, 2007; Westerlind *et al.*, 2008). Some polysaccharides show relatively high affinities for special cell types. Heparin for example has a 100-fold increase in affinity towards apoptotic cells (Gebska *et al.*, 2002).

Also vaccine approaches gave first promising results. The carbohydrate moiety is linked to an immunogenic protein like bovine serum albumine (BSA) or keyhole limetic hemocyanine (KLH). A concerted immune answer with immuno-globulin (Ig) G-release is the consequence when mice are vaccinated. But the cumulative stimulation of the innate and acquired immune system was successful in more cases. The carbohydrate units were coupled to T- and B-cell oligopeptide epitopes. Furthermore, different classes of cancer cell oligosaccharide patterns were coupled to the peptide. A globotriaosyl (Gb3) ceramide mimick and a mucin-type MUC5A-motif were alternatingly linked to a B- and T-cell oligopeptide epitope (Zhu *et al.*, 2009; figure 27). The introduction of multivalent carbohydrate-protein constructs enhanced the immunogenicity of the vaccine.

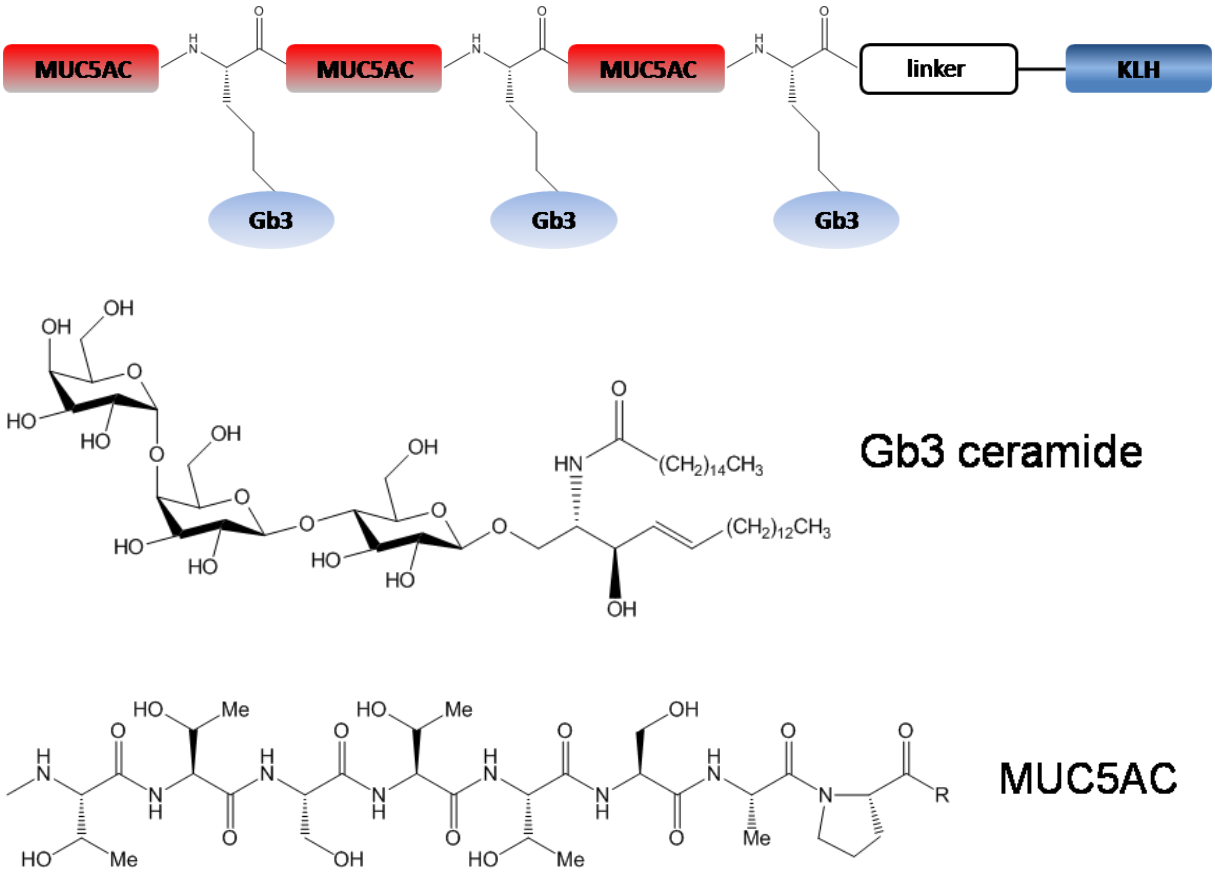

Figure 27 Second generation carbohydrate-based anti-cancer vaccine with remarkable immuno-stimulating activity (Zhu *et al.*, 2009).

2 Aim of this work

This thesis on the crossroads of biology and chemistry aims at the combination of chemical and enzymatic methods for the synthesis of defined natural carbohydrate oligosaccharides, their analogues and their chemical functionalisation. These target structures may interact with proteins during infections, inflammation and other cell signalling and cell-cell interaction processes.

The aim is the chemo-enzymatic synthesis of tailor-made oligosaccharides. Difficulties are their chemical similarity and laborious chemical synthesis. Therefore the chemical synthesis shall be supported and broadened by enzymatic glycosylation methods in order to expand the library of accessible oligosaccharide structures.

The first aim was the identification of novel glycosyltransferases. A novel fructosyltransferase SacB from *Bacillus megaterium* was identified in the group of Dieter Jahn (TU Braunschweig). Another fructosyltransferase (Suc1) from *Aspergillus niger* was identified in the group of Petra Dersch (Helmholtz-Centre for Infection Research and TU Braunschweig). The biochemical characterisation, cloning, expression, purification and crystallisation were performed in cooperation with the two mentioned groups from the Department of Microbiology at the TU Braunschweig and with the groups of Dirk Heinz from the Helmholtz-Centre for Infection Research. These studies shall be the basis for rational design approaches in order to create enzyme variants with altered product spectra. The biochemical characterisation includes the determination of the temperature- and pH optima, the kinetic parameters after Michaelis and Menten (K_m, k_{cat}) and the determination and analysis of the oligo- and polysaccharide product spectra. They shall be analysed by thin layer chromatography (TLC), high-performance anion-exchange chromatography (HPAEC), mass spectroscopy (MS) and nuclear magnetic resonance (NMR) spectroscopy.

Besides enzyme engineering, substrate engineering shall expand the diversity of carbohydrates to be synthesised. The established synthesis of sucrose analogues by the fructosyltransferase SacB from *Bacillus subtilis* shall be expanded to the fructosytransferase SacB from *Bacillus megaterium*. The fructosyltransferases SacB from *B. megaterium* and Suc1 from *Aspergillus niger* which synthesis natively short-

chain fructo-oligosaccharides shall be characterised biochemically. They are going to be expressed heterologously in *E. coli* in case of SacB or expressed homologously in a genetically engineered *A. niger* (Suc1). They shall be purified and, as Suc1 is a heavily glycosylated protein, the effects of the glycosylation pattern on the activity and product formation of Suc1 is going to be investigated. Novel oligofructosides shall be synthesised by a combined action of these two fructosyltransferases. The products shall be characterised regarding their prebiotic and immuno-stimulating properties using *Lactobacilli* and *Bifidobacteria* and human epithelial colorectal adenocarcinoma (Caco-2) cells, respectively. An eventual growth of the beneficial gut bacteria indicates prebiotic activity. Four different strains of *Lactobacilli* (*Lb. fructosus, Lb. plantarum, Lb. fermentum* and *Lb. delbrueckii*) and *Bifidobacterium lactis* are going to be investigated concerning the ability to metabolise fructo-oligosaccharides. Their growth rate on fructo-oligosaccharides of different chain length in a semi-defined medium with addition of the carbon source to be investigated shall be examined and compared. The immuno-stimulating ability of fructo-oligosaccharides shall be investigated by characterising the cytokine release of Caco-2 cells incubated in the presence of the novel oligofructosides.

Another issue of this thesis is the control of the carbohydrate linkage type. The chemical control is difficult because of the chemical similarity of the carbohydrate hydroxyl groups. The isomerisation possibilities of novel sucrose analogues synthesised by the fructosyltransferase SacB from *B. megaterium* shall be investigated. Sucrose isomerases are known to form isomaltulose and/or trehalulose from sucrose. The sucrose isomerase SmuA from *Protaminobacter rubrum*, a mainly isomaltulose-forming enzyme, shall be investigated regarding its substrate promiscuity. Thus, the linkage type of our newly synthesised sucrose analogues shall be controlled as a further step towards tailor-made oligosaccharides.

The last point of the thesis is the labelling of cell surfaces by functionalised carbohydrates. In cooperation with the group of Petra Dersch from the TU Braunschweig and the Helmholtz-Centre for Infection Research, the incorporation of chemically modified carbohydrates into the cell metabolism shall be investigated. These functionalised carbohydrates shall lead to modified cell surfaces containing glycoproteins with chemical tags. This tag has to fullfill restrictive characteristics. It has to be accessible for chemical modification, the chemical labelling reaction shall

be ideally non-toxic in order to take place *in vivo* and the tag has to be metabollically inert which is referred to as biological orthogonality. The azide-alkyne click-chemistry reaction shall be investigated if it is suitable for this purpose. The labelling reaction shall be performed with a fluorescent agent. It shall be investigated which conditions are suitable for the *in vivo* labelling. Different functionalised monosaccharides and different modified fluorescent agents are going to be examined in labelling human larynx carcinoma (HEp-2) and hamster ovary carcinoma (CHO) cells.

3 Materials and Methods

3.1 Instruments

Instrument	Type	Company
Autoclave	Westima	Sauter
Centrifuge, cooled	J2 21	Beckman
Rotor	JA-10, JS-13	Beckman
Clean bench	Heraeus LaminAir	Heraeus
Electrophoresis device	Power-phor-N	anamed
Fast Protein Liquid Chromatography (FPLC) device		
Pump	LKB Pump P-500	Pharmacia
Controller	Liquid Chromatography Controller LCC-500 Plus	Pharmacia
Detector	Biotech UV-MII	Pharmacia
Fraction collector	LKB Frac-100	Pharmacia
Column for SacB purification	CM-Sepharose	GE Healthcare
Column for Suc1 purification	Superdex 200	GE Healthcare
High-Performance Anion Exchange Liquid Chromatography (HPAEC) device		
Basic chromatography module	CHB	Dionex

Gradient pump	GPM-2	Dionex
Pre-column	CarboPac PA1 , 4*50 mm	Dionex
Main column	CarboPac PA1, 4*250 m	Dionex
Pulsed amperometric detector	PAD-2	Dionex
Autosampler	series 200 with tefzel valve	Perkin Elmer Rheodyne
Thermostate	Thermomix BU	Braun
Luminex system	Luminex 200	Luminex
MALDI-TOF Mass Spectrometry	Ultraflex	Bruker Daltonics
NMR		Bruker
Photometer	ultrospec 200	GE Healthcare
Sonotrode	MS72	Bandelin
Spektrophotometer	NanoDrop Spectrophotometer ND-100	peqLab Biotechnology
Thermoshaker:		GFL
Ultra pure water device	MilliQ	Millipore

3.2 Chemicals, media and solutions

All chemicals, media and biological kits were ordered at Roth, NEB, Sigma-Aldrich, Merck, Carbosynth, Glycon, Invitrogen or Bio-Rad.

3.2.1 Media for the cultivation of bacterial cells

3.2.1.1 Medium after Luria-Bertani (LB-medium)

Peptone	10 g l^{-1}
Yeast extract	5 g l^{-1}
NaCl	5 g l^{-1}

The medium was autoclaved for 20 min at 120 °C and 1 bar of overpressure. The antibiotics were sterilised by filtration.

3.2.1.2 LB-Medium supplements

Agar	15 g l^{-1}
Ampicillin	0.5 mM
IPTG	0.5 mM

The media containing antibiotics was cooled down to lower than 60 °C prior to antibiotic addition.

3.2.1.3 Medium after de Man, Rogosa and Sharp (MRS)

Universal peptone	10.0 g l^{-1}
Meat extract	5.0 g l^{-1}
Yeast extract	5.0 g l^{-1}
D(+)-Glucose	20.0 g l^{-1}
Dipotassium hydrogen phosphate	2.0 g l^{-1}
Diammonium hydrogen citrate	2.0 g l^{-1}
Sodium acetate	5.0 g l^{-1}
Magnesium sulfate	0.1 g l^{-1}
Manganous sulfate	0.05 g l^{-1}
optional: agar	12.0 g l^{-1}

3.2.1.4 Semi-defined medium after Vogel (Korakli *et al.*, 2003)

NH_4Cl	2 g l^{-1}
Na acetate	5 g l^{-1}
$MnSO_4$	0.05 g l^{-1}
K_2HPO_4	2 g l^{-1}
Yeast Nitrogen Base (Difco)	5 g l^{-1}
Bacto Pepton (Difco)	10 g l^{-1}
addition of the appropriate C-source	

3.2.2 Media for the cultivation of eukaryotic cells

3.2.2.1 Medium for the cultivation of Caco-2 and CHO-K1

RPMI-1640, Biochrom

add 7.5 % newborn calf serum (Invitrogen)

3.2.2.2 Medium for the cultivation of HEp-2

DMEM/Ham`s F12 (1:1), Biochrom

add 10 % fetal calf serum (Invitrogen)

optional: ampicillin 0.5 mM

3.2.3 Phosphate buffer after Sörensen

	pH 5.0	**pH 5.6**	**pH 6.0**	**pH 6.6**	**pH 7.0**	**pH 7.6**	**pH 8.0**
KH_2PO_4 (% v/v)	99.2	95.5	88.9	65.3	41.3	12.8	3.7
Na_2HPO_4 (% v/v)	0.8	4.5	11.1	34.7	58.7	87.2	96.3

3.2.4 Sodiumdodecylsulfate-polyacrylamide gel electrophoresis (SDS-PAGE)

Loading buffer

Roti-Load, Roth

10x denaturing Tris/Glycine buffer

Tris	30.0 g l^{-1}
SDS	30.0 g l^{-1}
Glycin	144.0 g l^{-1}

in water.

Fixing solution

Trichloroaceticacid 20 % (w/v)

in water

Staining solution

Solution A

Coomassie Blue 0,2 % (w/v)

in methanol

Solution B

Acetic acid 20 % (v/v)

→ Mix A and B in a ratio of 1:1.

Decolouration solution

Acetic acid	10 % (v/v)
Methanol	20 % (v/v)

in water

Prestained Protein Marker, Broad Range, New England Biolabs

175.0	kDa	MBP-ß-Galactosidase
83.0	kDa	MBP-Paramyosin
62.0	kDa	Glutarsäure Dehydrogenase
47.5	kDa	Aldolase
32.5	kDa	Triosephosphat-Isomerase
25.0	kDa	ß-Lactoglobulin A
16.5	kDa	Lysozym
6.5	kDa	Aprotinin

3.2.5 Carbohydrate analysis by thin layer chromatography (TLC)

Mobile phase

Ethylacetate	60 % (v/v)
Isopropanol	30 % (v/v)
Water	10 % (v/v)

Developing solution

Sulfuric acid	5 % (v/v)
N-N	0.3 % (w/v)
in methanol	

Carbohydrate standard

Glucose	0.1 g l^{-1}
Fructose	0.1 g l^{-1}
Sucrose	0.1 g l^{-1}
1-Kestose	0.1 g l^{-1}
1-Nystose	0.1 g l^{-1}

3.2.6 Carbohydrate analysis by high-performance anion-exchange chromatography (HPAEC)

Mobile phase

NaOH (solution)	0.1 mol l^{-1}

Elution phase

NaOH (solution)	0.1 mol l^{-1}
Sodium acetate	82.0 g l^{-1}

Carbohydrate standard

Glucose	0.1 g l^{-1}
Fructose	0.1 g l^{-1}
Sucrose	0.1 g l^{-1}
1-Kestose	0.1 g l^{-1}
1-Nystose	0.1 g l^{-1}

3.2.7 Metabolic labelling of cell surfaces

Solution for the click reaction

$CuSO_4$	2 mM
Sodium ascorbate	10 mM
TBTA	2 mM

in DMSO

add 2 mM of the labelling molecule (alkynylated tetramethylrhodamine (TAMRA), azido- or alkynylated fluorescein).

3.3 Bacterial strains

Strain	Characteristics	Source
Escherichia coli		
DH10β	ΔlacX74, deoR, recA1, endA1, araD139, Δ(ara, leu)7697, galU, galK λ^- rpsL, nupG	Gibco Life Technologies
BL21(DE3)	F^- dcm ompT hsdS (rB^- mB^-) gal λ(DE3)	Stratagene
Bacillus megaterium		
DSM319	wild-type	DSMZ
Protaminobacter rubrum		
Industrial strain from Südzucker	alginate-immobilised cells	Südzucker

3.4 Bacterial plasmids

Plasmids	Characteristics	Source
pET11d	Expression vector, T7/lac-promoter, amp^r	Novagen
pRBEc1	amp^r, *sacB* from *B. megaterium* without signal sequence in pET11d cloned by *Bam*HI and *Nco*I.	Department of Microbiology, TU Braunschweig

3.5 Eukaryotic strains

Strain	Characteristics	Source
Aspergillus niger AB 1.13	*pyrG*$^{-}$, *amp*^{r},	Department of Microbiology, TU Braunschweig
Aspergillus niger SKANIp8	control, empty plasmid	Department of Microbiology, TU Braunschweig
Aspergillus niger pSKAn1015	*suc1*$^{+}$, *pyrG*$^{-}$, *amp*^{r}	Department of Microbiology, TU Braunschweig
HEp-2	human larynx carcinoma cell line	Department of Microbiology, TU Braunschweig
Caco-2	human epithelial colorectal adenocarcinoma cell line	Department of Microbiology, TU Braunschweig
CHO-K1	chinese hamster ovary cell line	Rothkegel group, Department of Zoology, TU Braunschweig

3.6 Eukaryotic plasmids

Plasmid	Characteristics	Source
ANIp8	*pyrG*$^{+}$, *pkiA*, *amp*^{r}	Novagen

3.7 Methods

3.7.1 Methods of molecular biology

The basic methods of molecular biology are performed as described previously (Sambrook *et al.*, 1999). The studies of the fructosyltransferase SacB from *B. megaterium* were performed in cooperation with Rebekka Biedendieck and Martin Gamer from the group of Dieter Jahn (TU Braunschweig, Department of Microbiology) and Christian Strube from the group of Dirk Heinz (Helmholtz-Centre for Infection research). The studies of the fructosyltransferase Suc1 from *A. niger* were performed in cooperation with Andreas Roth from the group of Petra Dersch (Department of Microbiology, TU Braunschweig and Helmholtz-Centre for Infection research).

3.7.2 Heterologous protein expression of the fructosyltransferase SacB from *B. megaterium* and its variants in *Escherichia coli* BL21(DE3)

A novel fructosyltransferase from *Bacillus megaterium* was identified by Rebekka Biedendieck from the group of Dieter Jahn (Department of Microbiology, TU Braunschweig). This protein shall be heterologously expressed in *E. coli*. For cloning and cultivation, *E. coli* cells carrying the corresponding plasmid were grown in Luria–Bertani (LB) medium supplemented with 0.5 mM ampicillin at 37 °C in shaking flasks. Recombinant gene expression was induced with 0.5 mM IPTG after 3 hours and the temperature was lowered to 26 °C for 20 h.

3.7.3 Disruption of SacB-overexpressing *Escherichia coli* BL21(DE3) cells

The medium was centrifuged (10 min, 8000 rpm at 4 °C) and the supernatant was discarded. The cell pellet was dissolved in 25 ml of phosphate buffer after Sörensen (50mM, pH 6). After another centrifuge step at the same conditions, the pellet was

resuspended in 6.25 ml of Sörensen`s buffer. The cells were disrupted by sonication (50 % time, 70 % power) at 4 °C for 4 min.The cell extract was stored at -20 °C:

3.7.4 Purification of the fructosyltransferase SacB from *Bacillus megaterium*

The overexpressed fructosyltransferase SacB was purified by FPLC. The protein separation was performed by a CM-Sepharose column and monitored by a UV detector. The cell extract was centrifuged at 10,000 rpm for 5 min. The loading of the column with the crude cell extract was performed with a volume of 2.5 ml at a flow rate of 0.5 ml min^{-1}. The through-flow was collected. After the loading a straight baseline was achieved. Subsequently the elution program was started. The elution of SacB was performed at a flow rate of 1 ml min^{-1}. Fractions of 2 ml were collected. The elution process was monitored by the software Clarity (Ver. 2.4.1.77, Data Apex). The column was regenerated by the FPLC regeneration program.

Table 3 FPLC program

0 - 5 min		0 % buffer Sörensen, pH 6.6, 1 M
5 - 125 min	to	60 % buffer Sörensen, pH 6.6, 1 M
125 - 165 min	to	100 % buffer Sörensen, pH 6.6, 1 M
165 - 180 min		100 % buffer Sörensen, pH 6.6, 1 M

Table 4 FPLC regeneration program

30 min	100% buffer Sörensen, pH 6.6, 1 M
30 min	0% buffer Sörensen, pH 6.6, 1 M

3.7.5 Dialysis of the purified SacB from *Bacillus megaterium*

The fractions are desalted by dialysis. At high salt concentrations there is a decrease in protein solubility and some protein denaturing effects. Via dialysis a diffusion of the salt through a semi-permeable membrane occurs. The pore size of the membrane is crucial for the size of the molecules which are able to permeate.

For the dialysis of the purified protein fractions, a dialysis tube (Visking Dialysis tubing 27/32, mass weight cut off (MWCO) 12-14,000 Da, Serva) with a variable volume was used. It was filled with the FPLC fractions containing pure SacB and dialysed at 4 °C for 1 h in 1 l of phosphate buffer after Sörensen (50 mM, pH 6.6). Subsequently the tube was transferred into 3 l of buffer (same composition as above) and dialysed over night. To support the diffusion the buffer is stirred slowly (appr. 50 rpm).

3.7.6 Protein analysis via sodiumdodecylsulfat-polyacrylamide gel electrophoresis (SDS-PAGE)

By electrophoresis, proteins are seperated by their molecular weight. The proteins are denatured by β-mercaptoethanol and at the same time negatively charged. When a potential is applied they migrate through the polyacrylamide to the anode.

The probe was mixed in a ratio of 1:4 with the loading buffer (Roth) and incubated at 95 °C for 5 min. For the analysis commercially available gels were used (ProGel-Tris-Glycin-Gel, 10 %, anamed) with the appropriate electrophoresis conditions. The staining was performed according to the coomassie staining protocol.

Table 5 Elektrophoresis program

Collection step	80 V	30 mA3W	15 min
Seperation step 1	120 V	40 mA5W	45 min
Seperation step 2	150 V	50 mA10W	5 min

Table 6 Coomassie-staining protocol

Fixing solution	30 min
Staining solution	60 min
Decolouring solution	15 min
Decolouring solution	over night

3.7.7 Determination of protein concentrations

The determination of the SacB concentration in the dialysed FPLC product was performed via spectral photometry at 280 nm (NanoDrop 3300, Thermo Scientific). The spectral characteristics were converted into protein concentration considering a correction factor for SacB.

$$c_{FTF} = c \cdot 0{,}62 \qquad [3.1]$$

c_{FTF} = Concentration of the fructosyltransferase SacB in solution

c = measured protein concentration

1 µl of protein solution was pipetted onto the analysis device.

3.7.8 Determination of the activity of the purified Suc1 from *Aspergillus niger*

The Suc1 activity after FPLC purification was determined by TLC. 500 mM sucrose solution in Sörensen`s buffer, 50 mM, pH 5.6, was mixed with 10 µl of each FPLC fraction. After 3 h, 3 µl of the reaction mixture was analysed by TLC.

3.7.9 Purification of the fructosyltransferase Suc1 from *Aspergillus niger*

The fructosyltransferase Suc1 was purified by fast protein liquid chromatography (FPLC) using a Sephadex 200 (Invitrogen) column. In this column material, proteins of high molecular weight migrate faster than small proteins. 100 µl of crude supernatant of an *A. niger* SKAn1015 cultivation was applied. The mobile phase was phosphate buffer after Sörensen, 50 mM, pH 5.6 without a gradient. The FPLC process was monitored by the software Clarity (Ver. 2.4.1.77, Data Apex).

3.7.10 Deglycosylation of the purified Suc1 from *Aspergillus niger*

The purified fructosyltransferase Suc1 from *A. niger* was deglycosylated by the action of the glycosidase PNGaseF (New England Biolabs). The deglycosylation process was performed with the native and the denatured Suc1. The denaturation of the enzyme was performed by heating of the purified Suc1 for 10 min at 95 °C. The deglycosylation procedure was performed according to the instructions of the manufacturer (Sigma).

3.7.11 Determination of the activity of the purified deglycosylated Suc1 from *Aspergillus niger*

The Suc1 activity after the deglycosylation process was determined by TLC. 500 mM sucrose solution in Sörensen`s buffer, 50 mM, pH 5.6, was mixed with 10 µl of either the native deglycosylated or the denatured deglycosylated purified Suc1. The

reaction was performed at 37 °C and 200 rpm. After 3 h, 3 µl of the reaction mixture was analysed by TLC.

3.7.12 Qualitative carbohydrate analysis via thin layer chromatography (TLC)

By TLC the qualitative carbohydrate analysis was applied to get an overview of the enzyme activity and the resulting products. The sample to analyse was diluted to a total carbohydrate concentration of 1 - 3 g l^{-1}. 3 µl of the sample was applied on a TLC plate (TLC aluminium foil coated with silica 60, 20 x 20 cm with concentration zone, Merck). After drying the TLC was run in a TLC chamber equilibrated with the mobile phase. After 45 min the plate was dried and again incubated for 45 min. The staining of the carbohydrates was performed by a short dive into the developing solution and incubation at 150 °C for 5 min. An appropriate standard has to be applied each time.

3.7.13 Analysis of carbohydrates by high-performance anion-exchange chromatography (HPAEC)

HPAEC analysis was used to determine the kinetic parameters of the enzyme reactions and the optimal reaction conditions. The HPAEC is a modular high-performance liquid chromatography (HPLC) optimised for the analysis of carbohydrates. The pre-column (CarboPac PA1, 4*50 mm, Dionex) and the following seperation column (CarboPac PA1 4*250 mm, Dionex)) of the HPAEC device separate the analytes by anion-exchange and a gradient of the eluent. The samples were applied by an autosampler (Perkin Elmer). A degaser unit was used for removing oxygen and carbon dioxide from the mobile phase (sodium hydroxide, 100 mM in MilliQ water) and the eluent (sodium hydroxide, 100 mM and sodium acetate, 1 M in MilliQ water). A thermostat ensured a stable temperature of 15 °C. The flow rate was 1 ml min^{-1}. The total carbohydrate concentration has to be set to 100 – 200 mg l^{-1} correlating with the used detector sensitivity of “1k”. The chromatograms were recorded with the Clarity software (Ver. 2.4.1.77, DataApex).

Table 7 HPAEC program

0 - 5 min		0 % NaOH, NaAc
5 - 25 min	to	25 % NaOH, NaAc
25 - 30 min	to	50 % NaOH, NaAc
30 - 35 min		50 % NaOH, NaAc
35 - 37 min	to	0 % NaOH, NaAc
37 - 60 min		0 % NaOH, NaAc

3.7.14 Nuclear magnetic resonance (NMR)-spectroscopy analysis of carbohydrates

All samples to be analysed by NMR were freeze-dried and dissolved in D_2O (or 900 mM NaOD when indicated). Spectra were recorded on a Bruker DRX600 or Bruker DRX400 operating at 600 and 400 MHz, respectively. One-dimensional ^{1}H and ^{13}C spectra and phase-sensitive two-dimensional spectra (double-quantum-filtered COSY, NOESY (Nuclear overhauser and exchange spectroscopy), TOCSY (Total correlated spectroscopy), ^{1}H-^{13}C HSQC (Heteronuclear single quantum coherence) and HMBC (Heteronuclear multiple bond correlation)) were recorded using standard pulse programs at 38.8 °C, and data were analysed using the software packages XWINNMR (Bruker, Germany). Chemical shifts are calculated in the δ-scale (ppm) and coupling constants *J* in Hz.

3.7.15 Biochemical characterisation of the wild-type fructosyltransferase SacB from *Bacillus megaterium*

3.7.15.1 Determination of the optimal enzyme and substrate concentration

The optimal enzyme concentration was determined in 50 mM Sörensen's phosphate buffer (pH 6.6) at 37 °C and 500 mM sucrose. The tested enzyme concentrations were 73.60, 29.44, 14.72, 7.36, and 4.91 mg l^{-1} purified SacB, respectively. Reactions were stopped after 1 h by heating (100 °C, 10 min). The release of fructose and glucose from sucrose was analysed by TLC and HPAEC. The optimal substrate concentration for the transfructosylation was determined in 50 mM Sörensen's phosphate buffer (pH 6.6) at 37 °C at 7.36 mg l^{-1} purified SacB concentration. Sucrose concentrations tested were 1 M, 750, 500, and 250 mM, respectively. Reactions were stopped after 1 h by heating (100 °C, 10 min) and analysed as described above. The optimal reaction conditions for the wild-type and the variants were at an enzyme concentration of 7.36 mg l^{-1}, a substrate concentration of 500 mM sucrose, and a reaction time of 60 min. The release of glucose was measured by HPAEC.

3.7.15.2 Determination of the pH optimum

The influence of the pH on the fructosyltransferase reaction was investigated. The phosphate buffer was adjusted to six different pH values between 5 and 8 (table 10). The substrate concentration was 500 mM and the enzyme concentration was 7.36 mg l^{-1}. The mixture was shaken at 200 rpm and 37 °C for 1 h. Samples were taken after 2, 10 15, 30 and 60 min. The enzyme in the samples was inactivated by heating (100 °C, 10 min). The samples were analysed by TLC and HPAEC.

Table 8 Buffer after Sörensen, 50 mM, pH 5-8

	pH 5.0	**pH 5.6**	**pH 6.0**	**pH 6.6**	**pH 7.0**	**pH 7.6**	**pH 8.0**
KH_2PO_4 (% v/v)	99.2	95.5	88.9	65.3	41.3	12.8	3.7
Na_2HPO_4 (% v/v)	0.8	4.5	11.1	34.7	58.7	87.2	96.3

3.7.15.3 Determination of the temperature optimum

According to the Arrhenius function a small rise in temperature in the area of the temperature maximum leads to a fast inactivation of the enzyme. To avoid these denaturing effects the experiments were performed some degrees below the maximum activity of the enzyme. The determination of the temperature optimum was performed in Sörensen`s phosphate buffer at pH 6.6. The substrate concentration of sucrose was 500 mM. The concentration of the fructosyltransferase SacB was 7.36 mg l^{-1}. The mixtures were incubated at different temperatures (25, 30, 37, 40, and 50 °C) at 200 rpm. Samples were taken after 1, 6, 15, 30, 45 and 60 min. The enzyme was inactivated by heating for 10 min at 100 °C. The samples were analysed by TLC and HPAEC.

3.7.16 Determination of the kinetic parameters of the fructosyltransferase SacB from *Bacillus megaterium* and its variants

The kinetic parameters K_m and k_{cat} describe the architecture of the active site concerning substrate binding and turnover. The substrate affinity, reaction rate and catalytic efficiency are essential characteristics of an enzyme.

3.7.16.1 Determination of the specific activity

The wild-type fructosyltransferase SacB from *B. megaterium* in a concentration of 7.36 mg l^{-1} was mixed with a sucrose solution (500 mM) in phosphate buffer (50 mM, pH 6.6) and incubated at 37 °C. Samples were taken during one hour reaction time (after 30 sec, 1, 1.5, 2, 2.5, 3, 3.5, 10, 22, 30, 45 and 60 min). The samples were analysed by HPAEC.

The specific activity of an enzyme results from the slope of the tangent to the linear area of the saturation hyperbola. A regression was performed using the equation of Michaelis-Menten (equation [1.3]). The activity was determined by a regression to the linear area of the hyperbola (until 10 min reaction time).

3.7.16.2 Determination of the kinetic parameters after Michaelis-Menten

To determine the kinetic parameters K_m and k_{cat} of the fructosyltransferase SacB from *B. megaterium*, the purified enzyme was used in an end concentration of 7.36 mg l^{-1} at a pH of 6.6 and 37 °C. Substrate concentrations of 500 to 1 mM were used (500, 250, 100, 50, 25, 10, 5, 2.5 and 1 mM). The dilutions were made from a 1 M sucrose stock solution containing SacB so the enzyme was diluted proportionally. After 1 h the reaction was stopped by heating for 10 min at 100 °C. The samples were analysed by HPAEC.

The specific product formation velocity (v/U) was plotted with the substrate concentration (S). The K_m and v_{max} values were determined by a regression with the Michaelis-Menten function [1.3]. The determination of k_{cat} was performed according to equation 1.4. The catalytic efficiency results from the equation 1.6.

3.7.17 Analysis of the product spectrum of the wild-type fructosyltransferase SacB from *Bacillus megaterium* and its variants

The product spectrum of the wild-type fructosyltransferase and the mutants shall be determined to prove the postulated function of the exchanged amino acids. First, a

kinetic was performed with the wild-type enzyme under optimised reaction conditions (50 mM Sorenson's phosphate buffer, pH 6.6 and 500 mM sucrose at 37 °C) in order to get an overview of the reaction time and the wild-type product spectrum. The enzyme concentration was 100 mg l^{-1} to get a full conversion of sucrose. The sampling time points were 30 sec, 30 min, 60 min, 24 h and 72 h. The samples were analysed by TLC and HPAEC using standards (1-kestose, 6-kestose, 1-nystose). For the qualitative determination of the product spectra of the variants the incubation was performed under optimised reaction conditions for 72 h to ensure a complete conversion of sucrose regarding the wild-type. The product spectra of the variants were also analysed by TLC. All unidentified oligosaccharides were separated by silica gel column chromatography (3.5 x 500 mm, flow rate 500 μl min^{-1}) and analysed by NMR and mass spectroscopy.

Table 9 HPAEC protocol for mono- and disaccharide analysis

t [min]	% eluent
0-5	0
5-30	0-50
30-35	50
35-40	to 0
40-60	0

3.7.17.1 Characterisation of precipitated oligo- and polysaccharides synthesised by the fructosyltransferase SacB from *Bacilus megaterium*

The formation kinetic of the polysaccharide was examined in 50 mM Sorenson's phosphate buffer (pH 6.6) at 37 °C, 500 mM sucrose and 7.36 mg l^{-1} enzyme concentration. Samples were taken after 30 sec, 30 min, 60 min, 24 h, and 72 h, respectively, and analysed by TLC. The production of the polysaccharide was performed in Sorensen's phosphate buffer (50 mM, pH 6.6) at 37 °C with 100 mg l^{-1} SacB. After 10 min the polymer was precipitated with 1 volume of ethanol (99 %

(v/v)). After centrifugation (14,000 x *g*, 5 min, 4 °C) the supernatant was discarded and the precipitate was freeze-dried.

For the identification of the linkage type, the polysaccharides were produced as described above and dialysed with water at 4 °C over night (Slide-A-Lyzer Dialysis cassettes, Pierce, MWCO 30 kDa). The sample was centrifuged for 5 min at 14,000 *g* and the supernatant was discarded. The precipitate was washed four times with 1 ml of ethanol dissolved in water (66 % (v/v)). The polysaccharides were freeze-dried and dissolved in 900 mM NaOD for NMR spectroscopy.

Table 10 HPAEC protocol for oligosaccharide analysis

t [min]	% eluent
0-5	0
5-10	0-30
10-40	30
40-45	30-0
45-60	0

3.7.18 Synthesis of novel fructo-oligosaccharides by the concerted action of two fructosyltransferases from *Bacillus megaterium* and *Aspergillus niger*

3.7.18.1 Synthesis of sucrose analogues by the fructosyltransferase SacB from *Bacillus megaterium*

The fructo-oligosaccharides were synthesised in two steps. First, sucrose analogues were synthesised by the fructosyltransferase SacB from *B. megaterium* as described previously (Seibel *et al.*, 2006b). Briefly, the acceptor carbohydrate was used in a concentration of 1.2 M and sucrose in a concentration of 600 mM dissolved in phosphate buffer after Sörensen (50 mM, pH 6.6). SacB was applied in a final concentration of 10 mg l^{-1}. The reaction was performed at 200 rpm and 37 °C for 2 h.

The purification of the sucrose analogues was performed by a silica column with the mobile phase analogous to the TLC analysis of carbohydrates (60 % ethylacetate, 30 % isopropanol, 10 % water, all v/v). The products were analysed by TLC (Merck), HPAEC (Dionex) and 1D and 2D ^{1}H and ^{13}C NMR (Bruker).

3.7.18.2 Synthesis of 1-kestose and 1-nystose and their analogues by the fructosyltransferase Suc1 from *Aspergillus niger*

The subsequent synthesis step of 1-kestose and 1-nystose and their analogues was performed by the fructosyltransferase Suc1 from *A. niger*. The supernatant of a cultivation of *A. niger* SKAN1015 was used in a dilution of 1:50 (v/v). The Suc1 dilution was mixed with 500 mM of the sucrose analogue to be converted in Sörensen`s phosphate buffer (50 mM, pH 5.6). The reaction was performed at 45 °C and 200 rpm. The reaction time depends on the desired oligosaccharide to be synthesised (table 13).

Table 11 Reaction times and yields for the synthesis of novel fructo-oligosaccharides by the fructosyltransferase Suc1 from *A. niger*.

	t [min]	**Conversion [%]**
1-kestose (Glc-Fru_2)	18	81
1-nystose (Glc-Fru_3)	60	93
Man-Fru_2	60	71
Man-Fru_3	180	87
Gal-Fru_2	420	44
Gal-Fru_3	960	65
Xyl-Fru_2	20	75
Xyl-Fru_3	120	94
Fuc-Fru_2	60	65
Fuc-Fru_3	120	88

3.7.19 Growth screen of beneficial gut bacteria (probiotics) with different carbohydrate sources (prebiotics)

The growth screen of the *Lactobacilli* and *Bifidobacteria* was performed in cooperation with Andreas Roth from the group of Petra Dersch (Department of Microbiology, TU Braunschweig and Helmholtz-Centre for Infection Research).

Four different strains of *Lactobacilli* (*Lb. fructosus*, *Lb. plantarum*, *Lb. fermentum*, *Lb. delbrueckii,* Department of Microbiology) and *Bifidobacterium lactis* (DSMZ) were investigated regarding their potential growth on 1-kestose and 1-nystose. Oligofructosides are considered to act as prebiotics promoting the growth of beneficial gut bacteria.

The *Lactobacilli* were first cultivated at 37 °C in a full medium (MRS) over night. As microaerophiles they grow on the bottom of culture tubes. The *Bifidobacteria* were grown under anaerobic conditions in culture tubes containing MRS-medium overlayed with glycerin at 37 °C for 2 d.

The *Lactobacilli* and *Bifidobacteria* were screened for their ability to grow on 1-kestose and 1-nystose. Each strain was fed with glucose as a control, 1-kestose and 1-nystose in concentrations of 500 and 200 mM (glucose) or 100 and 75 mM (1-kestose and 1-nystose), respectively. A 96-well plate was prepared with MRS full medium or semi-defined medium (200 µl each) with glucose, 1-kestose and 1-nystose or no carbohydrates as negative control (table 14) (Korakli *et al.*, 2003). For the growth of the strictly anaerobic *Bifidobacteria* the well was overlayed with glycerin. The inoculation was performed with a culture of *Lactobacilli* or *Bifidobacteria* in MRS medium in the exponential growth phase with 1/10 volume. The 96-well plate was incubated at 37 °C and the OD_{580} was measured after 1, 24, 28 and 40 hours.

Table 12 Semi-defined medium for *Lactobacilli* and *Bifidobacteria* growth screen after Vogel (Korakli *et al.*, 2003).

Compound	**c [g L^{-1}]**
NH_4Cl	2
Na acetate	5
$MnSO_4$	0,05
K_2HPO_4	2
Yeast Nitrogen Base (Difco)	5
Bacto Pepton (Difco)	10

Glucose (500 mM, 200 mM), 1-kestose (150 mM, 75 mM) or 1-nystose (150 mM, 75 mM) were added as carbon source.

3.7.20 Cultivation of eukaryotic cells

3.7.20.1 Cultivation of HEp-2 cells

The cells were cultivated in 20 ml RPMI ("Roswell Park Memorial Insitute") medium containing 7.5 % newborn calf serum (NCS) at 37 °C in 5 % CO_2 atmosphere. At 80 % confluence (appr. 2-3 days) the medium was discarded and the cells were washed with PBS buffer (Gibco). By application of 1.5 ml of trypsin/EDTA mixture the cells were detached for 5 min at 37 °C. They were supplied with 8.5 ml of fresh medium and split in a ratio of 1:10.

3.7.20.2 Cultivation of Caco-2 cells

The cells were cultivated in 20 ml Dulbecco`s modified Eagle`s medium supplemented with HamsF12 nutrient (DMEM / HamsF12, ratio 1:1) containing 10 % fetal calf serum (FCS) at 37 °C and 5 % CO_2. At 80 % confluence (appr. 2-3 days) the medium was discarded and the cells were washed with PBS buffer (Gibco). By applying 1.5 ml of trypsin/ethylene diamine tetra acetate (EDTA) mixture the cells were detached for 5 min at 37 °C. They were supplied with 8.5 ml of fresh medium and split in a ratio of 1:10.

3.7.20.3 Cultivation of CHO-K1 cells

The cells were cultivated in 20 ml DMEM / HamsF12 (1:1) containing 10 % FCS at 37 °C and 5 % CO_2 atmosphere. At 80 % confluence the medium was discarded and the cells were washed with PBS buffer (Gibco). By the application of 1.5 ml of trypsin/EDTA mixture the cells were detached for 5 min at 37 °C. They were supplied with 8.5 ml of fresh medium and split in a ratio of 1:10.

3.7.21 Cytokine assay of Caco-2 cells

For the fructo-oligosaccharide assay, Caco-2 cells at 80 % confluence were split as described and cultivated in 24-well dishes (Biochrom). Each well was supplied with the oligofructoside to be tested in a concentration of 25 µM. After 48 h (80 % confluence) the supernatant medium was collected for cytokine analysis.

The assay was performed with a 25-plex human cytokine analysis kit according to the manufacturer`s instructions (Biosource, Invitrogen). Briefly, the supernatant medium was incubated with antibody-functionalised beads and detected with biotinylated secondary antibodies. Streptavidin-R-phycoerythrin (RPE) was used as fluorescence marker. The final analysis was performed by the luminex system (Qiagen) which recognises spectral properties of the beads and quantifies the bead load by the specific fluorescence intensity (figure 28). In the 96-well plate provided, we analysed 15 different oligosaccharides (sucrose, palatinose, 1-kestose, 1-nystose, Gal-Fru, Gal-Fru_2, Man-Fru. Man-Fru_2, Man-Fru_3, Fuc-Fru, Fuc-Fru_2, Fuc-Fru_3, Xyl-Fru, Xyl-Fru_2 and Xyl-Fru_3). The concentrations of 25 different cytokines and chemokines were analysed in each sample (Eotaxin, granulocyte macrophage colony stimulating factor (GM-CSF), Interferon (IFN)-α, IFN-γ, interleukin (IL)-1RA, IL- 1β, IL-2, IL-2R, IL-4, IL-5, IL-6, IL-7, IL-8, IL-10, IL-12p40/p70, IL-13, IL-15, IL-17, IP-10, monocyte chemotactic protein (MCP)-1, monokine induced by gamma interferon (MIG), macrophage inflammatory protein (MIP)-1α, MIP-1β, regulated upon activation, normal T-cell expressed and secreted (RANTES) and tumour necrosis factor (TNF)-α).

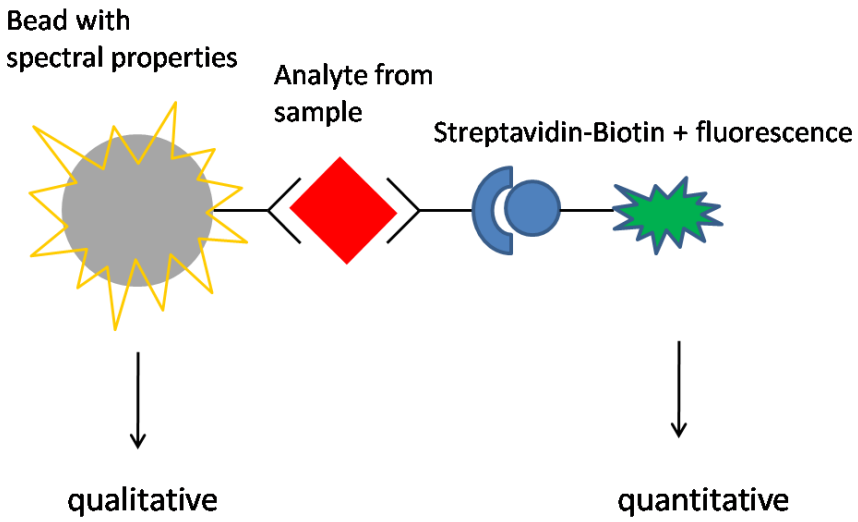

Figure 28 The analysis principle of the 25-plex human cytokine analysis kit (Biosource).

3.7.22 Metabolic labelling and modification of cell surfaces

HEp-2, CHO and CHOlec 3.2.8.1 cells were cultivated as described previously. For labelling experiments they were split at 80 % confluence into 6-well dishes and incubated in 2 ml of media suited for the individual cell line. The medium contained 25 µM of the modified carbohydrate to be incorporated (AcGlcNAz, GlcNAz, NeuNAz or NeuNHex). The incubation time was two days until 80 % confluence. The cells were detached using a cell scraper. 150 µl of each well were transferred into an 8-well microscopy cultivation slide and filled with 150 µl of the fresh medium appropriate for the cultivated cell line. The cells were cultivated at the described growth conditions until reattachment (control by microscopy). The medium was discarded and the cells were washed several times with PBS buffer (Gibco). The labelling reaction was performed in the dark with 2 mM of the desired labelling molecule (alkynylated tetramethylrhodamin (TAMRA), azido- or alkynylated fluorescein) with 2 mM $CuSO_4$, 10 mM sodium ascorbate and 2 mM Tris-[(1-benzyl-1-H-1,2,3-triazol-4-yl) methyl]amine (TBTA) in dimethylsulfoxide (DMSO). After 1 h each well was washed several times with DMSO/water (1:1) and subsequently examined by fluorescence microscopy.

3.7.23 *In silico* tools for carbohydrate and protein studies

Computers are getting more and more powerful concerning their calculation time for challenging simulation scenarios. The field of biology with many macromolecules like proteins, RNA and DNA and an overwhelmingly number of metabolic processes is a big challenge for computational approaches. In this chapter, some versatile software tools and web resources are introduced (tables 13 and 14).

The interactions of enzymes with a ligand can be simulated with Autodock (http://autodock.scripps.edu, Scripps Institute, LaJolla, CA, USA). The structure of the protein and the ligand has to be available in pdb, Mol2, MEAD, Gromacs or MMCIF format. The crucial problem is to find a balance between the computational effort and reasonable results. In Autodock it was realised by a grid-based energy evaluation and an efficient search for torsional freedom of the amino acid residues as well as the substrate to be docked. However, the limited flexibility of especially the protein is a drawback of this method.

The calculation of protein structures lacking a pdb entry was performed by ESyPred3d (http://www.fundp.ac.be/sciences/biologie/urbm/bioinfo/esypred). The software screens the RCSB pdb database (http://www.rcsb.org/pdb) for similar proteins and calculates the structure based on several multiple alignment programs. The resulting pdb file is created by the software MODELLER (Lambert *et al.*, 2002).

The prediction of potentially glycosylated arginine residues and *in silico* glycosylation of proteins is performed by GlyProt (Zentrale Spektroskopie, Molecular Modeling, Deutsches Krebsforschungszentrum, DKFZ, Heidelberg). It processes existing pdb files from the RCSB pdb database and accepts uploaded pdb files. The software predicts possible *N*-glycosylation sites based on a score function which includes accessibility and torsion angles of arginine candidates for glycosylation. The oligosaccharides to be attached can be selected from a list or defined manually.

Table 13 Software tools for protein and glycosylation analysis used in this thesis.

Tool	**Description**	**URL**
Autodock	Simulation of protein-ligand interactions	http://autodock.scripps.edu
GlyProt	*In silico* glycosylation of proteins	http://www.glycosciences.de/modeling/glyprot/php/main.php
ESyPred3D	Calculation of protein structures based on amino acid sequences	http://www.fundp.ac.be/sciences/biologie/urbm/bioinfo/esypred
GlycoWorkBench	Drawing of simplified glycan structures, MS fragmentation	http://www.ebi.ac.uk/eurocarb/gwb/home.action
DALI	Structural alignment of proteins	http://www.ebi.ac.uk/Tools/dalilite
Pymol	3D protein structure analysis	http://pymol.org/
NetNGlyc	Prediction of protein glycosylation sites	http://www.cbs.dtu.dk/services/NetNGlyc

Table 14 Databases for protein and carbohydrate analysis used in this thesis.

Database	**Description**	**URL**
RCSB pdb	Protein 3D structures	http://www.rcsb.org/pdb
BRENDA	Protein characteristics	http://www.brenda-enzymes.org
PubMed	Medical and biochemical literature	http://www.pubmed.gov
CFG	Glycan profiles of animal cells	http://www.functionalglycomics.org/glycomics/publicdata/glycoprofiling.jsp

4 Results and Discussion

4.1 Oligo- *versus* polysaccharide synthesis – Controlling the action of glycosyltransferases by enzyme engineering

The studies of the fructosyltransferase SacB from *B. megaterium* were performed in cooperation with Rebekka Biedendieck and Martin Gamer from the group of Dieter Jahn (TU Braunschweig, Department of Microbiology) and Christian Strube from the group of Dirk Heinz (Helmholtz-Centre for Infection Research)

4.1.1 Identification, cloning, expression and purification of the novel fructosyltransferase SacB from *Bacillus. megaterium*

When *B. megaterium* was cultivated in Luria-Bertani (LB)-medium supplemented with and without 0.5 % (w/v) sucrose, SDS-PAGE comparison of the secretome from both cultivations revealed a dominant protein solely produced in the presence of sucrose. This protein with a relative molecular mass of 52 kDa was identified by Rebekka Biedendieck from the group of Dieter Jahn (Department of Microbiology, TU Braunschweig). The analysed peptide fragments were homologous to fragments predicted for the levansucrase SacB, a 473 amino acid residue exo-enzyme of *B. subtilis*. BLAST searches of the *B. subtilis* SacB against the translated genome data of *B. megaterium* led to the identification of the SacB protein sequence and the genomic position of the corresponding *sacB* gene (Kunst *et al.*, 1997; Biedendieck, 2006; Sun. *et al.*, 2006; Homann *et al.*, 2007). *B. megaterium* SacB consists of 484 amino acids including the 29 amino acids of an *N*-terminal signal peptide. It shows 74 % identity at the amino acid sequence level to SacB from *B. subtilis*. Hence, the *B. megaterium* protein was also named SacB. Nine of the 11 additional amino acids found in *B. megaterium* SacB compared to SacB of *B. subtilis* are adjacent to one another at location 82–90 (*B. megaterium* SacB numbering). Like *sacB* of *B. subtilis, sacB* of *B. megaterium* is the first gene of an operon. It is followed by a gene consisting of 1,563 bp. The deduced protein sequence shows 66 % identity to the

levanase LevB from *B. subtilis*. *B. subtilis levB* is also the second gene in an operon (Sun. *et al.*, 2006). The third and last gene in the operon in *B. subtilis* encodes a 520 amino acid protein which might function as a permease (Sun. *et al.*, 2006). Interestingly, the protein encoded by a gene sequence following the levanase gene *sacB* in *B. megaterium* was annotated as bacterioferritin (Hundertmark, Hiller, Münch, Jahn, 2005; unpublished data). SacB from *B. megaterium* was heterologously expressed in *E. coli* and purified by FPLC (figures 29 and 30).

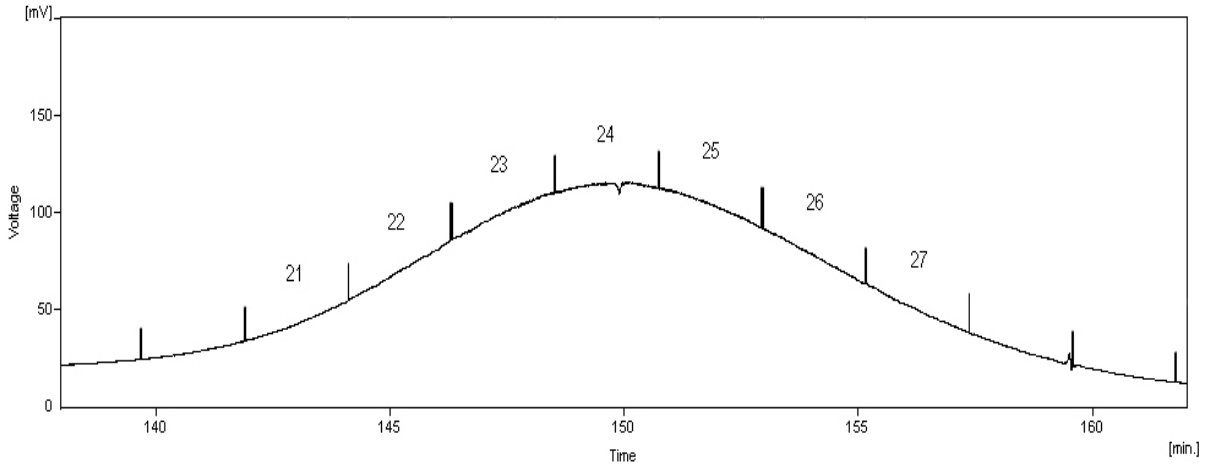

Figure 29 FPLC-purification of the wild-type fructosyltransferase SacB from *B. megaterium*. SacB was seperated by ion-exchange chromatography and eluted with 1 M Sörensen`s buffer, pH6.6.

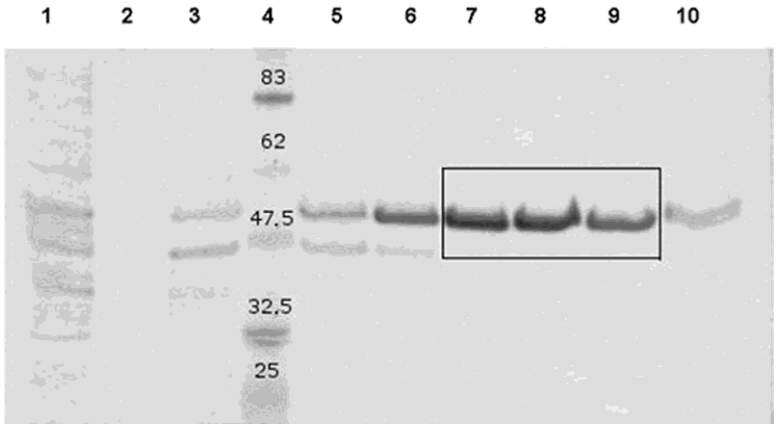

Figure 30 SDS-PAGE analysis of the FPLC fractions (figure 29). Lane 1 is the crude cell extract, 2 is the flow-through of the FPLC, 3 is the first FPLC peak fraction

(fraction 21, figure 29), 4 is the protein marker (New England Biolabs, relative molecular masses are indicated in kDa), lanes 5 to10 are the FPLC peak fractions (22-27, figure 29). The apparently pure SacB-containing fractions are boxed.

The pH optimum of the fructosyltransferase SacB from *B. megaterium* is pH 6.6 and the temperature optimum is 45 °C (figures 31 and 32, table 15). The linear area of the Michaelis-Menten plot was determined to be in between 10 min under the given reaction conditions (pH 6.6, 37 °C, 7.36 mg l^{-1} enzyme, 500 mM sucrose; figure 33).

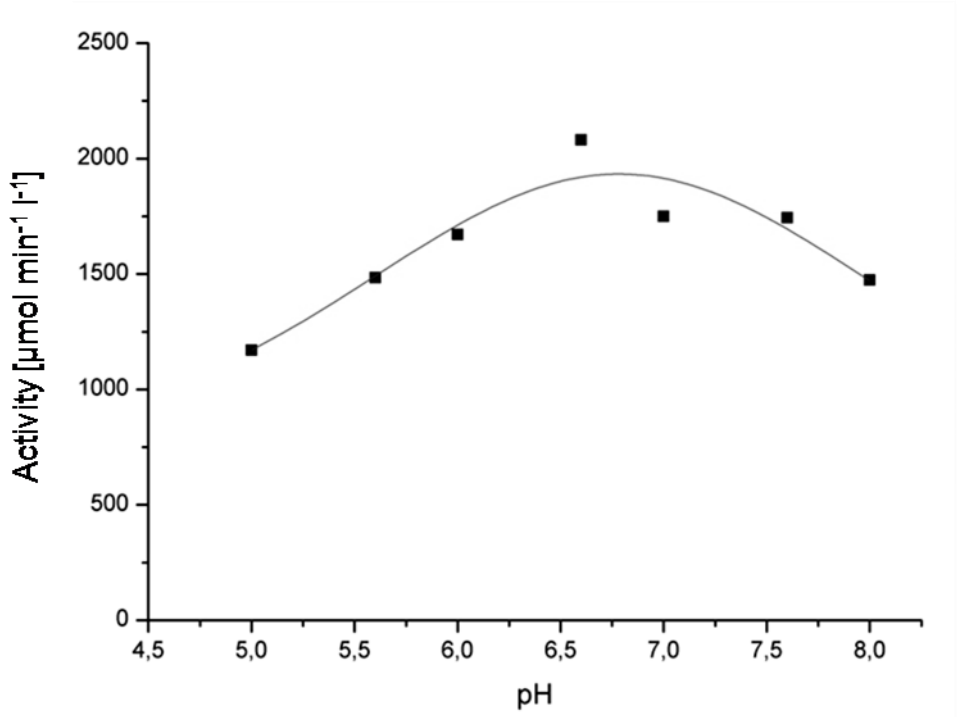

Figure 31 The pH-optimum of the wild-type fructosyltransferase SacB from *B. megaterium*. Reaction parameters were 37 °C, 500 mM sucrose, 7.36 mg l^{-1} purified SacB in 50 mM Sörensen phosphate buffer at pH values between 5 and 8. The reaction was stopped after 1 h by denaturation (100 °C, 10 min).

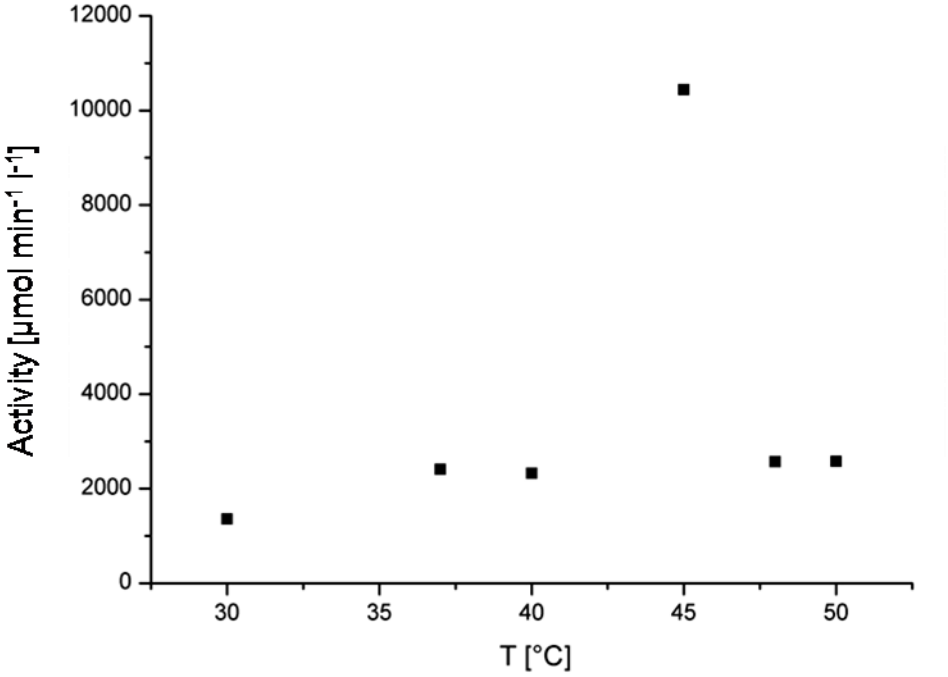

Figure 32 The temperature-optimum of the wild-type fructosyltransferase SacB from *B. megaterium*. Reaction parameters were pH 6.6, 500 mM sucrose, 7.36 mg l^{-1} purified enzyme in 50 mM Sörensen`s phosphate buffer between 30 and 50 °C. The reaction was stopped after 1 h by enzyme denaturation (100 °C, 10 min).

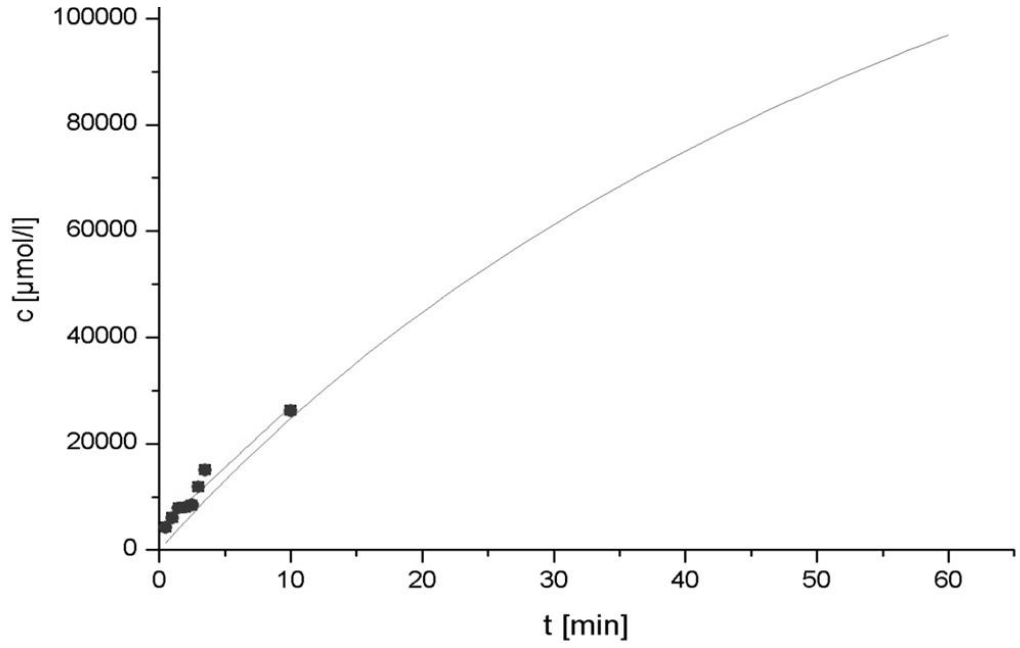

Figure 33 Determination of the linear plot region according to Michaelis-Menten of the wild-type fructosyltransferase SacB from *B. megaterium*. Reaction parameters

were 37 °C, 500 mM sucrose, 7.36 mg l^{-1} purified enzyme in 50 mM Sörensen`s phosphate buffer at pH 6.6. Samples were taken after 30 sec, 1, 1.5, 2, 2.5, 3, 3.5, and 10 min. The reaction was stopped by denaturation (100 °C, 10 min).

Table 15 The optimal reaction conditions for the fructosyltransferase SacB from *B. megaterium* are shown in comparison to the fructosyltransferase from *B. subtilis*.

	SacB from *B. subtilis* (BRENDA)	**SacB from *B. megaterium***
K_m	13.5 – 40 mM	6.6 mM
TO number (k_{cat})	0.6 – 165 s^{-1}	2272 s^{-1}
pH optimum	pH 6 for hydrolysis	pH 6.6 for hydrolysis
T optimum	37 – 50 °C	45 °C
stability	pH 3.5 to 7.5 at 4 °C, no time indicated	> 6 months at pH 6.6 and -20 °C

4.1.2 Kinetic studies and characterisation of the product spectrum of the wild-type fructosyltransferase SacB from *Bacillus megaterium*

The kinetic parameters were determined as described in materials and methods (3.7.16). The K_m value of 6.6 mM for hydrolysis measured for the wild-type SacB from *B. megaterium* is low compared to other levansucrases, *e.g*. SacB from *B. subtilis* with 13.5 to 40 mM according to BRENDA database (Schomburg *et al.*, 2002). This indicates a high affinity to the substrate sucrose supported by a very high k_{cat} (2272 s^{-1}) and a high catalytic efficiency (346 mM^{-1} s^{-1}; table 14). The reaction conditions used for the determination of the product spectrum favour hydrolysis (58.4 %) followed by synthesis of polyfructan (22.1 %). Further analysis showed that polyfructan synthesised by SacB from *B. megaterium* had a molecular weight of 2,711 kDa and consists of mainly β-(2,6) linkages. The polyfructan produced by SacB from *B. subtilis* had a M_w of 6,295 kDa and was described as β-(2,6)-linked levan with some β-(2,1) branches (Chambert *et al.*, 1974). Besides the polyfructan formation, the wild-type SacB of *B. megaterium* also synthesises five different detectable

oligosaccharides. Three products were identified by HPAEC as 1-kestose, 6-kestose, and 6-nystose which are known acceptors for the transfer of fructosyl units (van Hijum *et al.*, 2006; figure 37).

The two unknown by-products were isolated and analysed by 1- and 2D-NMR and mass spectroscopy (figures 34 and 35, tables 16 and 17). The 1-D proton spectrum of the first compound showed two anomeric protons (4.6-5.2 ppm) which correspond to an anomeric mixture of two non-reducing sugar residues. The 1-H signal the β-configurated glucoside-residue resonated at higher field (4.59 ppm) with a large coupling constant (d, 7.96Hz) where the 1-H signal (5.16 ppm) of the α-configured glucose appeared as minor signal of a reducing sugar in a ratio of α:β 1:2. Based on the results of the 2-D COSY spectrum, correlations were observed between the H-1`s of the glucose residues and the corresponding H-2`s (alpha 3.8-4.1 ppm; beta 3.20-3.16 ppm), which was coupled to H-3`s (alpha 3.63-3.68 ppm; beta 3.42-3.40 ppm). The assignments for the anomeric carbon signals (alpha 94.94 ppm; beta 98.79 ppm) and C-2s (alpha 74.27 ppm, beta 76.89 ppm) were achieved by 2-D HSQC spectrum analysis. In addition, ^{1}H ^{13}C HMBC long range ^{2}J and ^{3}J correlations were observed for the H-6 signal of glucose with the ^{13}C signals at δ_C 106.52 ppm (alpha, C-2') and 106.55 ppm (beta, C-2') of the fructofuranoside, respectively, which shows correlations for the fructofuranoside H-3' positions (beta 79.78 ppm; alpha 79.68 ppm/4.58 ppm) and H-4' positions (beta 77.45 ppm; alpha 77.31 ppm/4.07 ppm) (figure ???). All other carbon and proton signals were assigned from a combination of 2-D COSY, TOCSY, HMBC, and HSQC experiments. All experiments provide strong evidence of an 1:2 α:β mixture of β-(2,6)-Fru-α,β-Glc ((2,6)-*O*-β-D-fructofuranosyl-α,β-D-glucopyranoside, blastose).

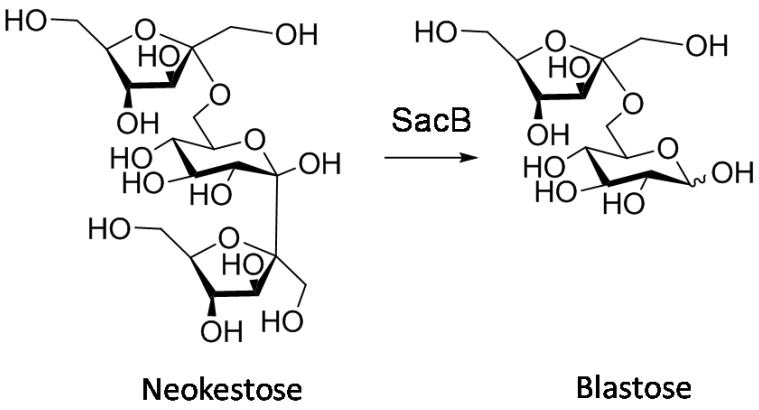

Figure 34 Unidirectional formation of blastose from neokestose as the accumulating product by the fructosyltransferase SacB from *B. megaterium*.

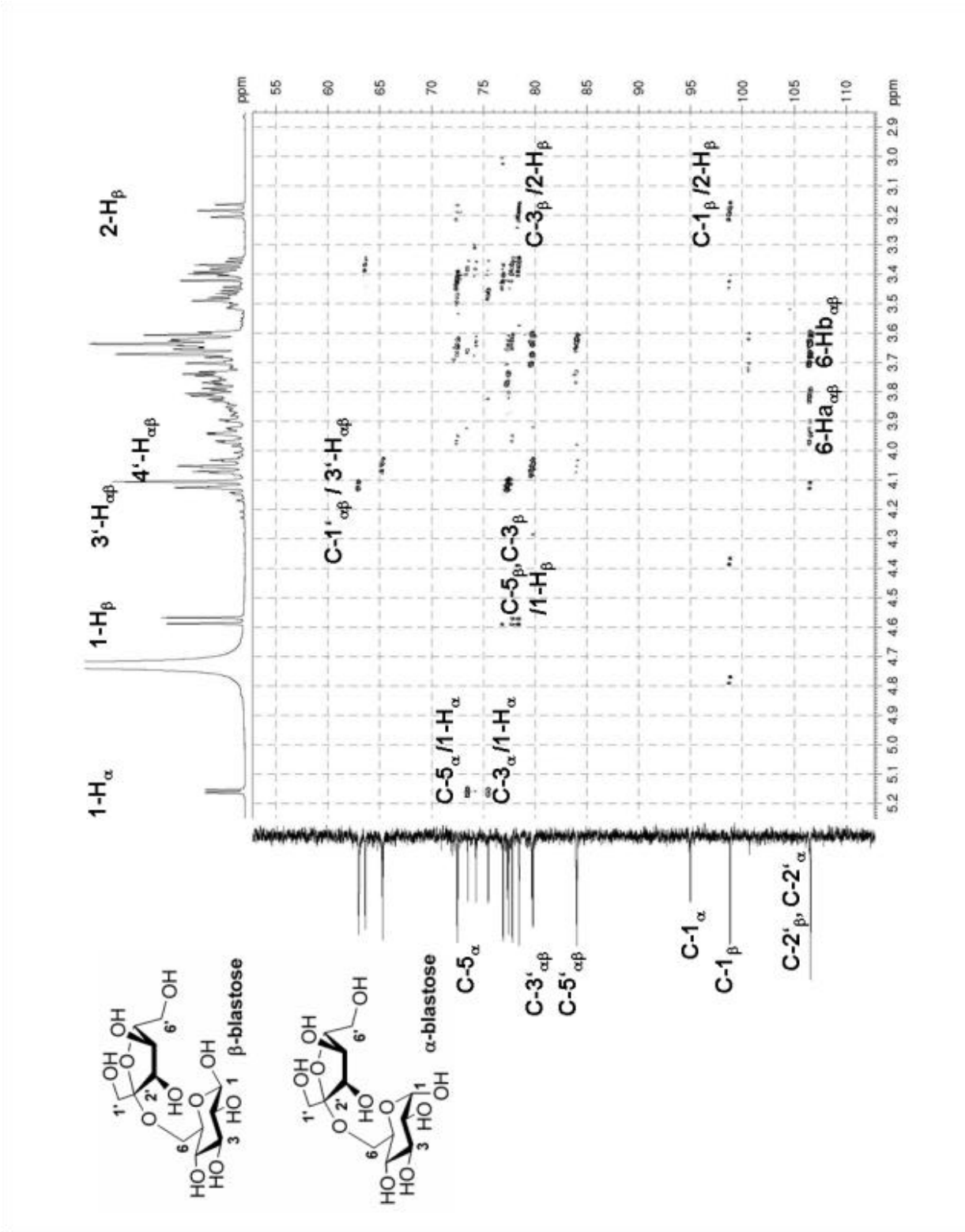

Figure 35 2D-NMR correlation spectrum of α,β blastose (HMBC)

Table 16 ^{13}C NMR data for the identification of blastose.

	α-blastose		**β-blastose**	
C-atom	δ_C	δ_H	δ_C	δ_H
C-1	94.94	5.16 (d, 3.70)	98.79	4.59-4.57 (d, 7.96)
C-2	74.27	3.49-3.46 (m)	76.89	3.20-3.16 (t, 8.70)
C-3	75.48	3.63-3.68 (m)	78.45	4.42-3.40 (m)
C-4	72.55	3.34-3.40 (m)	72.49	3.88-3.85 (m)
C-5	73.49	3.85-3.88 (m)	77.79	3.84-3.80 (m)
C-6	63.61	3.96-3.89, 3.67-3.62	63.61	3.96-3.89, 3.67-3.62
C-1’	62.99	3.70-3.62 (m)	62.99	3.70-3.62 (m)
C-2’	106.52	-	106.55	-
C-3’	79.68	4.58-4.56 (d, 8.26)	79.78	4.58-4.56 (d, 8.26)
C-4’	77.31	4.07-4.03 (t, 7.60)	77.45	4.07-4.03 (t, 7.60)
C-5’	83.97	3.82-3.76 (m)	84.02	3.82-3.76 (m)
C-6’	65.21	3.77-3.72 (m)	65.32	3.77-3.72 (m)

Table 17 ^{13}C NMR data for the identification of neokestose.

	neokestose	
C-atom	δ_C	δ_H
C-1	62.89	3.91-3.87, 3.76-3.73
C-2	106.45	-
C-3	79.47	4.16-4.13 (d, 8.5)
C-4	77.03	4.11-4.07 (t, 7.4)
C-5	83.88	3.84-3.80 (m)
C-6	65.17	3.83-3.73
C-1’	94.74	5.35 (d, 3.88)
C-2’	73.74	3.53-3.49 (dd, 3.90, 10.00)
C-3’	75.15	3.69-3.66 (m)
C-4’	74.76	3.92-3.88 (m)
C-5’	71.89	3.48-3.45 (m)
C-6’	62.03	3.58 (s)
C-1’’	64.14	3.73-3.69, 3.64-3.61
C-2’’	106.47	-
C-3’’	78.90	4.18-4.16 (d, 8.49)
C-4’’	76.64	4.04-4.00 (t, 8.5)

C-5''	84.08	3.87-3.83 (m)
C-6''	65.08	3.80-3.76, 3.68-3.64

The electro-spray ionisation mass spectrum (ESI/MS) of the second compound showed the molecule peak at *m/z* = 527 [M^+Na^+]. This trisaccharide is a non reducing oligosaccharide. In the 1-D proton spectrum the anomeric proton resonated at δ_H 5.35 ppm with a small J_{12} value of 3.90 Hz. This proton showed correlation in the 2D-HMBC spectrum with quaternary carbon C-2' (106.45 ppm) of a fructofuranoside residue. In the 2-D HMBC spectrum protons corresponding of the H-6 glucose residue showed correlations to the quaternary carbons C-2'' of a second fructofuranoside residue. Taken together, all signals assigned from the one dimensional and correlation spectroscopy (*i.e.* COSY, TOCSY, HMBC, DEPT and HSQC), the trisaccharide was identified as β-(2,6)-Fru-α-Glc-β-(1,2)-Fru ((2,6)-*O*-β-D-fructofuranosyl-α-D-glucopyranosyl-(1,2)-*O*-β-D-fructofuranoside, neokestose).

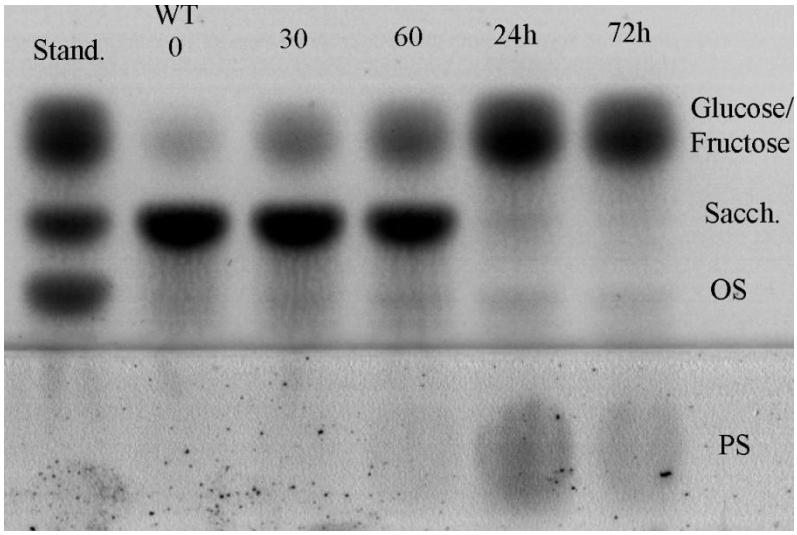

Figure 36 TLC analysis of the reaction product pattern of the wild-type fructosyltransferase SacB from *B. megaterium* at 7.36 mg l^{-1} enzyme, 0.5 M sucrose, pH 6.6, 37 °C. The sample times are indicated in minutes when not stated otherwise. Sacch. is sucrose, OS is oligosaccharides and PS is polysaccharide.

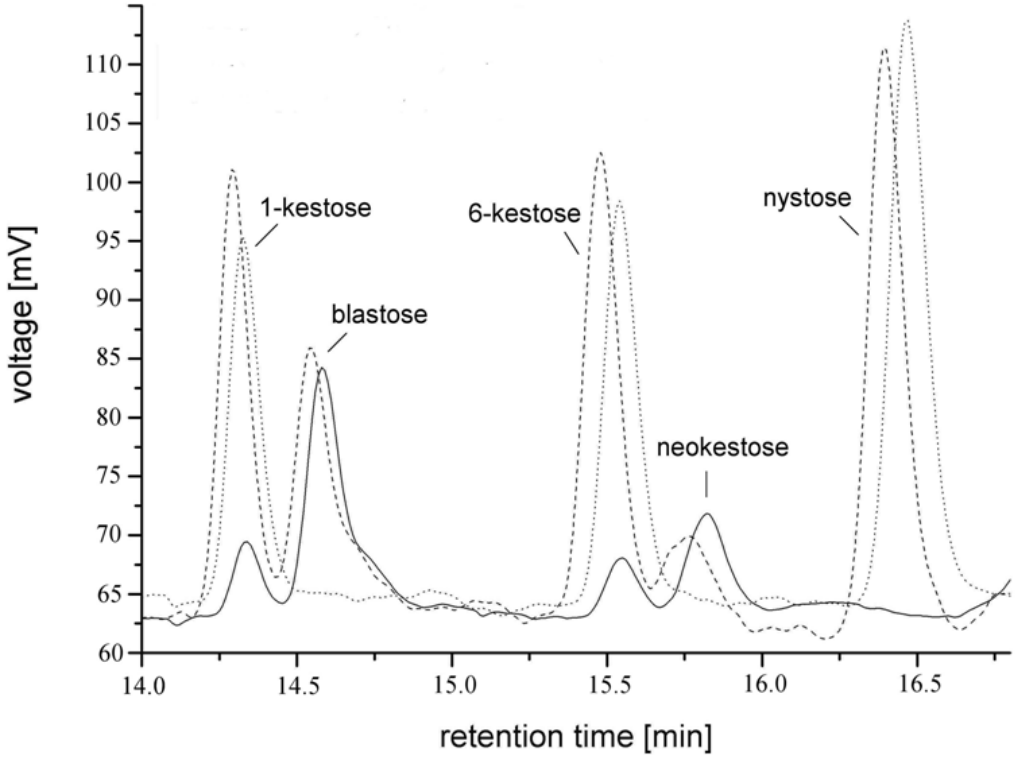

Figure 37 Identification of the transfructosylation products. The carbohydrates up to tetrasaccharides were identified by high-performance anion-exchange chromatography (HPAEC). The dotted line is the oligosaccharide standard (1-kestose, 6-kestose, nystose, all 0.01 g l^{-1}), the solid line is the wild-type SacB reaction (stopped after 19 h at 37 °C and 0.5 M sucrose in Sorensen`s phosphate buffer, 50 mM, pH 6.6, enzyme concentration was 0.1 g l^{-1}), the dashed line is the oligosaccharide standard (concentration as above) mixed with the same wild-type SacB sample.

4.2 Crystallisation of the fructosyltransferase SacB from *Bacillus megaterium*

The crystallisation and the structural refinement of the fructosyltransferase SacB from *B. megaterium* was performed by Christian Strube from the group of Dirk Heinz at the Helmholtz-Centre for Infection Research. The 3D structure (1.6 Å) shows essentially the same five-fold β-propeller motif as the SacB from *B. subtilis*. The active site contains the catalytic triad D95/D257/E352 with E352 acting as the acid/base catalyst and D95 as the nucleophile. The amino acid residue N252 is located in the +2-site

(figures 38 and 39). The interactions of the amino acids located in the active site with sucrose (figure 40) can be clearly identified as the analogous to SacB from *Bacillus subtilis* cocrystallised with sucrose.

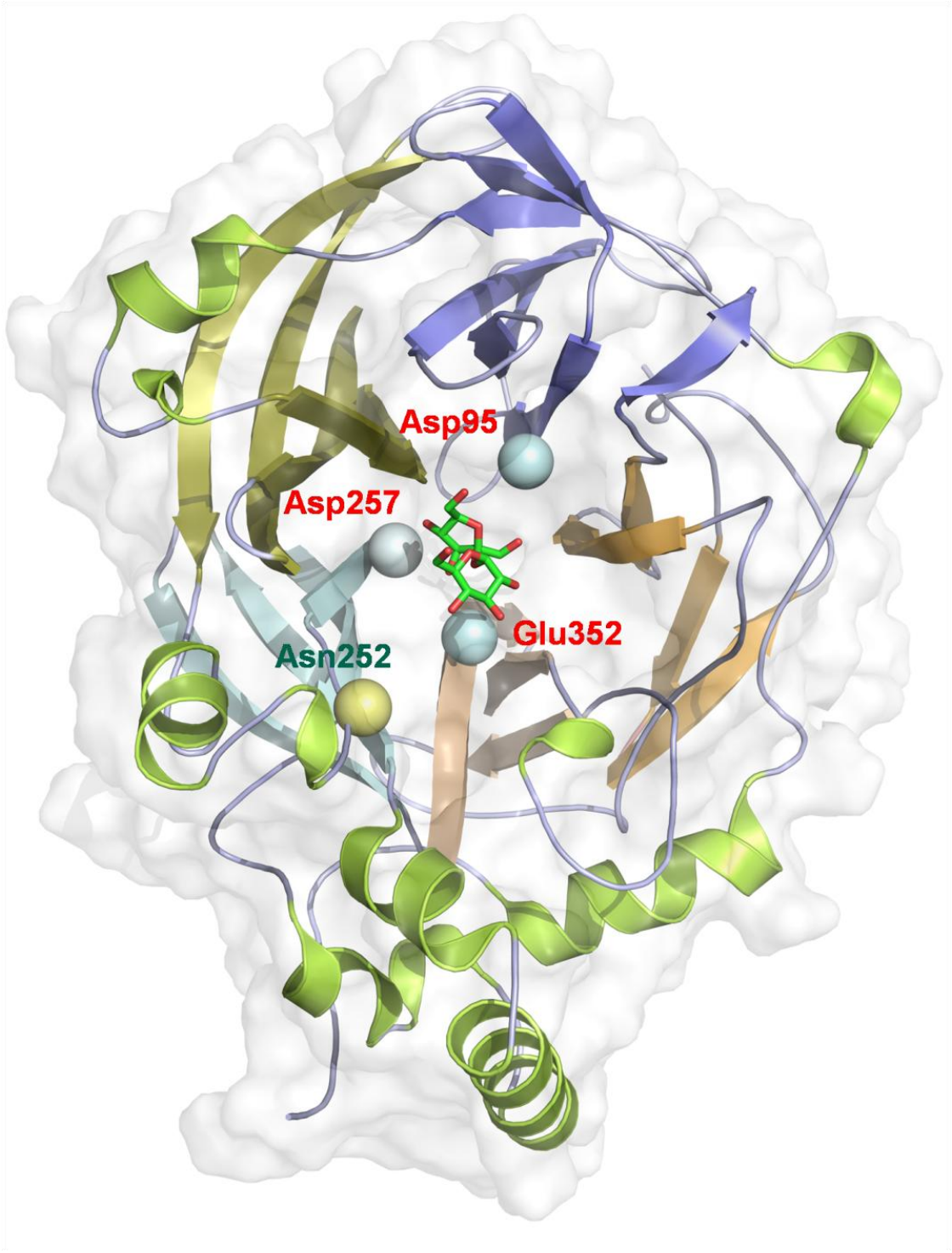

Figure 38 Crystal structure of the D257A variant of SacB from *B. megaterium* with sucrose modelled into the active site in a resolution of 1.6 Å. The catalytic triad is

shown in grey balls and red label. Asn252 in subsite +2 is shown as a yellow ball and green label. The structure refinement was performed by Christian Strube in the group of Dirk Heinz (Helmholtz-Centre for Infection Research).

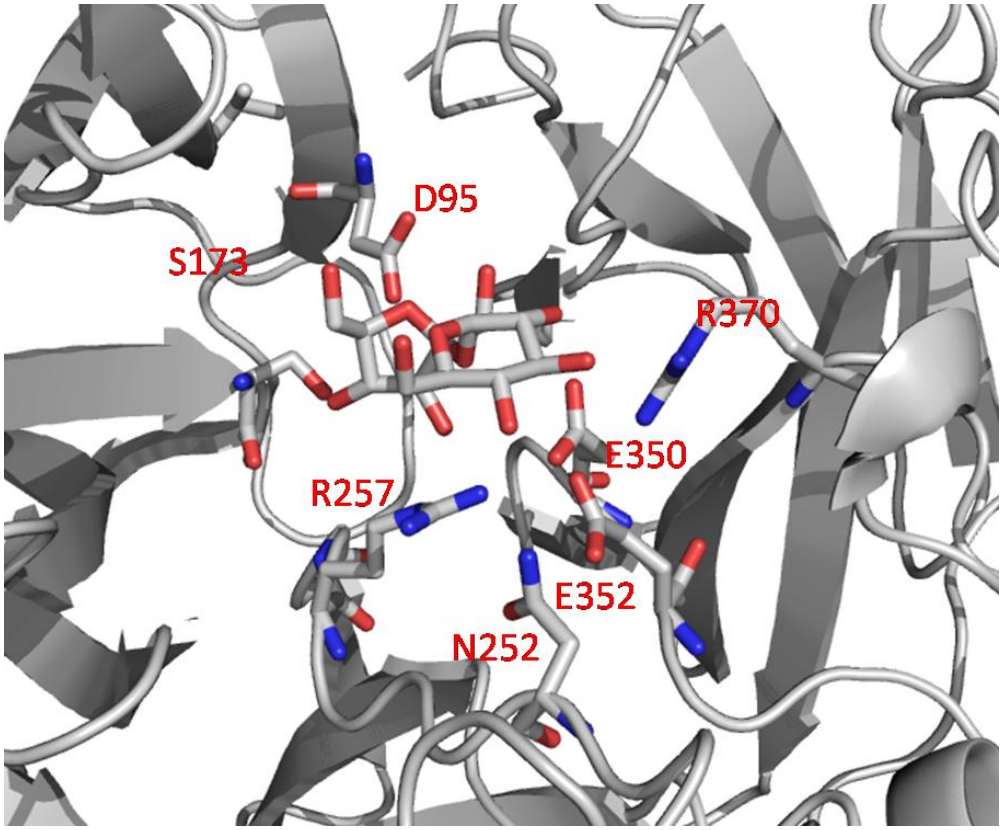

Figure 39 The active-site architecture of the fructosyltransferase SacB from *B. megaterium* with modelled sucrose.

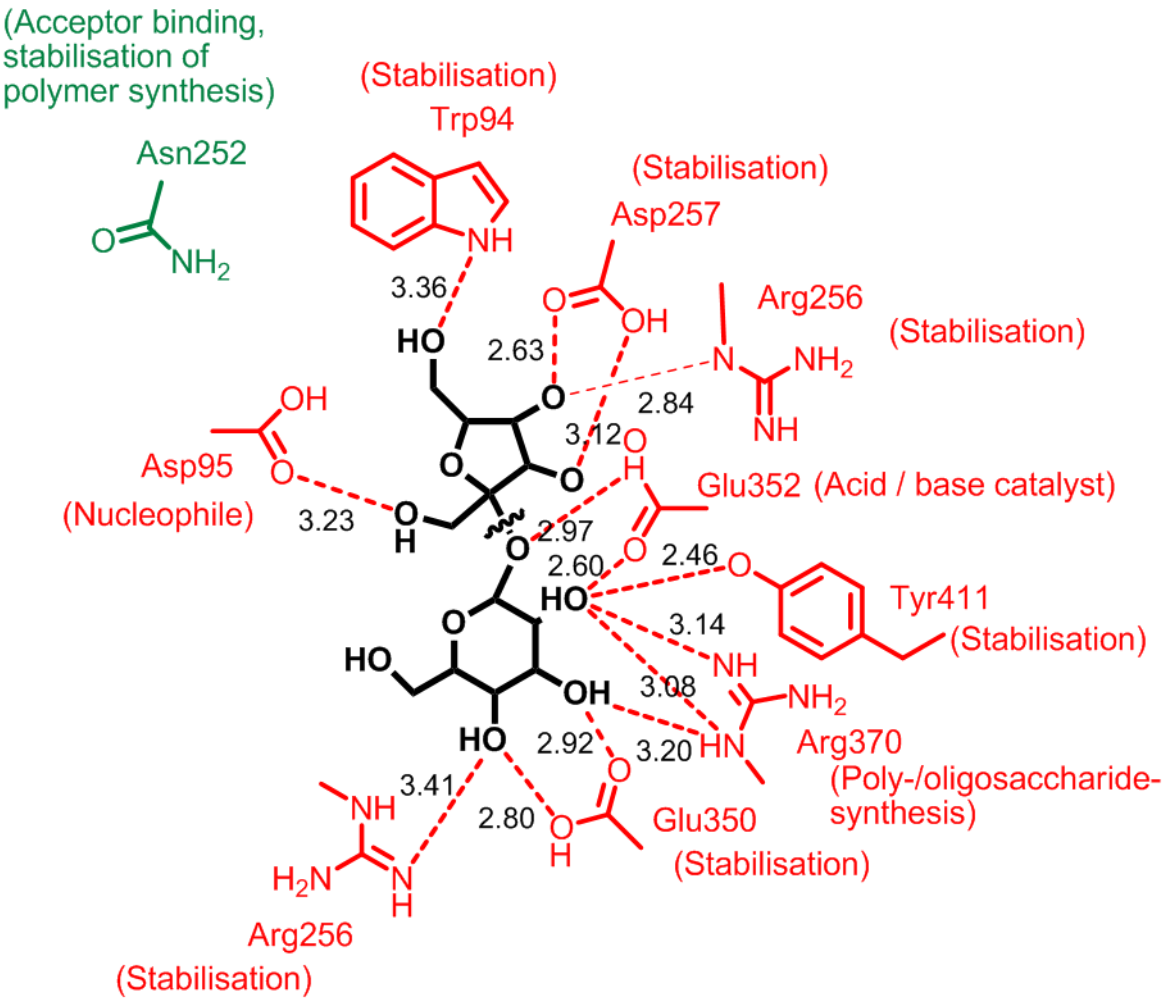

Figure 40 The interactions of the amino acids located in the active site of the fructosyltransferase SacB from *B. megaterium* variant D257A with the natural substrate sucrose (black). N252 which is not located in the active site is supposed to stabilise the third fructosyl unit for the transfructosylation process (indicated in green). The position of D257 was modelled by pymol (DeLano Scientific). The distances are given in Å.

4.3 Mutagenesis studies of the fructosyltransferase SacB from *B. megaterium*

4.3.1 Identification of amino acid residues located in the active site with impact on the enzyme activity and the transfructosylation reaction

By sequence alignments of the fructosyltransferase from *B. megaterium* with the levansucrase from *B. subtilis* and various other fructosyltransferases, we identified 11 amino acids in the active site (figure 41). The identified amino acid residues were exchanged to alanine in order to examine their functional role in SacB from *B. megaterium*.

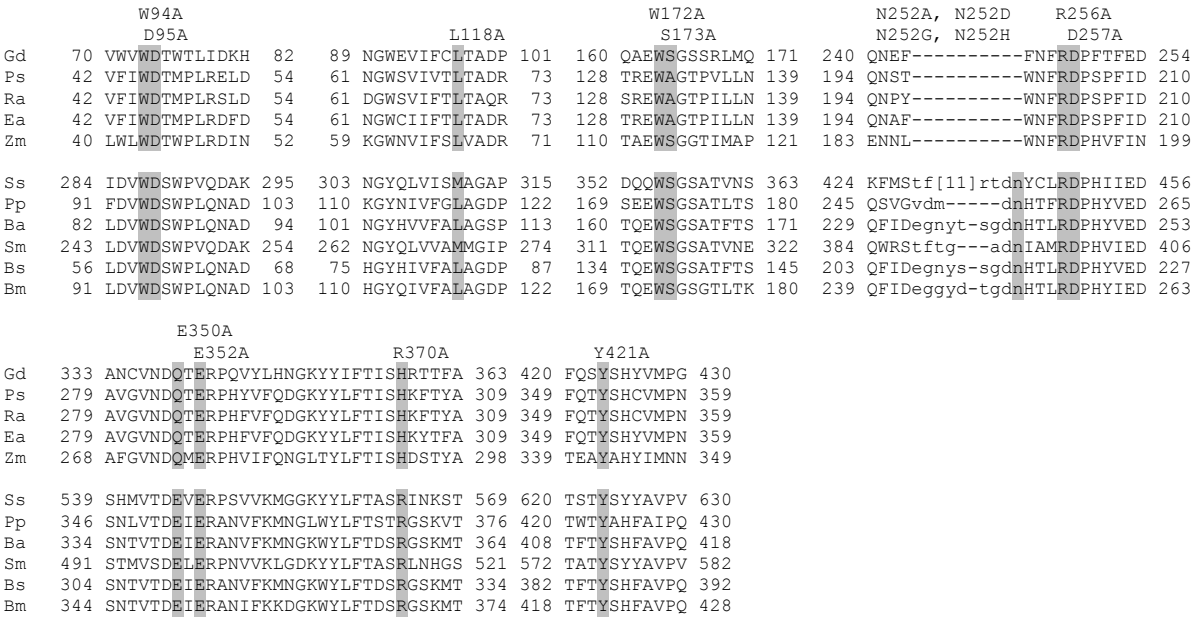

Figure 41 Sequence alignment of related levansucrases. Gd is *Gluconacetobacter diazotrophicus* (Martinez-Fleites *et al.*, 2005), Ps is *Pseudomonas syringae* (Hettwer *et al.*, 1998), Ra is *Rahnella aquatilis* (Song *et al.*, 1998), Ea is *Erwinia amylovora* (Geier *et al.*, 1993), Zm is *Zymomonas mobilis* (Song *et al.*, 1994), Ss is *Streptococcus salivarius* (Rathsam *et al.*, 1993), Pp is *Paenibacillus polymyxa* (Bezzate *et al.*, 2000), Ba is *Bacillus amyloliquefaciens* (Tang *et al.*, 1990), Sm is *Streptococcus mutans* (Ueda *et al.*, 1988), Bs is *Bacillus subtilis* (Meng *et al.*, 2003), Bm is *Bacillus megaterium*. The amino acids used for the mutagenesis study are indicated and the resulting variant is labelled above the sequence. N252 (*B.*

megaterium numbering) which is not located in the active site was identified by a random mutagenesis screen (Beine *et al.*, 2008).

Table 18 Postulated functions of chosen amino acid residues located in the active site of the fructosyltransferase SacB from *B. megaterium*. The effect of the functional knock-out of the amino acid residues is studied by an exchange to alanine.

Postulated function	**Bacillus m*egaterium* numbering**	***Bacillus subtilis* numbering**	**Interactions with sucrose**
Nucleophile	Asp95	Asp86	1'-OH 2.86
			C-2' 3.1
Stabilisation	Glu350	Glu340	4-OH 2.45,
			3-OH 2.83
Polymer synthesis	Arg370	Arg360	3-OH 3.14,
			2-OH 3.23
Stabilisation	Tyr421	Tyr411	2-OH 2.93
Acid/base catalyst	Glu352	Glu342	1-O 2.75,
			2-OH 3.00,
			3'-OH 2.75
Stabilisation	Trp94	Trp85	6'-OH 3.09
Stabilisation	Asp257	Asp247	4'-OH 2.76,
			3'-OH 2.85
Poly/oligosaccharide synthesis	Arg256	Arg246	3'-OH 2.80
	Trp172	Trp163	-

	Ser173	Ser164	-
	Leu 118	Leu109	-
	Val115	Val106	-
Screen for polymer formation	Asn252	Asn242	-

The amino acid residue Asn in position 242 was identified in a random mutagenesis screen of the levansucrase from *B. subtilis* to have a strong impact on transfructosylation. An exchange to alanine abolishes polymer formation. Sequence alignments and the structure from the fructosyltransferase SacB from *B. megaterium* shows that Asn252 is the analogous amino acid.

4.3.2 Identification of amino acid residues not located in the active site with potential impact on the linkage type of the synthesised oligo- and polysaccharides

In a sequence alignment with the inulosucrase from *Lactobacillus reuteri*, amino acid residues of the fructosyltransferase SacB from *B. megaterium* with impact on the linkage type formation of the fructosyl moieties of the formed oligo- and polysaccharide were identified. In contrast to the fructosyltransferase SacB from *B. megaterium* which synthesises β-(2,6)-linked levan, the inulosucrase from *Lb. reuteri* synthesises oligo- and polyfructosides with β-(2,1)-linkages (figure 42). As an attempt to control the linkage type of the oligo- and polyfructosides formed by the fructosyltransferase SacB from *B. megaterium*, the analogous amino acid residues were exchanged to the corresponding inulosucrase amino acid residues from *Lb. reuteri* (table 19).

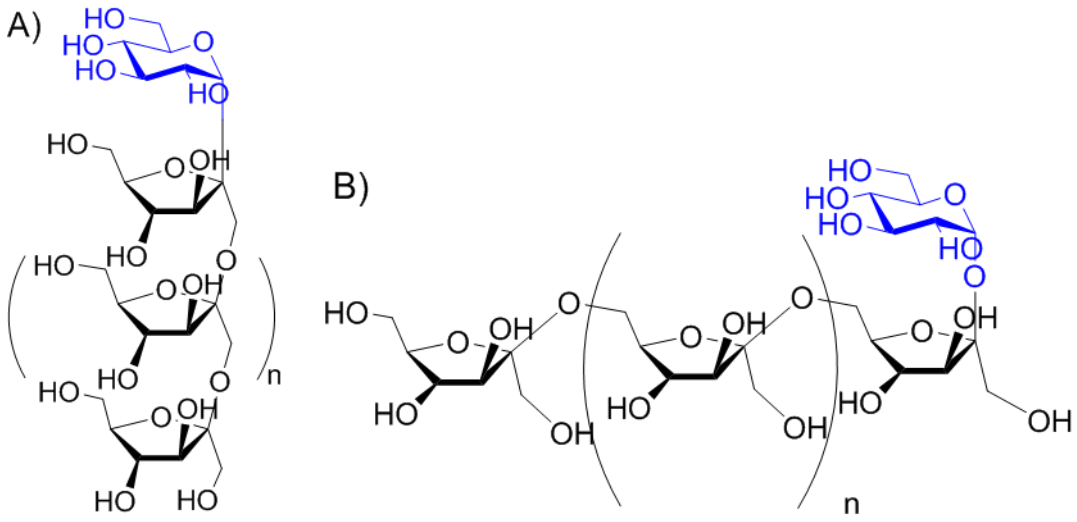

Figure 42 Structures of β–(2,1) linked inulin and β-(2,6) linked levan.

Table 19 Sequence aligment of SacB from *B. megaterium* (Bm) with the inulosucrase from *Lb. reuteri* (Lr).

Levansucrase Bm	**Inulosucrase Lr**
Y247	[Gap]
N312	D
K315	R
S372	N
K373	R
Q381	[Gap]
H423	Y
Y439	Y

4.3.3 Identification of amino acid residues not located in the active site with impact on the transfer *versus* hydrolysis activity

By sequence blasts and structural alignments of the fructosyltransferase from *Bacillus megaterium* with already crystallised fructosyltransferases from *Bacillus subtilis*, *Gluconacetobacter diazotrophicus* and an exo-inulinase from *Aspergillus awamori* (for kinetic data see table 20) we identified eight amino acids with potential impact on the transfructosylation *versus* hydrolysis process (table 21). The identified amino acid residues were chosen because of their location on the surface of SacB from *B. megaterium* (figure 43).

Table 20 Kinetic data of sucrose-active enzymes from Clan-j GH 32 (*Aspergillus awamori*) and GH 68 (*Bacillus subtilis* and *B. megaterium*, *Lactobacillus reuteri* and *Gluconacetobacter diazotrophicus*).

Organism	**Reaction conditions**	**K_m**	**k_{cat}**
Bacillus megaterium (this study)	pH 6.6, 37 °C	6.6	2272
Bacillus subtilis (Chambert *et al.*, 1991)	pH 6.0, 30 °C	40	0.583
Gluconacetobacter diazotrophicus (Martinez-Fleites *et al.*, 2005)	pH 5.0, 30 °C	11.9	1
Lactobacillus reuteri (Kralj *et al.*, 2004)	pH 5.4, 37 °C	9.7	147
Aspergillus awamori (Kulminskaya *et al.*, 2003)	pH 4.5, 37 °C	40	1150

Table 21 Amino acids outside the active site with impact on the transfructosylation process.

Amino acid	Exchange to	Variant	Postulated function
Y247	Alanin, Isoleucin, Tryptophan	Y247A, Y247I, Y247W	Polymer formation, (2-6) stereoselectivity
N312	Alanin	N312A	Polymer formation
K315	Alanin, Arginin	K315A, K315R	Polymer formation
S372	Alanin	S372A	Polymer formation
K373	Alanin, Arginin	K373A, K373R	Polymer formation, (2-1) stereoselectivity
Q381	Alanin	Q381A	Polymer formation, (2-1) Stereoselectivity
H423	Alanin, Tyrosin	H423A, H423Y	(2-1) stereoselectivity
Y439	Alanin	Y439A	(2-1) stereoselectivity

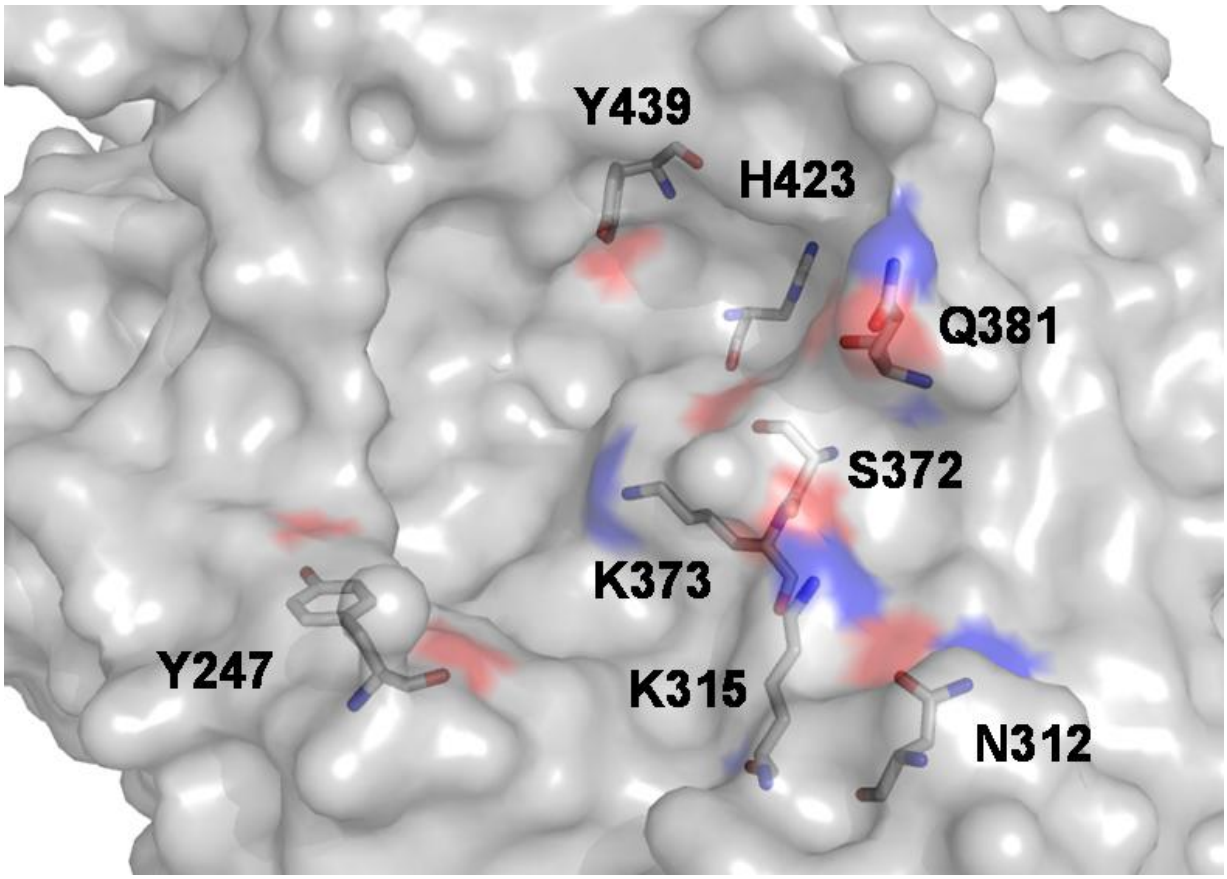

Figure 43 Location of the amino acid residues of the fructosyltransferase SacB from *B. megaterium* not located in the active site which were identified by sequence and structural alignments with other fructosyltransferases from *Aspergillus awamori*, *Bacillus subtilis, B. megaterium*, *Lactobacillus reuteri* and *Gluconacetobacter diazotrophicus*.

4.3.3 Functional role of the exchanged amino acids located in the active site and insights into the reaction mechanism of the fructosyltransferase SacB from *Bacillus megaterium*

Levansucrases belong to glycoside hydrolase family (GH) 68 according to CAZy (Cantarel *et al.*, 2009) which bind the substrate sucrose in subsite -1 (fructosyl residue) and +1 (glucosyl residue). In this family, two X-ray structures of the *B. subtilis* and *G. diazotrophicus* fructosyltransferases have been elucidated and both show a five-fold β-propeller topology (Meng *et al.*, 2003; Martinez-Fleites *et al.*, 2005).

The enzyme variants were incubated with sucrose (500 mM) for 72 h at 37 °C in Sörensen`s buffer, 50 mM, pH 6.6 and analysed by TLC (figures 44 and 45).

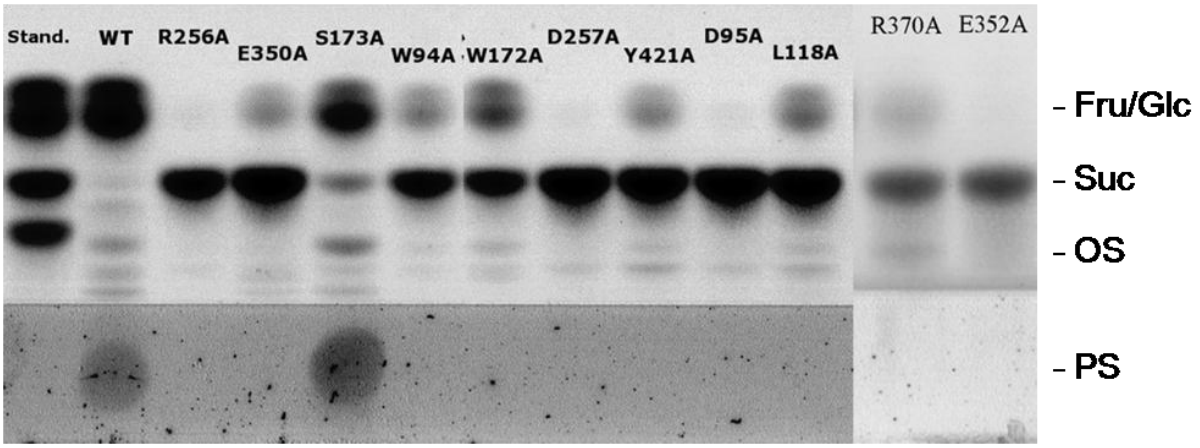

Figure 44 TLC analysis of the product spectrum of the wild-type fructosyltransferase SacB from *B. megaterium* and its variants of amino acid residues located in the active site after 24 h reaction time. Fru is fructose, Glc, is glucose, OS, is oligosaccharide, PS is polysaccharide.

Table 22 Product spectrum of the wild-type fructosyltransferase SacB from *B. megaterium* and indicated variants after 60 min reaction time. All values are given in mM. The sample used for the identification of neokestose is indicated.

	wild-type	**L118A**	**W172A**	**N252A**	**N252D**	**N252G**	**N252H**	**R370A**	**Y421A**
glc	428.0	85.1	13.0	447.9	463.4	334.9	118.6	138.7	12.2
fru	292.2	71.6	11.3	391.4	362.0	279.9	102.3	103.0	9.6
suc	41.9	407.1	487.0	17.1	0.0	141.8	381.4	321.3	487.5
1-kestose	15.9	3.4	0.0	5.2	3.5	6.9	0.0	3.4	0.0
α,β-blastose	6.4	0.0	0.0	7.3	17.3	9.7	0.0	3.9	0.0
6-kestose	3.5	0.0	0.0	15.0	4.2	6.8	0.0	0.0	0.0
neokestose	2.8	3.5	0.0	5.8	7.4	6.6	0.0	32.7	0.0
nystose	1.5	0.5	0.0	1.7	4.1	0.0	0.0	0.0	0.0

Table 23 Product spectrum of the wild-type fructosyltransferase SacB from *B. megaterium* and indicated variants after 19 h reaction time. All values are mM. The sample used for the identification of blastose is indicated.

	wild-type	L118A	W172A	N252A	N252D	N252G	N252H	R370A	Y421A
glc	449.8	304.1	101.1	459.9	443.8	448.7	431.1	414.4	97.8
fru	359.8	226.7	89.5	399.4	375.5	360.3	360.3	357.2	83.8
suc	0.0	172.2	389.7	0.0	0.0	0.0	27.4	0.0	389.5
1-kestose	7.6	4.5	2.1	4.0	7.7	7.0	6.0	6.0	4.7
α,β-blastose	24.5	7.4	1.1	14.1	21.5	26.3	16.7	69.7	1.1
6-kestose	4.9	4.1	0.6	11.9	14.8	6.7	4.5	1.2	0.0
neokestose	9.5	5.3	5.4	7.0	9.3	15.0	12.3	13.6	6.9
nystose	3.7	2.5	0.0	3.2	3.5	3.4	2.1	2.1	0.0

Amino acid sequence alignments of various levansucrase enzymes (figure 41) in combination with structural data of the family GH 32 members pointed towards functional relevant residues located in the active site of the fructosyltransferase SacB from *B. megaterium*. Subsequent site-directed mutagenesis of Trp94, Asp95, Val115, Leu118, Trp172, Ser173, Arg256, Asp257, Glu350, Glu352, Arg370 and Tyr421 was performed in order to explore the structural determinants which are responsible for the transfructosylation activity in *B. megaterium* SacB.

The residues Asp95, Glu352 and Asp257 are proposed to form the catalytic triad of the fructosyltransferase SacB from *B. megaterium* (figures 38 to 40). The substitution of Asp95 with alanine inhibited the enzyme activity (figure 44). Sequence alignments with other levansucrases from various bacteria as well as the structural information from the fructosyltransferase SacB from *B. megaterium* show that this amino acid residue acts as the nucleophile. It attacks the fructofuranosyl residue of the sucrose and forms an enzyme-fructosyl intermediate. The corresponding acid/base catalyst was Glu352. Consequently, an exchange to alanine led to a kock-out of the enzyme activity. The variant D257A also showed almost no activity. The residue Asp257 coordinates the fructofuranosly moiety in positions 3-OH and 4-OH.

Trp94, Arg256, Glu350, and Tyr421 were selected according to their corresponding amino acid residues of the SacB from *B. subtilis* (Chambert *et al.*, 1991; Meng *et al.*, 2003) which form hydrogen bonds to sucrose and position it in a productive orientation. Here, the substitution with alanine of each of these amino acid residues in the fructosyltransferase SacB from *B. megaterium* showed different effects. The variants R256A and E350A were nearly inactive. This agrees with the structural

information obtained for SacB from *B. subtilis* where the corresponding Arg246 formed hydrogen bonds to the 3-OH of the fructofuranoside and also to 4-OH of the glucopyranoside while Glu340 (*B. subtilis* SacB numbering) coordinated the 3-OH and 4-OH of the glucopyranoside. The SacB variant W94A from *B. megaterium* still carried 9 % of the catalytic efficiency (k_{cat}/K_m) while variant Y421A showed just 3 % of the wild-type activity. Considering the X-ray structure of SacB from *B. subtilis*, this Trp formed a hydrogen bond with 6-OH of the fructofuranoside and Tyr of the 2-OH of the glucopyranoside. Due to the low reaction rate hydrolysis was predominantly observed (tables 22 and 23). The substituted amino acid residues Trp172 and Ser173 were proposed to be part of interactions with amino acids of the active site. In the fructosyltransferase SacB from *B. subtilis*, this Trp forms a pocket for the glucopyranoside of the C-6-OH. The experiments with the SacB variant W172A from *B. megaterium* showed a 72-fold increase of the K_m and thus confirmed this function. It was very interesting to notice that subsitution of Ser in position 173 by alanine effected the catalytic efficiency dramatically, while the K_m was comparable to the wild-type SacB (table 24). Thus, it is proposed that Ser173 does not influence the binding mode of sucrose, but it must somehow participate in the subsequent catalysis.

4.3.4 Structure-functional aspects of the fructosyltransferase SacB from *Bacillus megaterium* - Hydrolysis *versus* fructosyl transfer

The substitution of Arg370 with alanine of *B. megaterium* SacB resulted in fundamental changes in product formation. The corresponding residue in SacB from *B. subtilis* in subsite -1 (Arg360), was previously described as a key residue for the formation of 1-kestose (Chambert *et al.*, 1991; Meng *et al.*, 2003). We observed the time-dependent accumulation of different oligosaccharides during the correspondent *B. megaterium* SacB variant R370A catalysis. After 60 min reaction time an accumulation of neokestose (2,6-β-Fru-α-Glc-1,2-β-Fru, 32.7 mM) was determined while after 19 h blastose (2,6-β-Fru-α,βGlc) was the main reaction product (69.7 mM). A four-fold K_m-value decrease compared to the wild-type enzyme supported the interactions of Arg370 with the 2-OH and 3-OH of the glucosyl residue in the active site. It is possible that the substitution to Ala favoured an unspecific substrate binding

and enabled a fructosylation at C-6 of the glucosyl residue of sucrose yielding neokestose. When the trisaccharide neokestose was accumulating and entering the active site of SacB variant R370A, the β-(2,1)-linkage is cleaved leading to the hydrolyzation product blastose. Blastose was supposed to be no donor substrate of the enzyme indicated by its strong accumulation due to an unfavourable β-(2,6)-linkage between glucose and fructose.

Residue Asn252 obviously plays an important role for the transfructosylation process of the fructosyltransferase SacB from *B. megaterium*. A substitution to Ala or Gly completely stopped the polysaccharide production at all, while the K_m and k_{cat} values were not affected (table 24). Catalysis of this variant was switched from mainly polysaccharide synthesis to hydrolysis (tables 22 and 23). In contrast, mutation of Asn252 to Asp252 affected just the downregulation of the polysaccharide synthesis (figure 45), also without changing K_m and k_{cat} values significantly. The X-ray structure of the fructosyltransferase SacB from *B. megaterium* enabled insights into the function of this amino acid residue. Due to its position in the +2-site, it stabilises the third fructosyl unit of the growing oligosaccharide chain and direct it as an acceptor substrate in the optimal position for further transfructosylation.

The mutation of Asn in position 252 to Asp obviously reduced the coordination of a fructosyl unit in the +2-site. However, it was still possible to some extend as indicated by the formation of a little amount of polysaccharide (figure 45). The mutations to alanine, glycine and histidine led to a complete knock-out of the polysaccharide formation. Recently, Ozimek *et al.* proposed a model of the sugar-binding subsites in two *Lb. reuteri* 121 fructosyltransferases (Ozimek *et al.*, 2006). For the fructan polymer synthesis, the subsites +2, and +3 need a high affinity for binding the growing fructan polymer chain. But no structural determinants have been reported so far.

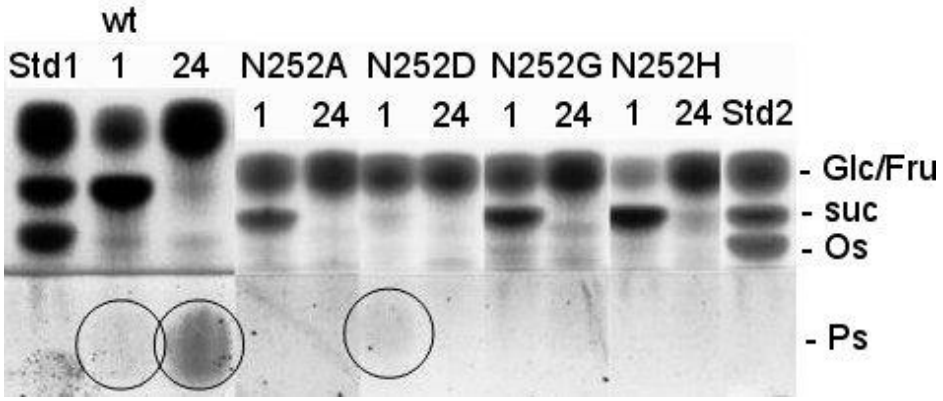

Figure 45 TLC analysis of the product spectrum of the wild-type fructosyltransferase SacB from *B. megaterium* and the variants of N252 after 24h reaction time. Fru is fructose, Glc, is glucose, Os, is oligosaccharide, Ps is polysaccharide.

The amino acid residues Arg370 and Asn252 which seem to be crucial for the polyfructan synthesis are found to be conserved in fructosyltransferases from Gram-positive bacteria. In contrast, the endophytic Gram-negative bacterium *G. diazotrophicus* SRT4 secretes a constitutively expressed levansucrase (LsdA, EC 2.4.1.10), which mainly converts sucrose into fructo-oligosaccharides. It contains a His419 instead of Arg370 at the equivalent position (figure 46). This His419 residue is found strictly conserved in Gram-negative levansucrases. Further, Asn252 is strictly conserved in Gram-positive bacteria while in Gram-negative ones this region shows variability. The corresponding part of the 3D-structure of LsdA was almost perfectly superimposable with the equivalent residues of the *B. subtilis* SacB in the active site. In contrast, the region +2 with the amino acid residue N252 was not perfectly superimposable (figure 46).

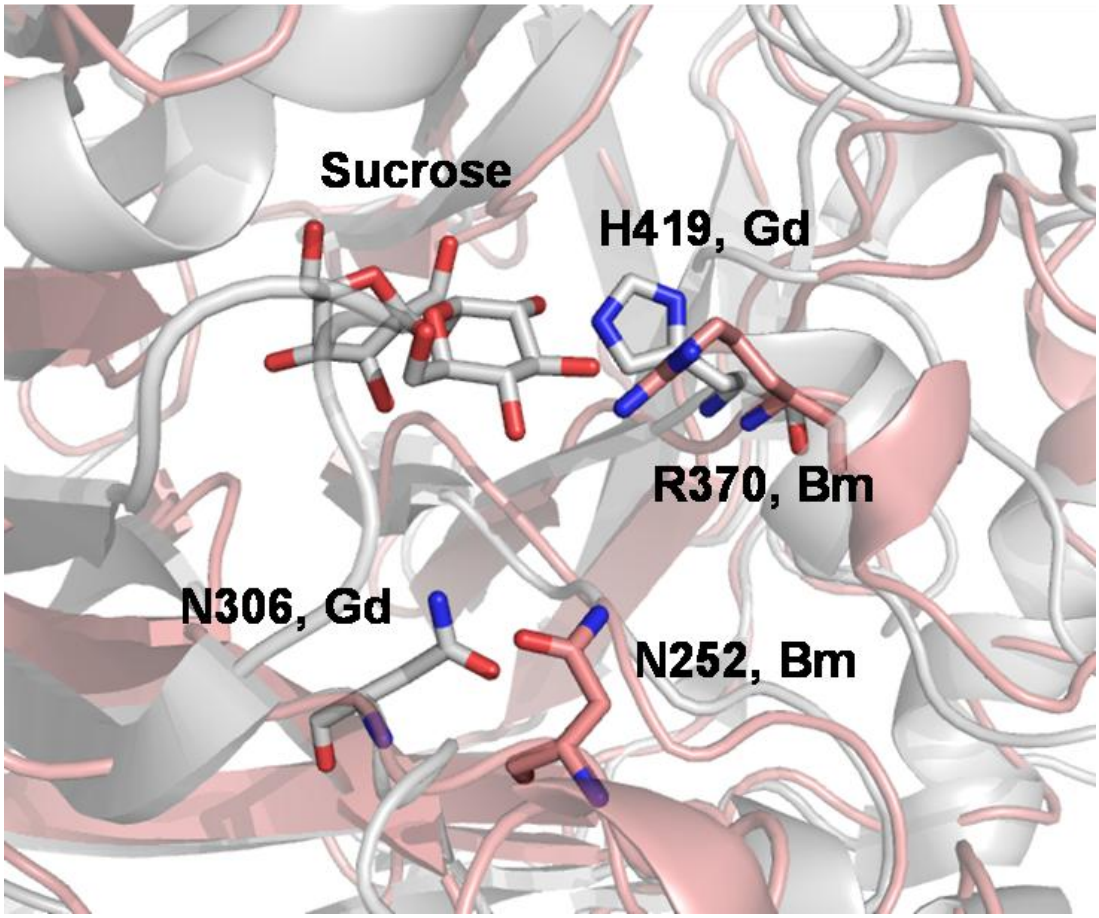

Figure 46 Local identification and alignment of the amino acid residues N252 and R370 from the fructosyltransferase SacB from *B. megaterium* crucial for polymer synthesis. SacB from *Bacillus megaterium* (Bm, rosé) and *Gluconacetobacter diazotrophicus* (Gd, grey) (Martinez-Fleites *et al.*, 2005) with sucrose in the active site are shown.

It was shown for the first time that a single amino acid substitution at the +2-subsite switches the enzymatic reaction from poly- to oligosaccharide formation conserving a high enzyme activity by changing from a processive to a non-processive mechanism. Based on these studies in the following chapters more structural details of the +2- and +3-subsites enable the redesign of this enzyme for the synthesis of tailor-made short-chain fructo-oligosaccharides.

Table 24 Kinetic parameters of the wild-type fructosyltransferase SacB from *B. megaterium* and its variants. The amino acids located in the active site are indicated in red. Mutations in subsite +2 and further away from the active site are shown in green colour.

Variant	**K_m [mM]**	**k_{cat} [s^{-1}]**	**k_{cat}/K_m [$mM^{-1}\ s^{-1}$]**
wild-type	6.6 ± 1.1	2272	346
W94A	31.9 ± 11.0	1000	31
D95A	inactive	inactive	inactive
L118A	66.6 ± 22.1	1231	19
W172A	480.4 ± 124.8	2396	5
S173A	2.3 ± 1.2	363	159
Y247A	9.0 ± 1.6	1505	167
Y247I	11.4 ± 3.0	2030	178
Y247W	2.1 ± 1.3	2653	1263
N252A	4.1 ± 1.7	1480	361
N252D	8.4 ± 2.3	3743	445
N252G	7.5 ± 0.8	2256	301
N252H	35.1 ± 30.7	1529	44
R256A	inactive	inactive	inactive
D257A	inactive	inactive	inactive
N312A	10.8 ± 3.0	776	72
K315A	5.3 ± 2.0	2415	456
K315R	9.5 ± 3.6	2122	223
E350A	inactive	inactive	inactive
E352A	inactive	inactive	inactive
R370A	29.2 ± 11.6	179	6
S372A	7.5 ± 2.4	2617	349
K373A	3.5 ± 1.4	699	200
K373R	11.0 ± 4.2	1708	155
Q381A	9.5 ± 1.9	3295	347
Y421A	51.9 ± 16.3	335	6

H423A	47.6 ± 8.4	2760	58
H423Y	13.2 ± 3.8	1722	130

4.3.5 The proposed reaction mechanism of the fructosyltransferase SacB from *Bacillus megaterium*

The fructosyltransferase SacB from *B. megaterium* cleaves sucrose and, via a covalent intermediate, transfers the fructosyl moiety to water (hydrolysis) or a growing oligofructoside chain (transfructosylation). The glycosyl transfer reaction follows a retaining mechanism. The carboxyl group of the nucleophile Glu352 protonates the glycosidic bond of sucrose. The formation of the enzyme-fructosyl-intermediate is performed by a covalent bond between Asp95 and the C2 of the fructosyl moiety of sucrose. The intermediate is stabilised by Asp257. A conformational change from 3T4 to E4 is the consequence (T, twist; E, envelope). A nucleophilic attack at the C2 position leads to hydrolysis or fructosyl transfer. The proposed mechanism was supported by docking experiments (Seibel *et al.*, 2006b). Asn252 most likely interacts with the oligofructoside chain supporting the transfructosylation process (Homann *et al.*, 2007; figure 47).

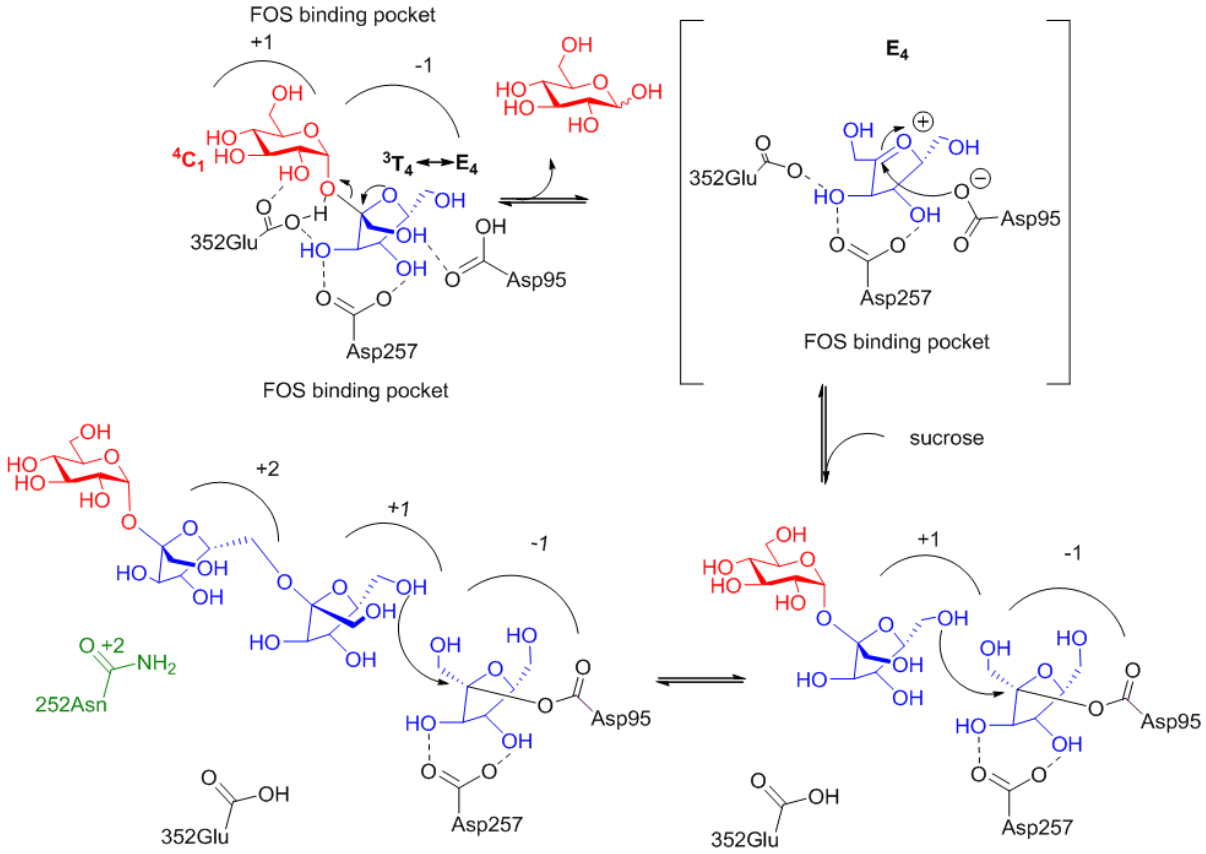

Figure 47 The acceptor reaction mechanism. The mechanism is based on the fructosyltransferase SacB from *B. megaterium* with sucrose as substrate (Homann *et al.*, 2007).

4.3.6 Impact of the amino acid residues not located in the active site on the transfructosylation process catalysed by the fructosyltransferase SacB from *Bacillus megaterium*

In a further investigation of amino acid residues influencing the transfructosylation process, 8 amino acid residues which are not located in the active site were identified. Variants were created based on sequence and structural alignments (table 20). Martin Gamer from the group of Dieter Jahn (Department of Microbiology, TU Braunschweig) created 13 variants of the fructosyltransferase SacB from *B. megaterium* (table 21) which were expressed in *E. coli*. After purification by FPLC the variants were characterised kinetically. All SacB variants have a K_m-value comparable to the wild-type except for H423A and Y439A. H423A has a seven-fold increased K_m which indicates a significant conformational change of the active site.

Variant Y439A is inactive. The K_m of the other variants differs from 2.1 (Y247W) to 13.2 mM (H423Y). That is not more than 50 % difference from the K_m of the wild-type. This indicates that the active-site architecture is maintained keeping the wild-type`s original substrate affinity.

Also the k_{cat} of all variants is comparable to the wild-type SacB, again except for two variants, K373A and N312A. These have a k_{cat} of roughly factor three lower than the wild-type. However, this value is still high compared to fructosyltransferases from other organisms (table 20). The other variants do not differ more than 40 % from the wild-type SacB`s turnover number.

For the first time we created variants of a fructosyltransferase with amino acid exchanges in positions away from the +1-site with high impact on the transfructosylation process. 12 out of 16 variants of amino acid residues not located in the active site (including the N252 variants) keep the wild-type`s substrate affinity and turnover rate while synthesising different mixtures of fructo-oligosaccharides (figure 48).

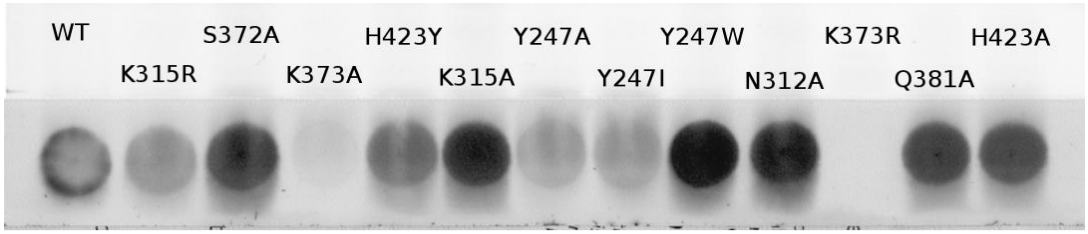

Figure 48 TLC analysis of the oligo- and polysaccharide formation of the wild-type fructosyltransferase SacB from *B. megaterium* and its variants after 72 h. The variant Y439A does not form any polymer.

Clear differences of the synthesised fructo-oligosaccharides are already visible by judging the intense of the TLC stain. The variant K373A hardly forms any oligo- or polysaccharide while variant K373R apparently does not form any transfructosylation product at all. Some of the variants have a lighter staining (T315R, Y247A, Y247I) and some a more intense compared to the wild-type SacB (S372A, T315A, Y247W, N312A). In order to elucidate their composition, the precipitated reaction products

were analysed by HPAEC. On the basis of a tetrasaccharide standard, the HPAEC peaks were assigned to the corresponding number of fructosyl units (figure 49).

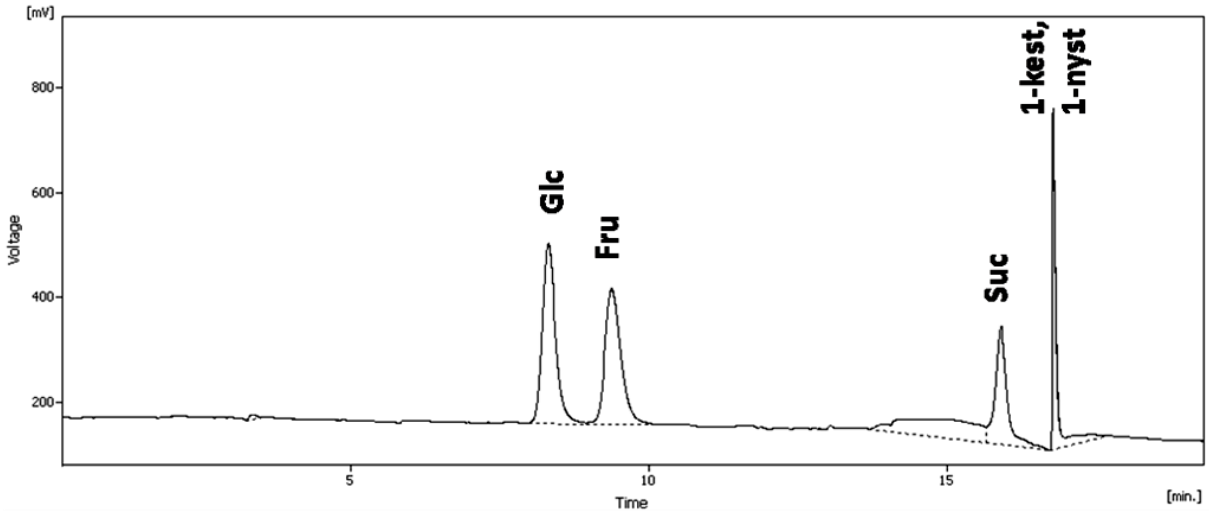

Figure 49 The standard HPAEC chromatogram up to the tetrasaccharide 1-nystose. Standards analysed are Glc, glucose, Fru, fructose, Suc, sucrose, 1-kest, 1-kestose and 1-nyst, 1-nystose. HPAEC was performed under the conditions for oligosaccharide analysis (table ???).

The amino acids Y247 and K373 have a clear impact on the transfructosylation process. The exchange of the amino acid K373 to alanine and arginine has different effects on the product formation. Regarding the variant K373A, the formation of tri- and tetrasaccharides is lowered while the synthesis of penta- and hexasaccharides is slightly enhanced. The knock-out of the amino group leads to shorter oligosaccharides (5 fructosyl units) than the exchange to arginine. Here, an oligosaccharide of up to 7 units is synthesised (figures 50 and 51).

K373 is located in the +2 subsite of the active site of SacB. There it interacts with R370 located in subsite +1. The HPAEC chromatogram data shows that variant K373A is not capable any more to position either arginine 370 nor any carbohydrate unit or -chain in the right position for further transfructosylation of more than 5 fructosyl units. The reason for the discrepancy of the amino acid position and the oligosaccharide chain length may be because of other, *i.e*. weaker, possible interactions of carbohydrates on the enzyme`s surface. That theory is supported by

the exchange of lysine in position 373 to arginine. Interactions between the arginine and the amino acid network as well as carbohydrate units are possible although not the whole range of oligosaccharides can be synthesised compared to the wild-type chromatogram (figure 51).

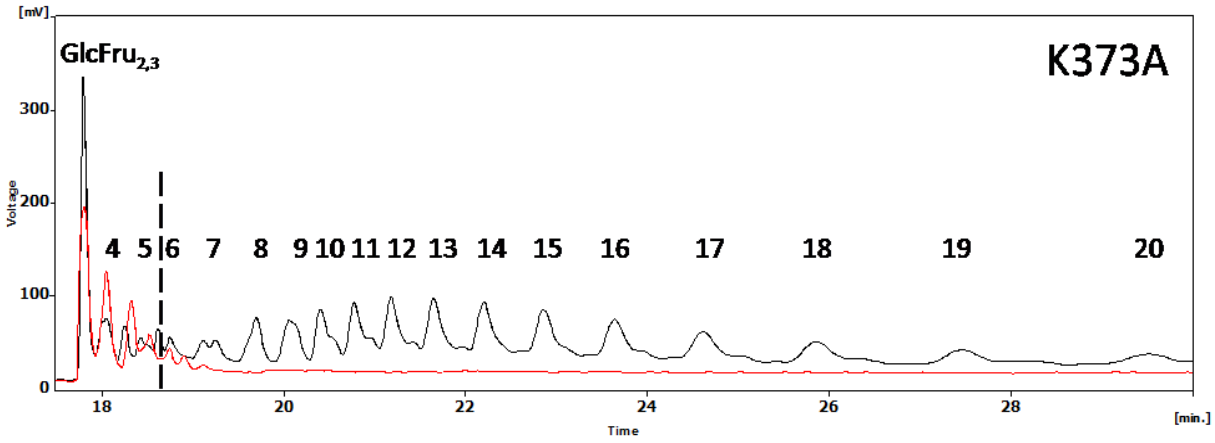

Figure 50 HPAEC analysis of the oligosaccharide product spectrum from the wild-type fructosyltransferase SacB from *B. megaterium* (black) and variant K373A (red).

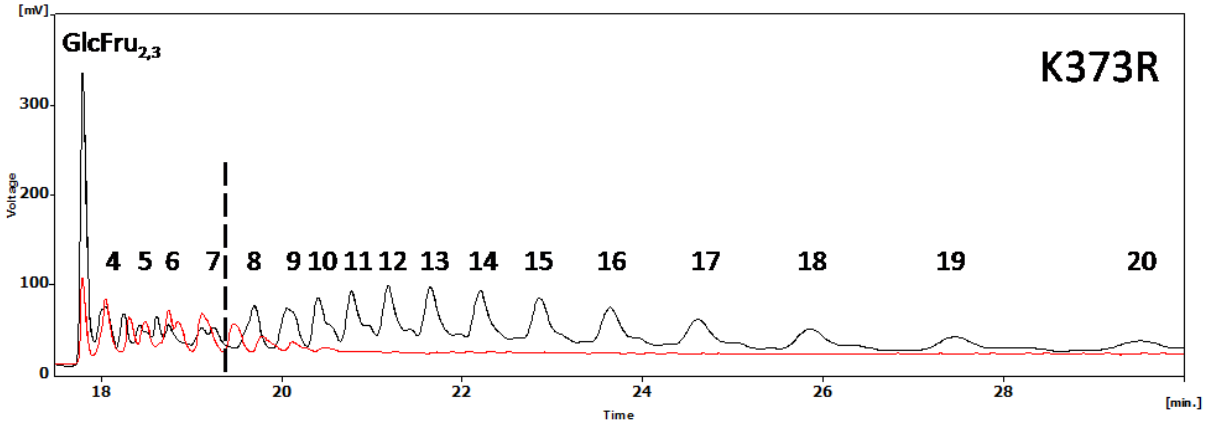

Figure 51 HPAEC analysis of the oligosaccharide product spectrum from the wild-type fructosyltransferase SacB from *B. megaterium* (black) and variant K373R (red).

The exchange of the tyrosine in position 247 to alanine leads to the formation of shorter oligosaccharides (figure 52). Nona- and decasaccharides are enhanced and the transfructosylation stops after approximately 9 fructosyl units. The distribution of

oligosaccharides synthesised by SacB variant Y247A is the same for the product spectrum of the variant Y247I. In contrast, the exchange of tyrosine to tryptophan yields the same oligosaccharide pattern as the wild-type SacB (figure 53). The reason may be that an unpolar favoured π-π-stacking mechanism is possible with tyrosine as well as tryptophan but not with alanine or isoleucine. The position of Y247 is supposed to be a key supporting function in an oligo- and polysaccharide-forming assembly line, possibly in collaboration with other interactions on the enzyme`s surface.

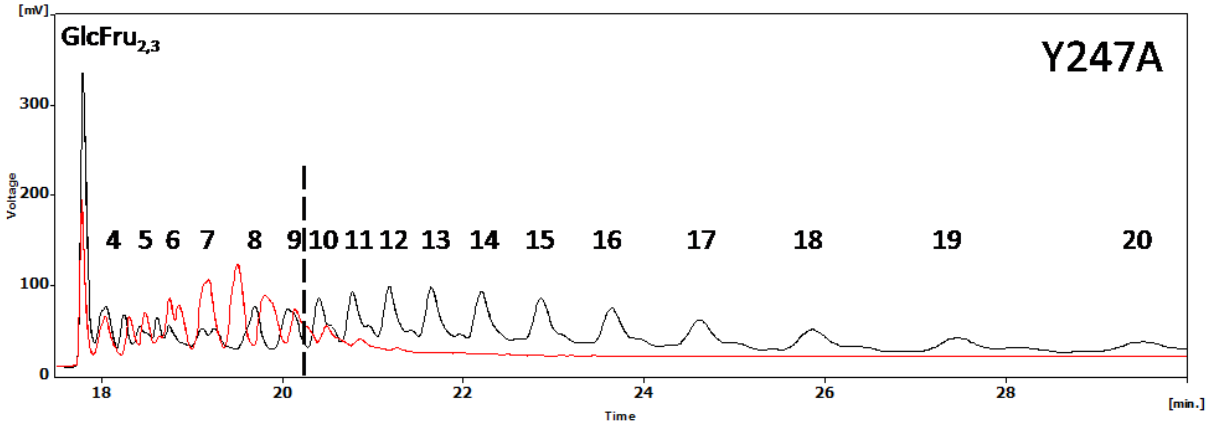

Figure 52 HPAEC analysis of the oligosaccharides synthesised by the wild-type SacB (black) and variant Y247A (red).

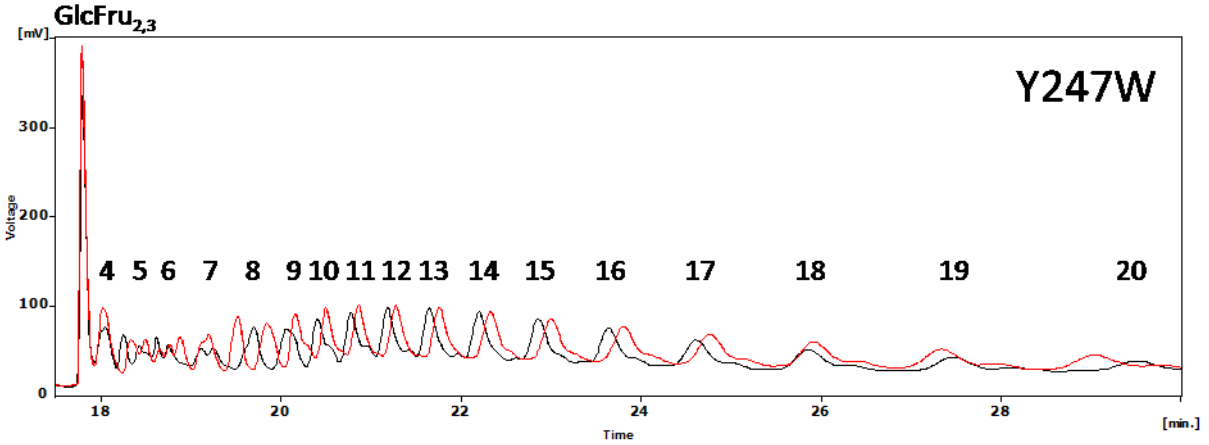

Figure 53 HPAEC analysis of the oligosaccharides synthesised by the wild-type SacB (black) and variant Y247W (red).

Interestingly, the hydrolysis activity of the variants is mostly enhanced compared to the wild-type except for H423Y and K315A (figure 56). According to its highly increased transfructosylation activity of 32 % (mol/mol), K315A forms significantly more oligosaccharides (figure 55). The K_m and k_{cat} of the variant are comparable to the wild-type SacB. Surprisingly, the exchange of lysine in position 315 to arginine does not have any effect that differs significantly from any wild-type parameter (figure 54).

The amino acid residue Lys315 is located in subsite +2 from the active site. It influences the formation of oligosaccharides apparently by indirect effects on other amino acid residues enhancing the oligofructoside formation.

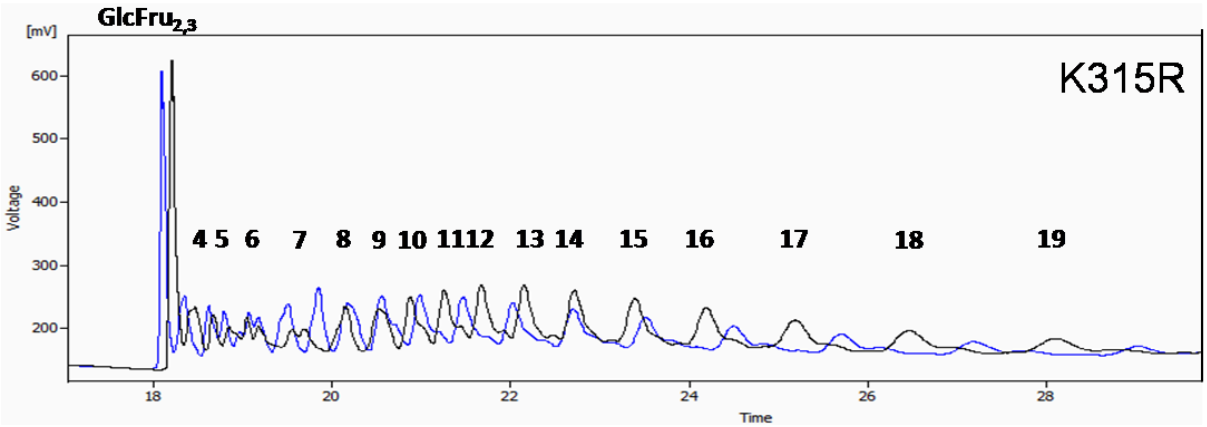

Figure 54 HPAEC analysis of the oligosaccharides synthesised by the wild-type SacB (black) and variant K315R (blue).

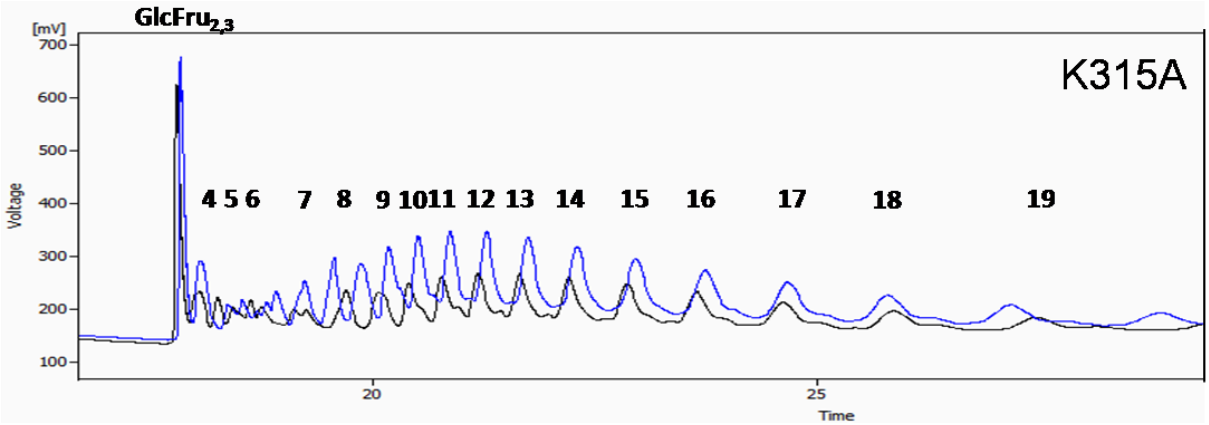

Figure 55 HPAEC analysis of the oligosaccharides synthesised by the wild-type SacB (black) and variant K315A (blue).

While the exchange of the histidine to tyrosine in position 423 has almost no influence on the K_m and k_{cat}, the transfructosylation activity is raised by 26 % [mol/mol]. The variant H423A has a seven-fold increased K_m while the k_{cat} remains in the wild-type range. Both HPAEC analysis` of the oligofructosides do not show any differences compared to the wild-type SacB.

The analysis of the absolute transfer and the enhancement of the transfer reaction elucidate the biochemical characteristics of the variants. The amount of glucose released which indicates hydrolysis was compared to the amount of free fructose. The difference must be transfer products (table 25, figure 56). The two variants with significantly enhanced transfer activity are H423Y (26 %) and K315A (32 %). The variants K315R and N312A show a hydrolysis/transfer activity similar to the wild-type. All other variants have an increased hydrolysis activity of up to 39 % (K373A). H423A and Y439A were inactive under the given reaction conditions.

Table 25 Concentrations of the hydrolysis products glucose (Glc) and fructose (Fru) determined by HPAEC. WT is the wild-type fructosyltransferase SacB from *B. megaterium*.

	Glc [mM]	**Fru [mM]**
WT	120	86
N312A	119	91
K315R	118	89
K315A	110	63
Y247A	121	97
Y247I	123	101
Y247W	130	91
S372A	126	96
K373R	115	102
K373A	124	119
Q381A	124	106
H423Y	108	71

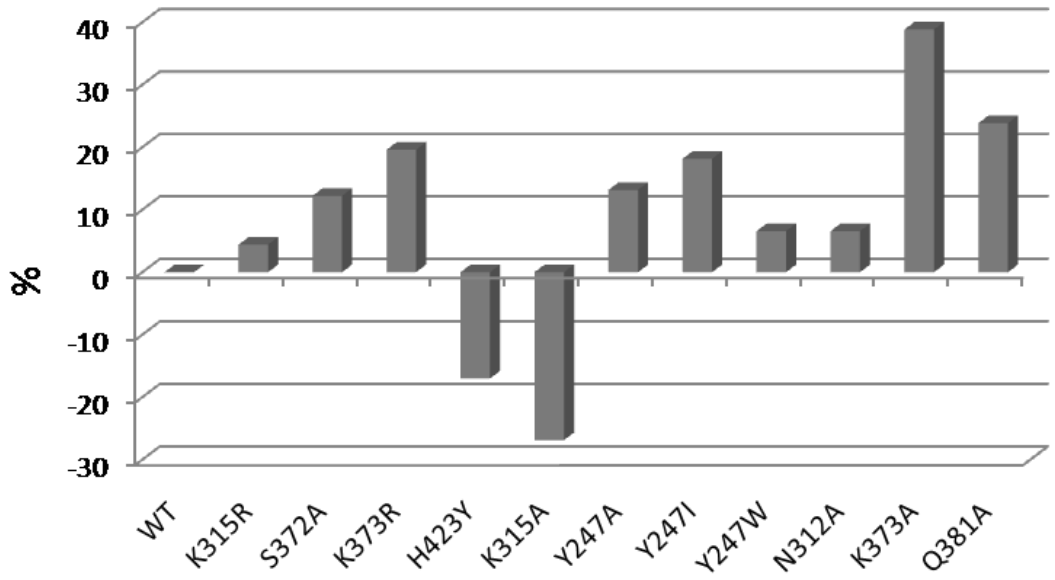

Figure 56 Hydrolysis activity of the wild-type fructosyltransferase SacB from *B. megaterium* (WT) and its variants. Deviance from the wild-type in % (mol/mol). The carbohydrate concentrations were determined by HPAEC.

The combination of biochemical data and structural information provide insights into the transfructosylation process. Clearly, the previously described arginine in position 370 interacts with the glucose unit in subsite +1. Our studies lead to the identification of many more amino acid residues not located in the active site. K373, N252 and Y247 form a nice platform for a possible stabilisation of the fructan chain. Although the biochemical data do not show definite abrogation of the polymerisation process, it is clearly visible that the variants K373A, N252A and Y247A synthesise unique mixtures of oligosaccharides of different chain length. With the help of the structural information, a clear subsite can be assigned to every amino acid residue (figures 57 and 59). However, it remains unclear if the oligosaccharide chain has a conformation that places more than one fructosyl unit in one subsite of the enzyme or if the oligosaccharide chain interacts with even more amino acid residues on the surface of the fructosyltransferase. Most likely, there`s a co-operation between the enzyme`s surface interaction with and the interaction between the fructosyl units of the oligosaccharide chain.

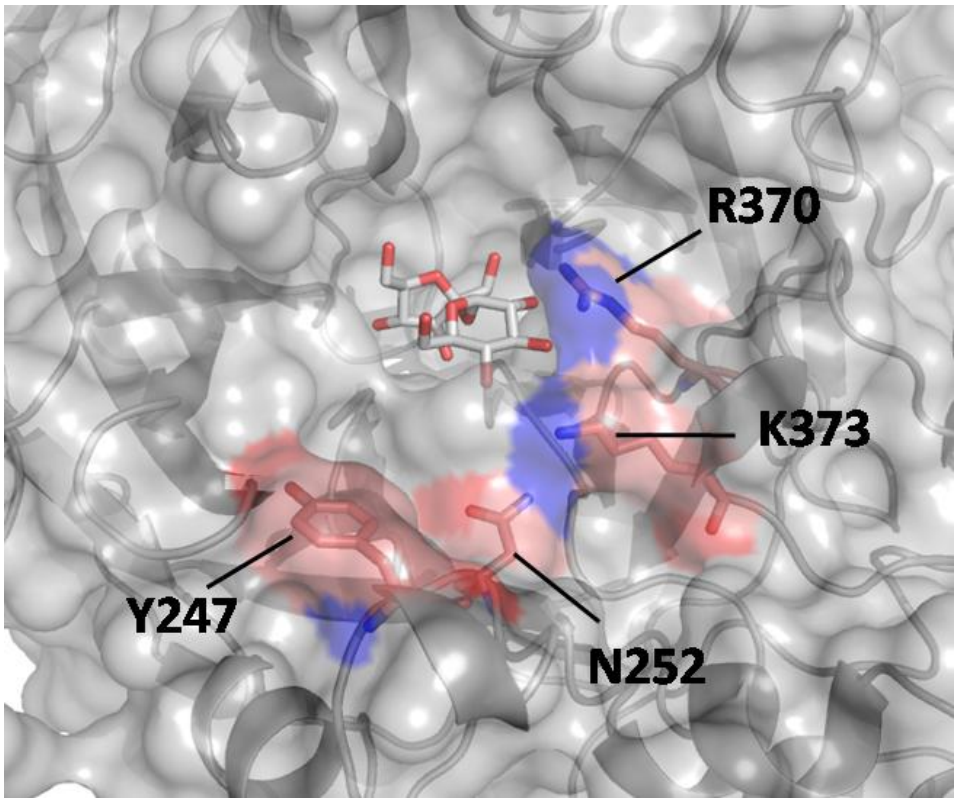

Figure 57 Surface model of the SacB from *B. megaterium* variant D257A with sucrose modelled in the active site. The amino acids with impact on the transfructosylation process are labelled and indicated by color.

The structural information along with the biochemical data suggests a possible attachment for the acceptor oligosaccharide chain on the surface of SacB. From the X-ray analysis` energy density data, it is observed that arginine in position 370 is flexible. The native enzyme shows an interaction of K373 with R370 (distance 3.13 Å) acting as a “fishhook” for the substrate sucrose already speculated by Meng and Fütterer. They crystallised the native enzyme and its substrate-bound conformation (Meng *et al.*, 2003; Meng *et al.*, 2008). The conformation of this arginine in the analogous position changes when the substrate sucrose binds in the active site.

Furthermore, in the native conformation a π-π-stacking of the fructan chain with the now accessible hydrophobic pocket formed by Y421 and H423 is possible (figure 58). In the substrate-bound conformation of R370, this pocket is blocked enabling the hydrolysis of sucrose (figure 58). The biochemical data for the mutagenesis studies of Y421 and H423 shows nearly wild-type K_m and k_{cat} values for variant H423Y. The tyrosine obviously is able to mimick the unpolar stacking interactions naturally

performed by histidine in this position. The variants Y421A and H423A have an increased K_m indicating a change in the active site interacting with the substrate sucrose. However, variant H423A keeps the wild-type turnover number.

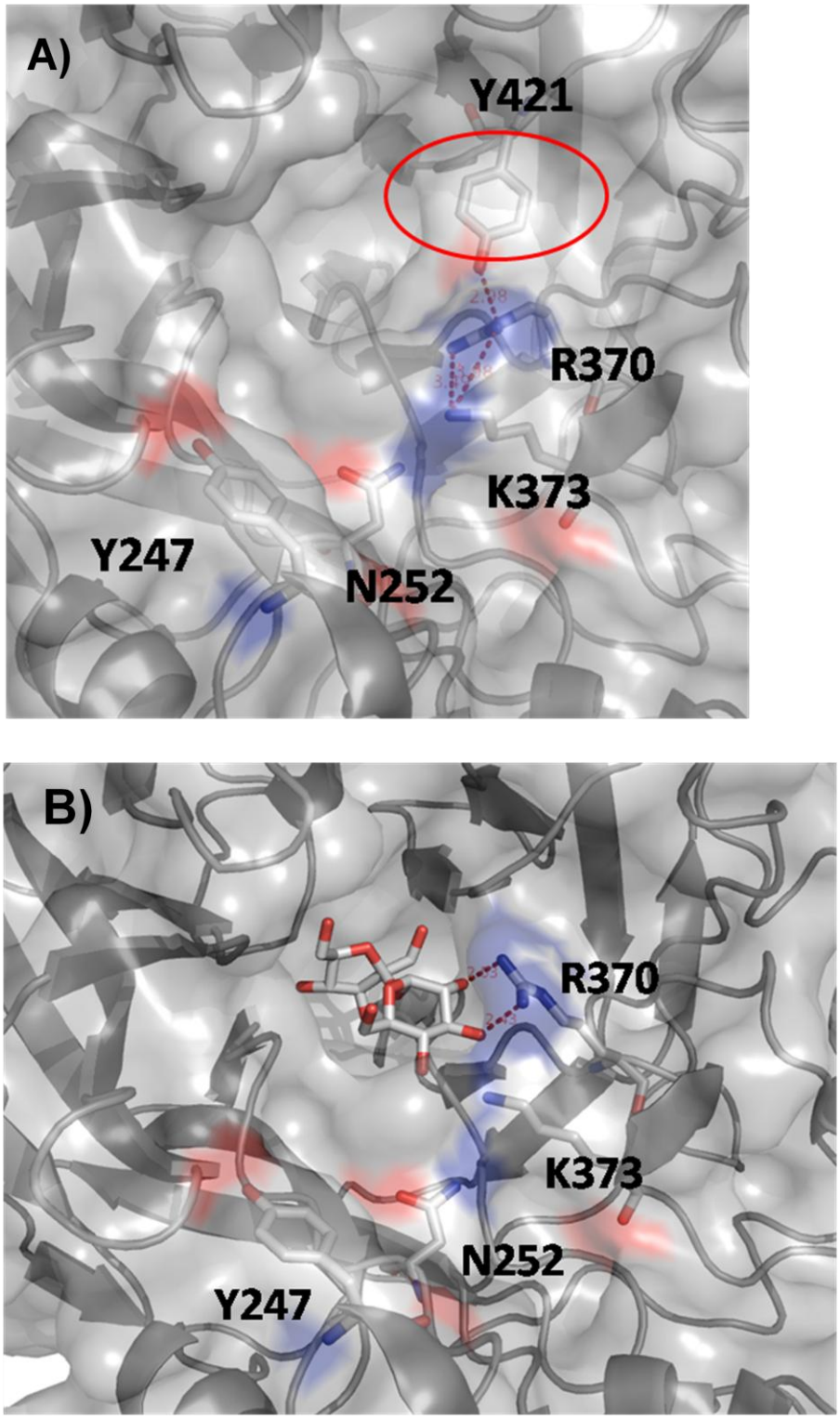

Figure 58 Surface of the fructosyltransferase SacB from *B. megaterium*. The amino acids with significant impact on the polymer formation are labelled. A) Crystallised conformation of SacB variant D257A with no substrate in the active site. R370 possibly interacts with Y421 and K373. B) Alternative conformation of R370 blocking the proposed stacking area formed by Y421. Sucrose is shown in the active centre.

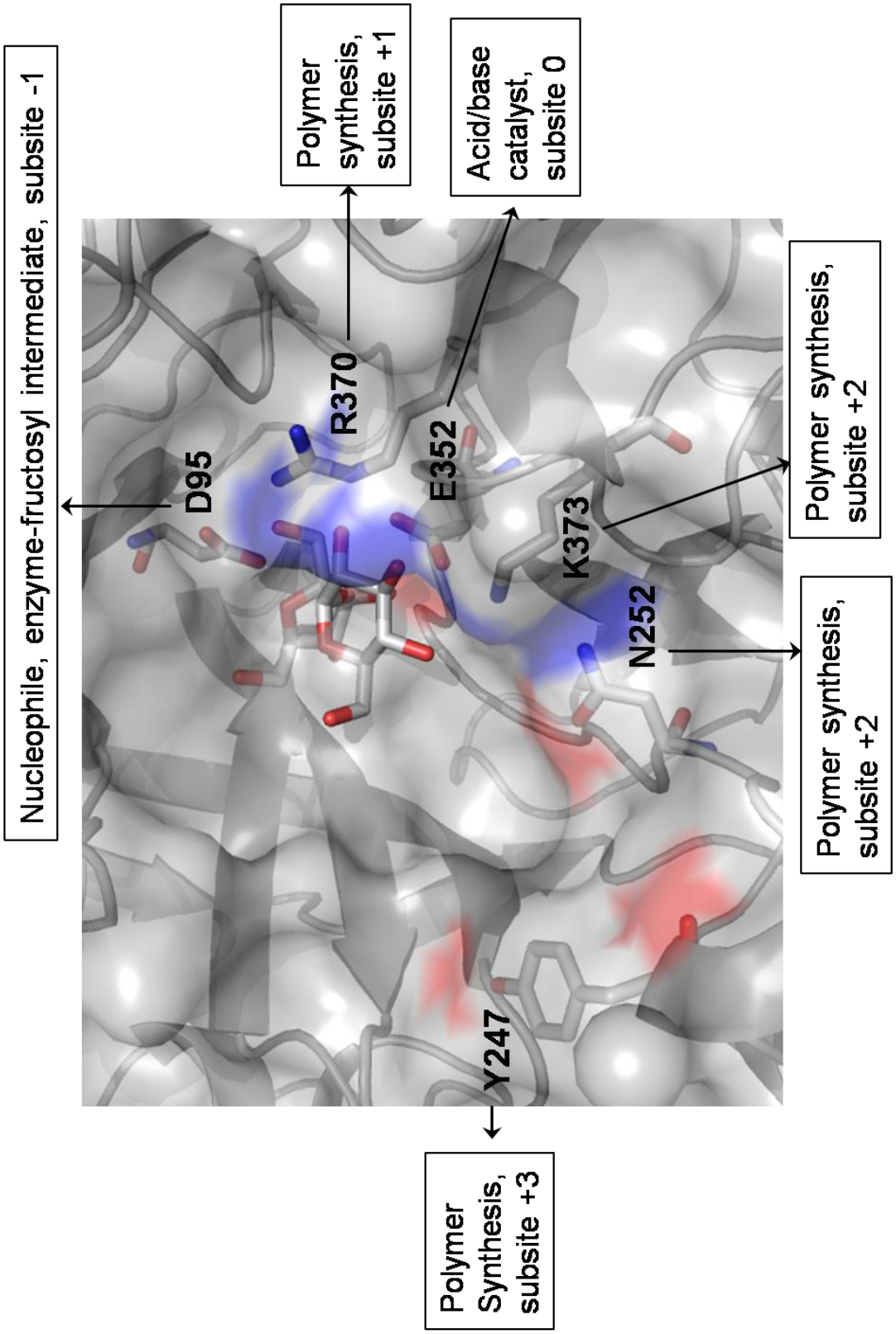

Figure 59 Summary of the most important amino acid residues of the fructosyltransferase SacB from *B. megaterium*.

4.4 Controlling the linkage type of sucrose and sucrose analogues – Impact of substrate engineering on the sucrose isomerase from *Protaminobacter rubrum*

A toolbox for the synthesis of tailor-made oligosaccharides is our aim. One step is the control of the carbohydrate linkage types. Here, we present the isomerisation of sucrose and a sucrose analogue, Gal-Fru, by the surcrose isomerase SmuA from *P. rubrum* (figure 60). Gal-Fru has been previously synthesised by a novel fructosyltransferase from *B. megaterium* according to the enzymatic synthesis by the fructosyltransferase from *B. subtilis* (Seibel *et al.*, 2006b).

Three sucrose isomerases, a trehalulose synthase from *Klebsiella* sp. LX3 (Zhang *et al.*, 2003), an isomaltulose synthase from *Pseudomonas mesoacidophilus* (Ravaud *et al.*, 2007) and a sucrose isomerase from *Protaminobacter rubrum* (Ravaud *et al.*, 2009) were previously crystallised and characterised. They belong to the large family GH13, which contains the well-characterised α-amylase. Also an oligo-(1,6)-glucosidase from *Neisseria* belongs to this family. The structure is an 8-stranded α/β-barrel containing the active site, interrupted by a ~70 amino acid calcium-binding domain protruding between β-strand 3 and α-helix 3, and a carboxyl-terminal β-barrel domain. Both structures contain the conserved catalytic triad with a glutamate acting as general acid/base catalyst. Both sucrose isomerases have a certain unspecificity concerning the formation of the isomerisation product. They form up to 90 % of isomaltulose or trehalulose respectively, depending on the bacterial strain. The sequences have an identity of 69 % and 80 % positive amino acids (figure 61). The sequence also shows an identity of 98 % compared to an α-glucosyltransferase from *Klebsiella*. Both structural informations show a central cavity for the disaccharide with a pair of phenyl residues on the entrance/exit (figure 64). Mutation of these phenylalanine shifts the enzyme to hydrolysis. The sucrose isomerase from *P. rubrum* contains a highly conserved active site and act via a double-displacement mechanism forming a glycosyl intermediate (Davies *et al.*, 1995; Mosi *et al.*, 1997; Yoshioka *et al.*, 1997; Uitdehaag *et al.*, 1999; Jensen *et al.*, 2004). The catalytic triad of the sucrose isomerase from *P. rubrum* consists of the amino acid residues D214, E268 and D342 (figures 62 and 63). An aromatic clamp with impact on the hydrolysis *versus* transfructosylation activity has been described for GH 5 enzymes*, i.e*. the

fungal exo-glucanase subfamily (Cutfield *et al.*, 1999) and an endocellulase (Ducros *et al.*, 1995). In the sucrose isomerase from *P. rubrum* it is formed by the amino acid residues F270 and F294 (Ravaud *et al.*, 2009; figure 64).

Recent findings describe mutations of two arginine residues of the sucrose isomerase from *Protaminobacter rubrum* yielding variants which synthesise predominantly isomaltulose (6-*O*-α-D-glucopyranosyl-β-D-fructose). With addition of an acceptor, in the published experiment glucose, an acceptor reaction towards enhanced isomaltose synthesis is observed. Our study shows the potential of the sucrose isomerase from *P. rubrum* to synthesise novel isomaltulose analogues by substrate engineering approaches (figure 60).

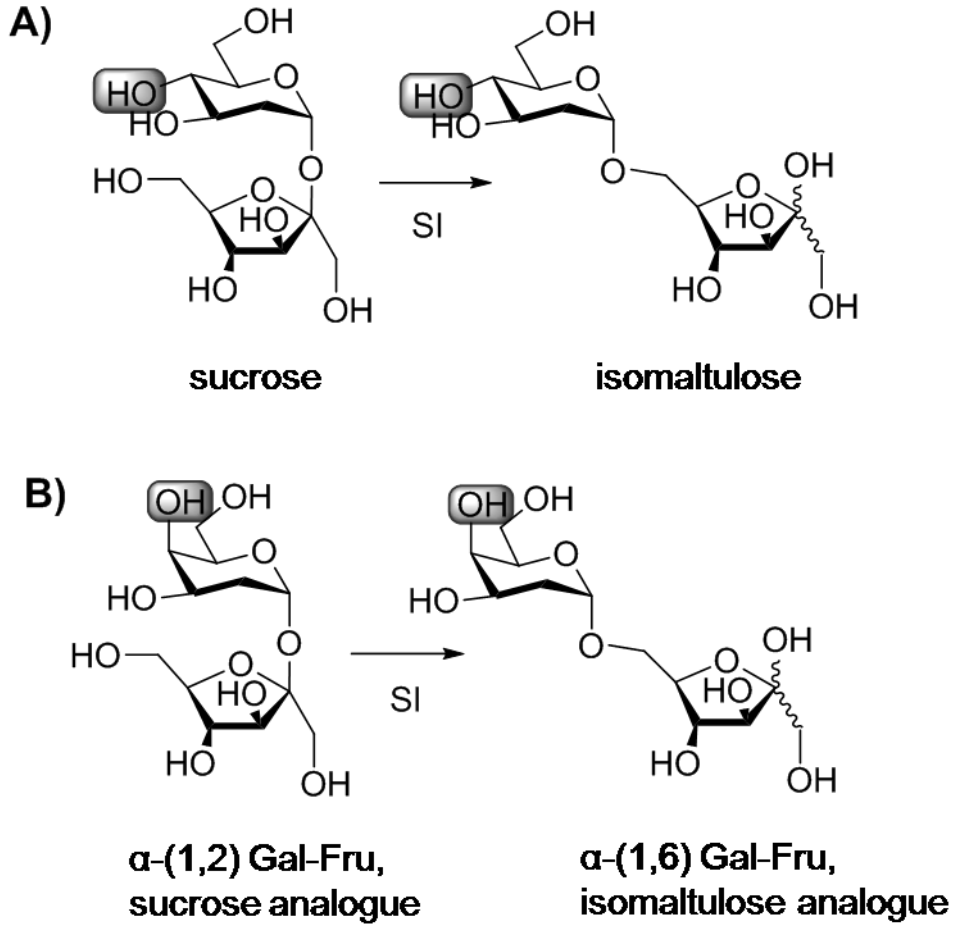

Figure 60 The isomerisation reaction catalysed by the sucrose isomerase (SI) from *P. rubrum*. A) The native reaction with sucrose as substrate yielding isomaltulose, B) the isomerisation of the sucrose analogue Gal-Fru (α-(1,2)-linkage) yielding the isomaltulose analogue (α-(1,6)-bound).

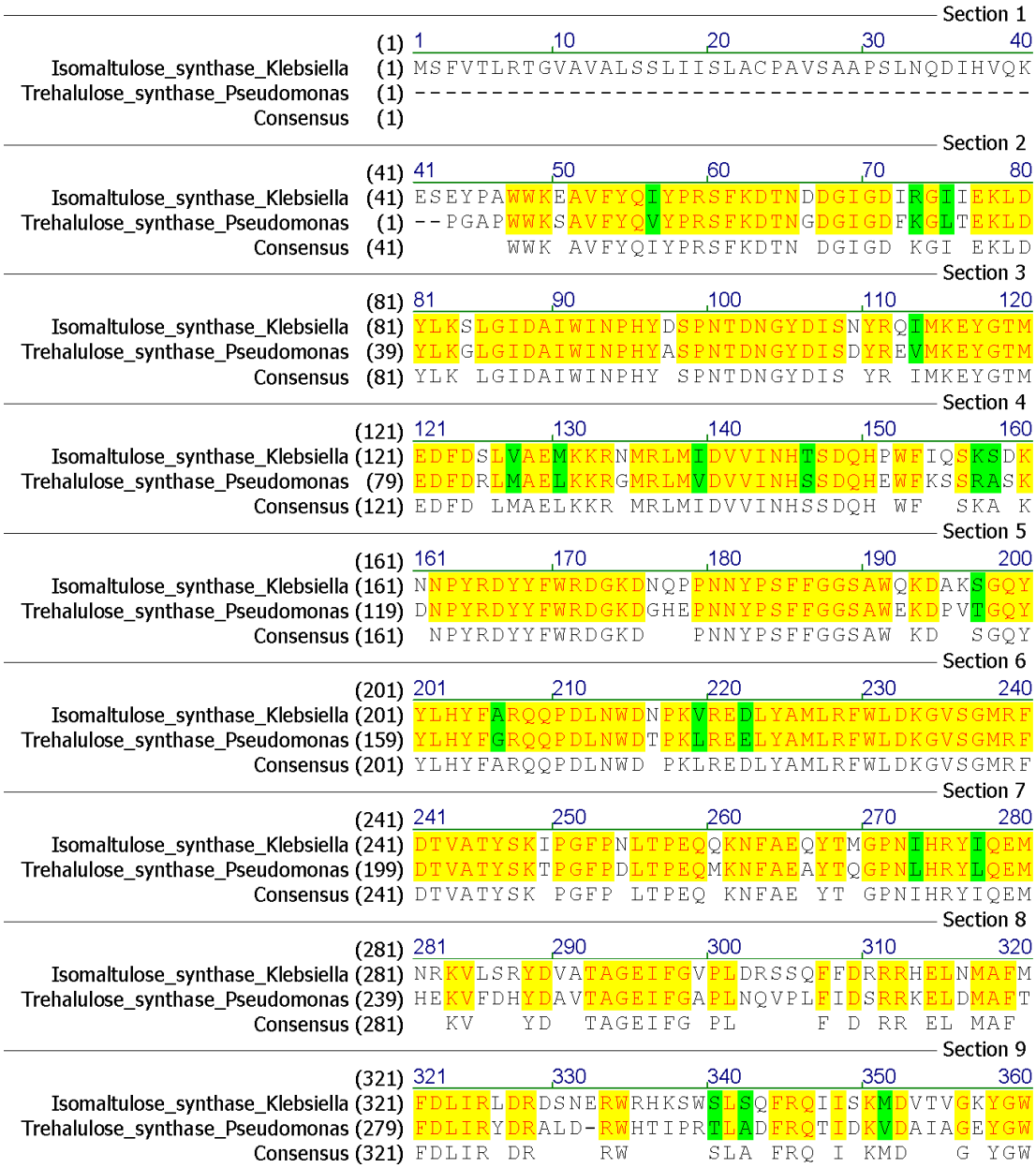

Figure 61 Alignment of the isomaltulose synthase from *Klebsiella sp*. LX3 and the trehalulose synthase from *Pseudomonas mesoacidophila*. Yellow background indicates the identical amino acid residues and in green the positive matches.

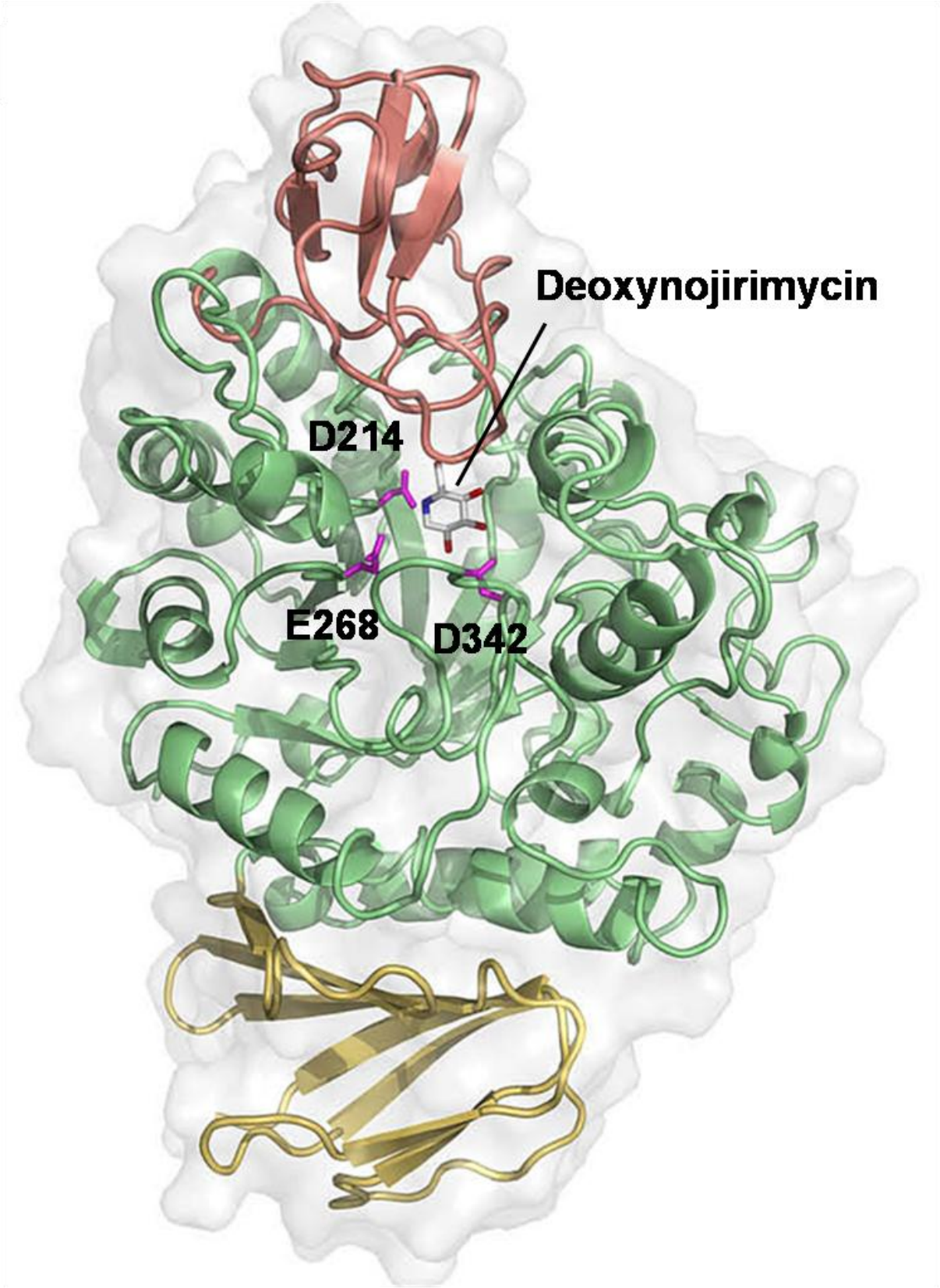

Figure 62 Structure of the sucrose isomerase SmuA from *P. rubrum* co-crystallised with the inhibitor deoxynojirimycin. The catalytic triad is highlighted in magenta (Ravaud *et al.*, 2009).

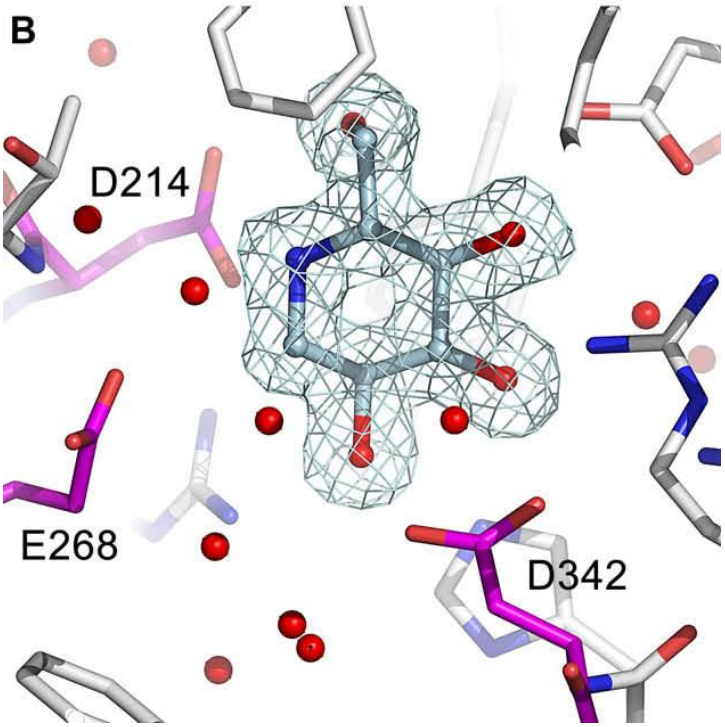

Figure 63 Adapted from Ravaud *et al.*, 2009: The active site of the sucrose isomerase SmuA from *P. rubrum* cocrystalliysed with the inhibitor deoxynojirimycin. The catalytic triad (D214, E268, D342) is highlighted in magenta.

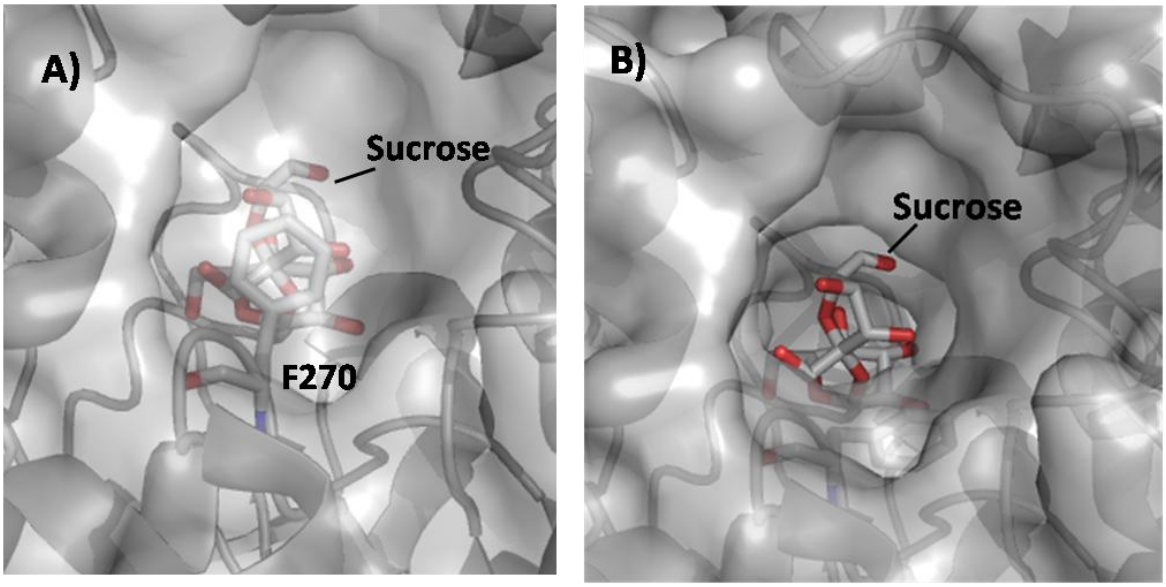

Figure 64 The location of amino acid residue Phe270 in the active site of SmuA from *P. rubrum* with modelled sucrose. A) The closed and B) the open conformation of Phe270 in the native active site of *P. rubrum*.

4.4.1 Docking studies of the sucrose isomerase from *Protaminobacter rubrum* with the sucrose analogue Gal-Fru as substrate

Our docking studies show a potential access for sucrose and sucrose analogues to the active site as well as possible conformations of the sucrose analogue Gal-Fru (figure 65). Docking studies were performed with the structure of the sucrose isomerase SmuA from *P. rubrum*. Sucrose and the sucrose analogue Gal-Fru were used as substrates. The results show the position of sucrose in the active site of the enzyme in a slightly different conformation compared to the cocrystallised sucrose in the active site of the highly similar trehalulose synthase from *Pseudomonas mesoacidophila*. This is potentially due to missing stacking interaction of the glucose moiety with a tyrosine in position 64 (SmuA numbering) which cannot be handled by the docking software. A comparison of the docked sucrose analogue Gal-Fru with the natural substrate sucrose shows a potential conformation slightly different to the crystallised sucrose. The pocket for the glucosyl or galactosyl moiety, respectively, in subsite -1 is limited by some unpolar and aromatic phenylalanine residues. Our docking results suggest that the axial O4 of the galactosyl residue is positioned like the O6 of glucose for maintaining the interaction with the transition state stabiliser D214 (figure 65). The O6 of the galactosyl is in the same position as the C6 of glucose thus not interfering sterically with adjacent amino acid residues (figure 65). The position of the glycosidic bond is also slightly shifted. It is estimated that in the case of Gal-Fru as a substrate D342 acts as the transition state stabiliser. In both figures, F270 positioned at the entrance/exit of the active site is shown.

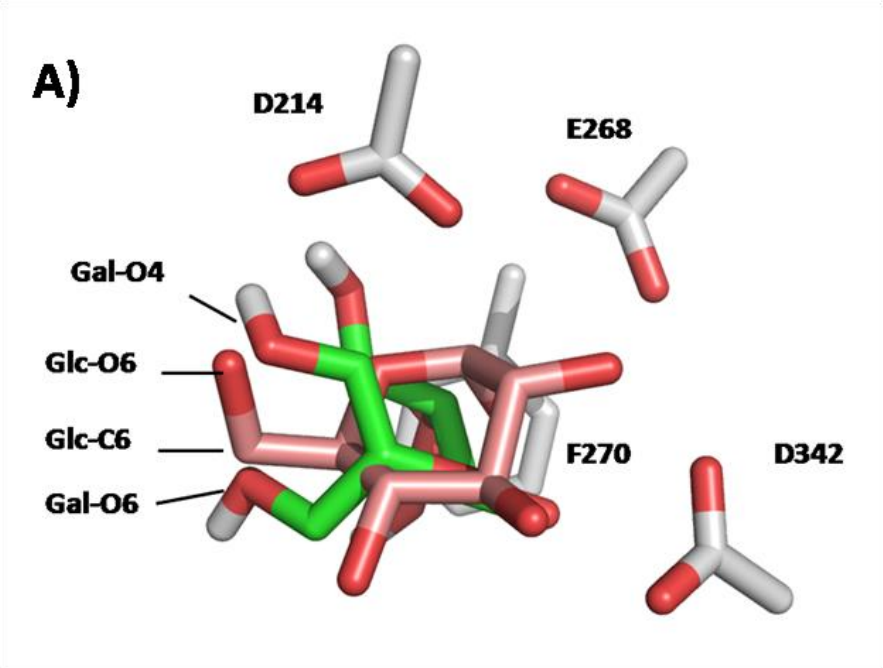

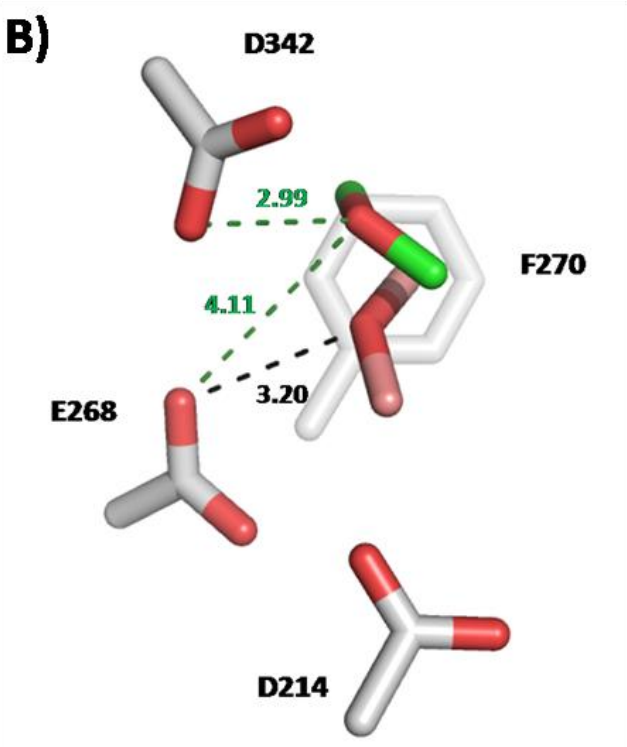

Figure 65 The active site of the sucrose isomerase SmuA from *P. rubrum*. The catalytic triad is formed by the amino acid residues D214 (transition state stabilizer), E268 (acid/base catalyst) and D342 (substrate orientation). F270 at the entrance/exit of the active site is shown as an orientation. A) The docked conformations of the glucosyl (rosé) and galactosyl (green) moiety of the natural substrate sucrose and the sucrose analogue Gal-Fru. B) Only the atoms of the glycosidic linkage and their

interaction with the amino acid residues of the catalytic triad are shown (colour scheme as in A). The docking procedure was performed with Autodock 4 (Scripps Research Institute, LaJolla, CA). The figure was drawn by pymol (DeLano scientific).

4.4.2 Substrate engineering of the sucrose isomerase from *Protaminobacter rubrum*

The action of the wild-type sucrose isomerase (SI) from *P. rubrum* on sucrose and sucrose analogues was investigated. The sucrose isomerisation reaction was first analysed in terms of the concentration of alginate-immobilised cells (w/v), temperature and pH by TLC and HPAEC (figures 66 and 67).

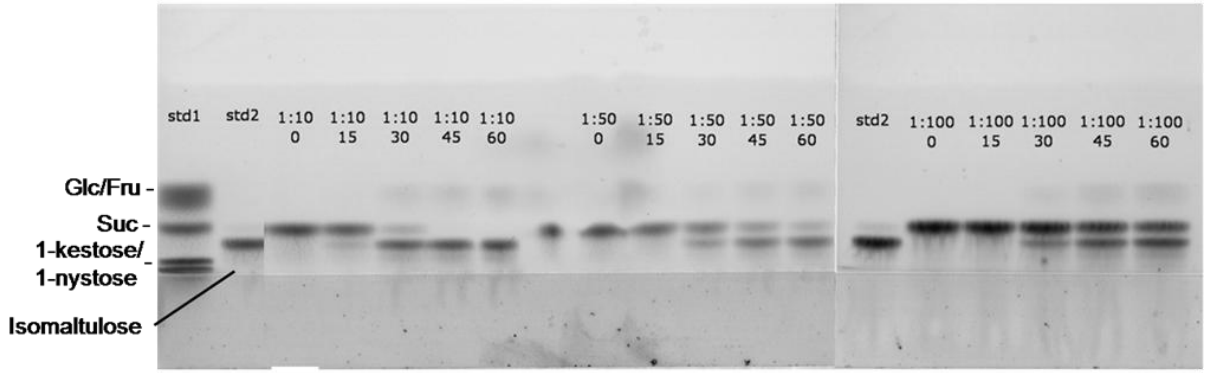

Figure 66 The isomaltulose synthesis was performed with sucrose isomerase (1:100 (w/v) of immobilized cells) at 37 °C and 500 mM of sucrose in Sörensen`s phosphate buffer, 50 mM, pH 6.6.

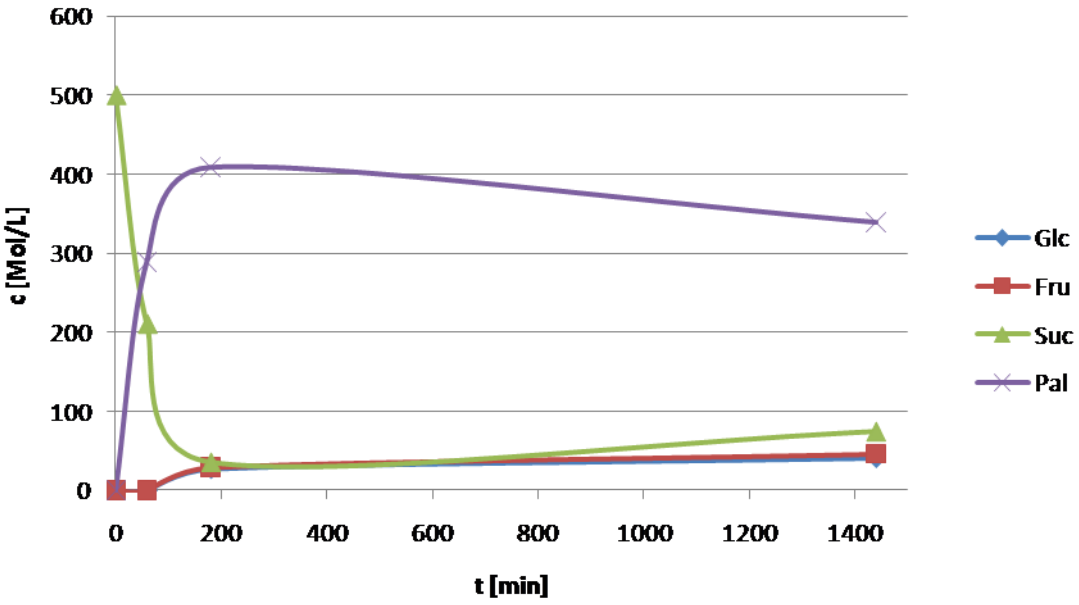

Figure 67 The sucrose isomerase SmuA from *P. rubrum* acting on sucrose (500 mM) at 37 °C and 1:100 (w/v) immobilised cells in Sörensen`s phosphate buffer, 50 mM, pH 6.6. Glc is glucose, Fru is fructose, Suc is sucrose and Pal is isomaltulose (synonymous to palatinose).

The optimum yield of isomaltulose was 82 % after 3 h at 37 °C and 1:100 (w/v) immobilised cells in Sörensen`s phosphate buffer, 50 mM, pH 6.6. With the identical reaction parameters we investigated Gal-Fru as substrate for the sucrose isomerase. The TLC analysis was promising, a new band appeared lower than sucrose (figure 68).

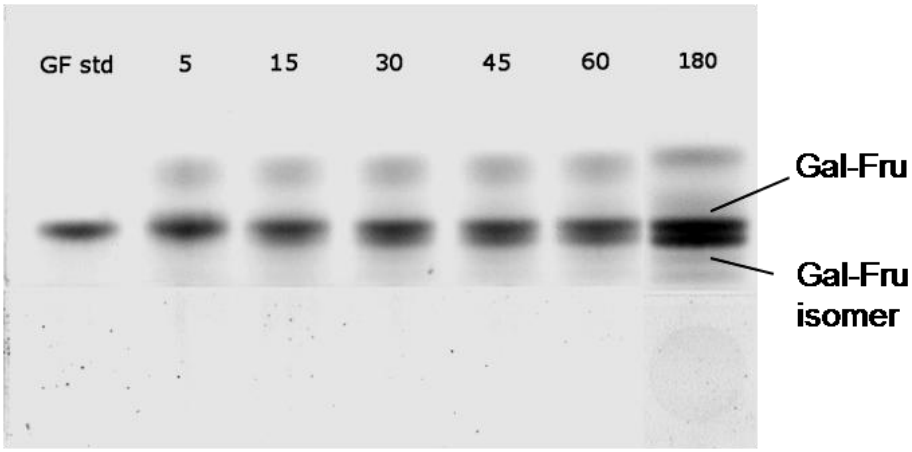

Figure 68 Formation of the isomaltulose analogue of Gal-Fru at 37°C and immobilised cells in a concentration of 1: 100 (w/v) in Sörensen`s phosphate buffer, 50 mM, pH 6.6.

Isolation of the molecule corresponding to the newly appeared band by silica and analysis by NMR proved the shift in the linkage type from α-(1,2) to α–(1,6). The ^{13}C-NMR data from isomaltulose (Thompson *et al.*, 2001) and the carbon spectrum of the Gal-Fru isomer are almost identical (table 26, figures 69 and 70). That indicates a linkage shift of Gal-Fru to α–(1,6). In the ^{1}H-NMR the H-4 of the galactosyl moiety was identified at 4.01 ppm as a doublet of a doublet with coupling constants of 3.71 and 8.25 Hz. The signal of the H-1 of the anomeric centre of the galactosyl moiety resonates at 4.87 ppm as a doublet with a coupling constant of 3.76 Hz. Thus, it can be concluded that the isolated compound is the galactosyl-containing analogue of isomaltulose.

Table 26 ^{13}C data for the α-/β-(1,6) isomer of the sucrose analogue Gal-Fru.

Carbon atom position	Galactose isomer of isomaltulose, δ_C
1	100.98
2	74.10
3	77.14
4	72.25
5	81.62
6	63.26
1´	65.25
2´	104.43
3´	75.67
4´	74.59
5´	77.87
6´	70.50

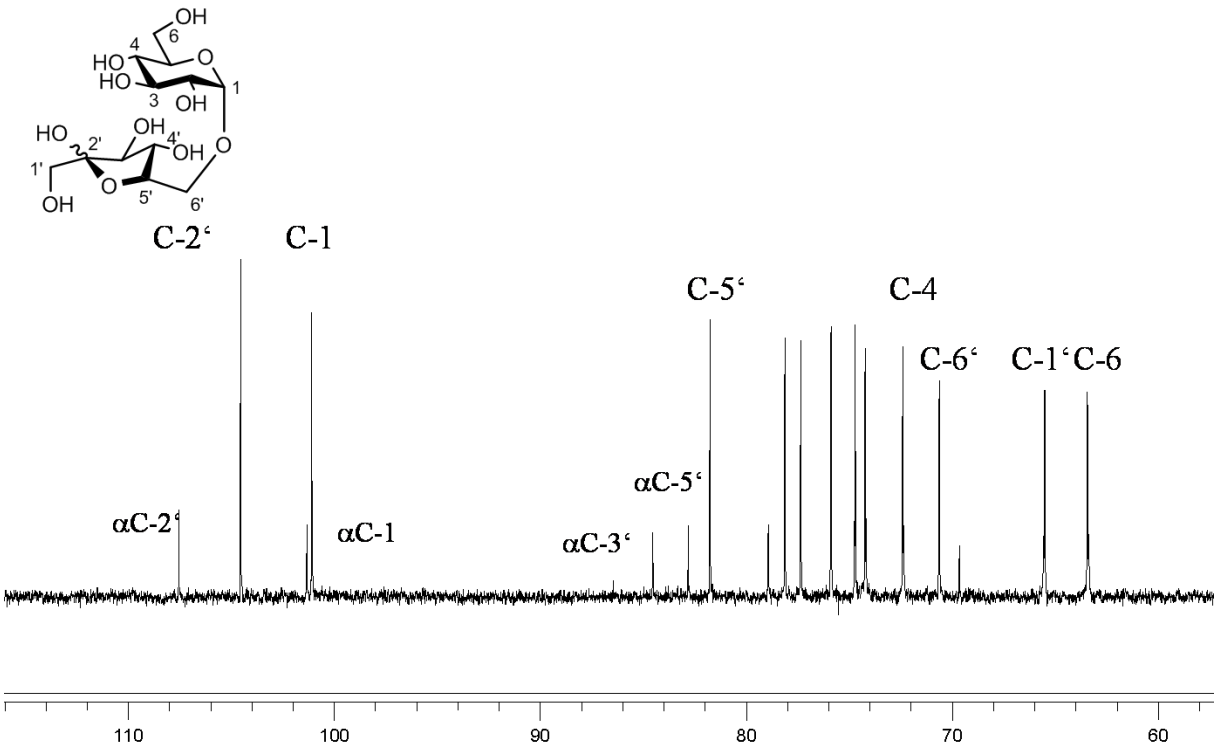

Figure 69 ^{13}C NMR spectrum of α-/β-isomaltulose synthesised by the sucrose isomerase from *P. rubrum*.

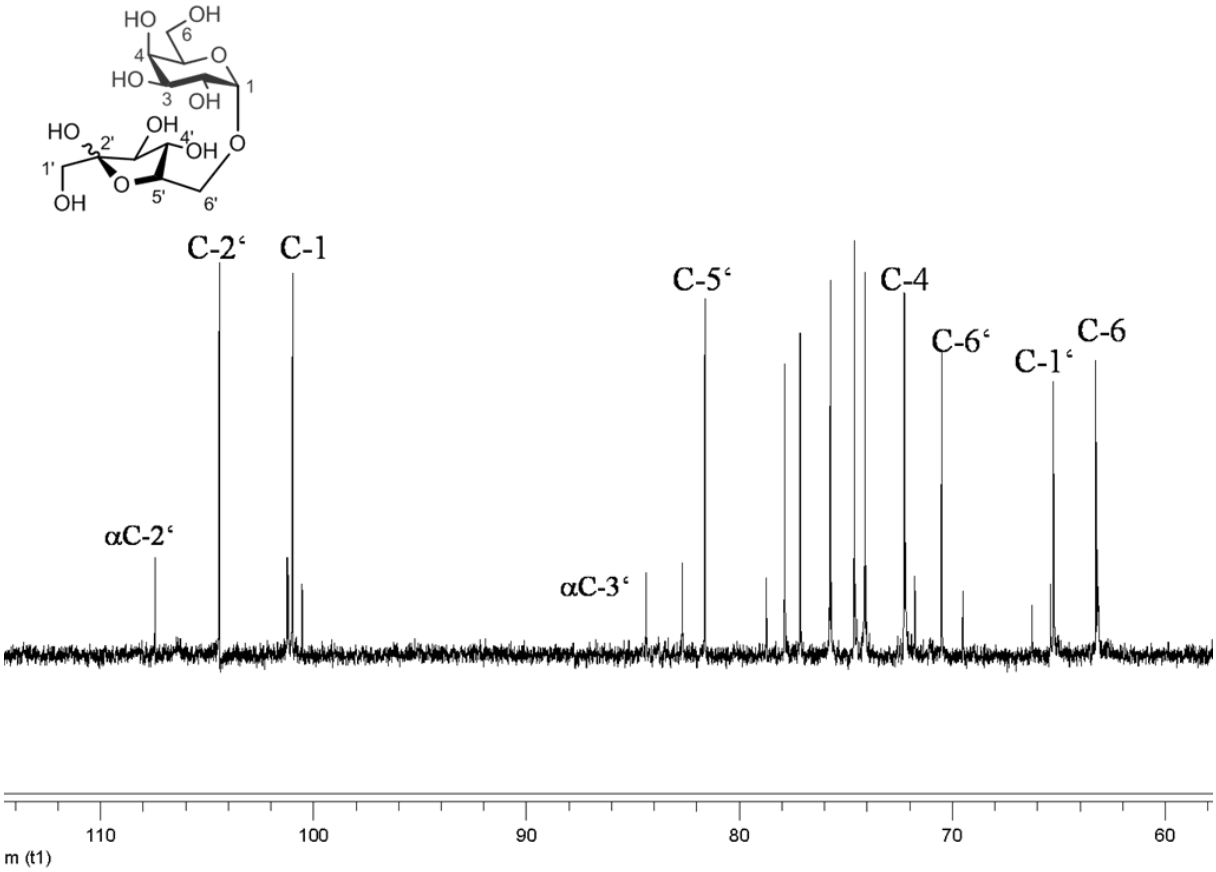

Figure 70 ^{13}C NMR spectrum of the α-/β-galactosylfructoside isomer synthesised by the sucrose isomerase from *P. rubrum*.

Our results show the potential of the sucrose isomerase from *P. rubrum* in performing a shift of the linkage type of sucrose analogues (α-(1,2)-) to isomaltulose analogues (α-(1,6))-linkages. By optimisation of the enzyme concentration and the reaction temperature we were able to follow the isomerisation reaction by TLC. Not only sucrose but also the sucrose analogue Gal-Fru was isomerised. The described potential of the enzyme to perform acceptor reactions when the arginine residues in position 325 and 328 are exchanged remains to be investigated.

4.5 Synthesis and physiological properties of novel fructo-oligosaccharides

Fructo-oligo- and polysaccharides have been known for several years as prebiotics. The growth of beneficial gut bacteria like *Lactobacilli* and *Bifidobacteria* is stimulated by these carbohydrate structures. Fructosyltransferases like inulosucrases and levansucrases which utilise fructans of various chain lengths as substrates are common in many different bacteria. However, although the structure of the levansucrase SacB from *Bacillus subtilis* was solved, the mechanism of fructosyl transfer and hydrolysis could not be elucidated until today. The reaction conditions like substrate concentration play a crucial role which products are formed. It was shown that the fructosyltransferases from *B. subtilis* and *B. megaterium* is able to synthesise sucrose analogues (Seibel *et al.*, 2006b). These act as substrates for the fructosyltransferase Suc1 from *Aspergillus niger* which synthesises defined kestose and nystose analogues (figure 71).

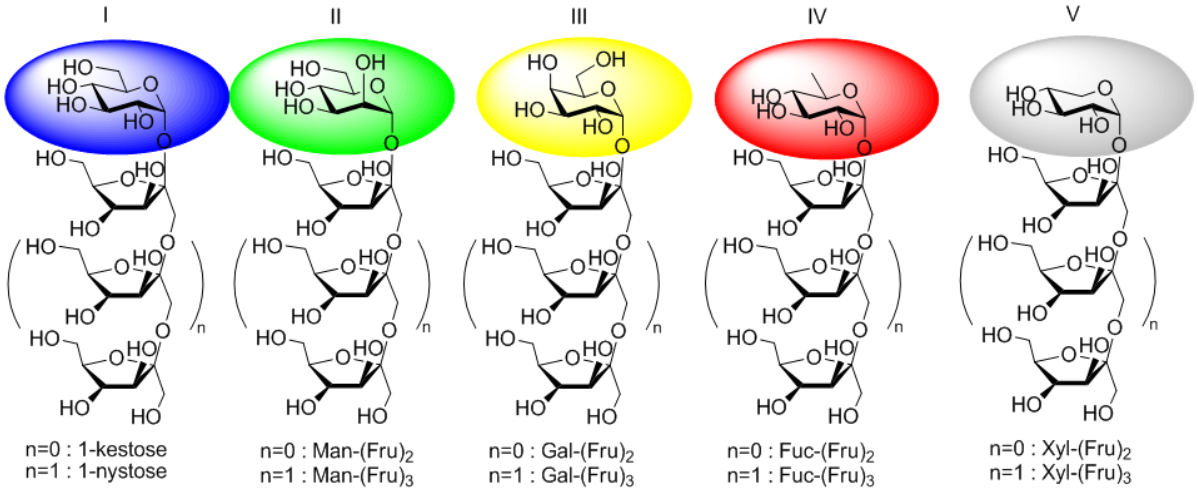

Figure 71 Fructo-oligosaccharide target structures. I) Established product on the market (1-kestose and 1-nystose). II) 1-kestose (Man-(Fru_2) or 1-nystose (Man-(Fru_3) analogue, III) 1-kestose (Gal-$(Fru)_2$) or nystose (Gal-$(Fru)_3$) analogue. IV) 1-kestose (Fuc-$(Fru)_2$) or 1-nystose (Fuc-$(Fru)_3$) analogue. V) 1-kestose (Xyl-$(Fru)_2$) or 1-nystose (Xyl-$(Fru)_3$) analogue.

The fructo-oligosaccharides were synthesised in order to be tested as substrates for beneficial gut bacteria and as immuno-stimulating agents in cultivations of human Caco-2 epithelial colorectal adenocarcinoma cells. The immunological response is the secretion of cytokines which have either direct or indirect influence on the activation of the immune system. Stimulation of the immune system by these novel pharmaceuticals can be useful to analyse inflammation processes. As auto-immune diseases like allergies are a growing problem in developed countries, specific stimulation of the immune system may prove useful to reduce this problem.

4.5.1 Synthesis of sucrose analogues by the fructosyltransferase SacB from *Bacillus megaterium*

The sucrose analogues were synthesized by a newly identified fructosyltransferase from *Bacillus megaterium*. *B. megaterium* is a rod-shaped Gram-positive soil bacterium. The fructosyltransferase SacB from *B. megaterium* was classified as EC 2.4.1.9 and GH 13 according to CAZy.

The synthesis of sucrose analogues was performed according to the synthesis of sucrose analogues with the fructosyltransferase SacB from *B. subtilis* published previously (Seibel *et al.*, 2006b). Briefly, the fructosyl moiety of sucrose is transferred to an acceptor monosaccharide of choice, *e.g.* mannose, galactose, xylose or fucose (figure 72). The acceptor reaction was performed with two-molar excess of the acceptor in Sörensen`s phosphate buffer (50 mM) at pH 6.6 and 37 °C. Purified enzyme in a concentration of about 10 mg l^{-1} or crude cell extract in an appropriate dilution was used. The acceptor reaction was followed by TLC (figure 73).

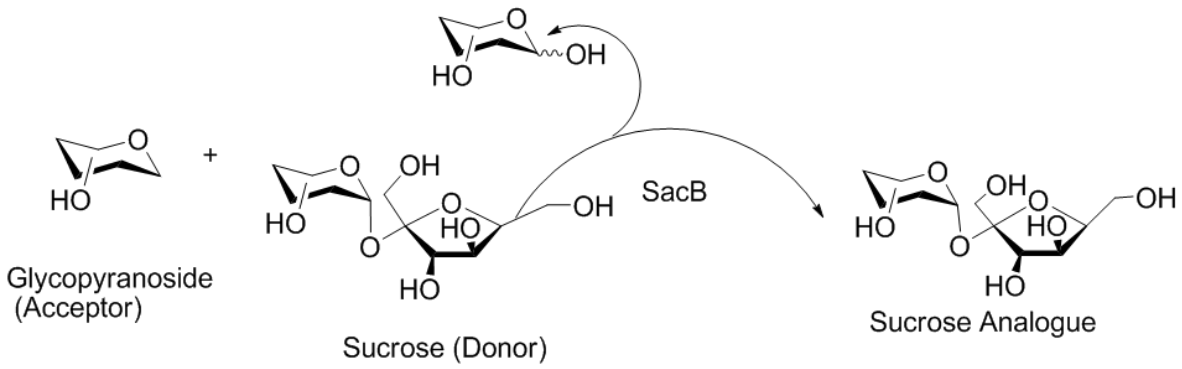

Figure 72 The synthesis of sucrose analogues performed by the fructosyltransferase SacB from *B. megaterium*.

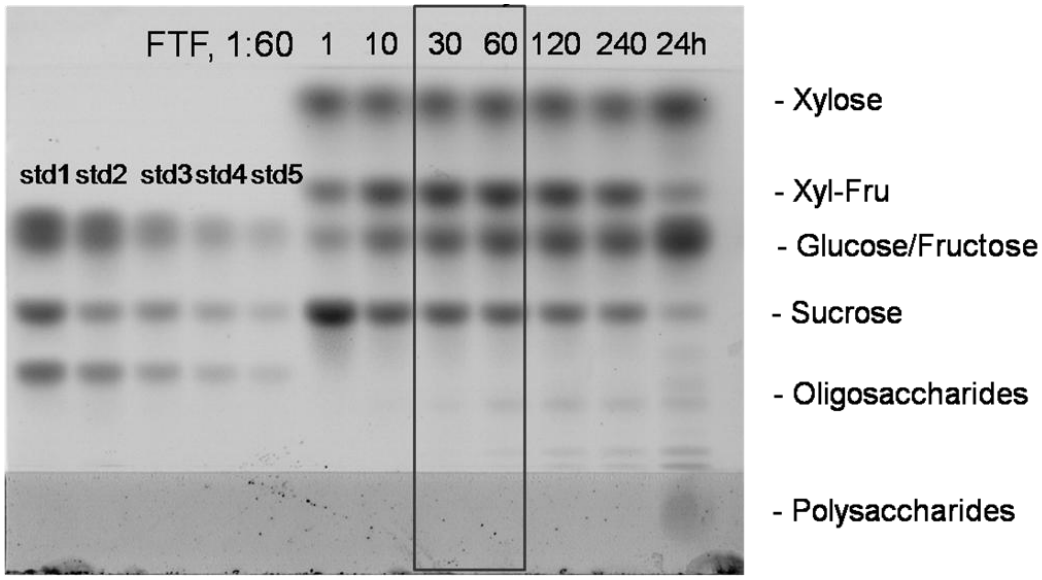

Figure 73 TLC analysis of the synthesis of the sucrose analogue xylosyl-fructoside (Xyl-Fru). The optimal time points for the best Xyl-Fru yield are boxed.

The resulting sucrose analogues were purified by silica columns.The products were analysed with standards by HPAEC. All the indicated target disaccharides as precursors for the synthesis of the novel fructo-oligosaccharides were synthesised (figure 71).

4.5.2 The fructosyltransferase Suc1 from *Aspergillus niger*

Cloning and expression of the fructosyltransferase Suc1 from *Aspergillus niger* was performed as previously described in cooperation with the group of Petra Dersch (Helmholtz-Centre for Infection Research) (Zuccaro *et al.*, 2008). Briefly, Suc1 from *Aspergillus niger* strain AB1.13 was identified after addition of sucrose to the growth medium. The gene of Suc1 was identified in the group of Petra Dersch (Department of Microbiology, TU Braunschweig and Helmholtz-Centre for Infection Research), amplified and cloned into the vector ANIp8 yielding the plasmid pSKAn1015. The plasmid was transformed back into the *A. niger* strain. An extract from a cultivation with the transformed *A. niger* pSKA1015 was analysed by SDS-PAGE. A band was identified at 120 kDa. The theoretical size of Suc1 calculated on the basis of the amino acid sequence is approximately 60 kDa. It is estimated that the difference in the molecular weight is due to post-translational modifications like glycosylation.

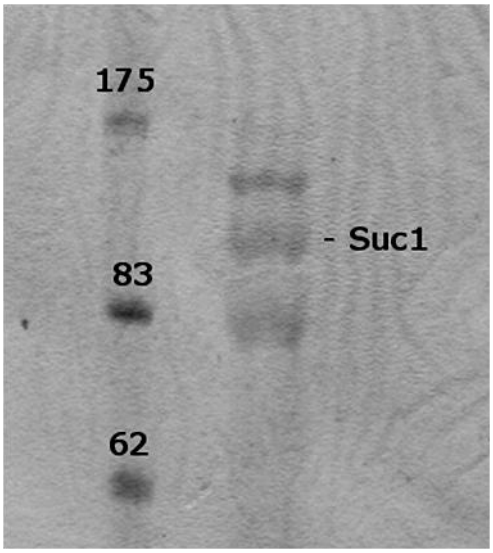

Figure 74 SDS-PAGE analysis of the culture supernatant from an *A. niger* SKAn1015 cultivation. The molecular weight of the standard proteins is indicated in kDa. Suc1 has an apparent molecular weight of about 120 kDa.

4.5.3 Purification of the fructosyltransferase Suc1 from *Aspergillus niger*

The purification of the fructosyltransferase Suc1 was performed as described in the methods part (3.7.9). FPLC size-exclusion chromatography was used for seperation of the proteins from the supernatant of the *A. niger* pSKAn1015 cultivation. The chromatogram shows 3 peaks (figure 75) most likely corresponding to the three bands visible on the gel from the SDS-PAGE analysis (figure 74).

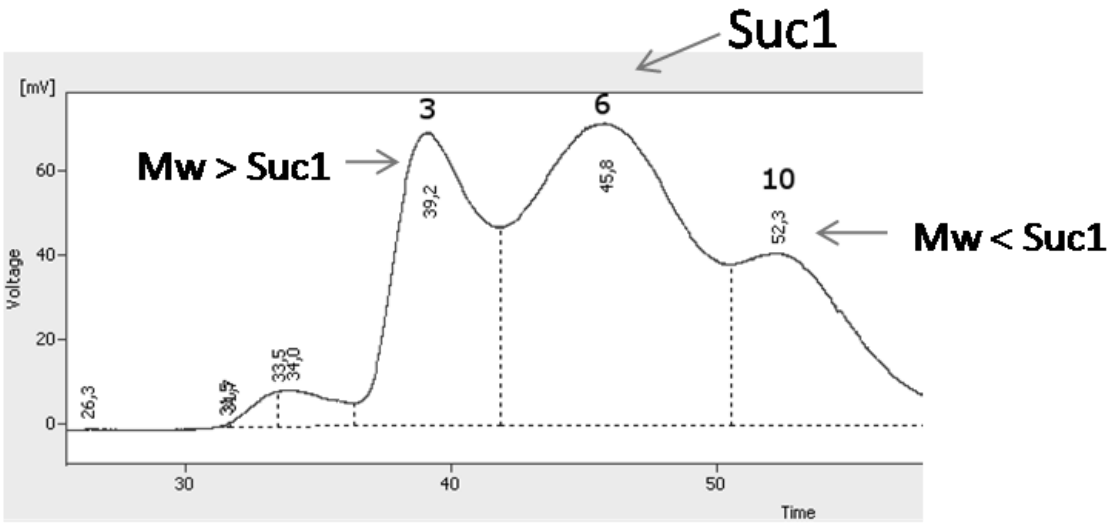

Figure 75 FPLC chromatogram of the Suc1 purification. Purification was performed by size-exclusion with Sephadex 200 (Invitrogen).

The activity test on sucrose of the peak fractions was performed according to the protocol described in the methods part (3.7.11). The TLC analysis shows the highest activity for the fractions 4 and 5 which are part of the peak indicated by “6” in the chromatogram (figure 76).

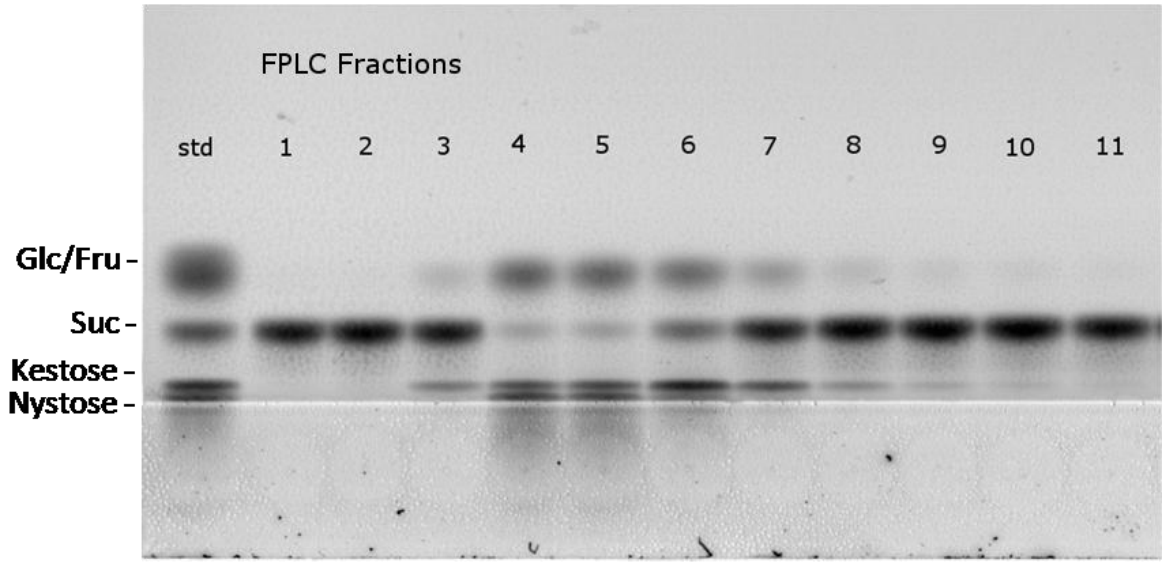

Figure 76 TLC analysis of the acitivity of the FPLC fractions peak fractions (figure 75) incubated with sucrose (500 mM) for 3 h at 40 °C, pH 5.6. The enzyme concentration was 1/20 of the reaction volume.

According to the results of the activity test (figure 76), the FPLC fractions 4 and 5 were mixed and analysed by SDS-PAGE (figure 77).

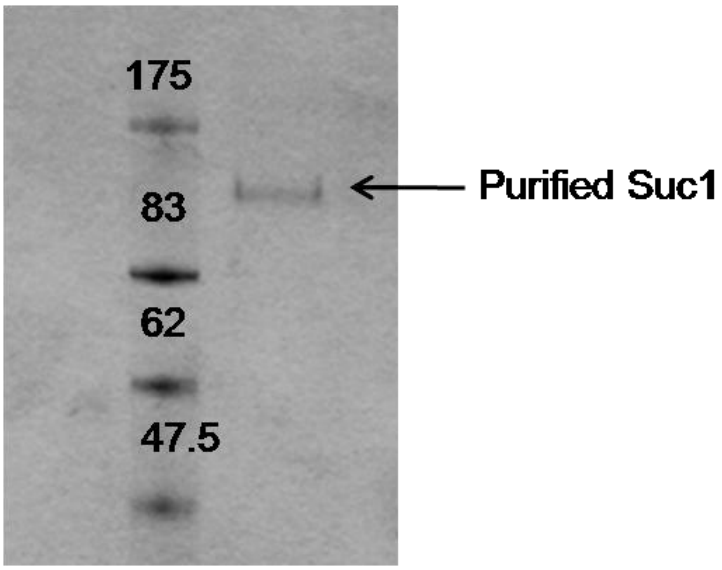

Figure 77 SDS-PAGE of the purified Suc1 with an apparent molecular weight of approximately 120 kDa. The molecular weight of the standard proteins is given in kDa.

4.5.4 Functional analysis of the glycosylation pattern of the fructosyltransferase Suc1 from *Aspergillus niger*

The apparent molecular weight of the fructosyltransferase Suc1 from *A. niger* was 120 kDa. It was assumed that the discrepancy to the theoretical molecular weight of 60 kDa is due to post-translational modifications. Glycosylation can lead to much higher molecular weights of proteins. The *N*-glycosylation motifs are generally large glycan patterns common for post-translational modifications of glycoproteins (figure 78).

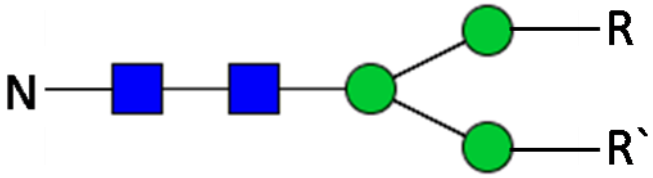

Figure 78 Simplified structure of the *N*-glycan core linked to an asparagine residue (N) of the sequon N-X-S/T. The blue squares are *N*-acetylglucosamine and the green circles are mannose. At the mannose residues R and R` further glycans may be attached yielding possibly large glycosylation motifs, *e.g.* high-mannose- or complex-type glycans.

In order to prove the glycosylation of Suc1, PNGase F was used to deglycosylate Suc1. After 24 h incubation, the PNGaseF digestion yielded a protein band in the range of the proposed size of deglycosylated Suc1 when analysed by SDS-PAGE (figure 79). The reason why the band is not seen in the range of the theoretical mass of 62 kDa may be due to altered migration characteristics compared to the standard proteins. Recently an altered SDS loading capacity was described for certain membrane proteins (Rath *et al.*, 2009). An activity test of the protein corresponding to this band proved it to be the deglycosylated Suc1 (figure 80).

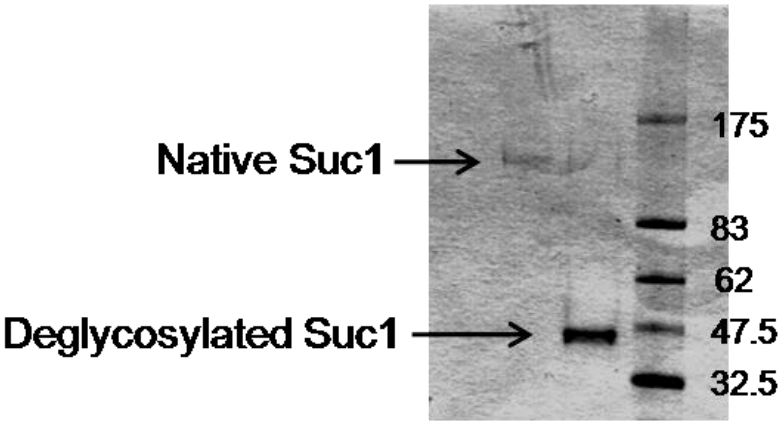

Figure 79 SDS-PAGE analysis of the deglycosylation of the fructosyltransferase Suc1 from *A. niger*. The left lane is the native purified Suc1, the middle lane is the deglycosylated protein. The right lane shows the standard [kDa].

An activity test of the native Suc1 and the deglycosylated form clarified whether the glycosylation pattern has any influence on the product formation activity. The test was performed according to the protocol described in the methods part (pH 5.6, 40 °C, 500 mM sucrose and 1/20 volume Suc1).

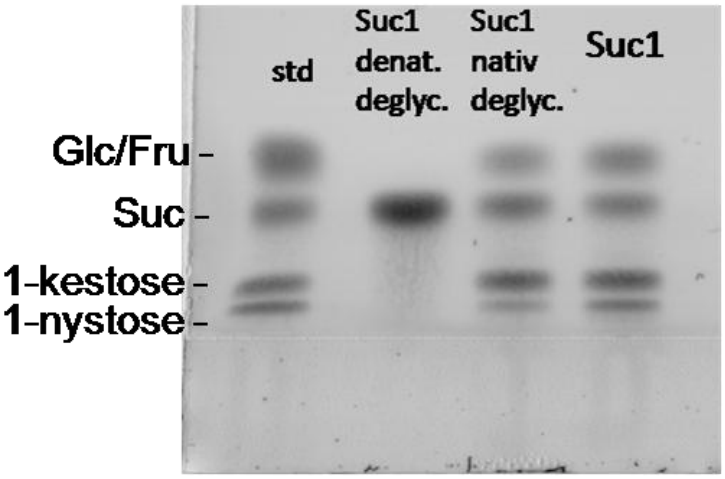

Figure 80 Activity test of the native glycoform and the deglycosylated Suc1. 1-kestose and 1-nystose are still synthesised by the deglycosylated Suc1.

In order to analyse the structure of the Suc1 and its mechanism of fructosyl transfer a structure of the enzyme is necessary. As there is no 3D-structure of an inulosucrase available yet, the amino acid sequence was the basis for an *in silico* calculation of the Suc1 structure. The modelling was performed by the web-based software ESyPred3D (http://www.fundp.ac.be/sciences/biologie/urbm/bioinfo/esypred).

The alignment of the fructosyltransferase Suc1 from *A. niger* with the exo-inulinase from *A. awamori* shows potential structural characteristics responsible for the transfer *vs*. hydrolysis reactions. The exo-inulinase which cleaves fructosyl moieties from a polysaccharide has a much smaller active site with an unpolar surface. Thus, an acceptor molecule can not attach to form acceptor products. The active site of Suc1 is wider and consists of some polar amino acid residues allowing a potential attachment of an acceptor molecule (figure 81).

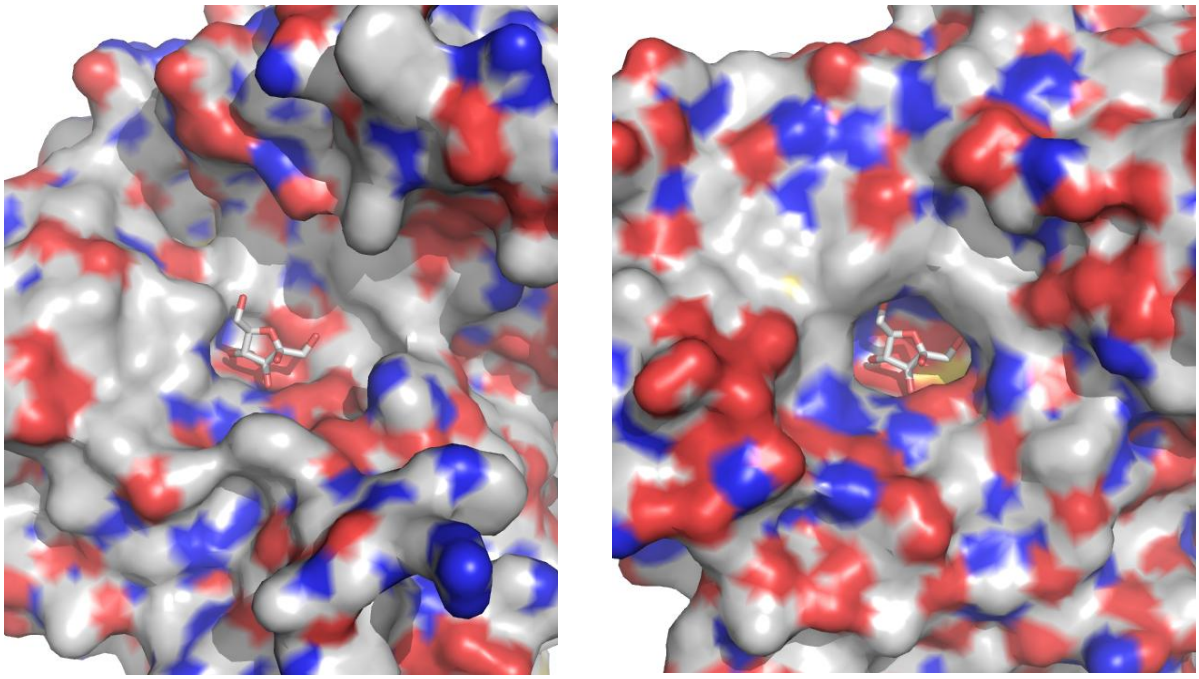

Figure 81 Comparison of the active site surface area of the fructosyltransferase Suc1 from *A. niger* (left side, modelled with EsyPred3D) and the exo-inulinase from *A. awamori* crystallised with fructose in the active site (on the right). The surface of the Suc1 shows a wider active site with more possibilities for the attachment of an acceptor.

Possible *N*-glycosylation sites in comparison to an exo-inulinase from *Aspergillus awamori* were determined by the web-based software NetNGlyc (Center for Biological Sequence Analysis, Department of Systems Biology, Technical University of Denmark, http://www.cbs.dtu.dk/services/NetNGlyc) (figure 82).

```
          1                                                    50
Exo-Inu   .......... .......... .........F NYDQPYRGQY HFS.PQKNWM
   Suc1   MKLQTASVLL GSAAAASPSM QTRASVVIDY NVAPPNLSTL PNGSLFETWR

          51                                                   100
Exo-Inu   NDPNGLLYHN GTYHLFFQYN PGGIEWGNIS WGHAISEDLT HWEEKPVALL
   Suc1   PRAHVLPPNG QIGDPCLHYT DPSTGLFHVG FLHDGSGISS ATTDDLATYK

          101                                                  150
Exo-Inu   ARGFGSDVTE MYFSGSAVAD VN.NTSGFGK DGKTPLVAMY TSYYPVAQTL
   Suc1   DLNQGNQVIV PGGINDPVAV FDGSVIPSGI NGLPTLLYTS VSYLPIHWSI

          151                                                  200
Exo-Inu   PSGQTVQEDQ QSQSIAYSLD DGLTWTTYDA ANPVIPNPPS PYEAEYQNFR
   Suc1   P....YTRGS ETQSLAVSSD GGSNFTKLDQ G.PVIPGPP. .FAYNVTAFR

          201                                                  250
Exo-Inu   DPFVFW...H DE.....SQK WVVVTSIAEL HK.....LAI YTSDNLKDWK
   Suc1   DPYVFQNPTL DSLLHSKNNT WYTVISGGLH GKGPAQFLYR QYDPDFQYWE

          251                                                  300
Exo-Inu   LVSEFG..PY NAQGGVWECP GLVKLPLDSG NSTKWVITSG LNPG....GP
   Suc1   FLGQWWHEPT NSTWGNGTWA GRWAFNFETG N.VFSLDEYG YNPHGQIFST

          301                                                  350
Exo-Inu   PGTVGSGTQY FVGEFDGTTF TPDADTVYPG .N.....STA NWMDWGPDFY
   Suc1   IGTEGSDQPV VPQLTSIHDM LWVSGNVSRN GSVSFTPNMA GFLDWGFSSY

          351                                                  400
Exo-Inu   AAAG...... ....YNGLSL NDHVHIGWMN ..NWQYGANI PTYP..WRSA
   Suc1   AAAGKVLPST SLPSTKSGAP DRFISYVWLS GDLFEQAEGF PTNQQNWTGT

          401                                                  450
Exo-Inu   MAIPRHMALK TIGSKATLVQ QPQE..AWSS ISNKRPIYSR TFKTLSEGST
   Suc1   LLLPRELRVL YIPNVVDNAL ARESGASWQV VSSDSSAGTV ELQTLGISIA

          451                                                  500
Exo-Inu   NTTTTGETFK VDLSFSAKSK ASTFAIALRA SAN...FTEQ TLVGYDFAKQ
   Suc1   RETKAALLSG TSFTESDRTL NSSGVVPFKR SPSEKFFVLS AQLSFPASAR

          501                                                  550
Exo-Inu   QIFLDR...T HSGDVSFDET FASVYHGPLT PDSTGVVKLS IFVDRSSVEV
   Suc1   GSGLKSGFQI LSSELESTTV YYQFSNESII VDRSNTSAAA RTTDGIDSSA

          551                                                597
Exo-Inu   FGGQGETTLT AQIFPSSDAV HARLASTGGT TEDVRADIYK IASTWN.
   Suc1   EAGKLRLFDV LNGGEQAIET LDLTLVVDNS VLEIYANGRF ALSTWVR
```

Figure 82 Sequence alignment and possible glycosylation sites of the modelled fructosyltransferase Suc1 from *A. niger* (blue, low score, and purple) and the exo-inulinase from *A. awamori* (red).

The *in silico* glycosylation was performed by GlyProt (http://www.glycosciences.de/modeling/glyprot). 11 possible *N*-glycosylation sites were detected and 10 were supposed to be suitable based on the scoring function of GlyProt. Standard complex-type glycans were attached which increase the gyration radius of Suc1 by 42 % (table 27, figure 83).

Table 27 Comparison of the native Suc1 with its glycoform calculated by GlyProt. The gyration radius increases by 42 %.

Deglycosylated Suc1	**Native Suc1**
22.9	32.4

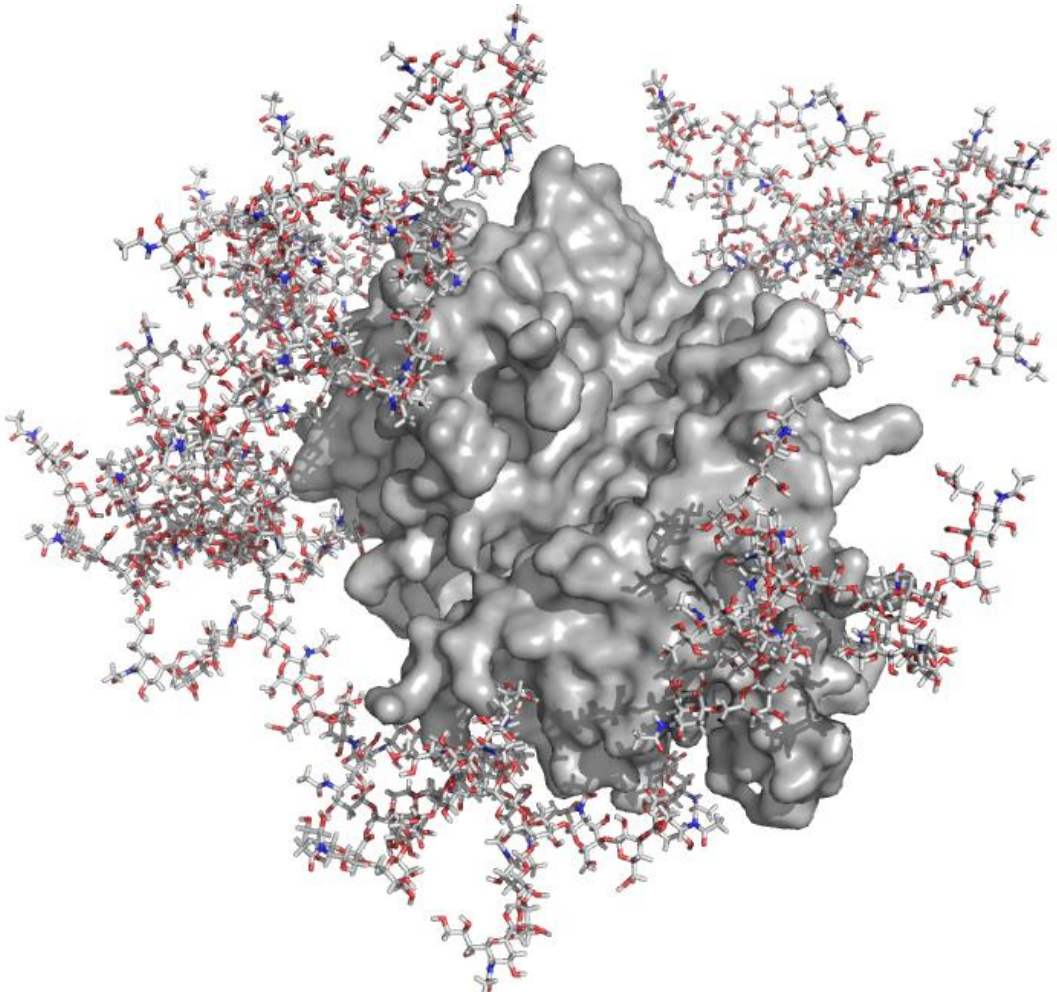

Figure 83 Glycosylated *in silico* model of the fructosyltransferase Suc1 from *A. niger*. The gyration radius increases by 42 %.

4.5.5 Synthesis of 1-kestose and 1-nystose by the fructosyltransferase Suc1 from *Aspergillus niger*

The fructosyltransferase Suc1 from *A. niger* transfers the fructosyl moiety from sucrose to a sucrose acceptor synthesising 1-kestose and 1-nystose. By substrate engineering it also utilises sucrose analogues yielding 1-kestose and 1-nystose analogues (Zuccaro *et al.*, 2008; figure 84).

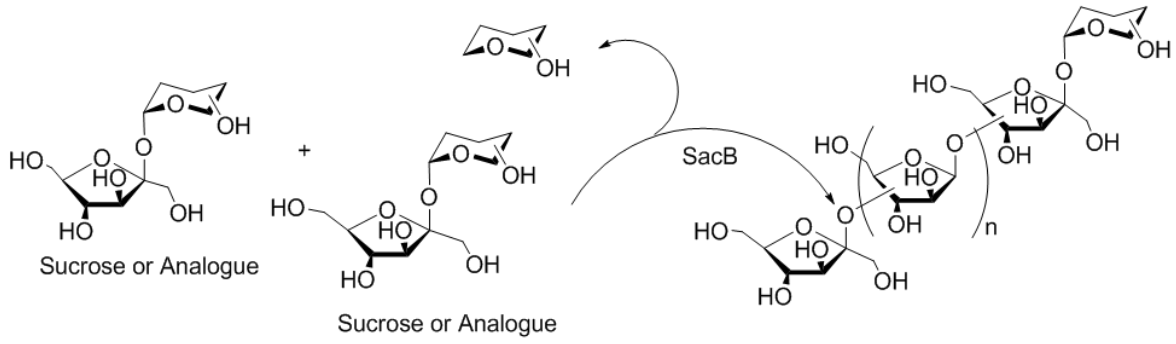

Figure 84 The transfer of a fructosyl moiety from sucrose or a sucrose analogue to another sucrose acceptor molecule or analogue.

The acitivity of the supernatant from a cultivation of *A. niger* SKAN1015 on sucrose was tested in different dilutions (1:100 and 1:200) and analysed by TLC (figure 85).

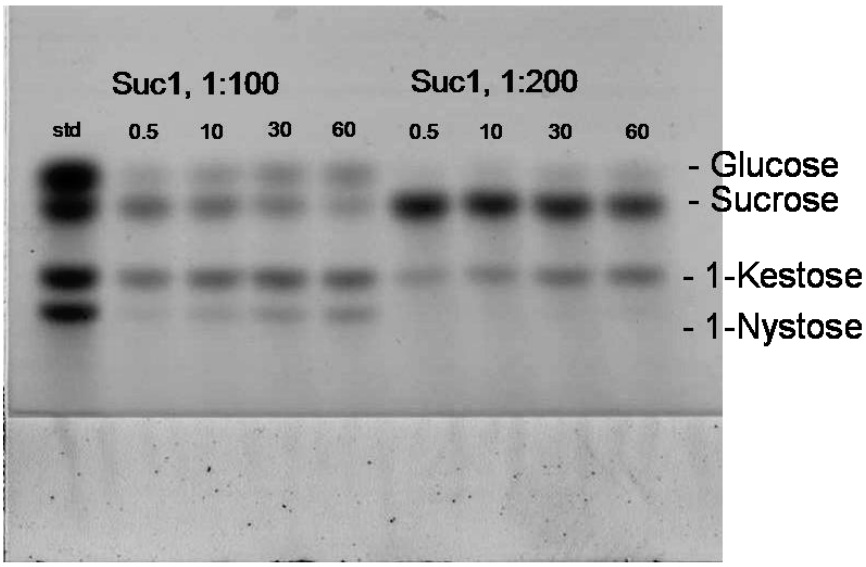

Figure 85 Activity of the fructosyltransferase Suc 1 from *A. niger*. Dilutions of 1:100 and 1:200 were investigated. The sucrose concentration was 500 mM. The sample time points are indicated in min.

The fructosyl transfer *vs*. hydrolysis activity of the Suc1 from *A. niger* SKAn1015 is relatively high compared to other *A. niger* strains, *e.g.* the industrially used strain ATCC20611 (table 28).

Table 28 Distribution of the transfructosylation (U_t) and hydrolytic activities (U_h) of fructosyltransferases similar to Suc1 from different organisms.

Organism	**U_t [U l^{-1}]**	**U_h [U l^{-1}]**	**U_t/U_h**
Aspergillus niger (SKANIp8)	1080	880	1.2
Aspergillus niger (SKAn1015)	244000	11000	21
A. niger ATCC20611	38800	2800	14
A. niger NRRL4337	5700	2800	2

A. oryzae IAM-2609pp13	3500	500	7
Aureobasidium pullulans	10600	1100	10

4.5.6 Growth screen of *Lactobacilli* and *Bifidobacteria* incubated with fructo-oligosaccharides as potential prebiotics

Four strains of *Lactobacilli* (*Lb. fructosus*, *Lb. plantarum*, *Lb. fermentum* and *Lb. delbrueckii*) and *Bifidobacterium lactis* were cultivated in semi-defined medium with the fructo-oligosaccharide to be examined as the sole carbon source. The results for the *Lactobacilli* were similar for each strain. Glucose and 1-kestose were the best carbon sources for promoting the growth of the examined bacteria. The slope and maximum of both curve fits are equal. The 1-nystose curve shows a growth delay at the beginning and an overall lower height. When grown in 75 mM of 1-nystose the optical density at 600 nm did not reach 0.6 (figure 86). 1-Kestose is apparently metabolised similar to the glucose consumption. The curve fits are nearly overlapping so just the fits for 1-kestose is shown in different concentrations being consistent with the given glucose concentrations.

The results show a growth of each bacterial strain with the fructo-oligosaccharides as the sole carbon source. TLC analysis of the metabolisation products indicates the action of a fructosyltransferase or fructosidase hydrolysing 1-kestose and 1-nystose to sucrose (figure 87). The involvement of different enzymatic processes requiring different glycosidases leads to a later consumption and metabolisation of fructo-oligosaccharides with more than two fructosyl moieties. Thus, it is likely that these structures persist longer in the intestinal tract and can potentially evoke effects like immuno-stimulation of gastrointestinal cells.

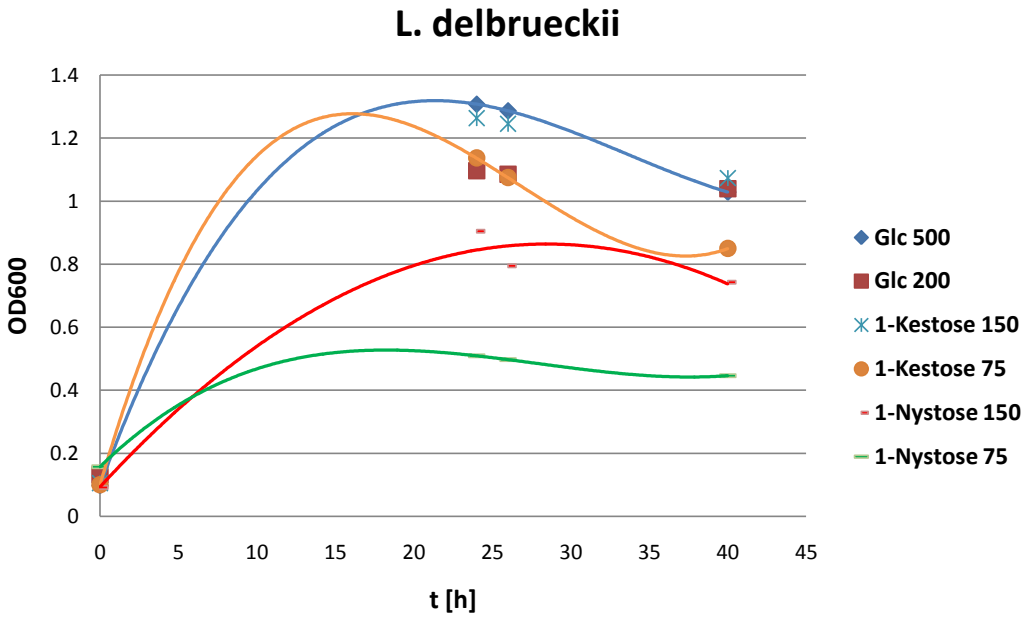

Figure 86 *Lactobacillus delbrueckii* growth curve fit. Glc, glucose. The concentrations of the investigated fructo-oligosaccharides are given in mM.

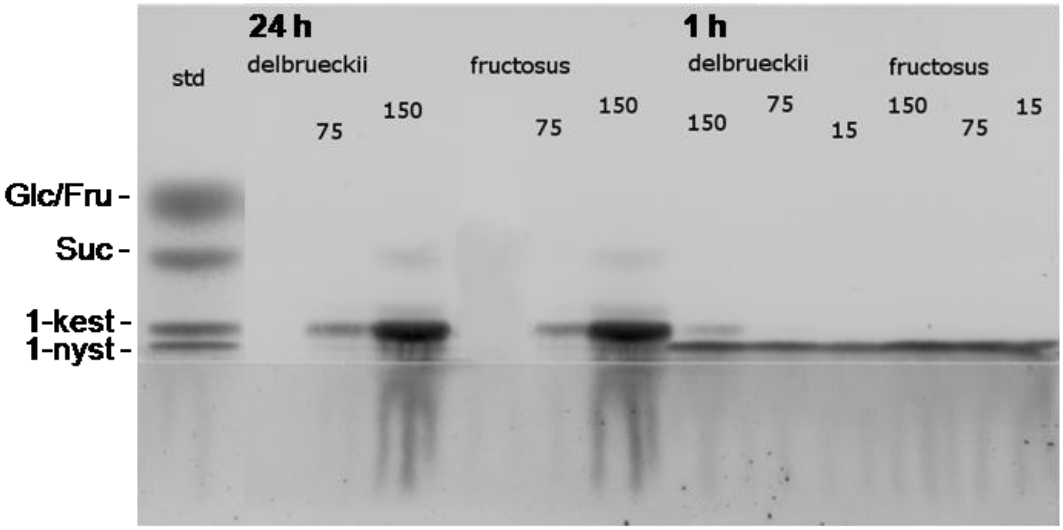

Figure 87 Metabolisation of 1-nystose by *Lb. delbrueckii* and *Lb. fructosus* after 1 and 24 hours. The starting concentration of 1-nystose (1-nyst) is indicated [mM]. 1-kest is 1-kestose.

4.5.7 Synthesis of novel 1-kestose and 1-nystose analogues by the fructosyltransferase Suc1 from *Aspergillus niger*

Suc1 is highly specific for the synthesis of defined 1-kestose and 1-nystose analogues depending on the reaction time and conditions. The reaction was performed at 40 °C in Sörensen`s phosphate buffer (50 mM) at pH 5.6. The substrate concentration was 500 mM. The yields were about 60 % for each analogue. The products were identified and analysed by TLC and HPAEC with appropriate standards (figure 88, table 29).

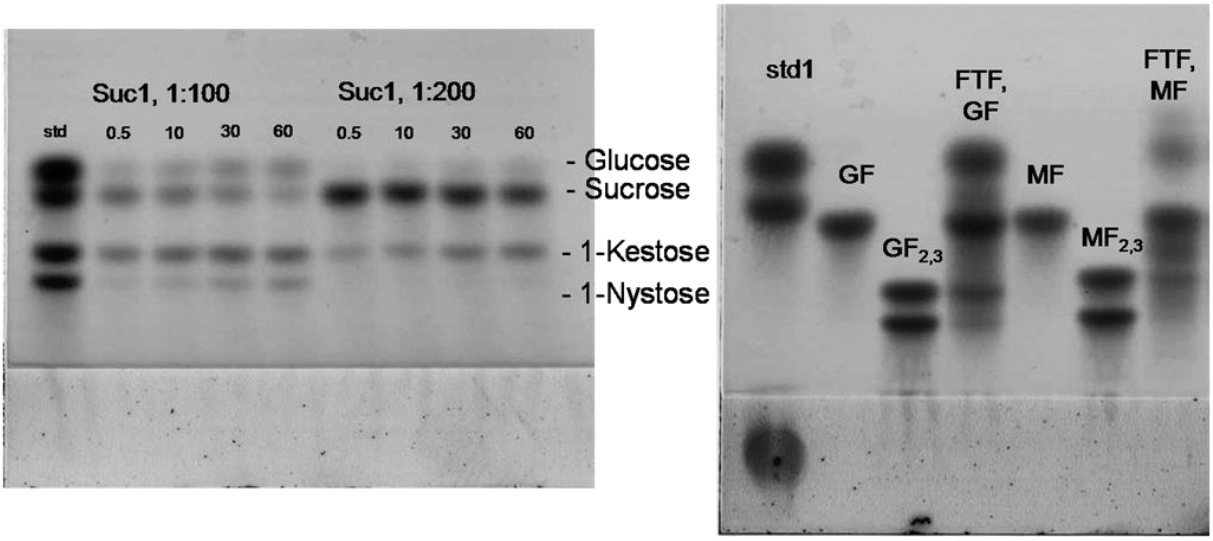

Figure 88 Synthesis of the 1-kestose and 1-nystose analogues of Gal-Fru and Man-Fru by the fructosyltransferase Suc1 from *A. niger* at 45 °C in Sörensen`s phosphate buffer (50 mM) at pH 5.6.

Table 29 Reaction times and conversion of the novel oligofructosides synthesised by the fructosyltransferase Suc1 from *A. niger*.

	t [min]	**Conversion [%]**
1-kestose (Glc-Fru_2)	18	81
1-nystose (Glc-Fru_3)	60	93
Man-Fru_2	60	71
Man-Fru_3	180	87
Gal-Fru_2	420	44
Gal-Fru_3	960	65
Xyl-Fru_2	20	75
Xyl-Fru_3	120	94
Fuc-Fru_2	60	65
Fuc-Fru_3	120	88

The combined action of the fructosyltransferase SacB from *B. megaterium* and the Suc1 from *A. niger* leads to a possible process for the synthesis of nutra- and pharmaceuticals (figure 89). The two production hosts are generally-regarded-as-safe (GRAS) organisms approved for the synthesis of products consumed by humans.

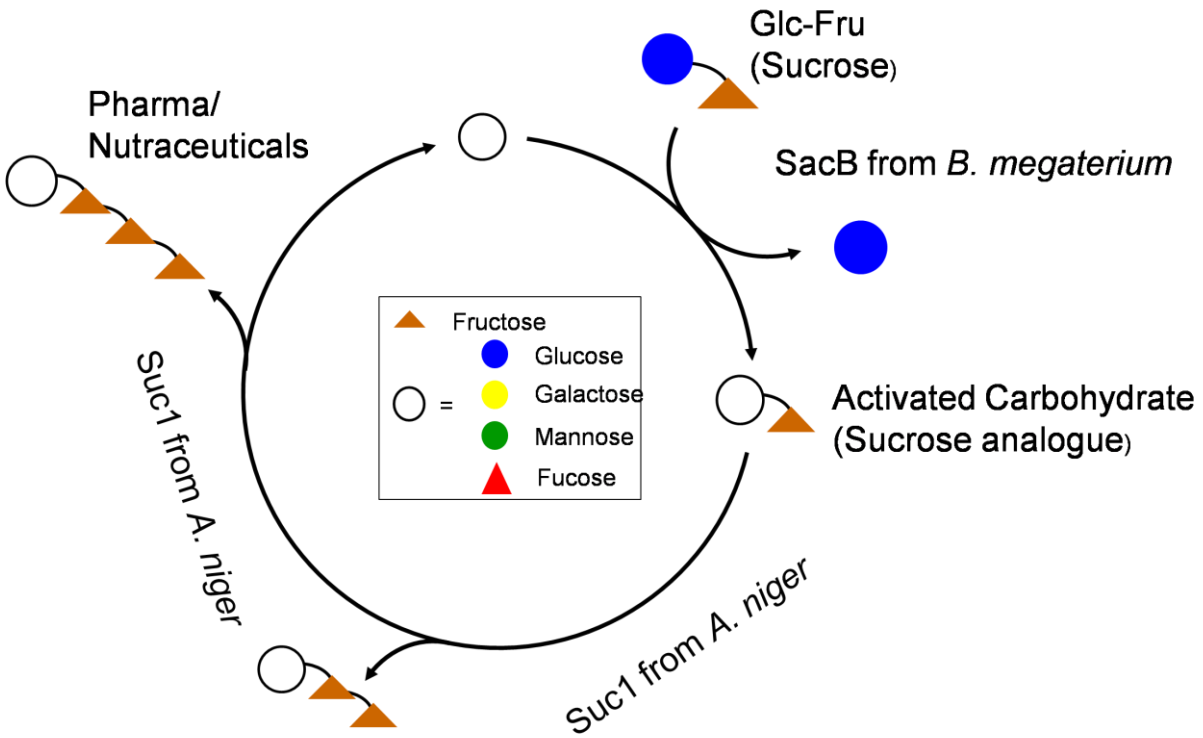

Figure 89 Possible process for the synthesis of novel pharma-/nutraceuticals by the concerted action of the fructosyltransferases from *B. megaterium* and *A. niger*.

4.5.8 Novel fructo-oligosaccharides as immuno-stimulating agents

Fructo-oligosaccharides were tested as substrates for beneficial gut bacteria and as immuno-stimulating agents in cultivations of human epithelial adenocarcinoma cells (Caco-2; figure 90). Carbohydrate-protein interactions are known to have broad effects on eukaryotic cells.

We examined the cytokine response of a human Caco-2 cell line (figure 90) after exposure to novel fructo-oligosaccharides (figure 71). The Caco-2 cell line is a model for the absorption of pharmacological products in the intestinal region (Artursson *et al.*, 2001; Shah *et al.*, 2006). Our strategy is to analyse and characterise the cytokine release into the growth medium in the presence of our novel oligosaccharides. A commercially available kit (Biosource, Invitrogen) gives access to the parallel analysis of 25 different cytokines and chemokines in one sample (Eotaxin, granulocyte macrophage colony stimulating factor (GM-CSF), Interferon (IFN)-α, IFN-γ, interleukin (IL)-1RA, IL- 1β, IL-2, IL-2R, IL-4, IL-5, IL-6, IL-7, IL-8, IL-10, IL-

12p40/p70, IL-13, IL-15, IL-17, IP-10, monocyte chemotactic protein (MCP)-1, monokine induced by gamma interferon (MIG), macrophage inflammatory protein (MIP)-1α, MIP-1β, regulated upon activation, normal T-cell expressed and secreted (RANTES) and tumour necrosis factor (TNF)-α). They were detected by fluorescent antibody-coated beads and quantified by a secondary fluorescence-labelling process (figure 92). The cytokines analysed have either direct or indirect influence on the cell signalling cascades and the activation of the immune system. Direct influence may be the release of cytokines by a cell line when it is cultivated in the presence of the novel oligosaccharides. Indirect stimulation of the immune system by these novel pharmaceuticals may include the growth of certain beneficial bacteria which in turn act as immuno-stimulating agents. As auto-immune diseases like allergies are a growing problem in developed countries, specific stimulation of the immune system may prove useful to reduce this problem.

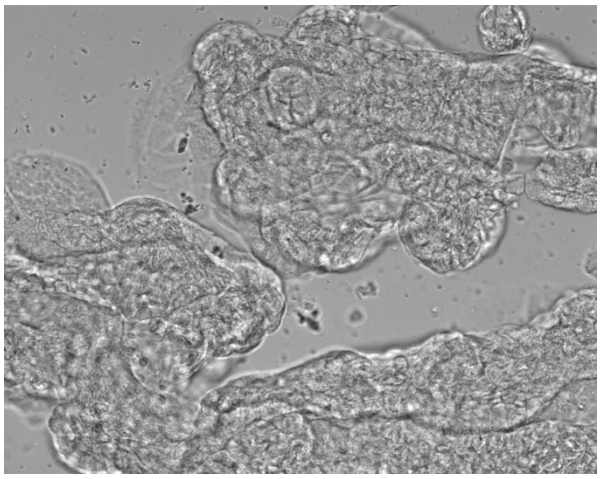

Figure 90 The Caco-2 cell line in a 200-fold magnification.

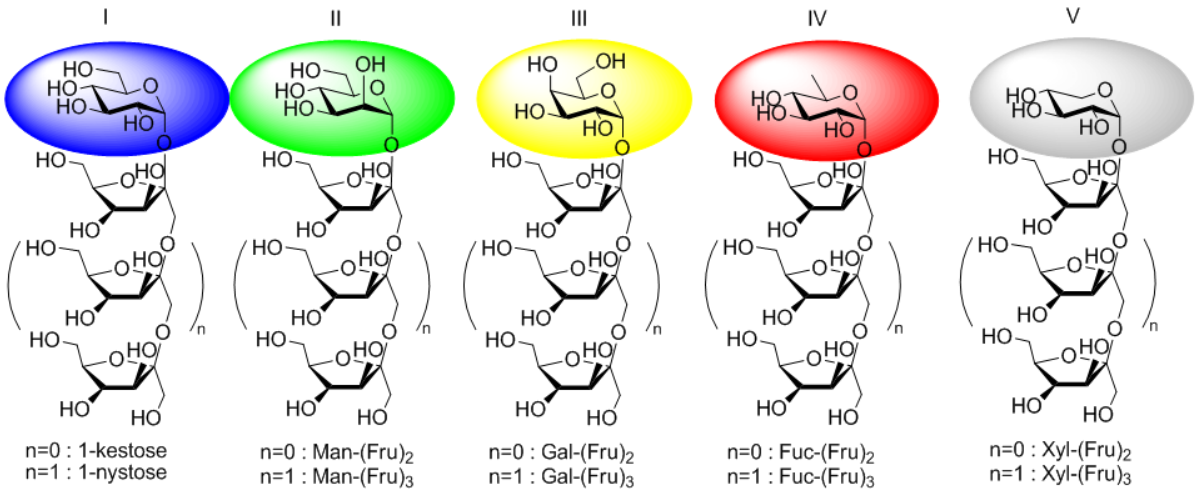

Figure 71 Fructo-oligosaccharide target structures. I) Established product on the market. II) 1- kestose (Man-$(Fru)_2$) or 1-nystose (Man-$(Fru)_3$) analogue. III) 1-kestose (Gal-$(Fru)_2$) or 1-nystose (Gal-$(Fru)_3$) analogue. IV) 1-kestose (Fuc-$(Fru)_2$) or 1-nystose (Fuc-$(Fru)_3$) analogue. V 1-kestose (Xyl-$(Fru)_2$) or 1-nystose (Xyl-$(Fru)_3$) analogue.

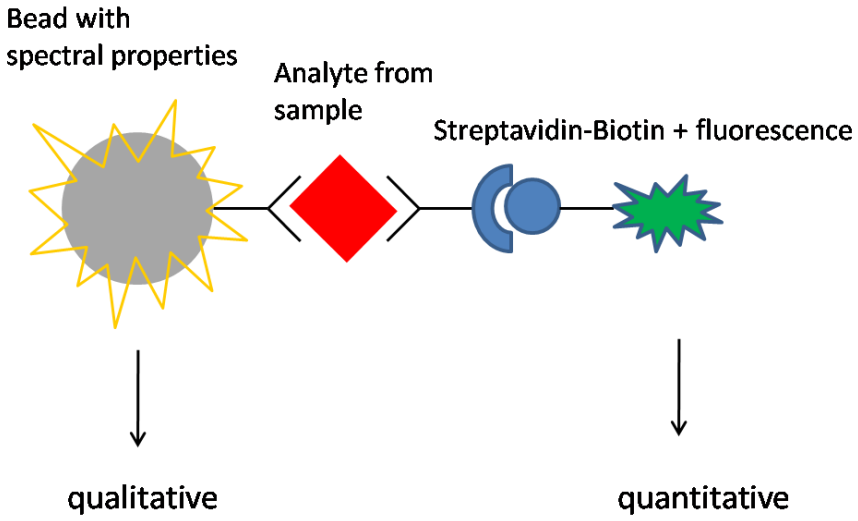

Figure 91 The analysis principle of the 25-plex human cytokine analysis kit (Biosource).

4.5.8.1 Immuno-assay of the human epithelial colorectal adenocarcinoma cell line Caco-2 incubated with novel fructo-oligosaccharides

Novel fructo-oligosaccharides were tested as immuno-stimulating agents in cultivations of human epithelial colorectal adenocarcinoma cells (Caco-2). Caco-2 cells were grown for 48 h in 24-well dishes containing the fructo-oligosaccharide to be investigated in a concentration of 25 µM (sucrose, palatinose, 1-kestose, 1-nystose, Gal-Fru, Gal-Fru_2, Man-Fru. Man-Fru_2, Man-Fru_3, Fuc-Fru, Fuc-Fru_2, Fuc-Fru_3, Xyl-Fru, Xyl-Fru_2 and Xyl-Fru_3). Five-fold repeats of each carbohydrate ensured the significance of the results.

Table 30 Fructo-oligosaccharides investigated in terms of immuno-stimulation.

suc	sucrose
pala	isomaltulose (palatinose)
kest	1-kestose
nyst	1-nystose
GF, GF_2	Gal-Fru, Gal-Fru_2
MF, $MF_{2,3}$	Man-Fru, Man-$Fru_{2,3}$
FF, $FF_{2,3}$	Fuc-Fru, Fuc-$Fru_{2,3}$
XF, $XF_{2,3}$	Xyl-Fru, Xyl-$Fru_{2,3}$

For the fructo-oligosaccharide assay, Caco-2 cells at 80 % confluence were split in a ration of 1:10 and cultivated in 24-well dishes. Each well was supplied with the oligofructoside to be tested in a concentration of 25 µM. After 48 h the medium was collected for cytokine analysis. The assay was performed with a 25-plex human cytokine analysis kit according to the manufacturer`s instructions (Biosource, Invitrogen). Briefly, the supernatant medium was incubated with antibody-functionalised beads and detected with biotinylated secondary antibodies. Streptavidin-R-phycoerythrin (RPE) was used as a fluorescence marker. The final analysis was performed by the luminex system (Quiagen) which recognises spectral properties of the beads and quantifies the bead load by the specific fluorescence

intensity. In the 96-well plate provided, we analysed 15 different oligosaccharides in five-fold repeats (sucrose, palatinose, 1-kestose, 1-nystose, Gal-Fru, Gal-Fru_2, Man-Fru. Man-Fru_2, Man-Fru_3, Fuc-Fru, Fuc-Fru_2, Fuc-Fru_3, Xyl-Fru, Xyl-Fru_2 and Xyl-Fru_3). The concentrations of 25 different cytokines were analysed in each sample (Eotaxin, granulocyte macrophage colony stimulating factor (GM-CSF), Interferon (IFN)-α, IFN-γ, interleukin (IL)-1RA, IL- 1β, IL-2, IL-2R, IL-4, IL-5, IL-6, IL-7, IL-8, IL-10, IL-12p40/p70, IL-13, IL-15, IL-17, IP-10, monocyte chemotactic protein (MCP)-1, monokine induced by gamma interferon (MIG), macrophage inflammatory protein (MIP)-1α, MIP-1β, regulated upon activation, normal T-cell expressed and secreted (RANTES) and tumour necrosis factor (TNF)-α).

IL-8 and MCP-1 were the only cyto- or chemokines, respectively, which gave a significant response compared to the background. Both standard curve fits show a correlation of over 99 % (figures 92 and 93). The measured fluorescence intensities are in the linear part of the standard curve indicating the significance of the data. The other cytokines gave no significant response under these conditions. MCP-1 generally shows a higher signal-to-background enhancement compared to the cultivation of Caco-2 cells without added carbohydrates (neg. or w/o feed). MCP-1 is up-regulated up to a factor of 2.7 (MF_3, figures 96 and 97, table 32). Longer fructosyl moieties seem to enhance this effect. For 1-nystose (factor 2.1), Man-Fru_3 (2.7), Fuc-Fru_3 (2.6) and Xyl-Fru_3 (1.8) the release of MCP-1 is clearly triggered. The stimulation of IL-8 is also visible when the fucose-containing 1-nystose analogue $FucFru_3$ is added (figures 94 and 95, table 31). An enhancement factor of 1.1 is detected. Also in the case of IL-8 longer fructosyl chains seem to enhance the release of this cytokine. In the samples containing 1-nystose, Gal-Fru_2, Man-Fru_3, Fuc-Fru_3 and Xyl-Fru_3 the highest concentration of IL-8 was detected. An interesting observation is the already high stimulation of IL-8 by sucrose.

One crucial question arises: Why are just two significant cytokine responses observable? The novel oligosaccharides have no effect on most of the tested cytokines. Only two out of 25 show significant up-regulation. Obviously it is not necessary for a cell in the intestine to synthesise cytokines and thus trigger the immune system upon contact with natural molecules of the carbohydrate metabolism. But it is crucial to release cytokines when the cell contacts potentially harmful structures, *e.g.* pathogens. Our novel oligosaccharide structures might mimick some

of these pathogen effects on cells. Mannose and fucose derivatives are the compounds which evoke the highest stimulation of MCP-1 and IL-8. This might be due to their participation in natural cell-cell communication processes, *e.g.* as terminal carbohydrate units in the Lewis X motif.

The experiment does not have a time-resolving component. The reaction time was 48 h but a cytokine can be released in several hours. The reason why we detect IL-8 and MCP-1 after 48 h might be due to their persisting synthesis or to another effect that leads to persistent release. An IL-8 accumulation was described in Weibel-Palade bodies of endothelial cells, where it colocalises with the von-Willebrand factor involved in blood coagulation (Sadler, 1998; Wolff *et al.*, 1998). There it is stored and released continuously upon repeated stimulation, for example by the novel oligosaccharide structures. Another explanation might be that MCP-1 triggers IL-8 release. So it might also be a secondary stimulation effect. Why exactly MCP-1 is detectable after 48 h remains to be investigated.

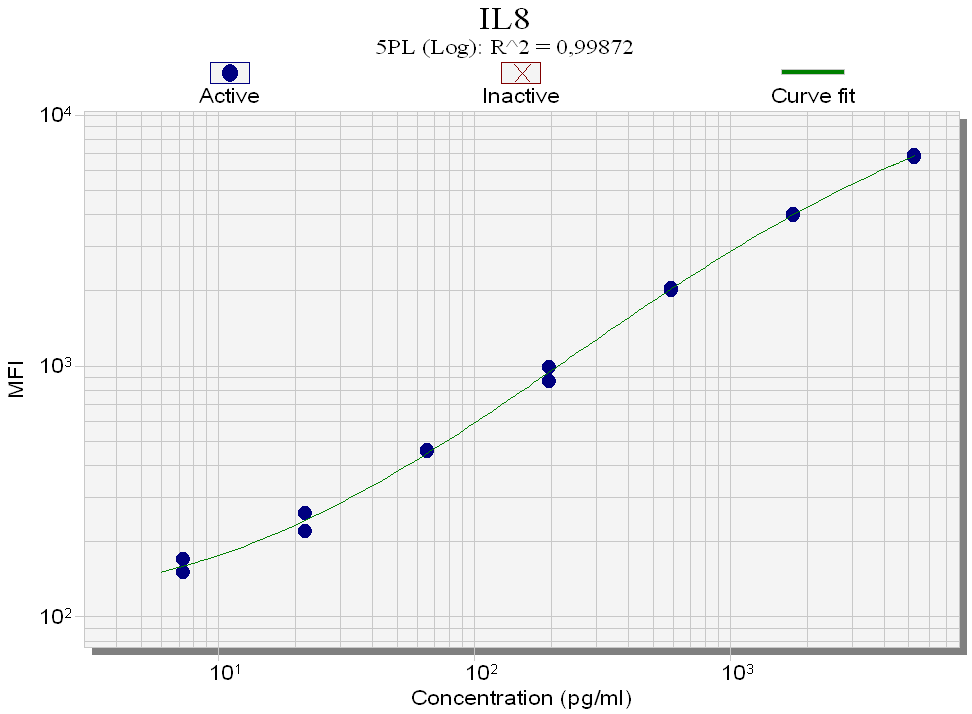

Figure 92 Standard curve fit for the luminex IL-8 analysis.

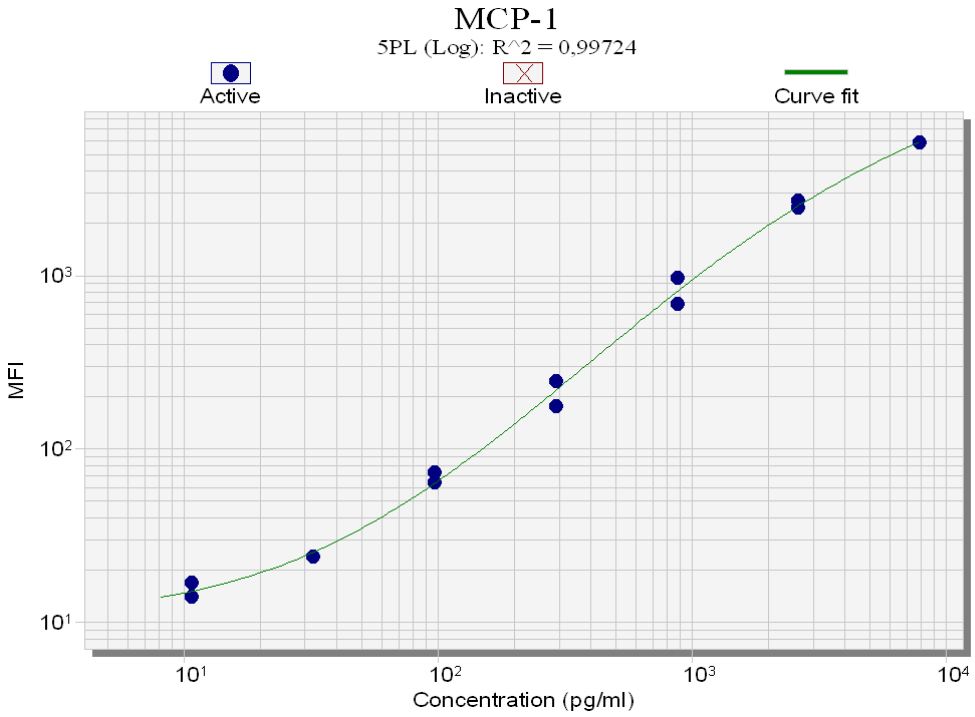

Figure 93 Standard curve fit for the luminex MCP-1 analysis.

The results for IL-8 and MCP-1 were correlated with the standard curve fit and converted to ng ml^{-1}.

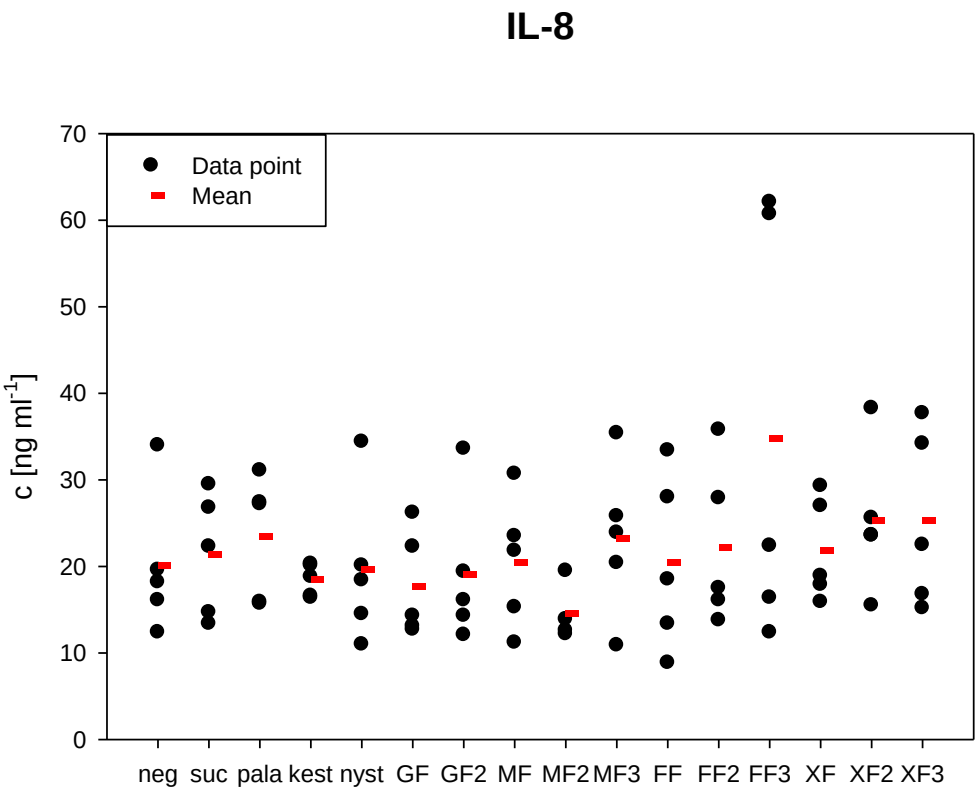

Figure 94 The concentration of IL-8 incubated with the target fructo-oligosaccharides and controls (table 30). The means of each dot plot column is indicated by a red bar.

Table 31 Factors of signal-to-background enhancement of the IL-8 release.

Carbohydrate	Factor
w/o feed	0,00
Suc	0,54
Pala	0,25
1-k	0,20
1-n	0,30
GF	0,00
GF_2	0,27
MF	0,06
MF_2	0,07
MF_3	0,40
FF	0,23
FF_2	0,34
FF_3	1,10
XF	0,32
XF_2	0,53
XF_3	0,53

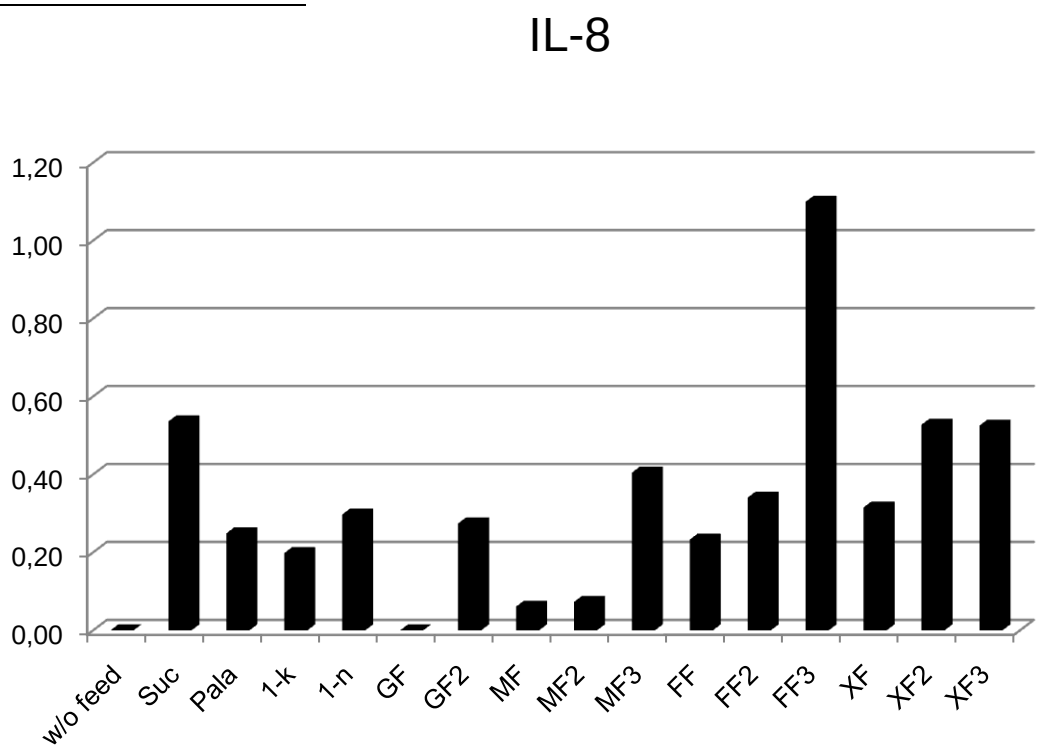

Figure 95 Factors of signal-to-background enhancement of the IL-8 concentration.

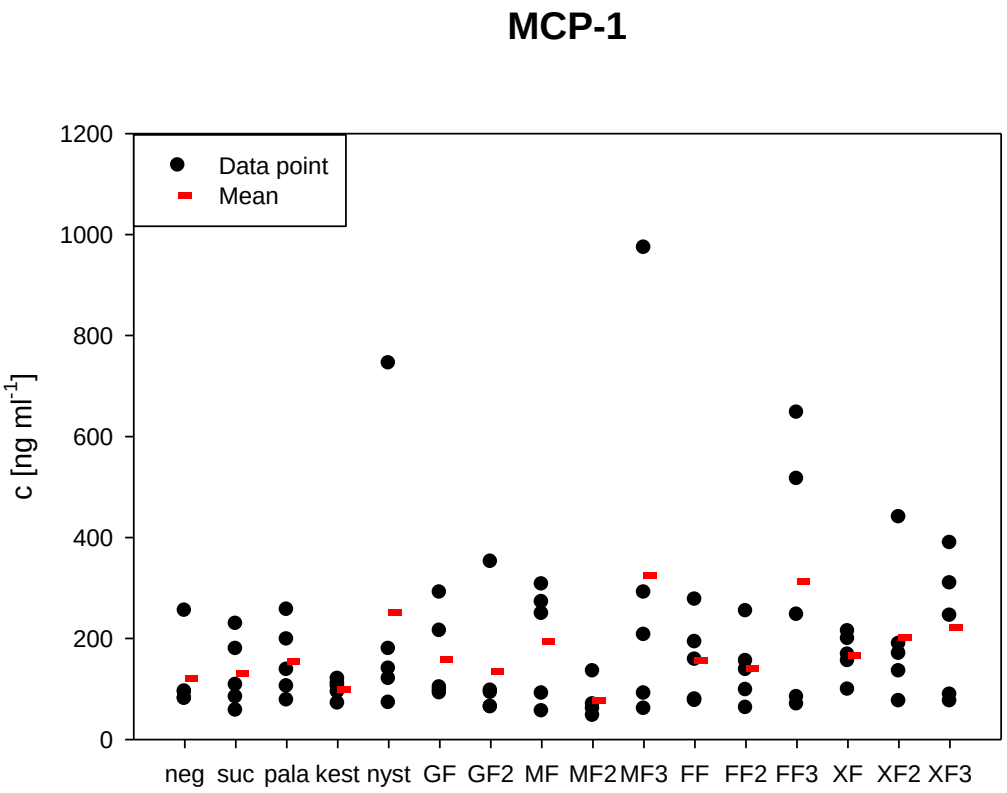

Figure 96 The concentration of MCP-1 incubated with the target fructo-oligosaccharides and controls (table 30). The means of each dot plot column is indicated by a red bar.

Table 32 Factors of signal-to-background enhancement of the MCP-1 release.

Carbohydrate	Factor
w/o feed	0,00
Suc	0,96
Pala	0,59
1-k	0,22
1-n	1,95
GF	0,50
GF2	0,81
MF	0,82
MF2	0,34
MF3	2,72
FF	0,79
FF2	0,62
FF3	2,58
XF	0,91
XF2	1,31
XF3	1,54

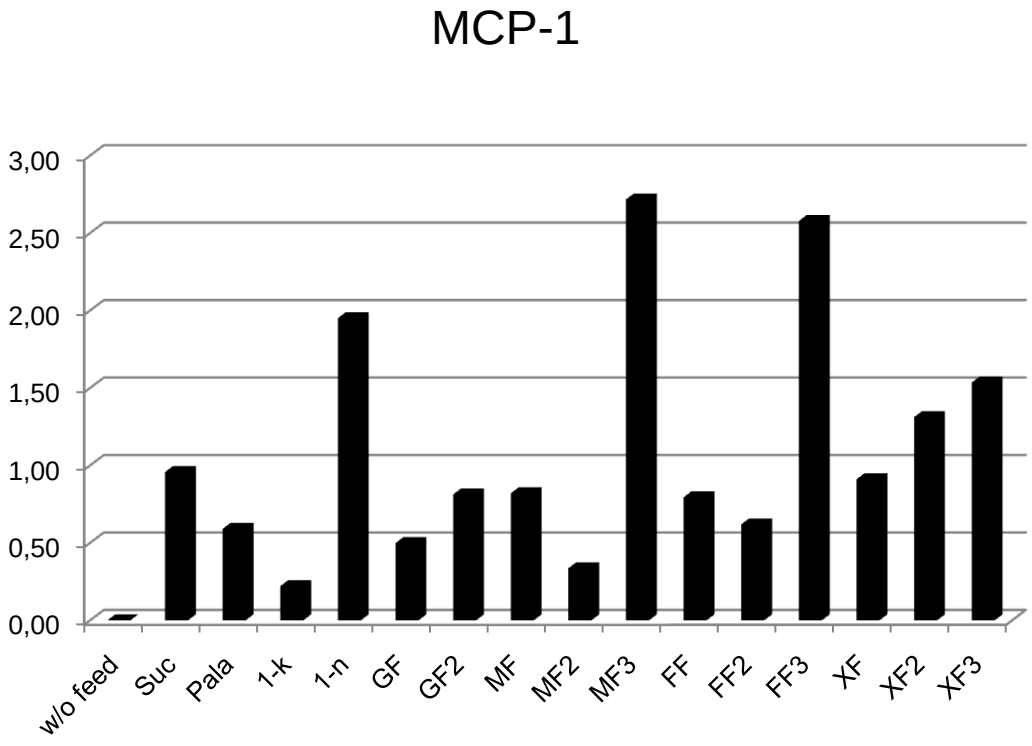

Figure 97 Factors of signal-to-background enhancement of the MCP-1 concentration.

4.6 Bioorthogonal metabolic engineering of HEp-2, CHO-K1 and CHO lec 3.2.8.1 cell lines for the investigation of cell-cell recognition processes

The surface of eukaryotic cells is highly decorated with glycan structures of various types forming the glycocalyx. Glycolipids and glycoproteins mediate cell-cell recognition and signal transduction processes (Varki, 2006). In 2002 Bertozzi and co-workers showed that functionalised carbohydrates can be incorporated into cells *in vitro* (Saxon *et al.*, 2002; Dube *et al.*, 2003; figure 103). This process works by active transporters and diffusion procedures depending on the modification of the carbohydrates. Acetylated sugars can easily pass the cell membrane whereas neuraminic acid derivatives carrying no acetylated hydroxyl groups enter the cell by special transporter systems (Bardor *et al.*, 2005). Acetylated monosaccharides are processed by unspecific deacetylases, activated by nucleotide transferases and metabolised by isomerases and epimerases (Prescher *et al.*, 2006; Chang *et al.*, 2007; Codelli *et al.*, 2008; Laughlin *et al.*, 2008; Chang *et al.*, 2009). These activated carbohydrates are incorporated into the natural carbohydrate patterns of the cell (figure 103). Some of the modified sugars are part of the glycosylated cell surface and therefore are accessible to chemical conversion without destruction of the cell. Depending on the modified carbohydrate added to the growth medium of the cell line or organism, *N*- or *O*-glycosylation patterns are addressed.

4.6.1 The alkyne-azide “click reaction” – Copper-catalysed formation of (1,3)-triazoles

Functionalised monosaccharides with azide or alkyne groups have been synthesised in our group (Riaz-ul-Qamar, 2007; Serim, 2008). The acetylated sugars are more hydrophobic than the deprotected ones and therefore can pass the cell membrane more easily. They are afterwards processed by unspecific deacetylases and incorporated into the carbohydrate metabolic system (Prescher *et al.*, 2006). But also the deprotected sugars are incorporated into cells by membrane transporter systems (Bardor *et al.*, 2005).

The metabolised modified sugars are subsequently labelled by fluorescent molecules. As described in the theoretical background part of the introduction, a molecule with an alkyne group can be quantitatively coupled to an azide group in the presence of Cu(I) and other catalysts by click chemistry (figure 98). However, there are some advantages and disadvantages in the use of this method *in vivo*. The strong advantage is the bioorthogonality of the alkyne and the azide. A drawback is the cytotoxicity of the copper catalyst and the organic solvent system.

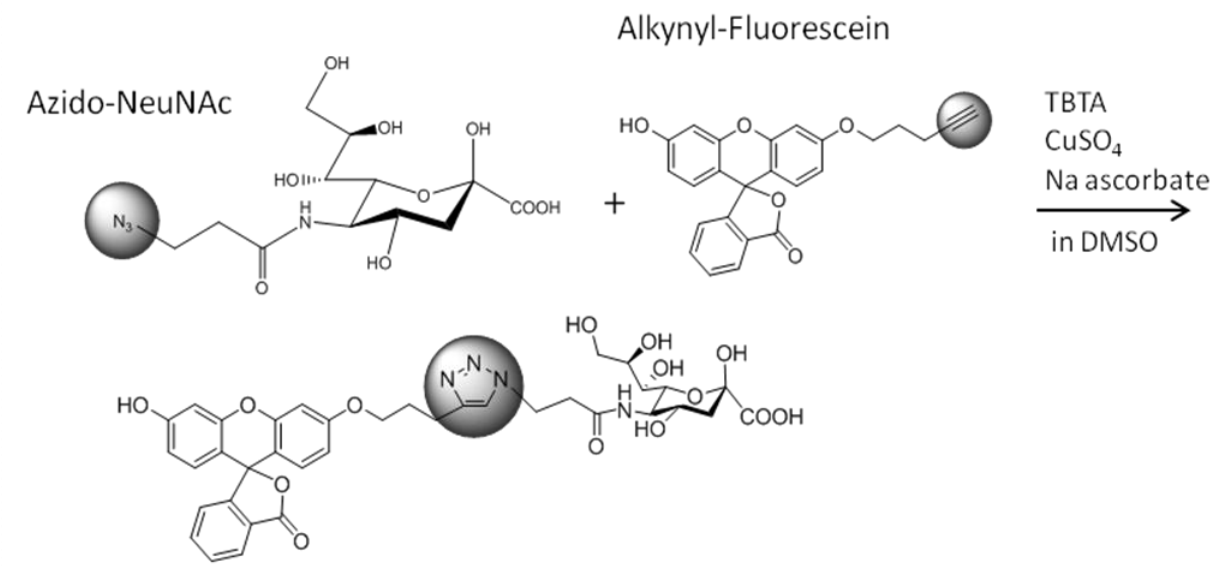

Figure 98 Labelling of azido-carbohydrates by an alkyne-functionalised fluorescence molecule by click chemistry.

4.6.2 Functionalised carbohydrates for bioorthogonal metabolic engineering

Four functionalised carbohydrates were synthesised chemically for the use in metabolic labelling studies, 2-azidoacetylamino-2-deoxy-(1,3,4,6)-tetraacetyl-β-D-glucopyranoside (AcGlcNAz), 2-azidoacetylamino-2-deoxy-β-D-glucopyranoside (GlcNAz; Serim, 2008), N-azido-acetylneuraminic acid (NeuNAz) and N-(1-oxohex-5inyl) neuraminic acid (NeuNHex; Riaz-ul-Qamar, 2007; figure 99).

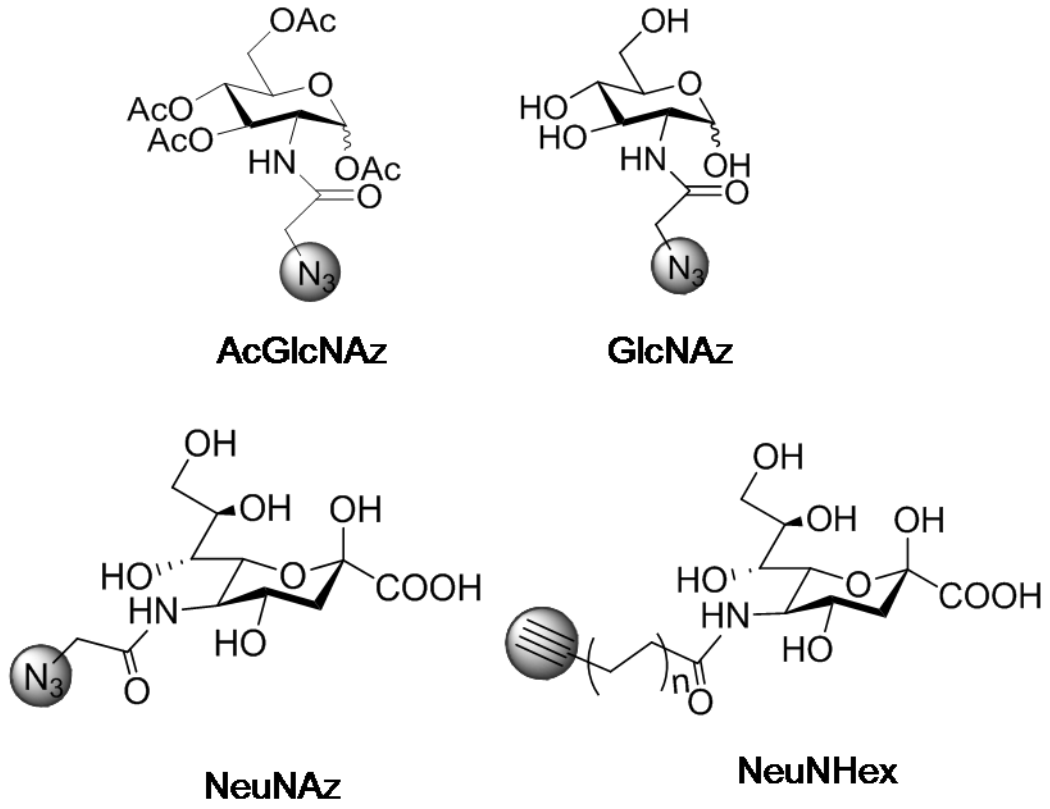

Figure 99 Functionalised carbohydrates synthesised by Riaz-ul-Qamar and Serim for the metabolic labelling of eukaryotic cells (Riaz-ul-Qamar, 2007; Serim, 2008).

4.6.3 *In vitro* promiscuity studies of a human neuraminic acid synthase

In first studies towards metabolic cell labelling, a human neuraminic acid synthase was investigated in terms of engineered substrate promiscuity. The native reaction is the conversion of *N*-acetylglucosamine with pyruvate to neuraminic acid.

The isomerisation of GlcNAc to the neuraminic acid synthase substrate ManNAc was performed by a shift to pH 10 (Blayer *et al.*, 1999). The following enzyme reaction took place at the described optimal pH 7.5 and, interestingly, also at the alkaline pH of 10 used for the epimerisation (figures 101 and 102). Due to the low amounts of enzyme availability, 0.1 U corresponding to a theoretical full conversion of GlcNAc or ManNAc were used, respectively, with pyruvate to form neuraminic acid in between 14 days. Sampling time was each day. However, the HPAEC analysis shows an optimal yield at 7 days reaction time (figure 102).

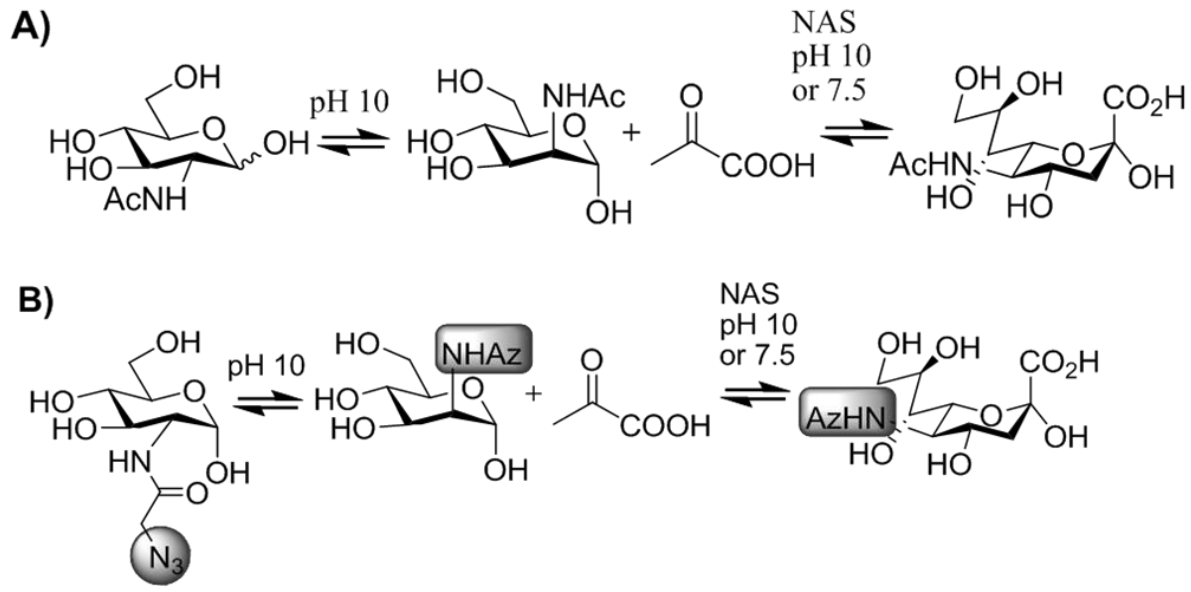

Figure 100 A) The native and B) engineered reaction of the human neuraminic acid synthase (NAS).

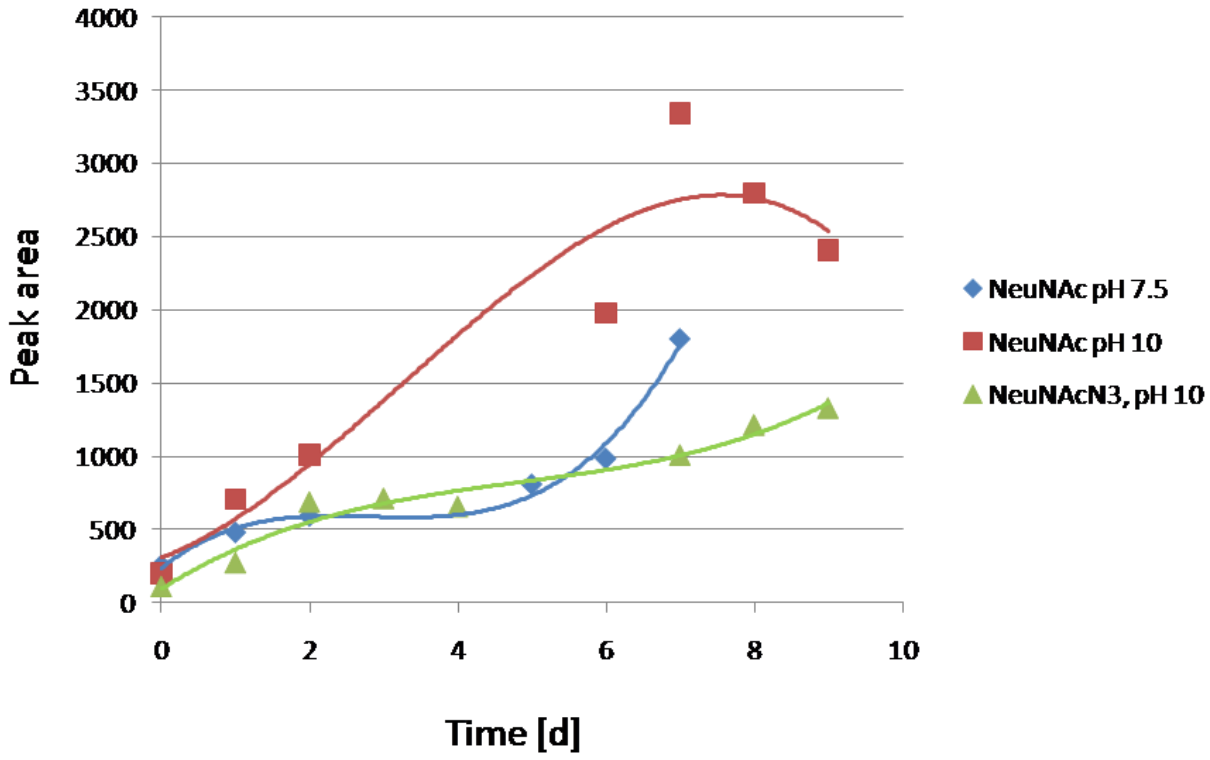

Figure 101 HPAEC analysis of the native and engineered conversion of ManNAc (pH 7.5), GlcNAc (pH 10) or engineered GlcNAz (pH 10) and pyruvate to NeuNAc or NeuNAz, respectively, by the neuraminic acid synthase.

4.6.4 Metabolic labelling experiments of HEp-2 cells with functionalised carbohydrates

Metabolic labelling of cell surfaces was established in order to study and characterise cell signalling and cell-cell interactions to examine inflammation and infection processes. The metabolic incorporation of functionalised carbohydrates was performed with HEp-2 cells. The carbohydrates were modified by introducing an azide or alkyne group and subsequent incubation with the cell lines indicated. The modified carbohydrates passed the natural carbohydrate biosynthetic pathway and were incorporated into the post-translational glycan patterns of proteins (figure 103).

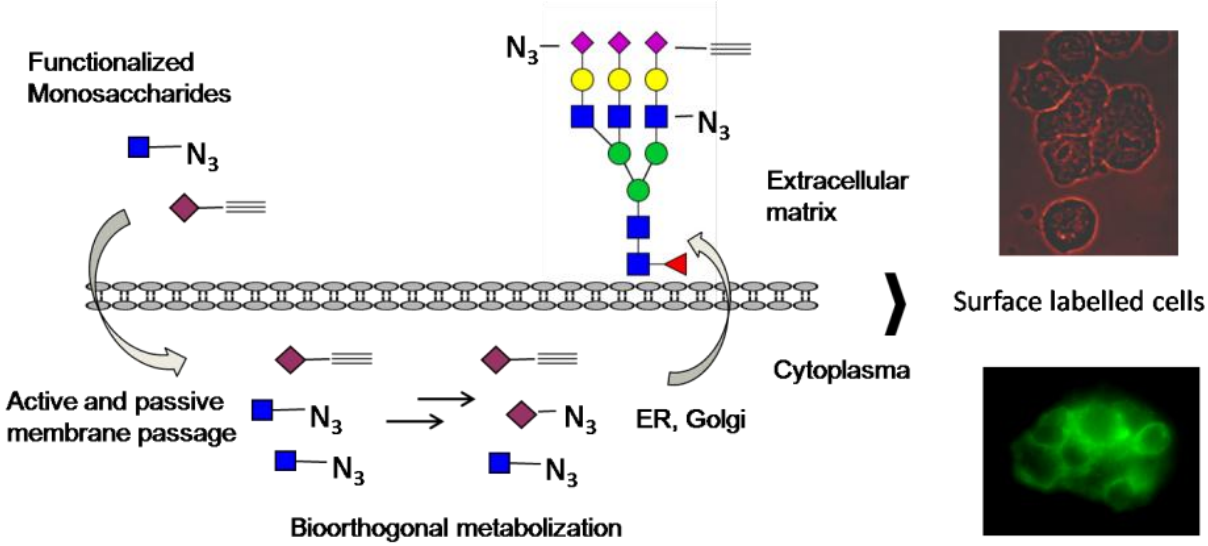

Figure 102 Incorporation of modified carbohydrates into the natural carbohydrate metabolic process of eukaryotic cells.

HEp-2 cells were incubated in the appropriate medium suitable for the cell line. At 80 % confluence they were split into 6-well plates with the appropriate medium containing the functionalised carbohydrates in a concentration of 25 µM (AcGlcNAz, GlcNAz, NeuNAz and NeuNHex). The subsequent click reaction for the fluorescent labelling of the cell surface was performed in 12-well microscopy slides (idbidi) with 50 µl detached cells in PBS buffer and 250 µl of the appropriate medium for the reattachment of the cells. After 24 h the medium was removed and the cells were washed three times with PBS. The functionalised fluorescent detection molecule and

the conditions for the click reaction ($CuSO_4$, sodium ascorbate and TBTA ligand) were applied in DMSO as solvent system. After one hour, the cells were analysed by fluorescence microscopy (phase contrast) or the appropriate wavelength for fluorescence.

The negative control was incubated in the medium suitable for the cell line to be analysed without any additional carbohydrate. The pictures were taken with a fluorescence microscope (brightfield and the appropriate wavelength, 580 for TAMRA and 525 nm for fluorescein staining).The fluorescence microscopy image does not show any significant background fluorescence (figures 104 and 105).

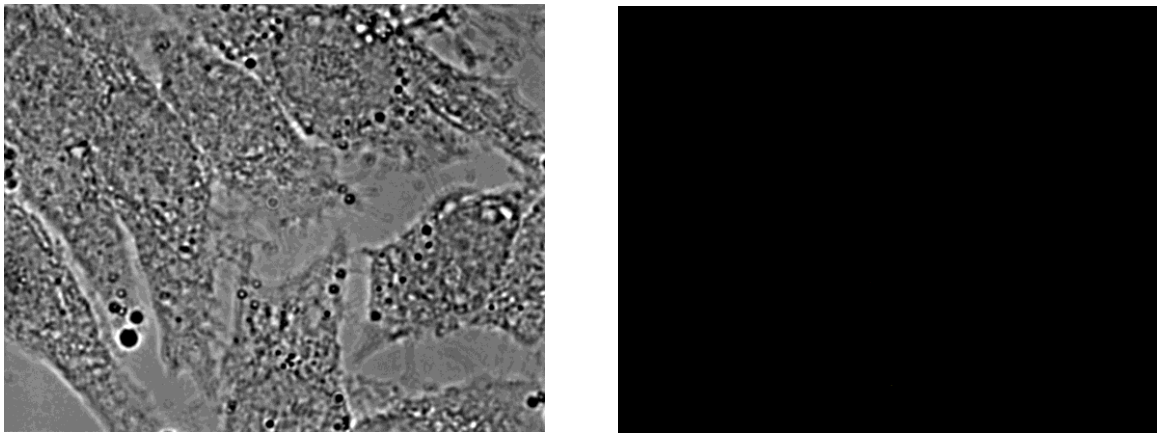

Figure 103 HEp-2 negative control w/o fed sugar (brightfield, left picture), TAMRA staining (580 nm, right picture)

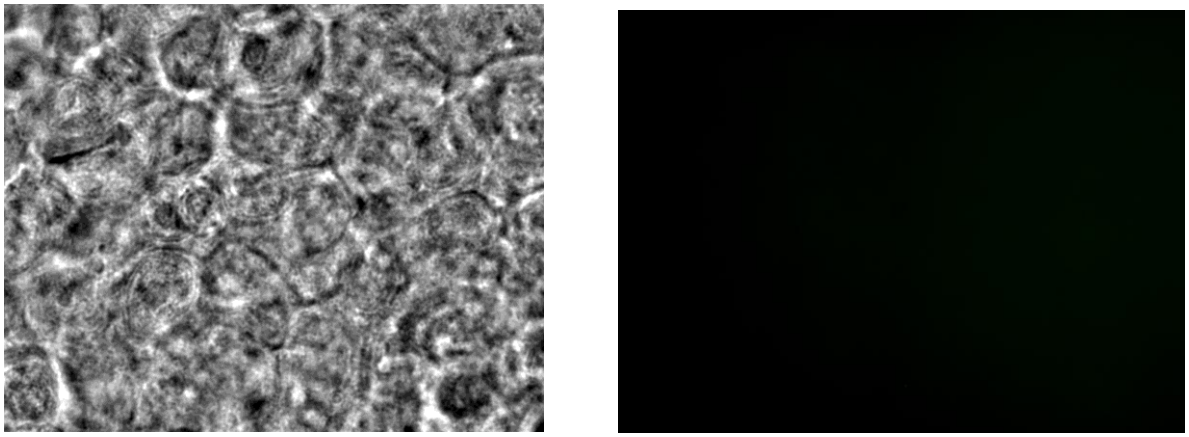

Figure 104 HEp-2 negative control w/o fed sugar (brightfield, left picture, fluorescein staining (525 nm, right picture).

The metabolic labelling of HEp-2 cells with GlcNAz was successful. We observed a clear alkynylated-TAMRA staining of the cell membrane in the expected wavelength (580 nm). However, also an unspecific staining of the nucleus membrane and some concentrated spots in the cytosol were visible. These may be glycoproteins in the ER, Golgi or endosomal vesicles containing our modified carbohydrates indicating an incorporation of the functionalised carbohydrates. Nevertheless our aim of cell membrane-functionalisation was achieved (figure 106).

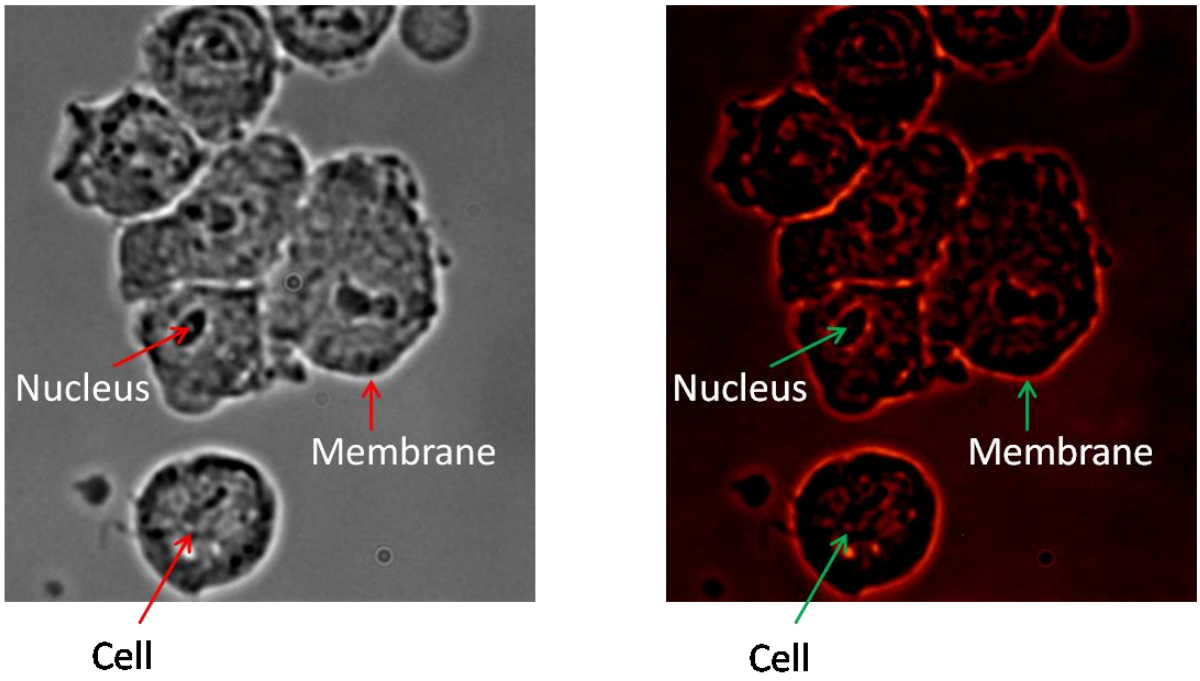

Figure 105 HEp-2 cells, 25 µM AcGlcNaz, 3 d, labelled with „Click-iT™ TAMRA (Tetramethylrhodamine) Glycoprotein Detection Kit“ (Invitrogen). Brightfield image on the left side, the right picture shows the alkynylated-TAMRA-stained cells at 580 nm.

In a further experiment, the incorporation of the sialic acid analogue NeuNHex into HEp-2 cells was studied. Also that incorporation process and labelling reaction proved to be successful (figure 107). The labelling of the cell surface was performed with alkyne-functionalised fluorescein.

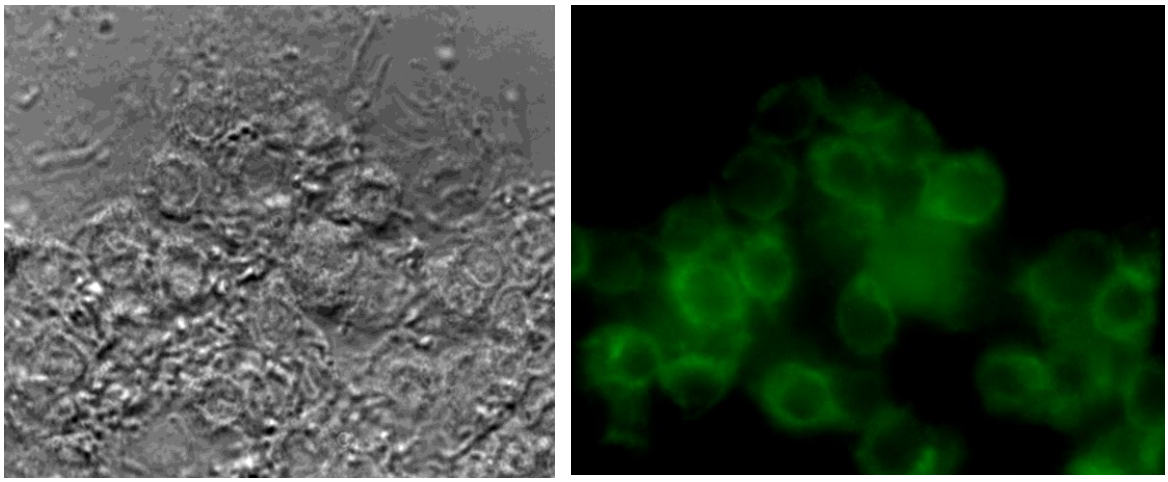

Figure 106 HEp-2 cells, 25 µM NeuNHex, 3 d, labelled with fluorescein azide. Brightfield image (right picture) and the fluorescein-labelled cell surface (525 nm, left picture).

In order to show the broad possibilities of the method, we incorporated in on experiment the GlcNAz and in another experiment the NeuNHex into CHO-K1 cells. The labelling reaction was performed with alkyne- or azide-functionalised fluorescein, respectively, under the same reaction conditions (25 µM of the modified carbohydrate, click reaction with Cu(I), sodium ascorbate and TBTA as copper-activating ligand). However, the results of this experiment are of minor quality regarding the cell membrane staining compared to the HEp-2 cells. This is most likely due to the staining click reaction which was performed over night. The click reaction proves best to be performed in between 1 h for optimal results. Another drawback of the reaction parameters and compounds used for the click reaction is the cytotpxicity of DMSO and copper. This problem for *in vivo* labelling can be overcome by different reaction conditions and different detection molecules. The strain-promoted click reaction with DIFO was introduced recently and proven to be suitable for *in vivo* labelling (Laughlin *et al.*, 2008).

5 Summary

Undoubtedly, carbohydrates play a crucial role in biological systems (Varki, 2006). They are involved in various processes like cell-cell recognition, tumour formation, inflammation and infections (Gruenberg *et al.*, 2006; Varki, 2006). Unfortunately, carbohydrate patterns are not encoded in a biological system like proteins are in the DNA. Posttranslational modifications like methylation, acetylation, phosphorylation, sulfation and glycosylation are usually dynamic. Once a carbohydrate structure is identified as crucial for an infection process, the task is not over at all. Much effort was taken over the years to synthesise and analyse carbohydrate target structures without a significant breakthrough for glycobiology. The holy grail of glycoscience is a toolbox to synthesise any desired carbohydrate pattern. The main problem is the chemical similarity or even identity of many carbohydrates. Due to this difficult accessibility by chemical synthesis alone, new chemo-enzymatic methods are helping to expand the library of carbohydrate structures. The promiscuity of natural carbohydrate-transferring enzymes known as glycosyltransferases accompanied by enzyme and substrate engineering is a possibility for the synthesis of the target structures and their analogues (Chang *et al.*, 2007; Lairson *et al.*, 2008). The goal can only be achieved when biology, chemistry, process engineering and many other disciplines of life sciences work together.

In this thesis, the synthesis and physiological analysis of biological-active tailor-made oligosaccharides is presented. Novel carbohydrate structures have been synthesised by a combination of enzyme and substrate engineering (Homann *et al.*, 2009). The previously described physiological activity turned our focus on fructo-oligosaccharides (Yun, 1996). As a first step, sucrose analogues were synthesised with the help of the fructosyltransferase SacB from *Bacillus megaterium*. This enzyme transfers the fructosyl moiety of sucrose to another monosaccharide of choice, *e.g.* galactose, mannose, xylose or fucose (Seibel *et al.*, 2006b). These sucrose analogues act as substrates for another fructosyltransferase from *Aspergillus niger* (Zuccaro *et al.*, 2008). By the consecutive action of these enzymes, 1-kestose and 1-nystose analogues with physiological functions were synthesised. In cooperation with the groups of Dieter Jahn (TU Braunschweig), Petra Dersch and Dirk Heinz (Helmholtz-Centre for Infection Research) the fructosyltransferases SacB

from *B. megaterium* and Suc1 from *A. niger* were identified, cloned, expressed, purified and characterised. Moreover, SacB from *B. megaterium* was crystallised and engineered to elucidate its transfructosylation mechanism for the synthesis of the oligosaccharide target structures. The two wild-type fructosyltransferases were screened for the acceptance of novel engineered substrate analogues synthesised in our group. Another point was the engineering of the enzymes to get functions exploitable for the synthesis of novel oligosaccharide structures. In order to elucidate the mechanism of transfructosylation, in cooperation with the group of Dieter Jahn, 27 variants of the fructosyltransferase SacB from *B. megaterium* based on random screens and rational mutagenesis were created. The kinetic data as well as the product spectra of each variant gave new insights into the mechanism of fructosyl transfer. By these mutagenesis studies the fructosyltransferase from *B. megaterium* was engineered in order to produce tailor-made fructo-oligosaccharides of different degrees of polymerisation. The variants H423Y and K315A have a higher transfructosylation activity keeping the wild-types K_m and k_{cat}. New amino acid residues not located in the active site were identified as crucial for oligosaccharide synthesis (N252, K373, Y247). These studies lead to a generalised understanding of carbohydrate transfer mechanisms (figures 56 and 59).

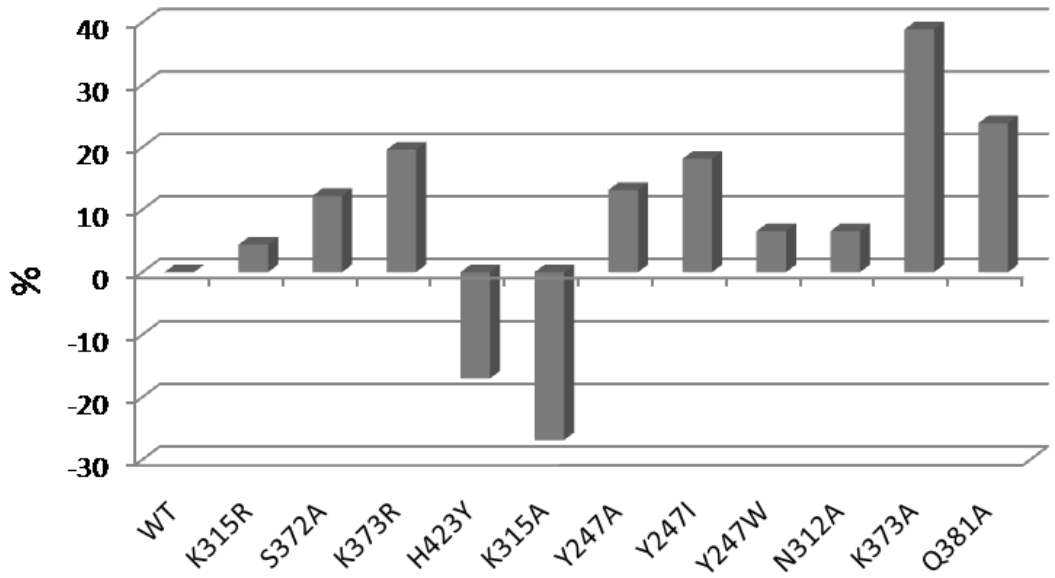

Figure 56 Hydrolysis activity of the wild-type fructosyltransferase SacB from *B. megaterium* (WT) and its variants. Deviance from the wild-type in % (mol/mol). The carbohydrate concentrations were determined by HPAEC.

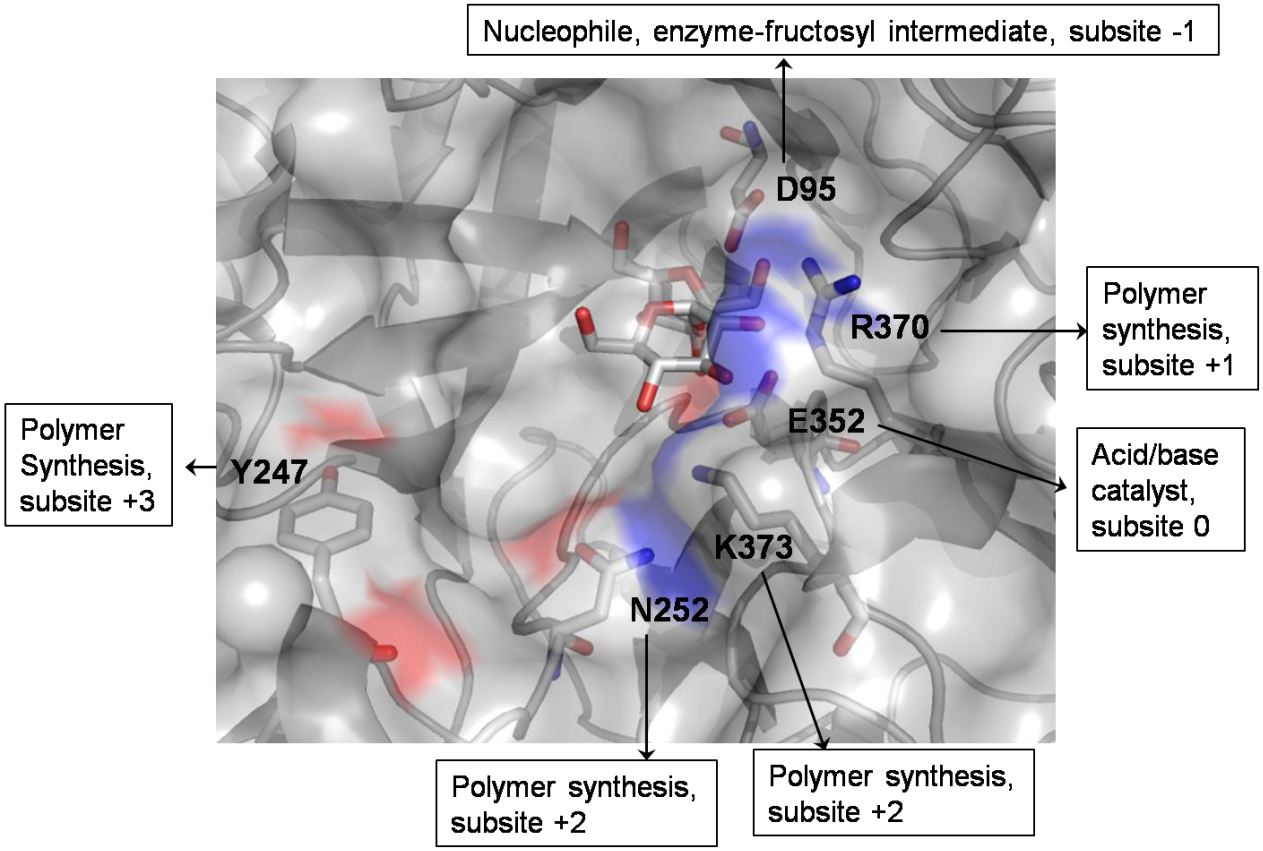

Figure 59 Summary of the most important amino acid residues of the fructosyltransferase SacB from *B. megaterium*

The sucrose isomerase from *Protaminobacter rubrum* provides insights into another aspect of tailor-made oligosaccharides. By the native and engineered fructosyltransferases from *B. megaterium* and *A. niger* we got control over the degree of polymerisation. By substrate engineering of a sucrose isomerase from *Protaminobacter rubrum* we changed the linkage type of the sucrose analogue galactosylfructoside (Gal-Fru). The α-(1,2) bond of the sucrose analogue of Gal-Fru was shifted to an α-(1,6) linkage yielding an isomaltulose analogue of Gal-Fru (figures 60b and 70). The control of the linkage specificity is one important component to expand the library of accessible oligosaccharide structures for the synthesis of tailor-made oligosaccharides.

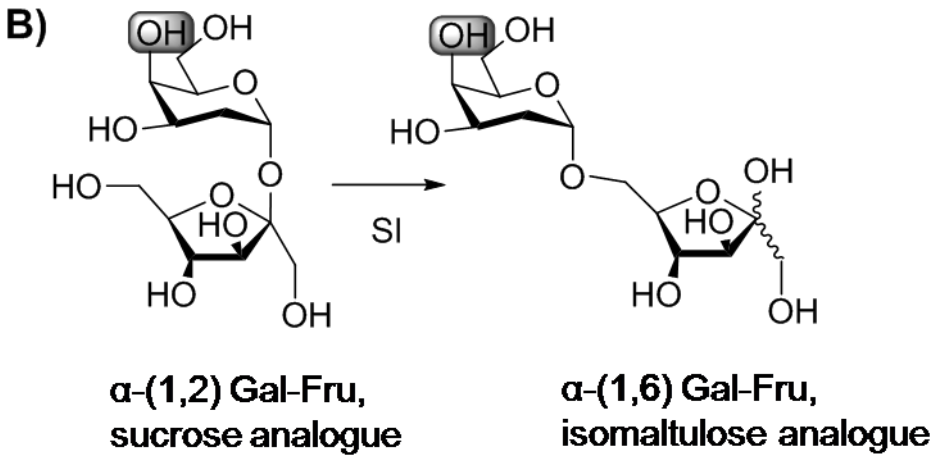

Figure 60 B) The isomerisation reaction catalysed by the sucrose isomerase (SI) from *P. rubrum* with the sucrose analogue Gal-Fru (α-(1,2)-linkage) yielding the isomaltulose analogue (α-(1,6)-bound).

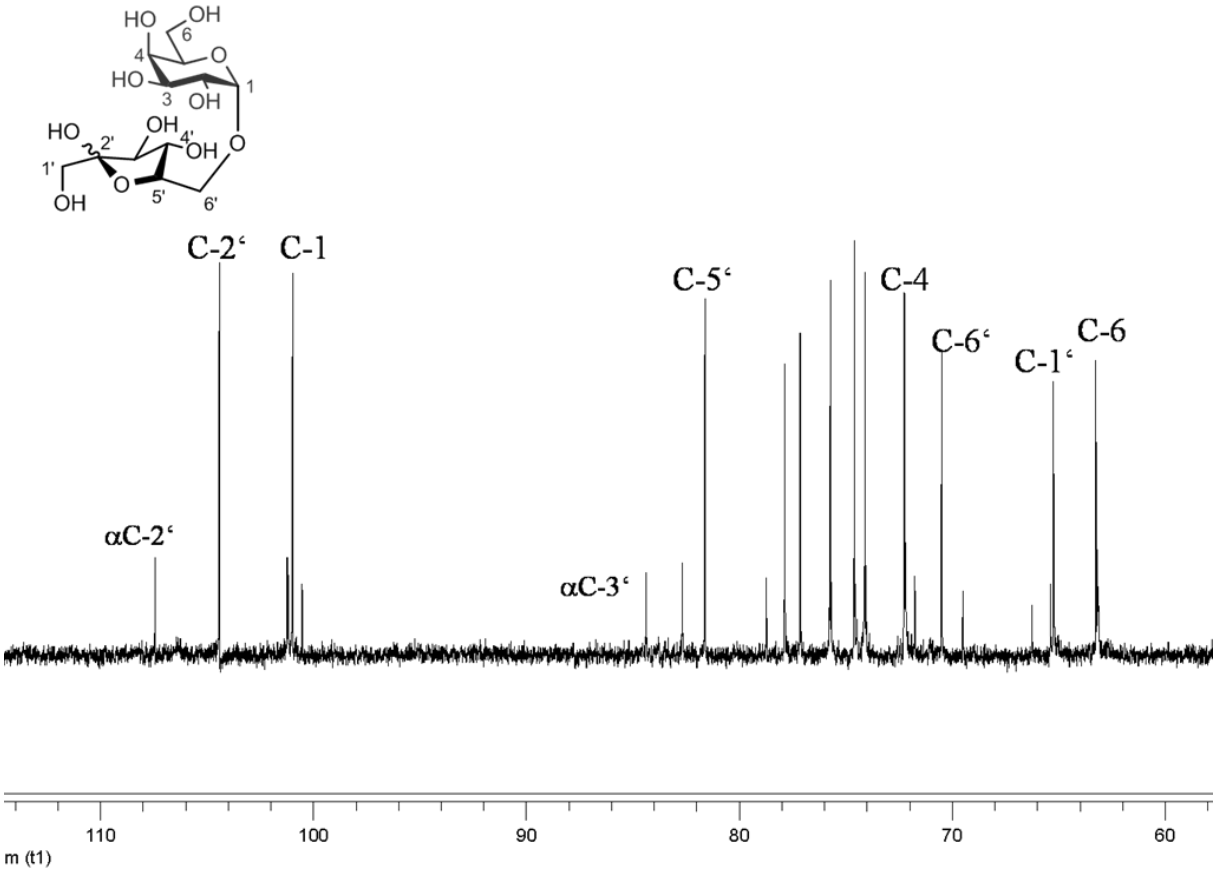

Figure 70 ^{13}C NMR spectrum of the α-/β-galactosylfructoside isomer synthesised by the sucrose isomerase from *P. rubrum*.

The physiological functions of the short-chain oligosaccharides were investigated in an assay with a human epithelial colorectal adenocarcinoma cell line (Caco-2). Their cytokine release pattern was characterised. The novel fructo-oligosaccharides synthesised by the concerted action of the two fructosyltransferases from *B. megaterium* and *A. niger* showed remarkable immuno-stimulating properties (figure 71). The chemokine MCP-1 was clearly triggered when Caco-2 cells are incubated in the presence of the novel fructo-oligosaccharides. The 1-nystose analogues MF_3 and FF_3 with exposed mannosyl and fucosyl moieties show an enhancement in the release of MCP-1 by factor 2.72 and 2.58, respectively (figure 97).

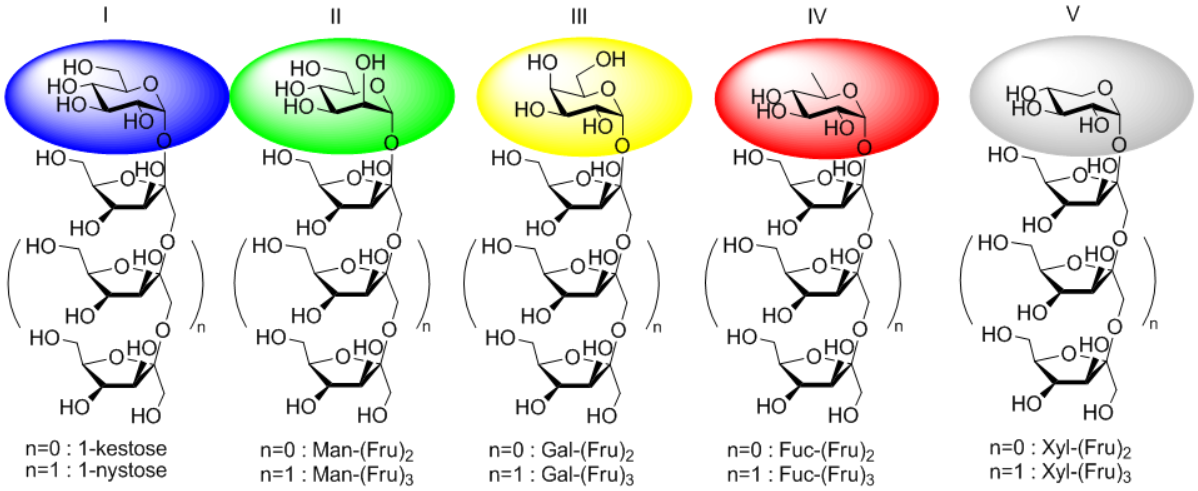

Figure 71 Fructo-oligosaccharide target structures. I) Established product on the market (1-kestose and 1-nystose). II) 1-kestose (Man-(Fru_2) or 1-nystose (Man-(Fru_3) analogue, III) 1-kestose (Gal-$(Fru)_2$) or nystose (Gal-$(Fru)_3$) analogue. IV) 1-kestose (Fuc-$(Fru)_2$) or 1-nystose (Fuc-$(Fru)_3$) analogue. V) 1-kestose (Xyl-$(Fru)_2$) or 1-nystose (Xyl-$(Fru)_3$) analogue.

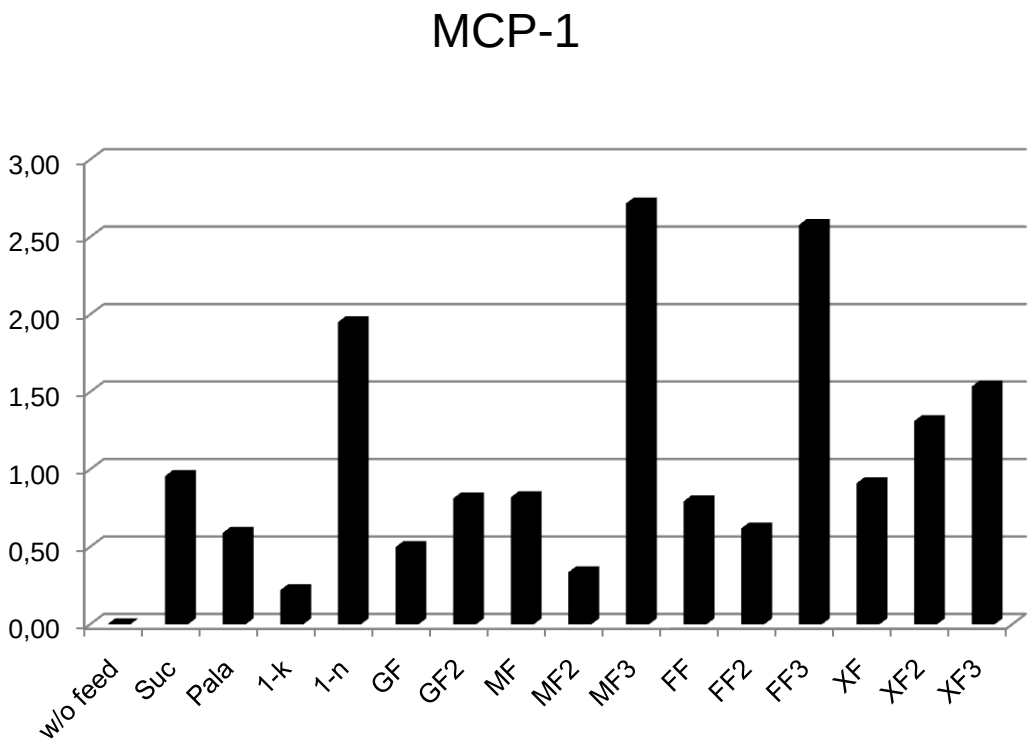

Figure 97 Factors of signal-to-background enhancement of the MCP-1 concentration.

In the last step towards tailor-made oligosaccharides and the investigation of their physiological properties, the application of chemically modified carbohydrates further broadens the product spectrum of glycosyltransferases and paves the way for novel biological applications and strategies. One example of a combined chemo-enzymatic strategy of bioorthogonal metabolic labelling is the so-called click chemistry. Huisgen and Sharpless developed a bioorthogonal, very specific quantitatively (1,3)-triazole formation of an azide and an alkyne group (Kolb *et al.*, 2001). Enzymes of the eukaryotic and human carbohydrate metabolism accept various functionalised monosaccharides as substrates *in vitro* and *in vivo* (Prescher *et al.*, 2006; Baskin *et al.*, 2007; Chang *et al.*, 2007). These modified carbohydrates are incorporated into glycoproteins and glycolipids (figure 102). The functionalised carbohydrate motifs can now be specifically addressed (Laughlin *et al.*, 2009). In this work, HEp-2 cells with specifically functionalised carbohydrates (GlcNAz, AcGlcNAz, NeuNAz and NeuNHEx) were tagged. After incorporation into the target cell line they were labelled with functionalised fluorescein or tetramethylrhodamine (TAMRA), respectively (figure 105). So basically all of the aims of this thesis have been achieved.

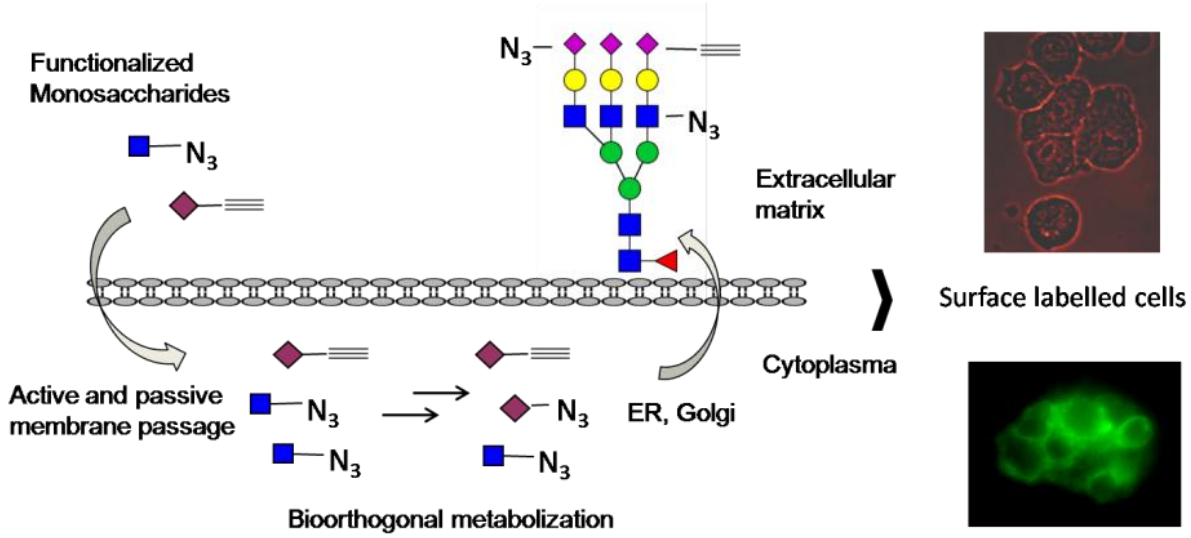

Figure 102 Incorporation of modified carbohydrates into the natural carbohydrate metabolic process of eukaryotic cells.

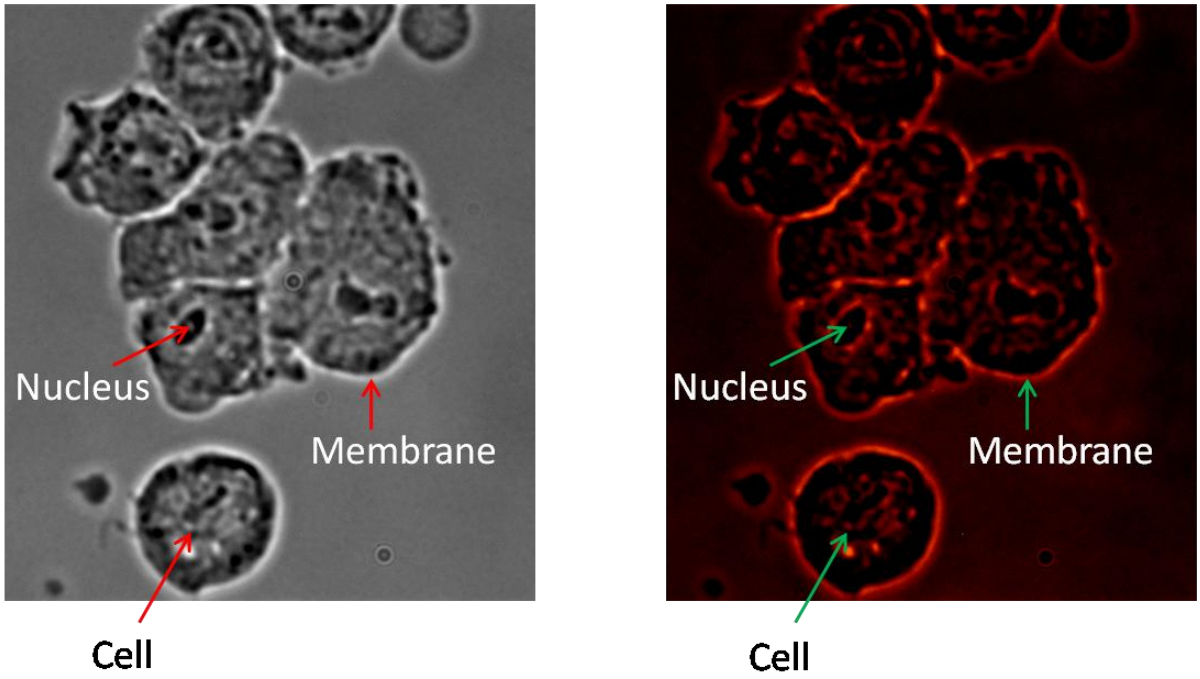

Figure 105 HEp-2 cells, 25 µM AcGlcNaz, 3 d, labelled with „Click-iT™ TAMRA (Tetramethylrhodamine) Glycoprotein Detection Kit“ (Invitrogen). Brightfield image on the left side, the right picture shows the alkynylated-TAMRA-stained cells at 580 nm.

6 References

Agard, N. J., J. A. Prescher and C. R. Bertozzi (2004). "A strain-promoted [3 + 2] azide-alkyne cycloaddition for covalent modification of biomolecules in living systems." J Am Chem Soc **126**(46): 15046-7.

Alam, R., M. A. Lett-Brown, P. A. Forsythe, D. J. Anderson-Walters, C. Kenamore, C. Kormos and J. A. Grant (1992). "Monocyte chemotactic and activating factor is a potent histamine-releasing factor for basophils." J Clin Invest **89**(3): 723-8.

Alberts, B., D. Bray, J. Lewis, M. Raff, K. Roberts and J. D. Watson (1995). Molekularbiologie der Zelle. 3. Auflage, VCH, Weinheim.

Arrhenius, S. (1889). "Über die Reaktionsgeschwindigkeit bei der Inversion von Rohrzucker durch Säuren." Z. Phys. Chemie **4**: 226-248.

Artursson, P., K. Palm and K. Luthman (2001). "Caco-2 monolayers in experimental and theoretical predictions of drug transport." Adv Drug Deliv Rev **46**(1-3): 27-43.

Bardor, M., D. H. Nguyen, S. Diaz and A. Varki (2005). "Mechanism of uptake and incorporation of the non-human sialic acid N-glycolylneuraminic acid into human cells." J Biol Chem **280**(6): 4228-37.

Baskin, J. M., J. A. Prescher, S. T. Laughlin, N. J. Agard, P. V. Chang, I. A. Miller, A. Lo, J. A. Codelli and C. R. Bertozzi (2007). "Copper-free click chemistry for dynamic in vivo imaging." Proc Natl Acad Sci U S A **104**(43): 16793-7.

Bause, E. (1983). "Structural requirements of N-glycosylation of proteins. Studies with proline peptides as conformational probes." Biochem J **209**(2): 331-6.

Beine, R., R. Moraru, M. Nimtz, S. Na'amnieh, A. Pawlowski, K. Buchholz and J. Seibel (2008). "Synthesis of novel fructooligosaccharides by substrate and enzyme engineering." J Biotechnol **138**(1-2): 33-41.

Bezzate, S., S. Aymerich, R. Chambert, S. Czarnes, O. Berge and T. Heulin (2000). "Disruption of the Paenibacillus polymyxa levansucrase gene impairs its ability to aggregate soil in the wheat rhizosphere." Environ Microbiol **2**(3): 333-42.

Biedendieck, R. (2006). TU Braunschweig, PhD thesis.

Bischoff, S. C., M. Krieger, T. Brunner and C. A. Dahinden (1992). "Monocyte chemotactic protein 1 is a potent activator of human basophils." J Exp Med **175**(5): 1271-5.

Blayer, S., J. M. Woodley, M. J. Dawson and M. D. Lilly (1999). "Alkaline biocatalysis for the direct synthesis of N-acetyl-D-neuraminic acid (Neu5Ac) from N-acetyl-D-glucosamine (GlcNAc)." Biotechnol Bioeng **66**(2): 131-6.

Boehm, G., J. Jelinek, B. Stahl, K. van Laere, J. Knol, S. Fanaro, G. Moro and V. Vigi (2004). "Prebiotics in infant formulas." J Clin Gastroenterol **38**(6 Suppl): S76-9.

Buskas, T., S. Ingale and G. J. Boons (2005). "Towards a fully synthetic carbohydrate-based anticancer vaccine: synthesis and immunological evaluation of a lipidated glycopeptide containing the tumor-associated tn antigen." Angew Chem Int Ed Engl **44**(37): 5985-8.

Callard, R. and A. Gearing, Eds. (1994). The cytokine facts book. London, academic press.

Cantarel, B. L., P. M. Coutinho, C. Rancurel, T. Bernard, V. Lombard and B. Henrissat (2009). "The Carbohydrate-Active EnZymes database (CAZy): an expert resource for Glycogenomics." Nucleic Acids Res **37**(Database issue): D233-8.

Carr, M. W., S. J. Roth, E. Luther, S. S. Rose and T. A. Springer (1994). "Monocyte chemoattractant protein 1 acts as a T-lymphocyte chemoattractant." Proc Natl Acad Sci U S A **91**(9): 3652-6.

Chambert, R. and M. F. Petit-Glatron (1991). "Polymerase and hydrolase activities of Bacillus subtilis levansucrase can be separately modulated by site-directed mutagenesis." Biochem J **279 (Pt 1)**: 35-41.

Chambert, R., G. Treboule and R. Dedonder (1974). "Kinetic studies of levansucrase of Bacillus subtilis." Eur. J. Biochem. **41**(2): 285-300.

Chandra, R. A., E. S. Douglas, R. A. Mathies, C. R. Bertozzi and M. B. Francis (2006). "Programmable cell adhesion encoded by DNA hybridization." Angew Chem Int Ed Engl **45**(6): 896-901.

Chang, P. V., X. Chen, C. Smyrniotis, A. Xenakis, T. Hu, C. R. Bertozzi and P. Wu (2009). "Metabolic labeling of sialic acids in living animals with alkynyl sugars." Angew Chem Int Ed Engl **48**(22): 4030-3.

Chang, P. V., J. A. Prescher, M. J. Hangauer and C. R. Bertozzi (2007). "Imaging cell surface glycans with bioorthogonal chemical reporters." J Am Chem Soc **129**(27): 8400-1.

Cheetham, P. S. (1984). "The extraction and mechanism of a novel isomaltulose-synthesizing enzyme from Erwinia rhapontici." Biochem J **220**(1): 213-20.

Clore, G. M., E. Appella, M. Yamada, K. Matsushima and A. M. Gronenborn (1990). "Three-dimensional structure of interleukin 8 in solution." Biochemistry **29**(7): 1689-96.

Codelli, J. A., J. M. Baskin, N. J. Agard and C. R. Bertozzi (2008). "Second-generation difluorinated cyclooctynes for copper-free click chemistry." J Am Chem Soc **130**(34): 11486-93.

Comstock, L. E. (2009). "Importance of glycans to the host-bacteroides mutualism in the mammalian intestine." Cell Host Microbe **5**(6): 522-6.

Cutfield, S. M., G. J. Davies, G. Murshudov, B. F. Anderson, P. C. Moody, P. A. Sullivan and J. F. Cutfield (1999). "The structure of the exo-beta-(1,3)-glucanase from Candida albicans in native and bound forms: relationship between a pocket and groove in family 5 glycosyl hydrolases." J Mol Biol **294**(3): 771-83.

Davies, G. and B. Henrissat (1995). "Structures and mechanisms of glycosyl hydrolases." Structure **3**(9): 853-9.

Ding, N., N. Wu, Q. Xu, K. Chen and C. Zhang (2009). "Molecular evolution of novel swine-origin A/H1N1 influenza viruses among and before human." Virus Genes.

Donlan, R. M. and J. W. Costerton (2002). "Biofilms: survival mechanisms of clinically relevant microorganisms." Clin Microbiol Rev **15**(2): 167-93.

Dube, D. H. and C. R. Bertozzi (2003). "Metabolic oligosaccharide engineering as a tool for glycobiology." Curr Opin Chem Biol **7**(5): 616-25.

Ducros, V., M. Czjzek, A. Belaich, C. Gaudin, H. P. Fierobe, J. P. Belaich, G. J. Davies and R. Haser (1995). "Crystal structure of the catalytic domain of a bacterial cellulase belonging to family 5." Structure **3**(9): 939-49.

Dziadek, S. and H. Kunz (2004). "Synthesis of tumor-associated glycopeptide antigens for the development of tumor-selective vaccines." Chem Rec **3**(6): 308-21.

Eltis, L. D. and S. G. Withers (2008). "Nature teaches but can be bettered." Curr Opin Chem Biol **12**(2): 115-7.

Fazio, F., M. C. Bryan, O. Blixt, J. C. Paulson and C. H. Wong (2002). "Synthesis of sugar arrays in microtiter plate." J Am Chem Soc **124**(48): 14397-402.

Gantt, R. W., R. D. Goff, G. J. Williams and J. S. Thorson (2008). "Probing the aglycon promiscuity of an engineered glycosyltransferase." Angew Chem Int Ed Engl **47**(46): 8889-92.

Gartner, Z. J. and C. R. Bertozzi (2009). "Programmed assembly of 3-dimensional microtissues with defined cellular connectivity." Proc Natl Acad Sci U S A **106**(12): 4606-10.

Gebska, M. A., I. Titley, H. F. Paterson, R. M. Morilla, D. C. Davies, A. M. Gruszka-Westwood, V. V. Kakkar, S. Eccles and M. F. Scully (2002). "High-affinity binding sites for heparin generated on leukocytes during apoptosis arise from nuclear structures segregated during cell death." Blood **99**(6): 2221-7.

Geier, g. and K. K. Geider (1993). "Characterization and influence on virulence of the levansucrase gene from the fireblight pathogen Erwinia amylovora." Physiol Mol Plant Pathol **42**: 387-404.

Green, R. S., E. L. Stone, M. Tenno, E. Lehtonen, M. G. Farquhar and J. D. Marth (2007). "Mammalian N-glycan branching protects against innate immune self-recognition and inflammation in autoimmune disease pathogenesis." Immunity **27**(2): 308-20.

Gruenberg, J. and F. G. van der Goot (2006). "Mechanisms of pathogen entry through the endosomal compartments." Nat Rev Mol Cell Biol **7**(7): 495-504.

Hafez, M., K. Hayes, M. Goldrick, G. Warhurst, R. Grencis and I. S. Roberts (2009). "The K5 capsule of Escherichia coli strain Nissle 1917 is important in mediating interactions with intestinal epithelial cells and chemokine induction." Infect Immun **77**(7): 2995-3003.

Hancock, S. M., M. D. Vaughan and S. G. Withers (2006). "Engineering of glycosidases and glycosyltransferases." Curr Opin Chem Biol **10**(5): 509-19.

Handel, T. M. and P. J. Domaille (1996). "Heteronuclear (1H, 13C, 15N) NMR assignments and solution structure of the monocyte chemoattractant protein-1 (MCP-1) dimer." Biochemistry **35**(21): 6569-84.

Hanson, S. R., E. K. Culyba, T. L. Hsu, C. H. Wong, J. W. Kelly and E. T. Powers (2009). "The core trisaccharide of an N-linked glycoprotein intrinsically accelerates folding and enhances stability." Proc Natl Acad Sci U S A **106**(9): 3131-6.

Heidecke, C. D., Z. Ling, N. C. Bruce, J. W. Moir, T. B. Parsons and A. J. Fairbanks (2008). "Enhanced glycosylation with mutants of endohexosaminidase A (endo A)." Chembiochem **9**(13): 2045-51.

Hellmuth, H., L. Hillringhaus, S. Hobbel, S. Kralj, L. Dijkhuizen and J. Seibel (2007). "Highly Efficient Chemoenzymatic Synthesis of Novel Branched Thiooligosaccharides by Substrate Direction with Glucansucrases." Chembiochem **8**(3): 273-276.

Hettwer, U., F. R. Jaeckel, J. Boch, M. Meyer, K. Rudolph and M. S. Ullrich (1998). "Cloning, nucleotide sequence, and expression in Escherichia coli of levansucrase genes from the plant pathogens Pseudomonas syringae pv. glycinea and P. syringae pv. phaseolicola." Appl Environ Microbiol **64**(9): 3180-7.

Hirayama, K. and K. Itoh (2005). "Human flora-associated (HFA) animals as a model for studying the role of intestinal flora in human health and disease." Curr Issues Intest Microbiol **6**(2): 69-75.

Homann, A., R. Biedendieck, S. Gotze, D. Jahn and J. Seibel (2007). "Insights into polymer versus oligosaccharide synthesis: mutagenesis and mechanistic studies of a novel levansucrase from Bacillus megaterium." Biochem J **407**(2): 189-98.

Homann, A. and J. Seibel (2009). "Towards tailor-made oligosaccharides-chemo-enzymatic approaches by enzyme and substrate engineering." Appl Microbiol Biotechnol **83**(2): 209-16.

Ingale, S., M. A. Wolfert, J. Gaekwad, T. Buskas and G. J. Boons (2007). "Robust immune responses elicited by a fully synthetic three-component vaccine." Nat Chem Biol **3**(10): 663-7.

Jensen, M. H., O. Mirza, C. Albenne, M. Remaud-Simeon, P. Monsan, M. Gajhede and L. K. Skov (2004). "Crystal structure of the covalent intermediate of amylosucrase from Neisseria polysaccharea." Biochemistry **43**(11): 3104-10.

Jiang, Y., D. I. Beller, G. Frendl and D. T. Graves (1992). "Monocyte chemoattractant protein-1 regulates adhesion molecule expression and cytokine production in human monocytes." J Immunol **148**(8): 2423-8.

Jones, J., S. S. Krag and M. J. Betenbaugh (2005). "Controlling N-linked glycan site occupancy." Biochim Biophys Acta **1726**(2): 121-37.

Kim, N. Y., H. G. Kim, Y. H. Kim, I. S. Chung and J. M. Yang (2008). "Expression and characterization of human N-acetylglucosaminyltransferases and alpha2,3-sialyltransferase in insect cells for in vitro glycosylation of recombinant erythropoietin." J Microbiol Biotechnol **18**(2): 383-91.

Kim, Y. W., A. L. Lovering, H. Chen, T. Kantner, L. P. McIntosh, N. C. Strynadka and S. G. Withers (2006). "Expanding the thioglycoligase strategy to the synthesis of alpha-linked thioglycosides allows structural investigation of the parent enzyme/substrate complex." J Am Chem Soc **128**(7): 2202-3.

Kline, K. A., S. Falker, S. Dahlberg, S. Normark and B. Henriques-Normark (2009). "Bacterial adhesins in host-microbe interactions." Cell Host Microbe **5**(6): 580-92.

Kolb, H. C., M. G. Finn and K. B. Sharpless (2001). "Click Chemistry: Diverse Chemical Function from a Few Good Reactions." Angew Chem Int Ed Engl **40**(11): 2004-2021.

Korakli, M., M. Pavlovic, M. G. Ganzle and R. F. Vogel (2003). "Exopolysaccharide and kestose production by Lactobacillus sanfranciscensis LTH2590." Appl Environ Microbiol **69**(4): 2073-9.

Kralj, S., G. H. van Geel-Schutten, M. J. van der Maarel and L. Dijkhuizen (2004). "Biochemical and molecular characterization of Lactobacillus reuteri 121 reuteransucrase." Microbiology **150**(Pt 7): 2099-112.

Kulminskaya, A. A., M. Arand, E. V. Eneyskaya, D. R. Ivanen, K. A. Shabalin, S. M. Shishlyannikov, A. N. Saveliev, O. S. Korneeva and K. N. Neustroev (2003). "Biochemical characterization of Aspergillus awamori exoinulinase: substrate binding characteristics and regioselectivity of hydrolysis." Biochim Biophys Acta **1650**(1-2): 22-9.

Kuna, P., S. R. Reddigari, D. Rucinski, J. J. Oppenheim and A. P. Kaplan (1992). "Monocyte chemotactic and activating factor is a potent histamine-releasing factor for human basophils." J Exp Med **175**(2): 489-93.

Kunisaki, K. M. and E. N. Janoff (2009). "Influenza in immunosuppressed populations: a review of infection frequency, morbidity, mortality, and vaccine responses." Lancet Infect Dis **9**(8): 493-504.

Kunst, F., N. Ogasawara, I. Moszer, A. M. Albertini, G. Alloni, V. Azevedo, M. G. Bertero, P. Bessieres, A. Bolotin, S. Borchert, R. Borriss, L. Boursier, A. Brans, M. Braun, S. C. Brignell, S. Bron, S. Brouillet, C. V. Bruschi, B. Caldwell, V. Capuano, N. M. Carter, S. K. Choi, J. J. Codani, I. F. Connerton, A. Danchin and et al. (1997). "The complete genome sequence of the gram-positive bacterium Bacillus subtilis." Nature **390**(6657): 249-56.

Lairson, L. L., B. Henrissat, G. J. Davies and S. G. Withers (2008). "Glycosyltransferases: structures, functions, and mechanisms." Annu Rev Biochem **77**: 521-55.

Lairson, L. L., A. G. Watts, W. W. Wakarchuk and S. G. Withers (2006). "Using substrate engineering to harness enzymatic promiscuity and expand biological catalysis." Nat Chem Biol **2**(12): 724-8.

Lambert, C., N. Leonard, X. De Bolle and E. Depiereux (2002). "ESyPred3D: Prediction of proteins 3D structures." Bioinformatics **18**(9): 1250-6.

Lasch, J., Ed. (1987). Enzymkinetik. Heidelberg, Springer Verlag.

Laughlin, S. T., J. M. Baskin, S. L. Amacher and C. R. Bertozzi (2008). "In vivo imaging of membrane-associated glycans in developing zebrafish." Science **320**(5876): 664-7.

Laughlin, S. T. and C. R. Bertozzi (2009). "Imaging the glycome." Proc Natl Acad Sci U S A **106**(1): 12-7.

Lina, B. A., D. Jonker and G. Kozianowski (2002). "Isomaltulose (Palatinose): a review of biological and toxicological studies." Food Chem Toxicol **40**(10): 1375-81.

Maira-Litran, T., A. Kropec, C. Abeygunawardana, J. Joyce, G. Mark, 3rd, D. A. Goldmann and G. B. Pier (2002). "Immunochemical properties of the staphylococcal poly-N-acetylglucosamine surface polysaccharide." Infect Immun **70**(8): 4433-40.

Mantovani, Gezzi and Dinarello, Eds. (2000). Pharmacology of cytokines. Oxford, Oxford University Press.

Martinez-Fleites, C., M. Ortiz-Lombardia, T. Pons, N. Tarbouriech, E. J. Taylor, J. G. Arrieta, L. Hernandez and G. J. Davies (2005). "Crystal structure of levansucrase from the Gram-negative bacterium Gluconacetobacter diazotrophicus." Biochem J **390**(Pt 1): 19-27.

Massion, P. P., C. A. Hebert, S. Leong, B. Chan, H. Inoue, K. Grattan, D. Sheppard and J. A. Nadel (1995). "Staphylococcus aureus stimulates neutrophil recruitment by stimulating interleukin-8 production in dog trachea." Am J Physiol **268**(1 Pt 1): L85-94.

McKenney, D., K. L. Pouliot, Y. Wang, V. Murthy, M. Ulrich, G. Doring, J. C. Lee, D. A. Goldmann and G. B. Pier (1999). "Broadly protective vaccine for Staphylococcus aureus based on an in vivo-expressed antigen." Science **284**(5419): 1523-7.

Meng, G. and K. Futterer (2003). "Structural framework of fructosyl transfer in Bacillus subtilis levansucrase." Nat Struct Biol **10**(11): 935-41.

Meng, G. and K. Futterer (2008). "Donor substrate recognition in the raffinose-bound E342A mutant of fructosyltransferase Bacillus subtilis levansucrase." BMC Struct Biol **8**: 16.

Miller, E. J., A. B. Cohen and B. T. Peterson (1996a). "Peptide inhibitor of interleukin-8 (IL-8) reduces staphylococcal enterotoxin-A (SEA) induced neutrophil trafficking to the lung." Inflamm Res **45**(8): 393-7.

Miller, E. J., S. Nagao, F. K. Carr, J. M. Noble and A. B. Cohen (1996b). "Interleukin-8 (IL-8) is a major neutrophil chemotaxin from human alveolar macrophages stimulated with staphylococcal enterotoxin A (SEA)." Inflamm Res **45**(8): 386-92.

Mosi, R., S. He, J. Uitdehaag, B. W. Dijkstra and S. G. Withers (1997). "Trapping and characterization of the reaction intermediate in cyclodextrin glycosyltransferase by use of activated substrates and a mutant enzyme." Biochemistry **36**(32): 9927-34.

Nagai, Y., T. Sugitani and K. Tsuyuki (1994). "Characterization of alpha-glucosyltransferase from Pseudomonas mesoacidophila MX-45." Biosci Biotechnol Biochem **58**(10): 1789-93.

Ozimek, L. K., S. Kralj, M. J. van der Maarel and L. Dijkhuizen (2006). "The levansucrase and inulosucrase enzymes of Lactobacillus reuteri 121 catalyse processive and non-processive transglycosylation reactions." Microbiology **152**(Pt 4): 1187-96.

Pachamuthu, K. and R. R. Schmidt (2006). "Synthetic routes to thiooligosaccharides and thioglycopeptides." Chem Rev **106**(1): 160-87.

Paul, W. E., Ed. (2008). Fundamental Immunology, Lippincott Williams & Wilkins.

Perez, L. and S. J. Danishefsky (2007). "Chemistry and biology in search of antimetastatic agents." ACS Chem Biol **2**(3): 159-62.

Potera, C. (1999). "Forging a link between biofilms and disease." Science **283**(5409): 1837, 1839.

Prescher, J. A. and C. R. Bertozzi (2005). "Chemistry in living systems." Nat Chem Biol **1**(1): 13-21.

Prescher, J. A. and C. R. Bertozzi (2006). "Chemical technologies for probing glycans." Cell **126**(5): 851-4.

Rath, A., M. Glibowicka, V. G. Nadeau, G. Chen and C. M. Deber (2009). "Detergent binding explains anomalous SDS-PAGE migration of membrane proteins." Proc Natl Acad Sci U S A **106**(6): 1760-5.

Rathsam, C., P. M. Giffard and N. A. Jacques (1993). "The cell-bound fructosyltransferase of Streptococcus salivarius: the carboxyl terminus specifies attachment in a Streptococcus gordonii model system." J Bacteriol **175**(14): 4520-7.

Ravaud, S., X. Robert, H. Watzlawick, R. Haser, R. Mattes and N. Aghajari (2007). "Trehalulose synthase native and carbohydrate complexed structures provide insights into sucrose isomerization." J Biol Chem **282**(38): 28126-36.

Ravaud, S., X. Robert, H. Watzlawick, R. Haser, R. Mattes and N. Aghajari (2009). "Structural determinants of product specificity of sucrose isomerases." FEBS Lett **583**(12): 1964-8.

Ravaud, S., H. Watzlawick, R. Haser, R. Mattes and N. Aghajari (2005). "Expression, purification, crystallization and preliminary X-ray crystallographic studies of the

trehalulose synthase MutB from Pseudomonas mesoacidophila MX-45." Acta Crystallogr Sect F Struct Biol Cryst Commun **61**(Pt 1): 100-3.

Ravaud, S., H. Watzlawick, R. Haser, R. Mattes and N. Aghajari (2006). "Overexpression, purification, crystallization and preliminary diffraction studies of the Protaminobacter rubrum sucrose isomerase SmuA." Acta Crystallogr Sect F Struct Biol Cryst Commun **62**(Pt 1): 74-6.

Riaz-ul-Qamar (2007). TU Braunschweig, Master Thesis.

Rollins, B. J. (1997). "Chemokines." Blood **90**(3): 909-28.

Saavedra, J. M. and A. Tschernia (2002). "Human studies with probiotics and prebiotics: clinical implications." Br J Nutr **87 Suppl 2**: S241-6.

Sadler, J. E. (1998). "Biochemistry and genetics of von Willebrand factor." Annu Rev Biochem **67**: 395-424.

Sambrook, J., E. F. Fritsch and T. Maniatis, Eds. (1999). Molecular Cloning, a laboratory manual. Cold Spring Harbor, New York, Cold Spring Harbor Laboratory Press.

Saxon, E., S. J. Luchansky, H. C. Hang, C. Yu, S. C. Lee and C. R. Bertozzi (2002). "Investigating cellular metabolism of synthetic azidosugars with the Staudinger ligation." J Am Chem Soc **124**(50): 14893-902.

Schlegel, H., Ed. (1992). Allgemeine Mikrobiologie, Thieme.

Schmidt-Dannert, C. and F. H. Arnold (1999). "Directed evolution of industrial enzymes." Trends Biotechnol **17**(4): 135-6.

Schomburg, I., A. Chang and D. Schomburg (2002). "BRENDA, enzyme data and metabolic information." Nucleic Acids Res **30**(1): 47-9.

Seibel, J., H. Hellmuth, B. Hofer, A. M. Kicinska and B. Schmalbruch (2006a). "Identification of new acceptor specificities of glycosyltransferase R with the aid of substrate microarrays." Chembiochem **7**(2): 310-20.

Seibel, J., R. Moraru, S. Gotze, K. Buchholz, S. Na'amnieh, A. Pawlowski and H. J. Hecht (2006b). "Synthesis of sucrose analogues and the mechanism of action of Bacillus subtilis fructosyltransferase (levansucrase)." Carbohydr Res **341**(14): 2335-49.

Serim, S. (2008). TU Braunschweig, Master Thesis.

Shah, P., V. Jogani, T. Bagchi and A. Misra (2006). "Role of Caco-2 cell monolayers in prediction of intestinal drug absorption." Biotechnol Prog **22**(1): 186-98.

Shaikh, F. A. and S. G. Withers (2008). "Teaching old enzymes new tricks: engineering and evolution of glycosidases and glycosyl transferases for improved glycoside synthesis." Biochem Cell Biol **86**(2): 169-77.

Sinclair, A. M. and S. Elliott (2005). "Glycoengineering: the effect of glycosylation on the properties of therapeutic proteins." J Pharm Sci **94**(8): 1626-35.

Sletten, E. M. and C. R. Bertozzi (2009). "Bioorthogonal chemistry: fishing for selectivity in a sea of functionality." Angew Chem Int Ed Engl **48**(38): 6974-98.

Soell, M., M. Diab, G. Haan-Archipoff, A. Beretz, C. Herbelin, B. Poutrel and J. P. Klein (1995). "Capsular polysaccharide types 5 and 8 of Staphylococcus aureus bind specifically to human epithelial (KB) cells, endothelial cells, and monocytes and induce release of cytokines." Infect Immun **63**(4): 1380-6.

Song, K. B., S. K. Lee, H. K. Joo and S. K. Rhee (1994). "Nucleotide and derived amino acid sequences of an extracellular sucrase gene (invB) of Zymomonas mobilis ZM1 (ATCC10988)." Biochim Biophys Acta **1219**(1): 163-6.

Song, K. B., J. W. Seo, M. G. Kim and S. K. Rhee (1998). "Levansucrase of Rahnella aquatilis ATCC33071. Gene cloning, expression, and levan formation." Ann N Y Acad Sci **864**: 506-11.

Springer, T. A. (1994). "Traffic signals for lymphocyte recirculation and leukocyte emigration: the multistep paradigm." Cell **76**(2): 301-14.

Standiford, T. J., D. A. Arenberg, J. M. Danforth, S. L. Kunkel, G. M. VanOtteren and R. M. Strieter (1994). "Lipoteichoic acid induces secretion of interleukin-8 from human blood monocytes: a cellular and molecular analysis." Infect Immun **62**(1): 119-25.

Stevens, D. L. (1997). "Superantigens: their role in infectious diseases." Immunol Invest **26**(1-2): 275-81.

Stoll, V. and J. Blanchard (1990). "Buffers: principles and practice." Meth. Enzymol. **182**(24-38).

Stoppok, E., J. Walter and K. Buchholz (1995). "The effect of pH and oxygen concentration on the formation of 3-ketodisaccharides by Agrobacterium tumefaciens." Appl Microbiol Biotechnol **43**(4): 706-12.

Sun., J., W. Wang, C. Hundertmark, A. P. Zeng, D. Jahn and W. D. Deckwer (2006). "A protein database constructed from low-coverage genomic sequence of Bacillus megaterium and its use for accelerated proteomic analysis." J Biotechnol **124**(3): 486-95.

Tang, L. B., R. Lenstra, T. V. Borchert and V. Nagarajan (1990). "Isolation and characterization of levansucrase-encoding gene from Bacillus amyloliquefaciens." Gene **96**(1): 89-93.

Thompson, J., S. A. Robrish, A. Pikis, A. Brust and F. W. Lichtenthaler (2001). "Phosphorylation and metabolism of sucrose and its five linkage-isomeric alpha-D-glucosyl-D-fructoses by Klebsiella pneumoniae." Carbohydr Res **331**(2): 149-61.

Totani, K., Y. Ihara, I. Matsuo, T. Tsujimoto and Y. Ito (2009). "The Recognition Motif of the Glycoprotein-Folding Sensor Enzyme, UDP-Glc: Glycoprotein Glucosyltransferase." Biochemistry.

Ueda, S., T. Shiroza and H. K. Kuramitsu (1988). "Sequence analysis of the gtfC gene from Streptococcus mutans GS-5." Gene **69**(1): 101-9.

Uitdehaag, J. C., R. Mosi, K. H. Kalk, B. A. van der Veen, L. Dijkhuizen, S. G. Withers and B. W. Dijkstra (1999). "X-ray structures along the reaction pathway of cyclodextrin glycosyltransferase elucidate catalysis in the alpha-amylase family." Nat Struct Biol **6**(5): 432-6.

Ulevitch, R. J. and P. S. Tobias (1995). "Receptor-dependent mechanisms of cell stimulation by bacterial endotoxin." Annu Rev Immunol **13**: 437-57.

Uliczka, F., T. Kornprobst, J. Eitel, D. Schneider and P. Dersch (2009). "Cell invasion of Yersinia pseudotuberculosis by invasin and YadA requires protein kinase C, PLC-gamma1 and Akt kinase." Cell Microbiol.

Ungar, D. (2009). "Golgi linked protein glycosylation and associated diseases." Semin Cell Dev Biol.

Vaddi, K. and R. C. Newton (1994). "Regulation of monocyte integrin expression by beta-family chemokines." J Immunol **153**(10): 4721-32.

van Hijum, S. A., S. Kralj, L. K. Ozimek, L. Dijkhuizen and I. G. van Geel-Schutten (2006). "Structure-function relationships of glucansucrase and fructansucrase enzymes from lactic acid bacteria." Microbiol Mol Biol Rev **70**(1): 157-76.

Varki, A. (2006). "Nothing in glycobiology makes sense, except in the light of evolution." Cell **126**(5): 841-5.

Veronese, T. and P. Perlot (1998). "Proposition for the biochemical mechanism occurring in the sucrose isomerase active site." FEBS Lett **441**(3): 348-52.

Watson, J. D. and F. H. Crick (1953). "Molecular structure of nucleic acids; a structure for deoxyribose nucleic acid." Nature **171**(4356): 737-8.

Westerlind, U., A. Hobel, N. Gaidzik, E. Schmitt and H. Kunz (2008). "Synthetic vaccines consisting of tumor-associated MUC1 glycopeptide antigens and a T-cell epitope for the induction of a highly specific humoral immune response." Angew Chem Int Ed Engl **47**(39): 7551-6.

Wittrock, S., T. Becker and H. Kunz (2007). "Synthetic vaccines of tumor-associated glycopeptide antigens by immune-compatible thioether linkage to bovine serum albumin." Angew Chem Int Ed Engl **46**(27): 5226-30.

Wolff, B., A. R. Burns, J. Middleton and A. Rot (1998). "Endothelial cell "memory" of inflammatory stimulation: human venular endothelial cells store interleukin 8 in Weibel-Palade bodies." J Exp Med **188**(9): 1757-62.

Wu, L. and R. G. Birch (2005). "Characterization of the highly efficient sucrose isomerase from Pantoea dispersa UQ68J and cloning of the sucrose isomerase gene." Appl Environ Microbiol **71**(3): 1581-90.

Yao, L., J. W. Berman, S. M. Factor and F. D. Lowy (1997). "Correlation of histopathologic and bacteriologic changes with cytokine expression in an experimental murine model of bacteremic Staphylococcus aureus infection." Infect Immun **65**(9): 3889-95.

Yoshioka, Y., K. Hasegawa, Y. Matsuura, Y. Katsube and M. Kubota (1997). "Crystal structures of a mutant maltotetraose-forming exo-amylase cocrystallized with maltopentaose." J Mol Biol **271**(4): 619-28.

Yun, J. W. (1996). "Fructooligosaccharides - occurence, preparation and application." Enz. Microb. Technol. **19**: 107-117.

Zhang, D., N. Li, S. M. Lok, L. H. Zhang and K. Swaminathan (2003). "Isomaltulose synthase (PalI) of Klebsiella sp. LX3. Crystal structure and implication of mechanism." J Biol Chem **278**(37): 35428-34.

Zhu, J., Q. Wan, G. Ragupathi, C. M. George, P. O. Livingston and S. J. Danishefsky (2009). "Biologics through chemistry: total synthesis of a proposed dual-acting vaccine targeting ovarian cancer by orchestration of oligosaccharide and polypeptide domains." J Am Chem Soc **131**(11): 4151-8.

Zuccaro, A., S. Gotze, S. Kneip, P. Dersch and J. Seibel (2008). "Tailor-made fructooligosaccharides by a combination of substrate and genetic engineering." Chembiochem **9**(1): 143-9.